VOLUME 36 JUNE 1958 NUMBER 6

Canadian Journal of Chemistry

Published by THE NATIONAL RESEARCH COUNCIL

OTTAWA CANADA

CANADIAN JOURNAL OF CHEMISTRY

(Formerly Section B, Canadian Journal of Research)

Under the authority of the Chairman of the Committee of the Privy Council on Scientific and Industrial Research, the National Research Council issues THE CANADIAN JOURNAL OF CHEMISTRY and five other journals devoted to the publication, in English or French, of the results of original scientific research. Matters of general policy concerning these journals are the responsibility of a joint Editorial Board consisting of: members representing the National Research Council of Canada; the Editors of the Journals; and members representing the Royal Society of Canada and four other scientific societies.

The Chemical Institute of Canada has chosen the Canadian Journal of Chemistry as its medium of publication for scientific papers.

Manuscripts for publication should be submitted to Dr. Léo Marion, Editor, Canadian Journal of Chemistry, National Research Council, Ottawa 2, Canada.
(For instructions on preparation of copy, see **Notes to Contributors** (inside back cover).)

Proof, correspondence concerning proof, and orders for reprints should be sent to the Manager, Editorial Office (Research Journals), Division of Administration and Awards, National Research Council, Ottawa 2, Canada.

Subscriptions, renewals, requests for single or back numbers, and all remittances should be sent to Division of Administration and Awards, National Research Council, Ottawa 2, Canada. Remittances should be made payable to the Receiver General of Canada, credit National Research Council.

The journals published, frequency of publication, and prices are:

Canadian Journal of Biochemistry and Physiology	Monthly	$3.00 a year
Canadian Journal of Botany	Bimonthly	$4.00 a year
Canadian Journal of Chemistry	Monthly	$5.00 a year
Canadian Journal of Microbiology	Bimonthly	$3.00 a year
Canadian Journal of Physics	Monthly	$4.00 a year
Canadian Journal of Zoology	Bimonthly	$3.00 a year

The price of regular single numbers of all journals is 75 cents.

Canadian Journal of Chemistry

Issued by THE NATIONAL RESEARCH COUNCIL OF CANADA

VOLUME 36 JUNE 1958 NUMBER 6

HYDROGEN PEROXIDE AND ITS ANALOGUES

VIII. EXCESS FUNCTIONS FOR THE BINARY SYSTEMS H_2O–H_2O_2 AND D_2O–D_2O_2 [1]

PAUL A. GIGUÈRE, OSVALD KNOP,[2] AND MICHAEL FALK[3]

ABSTRACT

Recent volumetric and calorimetric data have been used to calculate the excess functions for mixtures of water and hydrogen peroxide over the entire concentration range. The results are compared with those for the corresponding deuterium compounds. The existing calorimetric and vapor-pressure measurements are not comprehensive nor accurate enough to support discussion of the finer details of the excess quantities. A maximum in the excess-volume curves, presumably related to the formation of the compound $H_2O_2.2H_2O$, persists in the liquid mixtures over an appreciable temperature range above the melting point of that compound. A possible crystal structure is proposed for the latter.

New density determinations were carried out on mixtures of heavy water and deuterium peroxide at 0° and 20° C. and the effect of deuterium peroxide on the temperature of maximum density of heavy water was measured and compared with that of deuterated alcohols. It is concluded that the structure of liquid water is easily penetrated by hydrogen peroxide molecules.

INTRODUCTION

Mixtures of hydrogen peroxide and water represent one of the simplest possible examples of a binary system of strongly polar liquids with extensive hydrogen bonding. So far the investigation of solutions on non-electrolytes for the purpose of testing the existing theories has been largely confined to non-polar systems. However, if the theory is to be extended to hydrogen-bonded systems, the gaps in the present experimental data on such systems will have to be lessened. With this aim in mind we are presenting here a comparative study of the associative properties, in the form of excess functions, of the binary system H_2O–H_2O_2 and its deuterated analogue D_2O–D_2O_2. The excess functions are based in part on our calorimetric measurements reported in paper VII of this series (1).*

SYMBOLS AND DEFINITIONS

T	temperature in ° K.
N_p	mole fraction of hydrogen (or deuterium) peroxide.
N_w	mole fraction of water (or heavy water).

[1]*Manuscript received January 2, 1958.*
Contribution from the Department of Chemistry, Laval University, Quebec, Que.
[2]*On leave of absence from the Nova Scotia Technical College, Halifax, N.S.*
[3]*Holder of a Shawinigan Chemicals Co. research fellowship.*

**Shortly after our data were published a new diphenyl ether calorimeter was described by R. S. Jessup of the National Bureau of Standards, Washington, D.C. (2). The calibration factor of this instrument, 18.90, is slightly different from the one we used, 19.01 cal./g. Hg (3). There is little doubt that the factor found by Jessup is more accurate, as both his apparatus and calibration technique were much more elaborate than ours. Furthermore, most causes of error will give too high a factor, and Jessup's value is the lowest of all those reported so far. The resulting uncertainty in our published results (less than 0.5%) affects in no way the present discussion.*

V_p, V_w	molar volume of peroxide and water, respectively.
V	actual volume of one mole of solution.
$V^\circ = N_w V_w + N_p V_p$	ideal volume of one mole of solution.
$V^E = V - V^\circ$	excess volume of mixing.
$\theta = -100 V^E / V^\circ$	per cent volume contraction.
C_p	actual heat capacity of solution (average value between 0° and 26.9° C.).
$C^E_p = C_p - C^\circ_p$	excess heat capacity of solution (called $\Delta_m C_p$ in paper VII).
$H^E = H^M$	excess heat of mixing (called $\Delta_m H_{mix}$ in paper VII).
$F^E = F^M - F^\circ$	excess free energy of mixing.
$S^E = S^M - S^\circ$	excess entropy of mixing.

MOLAR VOLUMES

Several sets of density determinations on aqueous solutions of hydrogen peroxide can be found in the literature. The most recent ones, showing good mutual consistency, have been combined into cubic polynomials in either weight fraction of peroxide or temperature (4). From these expressions we have calculated the molar volumes and the excess volumes of mixing over the entire composition range and from 0° to 96° C. The temperature range was extended, though with reduced accuracy, down to the liquidus curve of the system (Table I) by including the low-temperature measurements of Giguère and Geoffrion (5). The ideal volumes below 0° C. were estimated by graphical extrapolation since the density of supercooled hydrogen peroxide is not known and that of supercooled water is known only down to −20° C.

TABLE I

EXCESS VOLUMES OF MIXING OF H_2O–H_2O_2 SOLUTIONS AT LOW TEMPERATURES

Composition		$-V^E$				
w_p	N_p	−10° C.	−20° C.	−30° C.	−40° C.	−50° C.
0.1927	0.1122	0.280	—	—	—	—
0.2954	0.1817	0.356	0.442	—	—	—
0.4123	0.2709	0.417	0.505	0.605	0.715	0.833
0.4987	0.3451	0.434	0.517	0.611	0.716	0.828
0.6837	0.5338	0.381	0.441	0.517	—	—
0.7861	0.6606	0.312	0.360	—	—	—
0.8964	0.8209	0.200	—	—	—	—

The excess volume of the mixtures is everywhere negative, as may be seen from the plots in Fig. 1. The variation of θ with temperature and composition is shown in Fig. 2. The pronounced maxima in the curves of Fig. 1 correspond to the maximum deviation from ideality, max θ. Fig. 3 illustrates the temperature dependence of the position of max θ. The equation of the best straight line fitting all the points of that curve up to 50° C. was found by least squares to be

[1] $$\log \max \theta = -8.391 \times 10^{-3} T + 2.512.$$

At higher temperatures the uncertainty in the density measurements was too great to yield reliable values of the maximum.

The position of max θ converges with decreasing temperature towards $N_p = 1/3$, that is

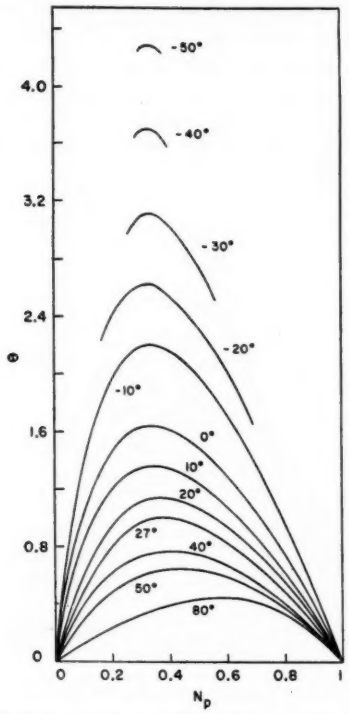

FIG. 1. Per cent volume contraction of mixtures of water and hydrogen peroxide at different temperatures.

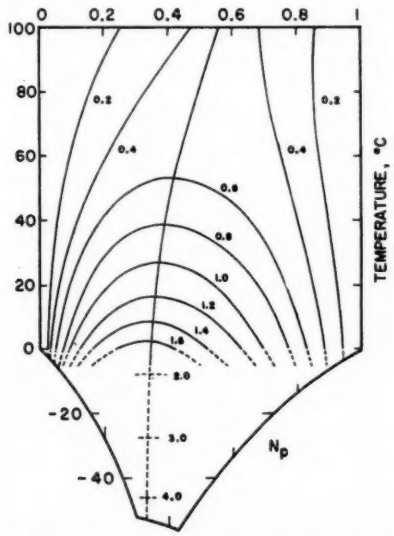

FIG. 2. Per cent volume contraction of mixtures of water and hydrogen peroxide as a function of temperature and composition.

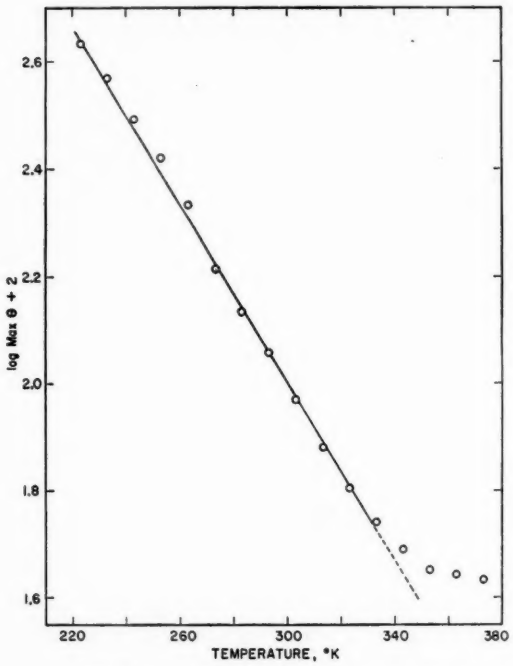

FIG. 3. Dependence of max θ on temperature.

towards the composition of the only crystalline compound, $H_2O_2.2H_2O$, in the system. The near coincidence, though not the convergence, of the position of max θ in these mixtures at ordinary temperatures with the composition of the compound had already been pointed out in somewhat different terms in a paper which recently came to our attention (6).

The experimental data for the mixtures of deuterated compounds are naturally much fewer and less accurate than for the hydrogen compounds. To supplement the first

TABLE II

DENSITIES AND EXCESS VOLUMES OF MIXING OF D_2O–D_2O_2 SOLUTIONS

	Density (g./cm.^{3})		V		$-V^E$	
N_p	0° C.	20° C.	0° C.	20° C.	0° C.	20° C.
0	1.1040	1.1050	18.131	18.113	0	0
0.1978	1.2328	1.2210	18.815	18.997	0.305	0.178
0.2498	1.2630	1.2495	19.023	19.230	0.357	0.223
0.3395	1.3089	1.2929	19.453	19.694	0.375	0.241
0.3637	1.3213	1.3034	19.563	19.832	0.386	0.233
0.4819	1.3727	1.3554	20.208	20.466	0.322	0.233
0.5236	1.3907	1.3717	20.427	20.711	0.321	0.211
0.7281	1.4693	1.4478	21.575	21.896	0.196	1.124
1	1.5577*	1.5348*	23.130*	23.479*	0	0

**Extrapolated.*

set of measurements made in this laboratory some years ago (7) we have repeated a number of determinations to define better the region of max θ. The results (Table II) show definite improvement over those of the first series owing to the larger quantity of deuterium peroxide available this time. As far as can be judged from Fig. 4, max θ occurs at the same composition in the two systems, but there is an increase in the absolute value for the deuterium system amounting to about 17% at 0° C. and about 5% at 20°.

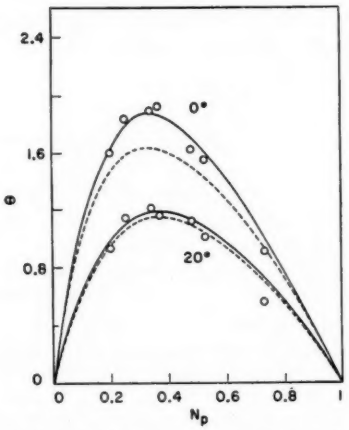

FIG. 4. Per cent volume contraction of mixtures of heavy water and deuterium peroxide at 0° and 20° C. Broken lines are the corresponding curves for the system H_2O–H_2O_2.

THERMODYNAMIC EXCESS FUNCTIONS

Another measure of the associative properties of solutions is given by the excess functions. These quantities are usually derived from vapor pressures and calorimetric data through the equations

$$F^E = RT \sum N_i \ln \gamma_i, \quad [2]$$

$$TS^E = H^E - F^E, \quad [3]$$

where the γ's are the activity coefficients. Unfortunately no complete set of data is available yet for both properties *at the same temperature.* The latest and most extensive determinations of vapor pressure and vapor composition by Scatchard *et al.* (8) were carried out at 60°, 75°, and 90° C. over a wide concentration range, and at 44.5° and 105° each for equimolar mixtures.* But the heat of mixing has been measured so far only at 0° and 26.9°, and the latter corrected to 25°. For correlation purposes one must either recalculate the H^E to 60°, 75°, and 90° or else extrapolate the vapor-pressure data down to 0° and 25°. The former procedure was deemed less reliable at this stage because it requires accurate knowledge of the heat capacity of the solutions, and the only existing set (1) consists of average values between 0° and 26.9°.

On the other hand extrapolation of the vapor pressures is not without risk. Indeed, in consolidating their results Scatchard *et al.* estimated that their vapor-composition

**However, in a paper presented at the Am. Chem. Soc. meeting in Dallas, April 1956, J. D. Floyd, J. W. Turner, and P. M. Gross, Jr. reported on measurements of vapor pressure and vapor composition of hydrogen peroxide – water mixtures at 25°, 40°, 50°, 60°, and 75° C. over the entire concentration range.*

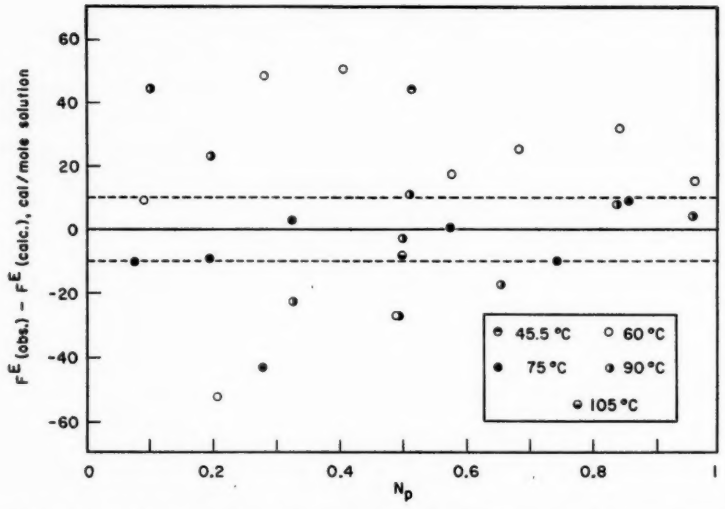

FIG. 5. Deviation of the F^E values based on individual vapor-pressure and vapor-composition measurements of Scatchard *et al.* (8) from their smoothed values obtained through equation [4].

measurements were not accurate enough for calculation of the activity coefficients.* Instead they assumed for the excess free energy an equation of the form

$$[4] \qquad F^E = N_w N_p [B_0(T) + B_1(N_p - N_w) + B_2(N_p - N_w)^2]$$

and obtained the numerical value of the B coefficients by successive graphical and analytical fitting of the experimental vapor pressures to an equation derived from [4] through the excess chemical potentials. Furthermore, in view of the rather narrow temperature range covered they used only one set of coefficients, smoothed with respect to temperature. Therefore, their calculated excess heat and entropy of mixing are temperature independent. The extent of deviation of the former quantity from our own calorimetric determinations at 0° and 26.9° has already been pointed out (Fig. 4 of paper VII). As regards the excess entropy given by their equation

$$[5] \qquad S^E = -0.97 N_p (1 - N_p)$$

it is necessarily symmetrical with respect to concentration about the middle value $N_p = 0.5$ as shown by the broken line in Fig. 6. This is to be compared with the excess-entropy curves based on our calorimetric data for 0° and 25°. Not only are they markedly unsymmetrical, but the entropy term becomes positive at 0° for dilute solutions ($N_p < 0.2$). One might be tempted to relate this feature to some property of the pure components, like the density anomaly of liquid water near the melting point. However, such inferences must be viewed with caution considering the present status of experimental evidence. Because the entropy term is obtained as the difference between two large quantities [3], even its sign in that concentration range remains uncertain pending more extensive and more accurate thermal and vapor-pressure measurements. Considerable effort will be

**In that connection it is interesting to note that although their equilibrium still was capable of greater accuracy than the static method used before by Giguère and Maass (9) their "experimental" points still show considerable spread (Fig. 5).*

needed to improve significantly over the present data owing to the tendency of hydrogen peroxide to decompose spontaneously.

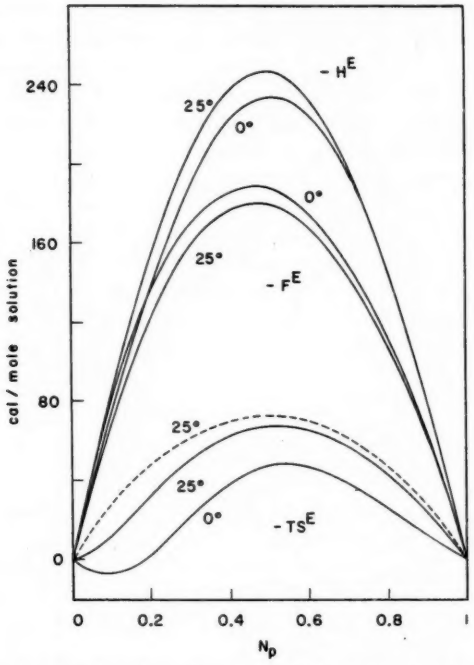

FIG. 6. Thermodynamic excess functions of aqueous solutions of hydrogen peroxide at 0° and 25° C. from calorimetric values of the heat of mixing and extrapolated vapor-pressure data.

CORRELATION OF VOLUME AND THERMODYNAMIC PROPERTIES

The excess volume of mixing is related to the other excess functions through equations

[6] $$V^E = \partial F^E/\partial p = RT \sum N_i(\partial \ln \gamma_i/\partial p)$$

and

[7] $$H^M = RT^2 \sum N_i(\partial \ln \gamma_i/\partial T).$$

Unfortunately certain information, such as the compressibility of peroxide solutions, is lacking for use in these equations, so that some sort of empirical relationship must be resorted to. A priori it seems reasonable to expect that both V^E and H^E are directly related to the number of hydrogen bonds formed on mixing. This is by no means the only factor responsible for the deviations from ideality, as proved by the fact that the curves for these two properties do not coincide. Moreover, instances are known of strongly associated binary mixtures for which the two excess quantities have opposite signs (10). However, in the present case the two are negative at all concentrations, suggesting that the assumption of proportionality to hydrogen-bond formation is tenable. Existence of such a relationship may be illustrated by plotting against composition the differences between the experimental values at 0° and at 26.9° for the three excess functions H^E, θ, and V^E, all normalized to C^E_p. Since all the points fall closely

on the same curve (Fig. 7) whatever factors, besides the number of extra hydrogen bonds formed in that temperature interval, may be responsible for the non-ideal behavior, they must affect equally the thermal and the volume excess functions of the peroxide solutions. Whether the excess heat capacity corresponds to the same modes as in the pure components cannot be decided because of the complexity of this binary system.

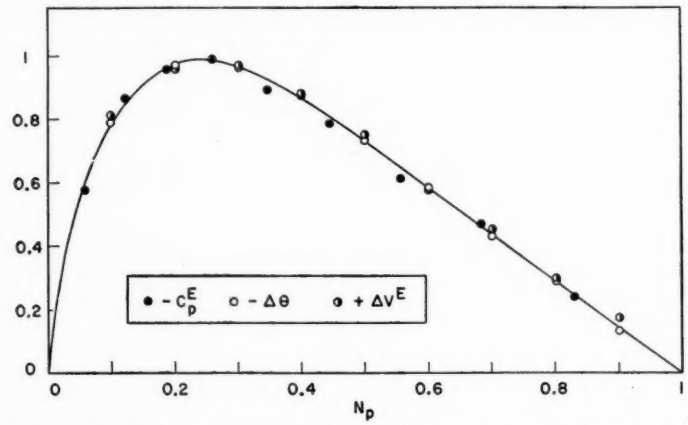

FIG. 7. Normalized values of the difference in $H^E = C_p{}^E \Delta T$, θ and V^E taken between 0° and 26.9° C.

The normalizing factor employed above in converting θ to $C^E{}_p$ may be used in turn to obtain a set of values for H^E from θ at various temperatures relative to its value at 26.9°. Obviously this procedure is open to criticism as it stands or falls with the relative

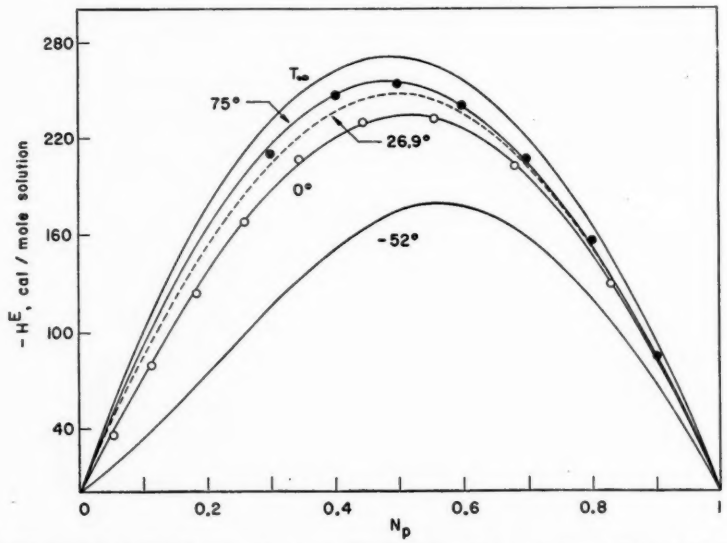

FIG. 8. Heats of mixing of water and hydrogen peroxide from the correlation of H^E and V^E. The experimental points for 75° are taken from Scatchard *et al.* (8), those at 0° from Ref. (1).

constancy of the average C^E_p at higher temperatures. Nevertheless, a fair agreement is obtained (Fig. 8) with the calculated H^E of Scatchard *et al.*, for 75°, their most favorable temperature. Actually the agreement is not too surprising since the excess heat of mixing is not particularly sensitive to temperature. Extension of the calculation to the high-temperature (T_∞) and the low-temperature limits (−52°, the melting point of the solid hydrate) gives an idea of the extent of variation of H^E.

Next to the number of extra hydrogen bonds, the most important factor should be the relative strength of such bonds between unlike molecules. The two factors are by no means equivalent, the former being essentially of a configurational nature. Indeed, a peroxide molecule with one site engaged in hydrogen bonding still has five other sites available for potential bond formation: either three acceptors and two donors or four acceptors and one donor. A water molecule in similar circumstances has only three sites available. Thus addition of hydrogen peroxide to water may have a cementing effect on the open, fragmentary ice structure which persists in the liquid above its melting point. This is borne out by the large effect of hydrogen peroxide in lowering the temperature of maximum density of water, as already pointed out (11), in contrast with the behavior of alcohols (Fig. 9).

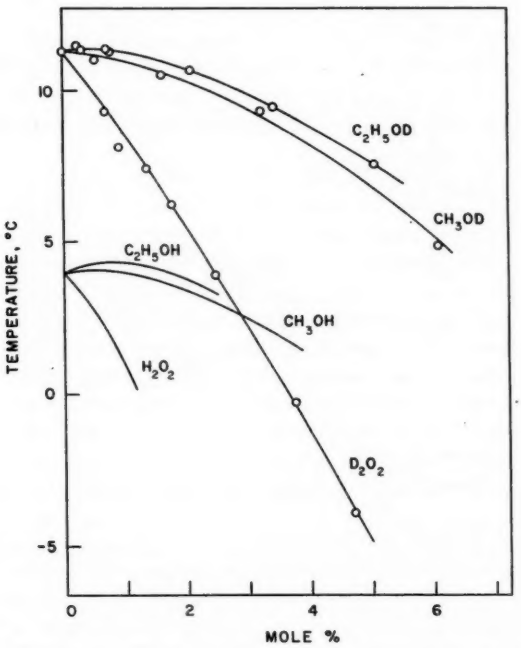

FIG. 9. Effect of different solutes on the temperatures of maximum density of water and heavy water. The curves for water are from Ref. (11).

As regards the strength of hydrogen bonds in the solutions relative to those in the pure components, the experimental evidence is meager and inconclusive. Bain (12) observed a slight shift of the O—H stretching fundamentals in the infrared spectra of peroxide solutions but he did not investigate its dependence on composition. In the

Raman spectra Taylor and Cross (13) detected a shoulder on the low-frequency side of the O—H stretching bands whose intensity increased with peroxide concentration up to a distinct maximum in the range $N_p = 0.2$ to 0.4 at $-40°$ C. At room temperature the intensity increased likewise but did not reach a maximum. The same authors also observed a concentration-dependent shift towards higher frequencies of the bending vibration ν_2 of both the water and hydrogen peroxide molecules. A systematic infrared study of these mixtures in the solid state at low temperatures (14) has confirmed these results and revealed, in addition, a number of extra bands in the low-frequency region with maximum intensity at about $N_p = 0.3$. It has been concluded (13) that an increase in the number of hydrogen bonds on mixing must be responsible for the above shifts of the bending modes towards higher frequencies, this being the experience also with other liquids. However, it is practically impossible with these methods to differentiate between varying hydrogen-bond strength and number of bonds. Refined X-ray diffraction techniques coupled with nuclear magnetic resonance investigations of the hydrate should provide useful structural data to supplement the thermodynamic arguments.

The maxima in the V^E of θ curves (Fig. 1) are obviously related in some way to the existence of the crystalline hydrate $H_2O_2.2H_2O$. In view of the presumably three-dimensional structural network and the low stability of the solid, the latter confirmed by the shape of the liquidus curve, it may not be appropriate to speak of persistence of the hydrate in the liquid above its melting point. It seems certain, however, that the packing and bonding factors are particularly favorable in liquid mixtures of water and hydrogen peroxide at N_p close to 1/3, so that optimum association ensues. The distinction between the two ways of stating the situation is mainly a matter of wording.

THE CRYSTALLINE HYDRATE

Knowledge of the structure of the solid hydrate would be valuable for interpreting the excess properties of the liquid mixtures. Unfortunately very little is known about it. Natta and Rigamonti (15) obtained an X-ray powder diffraction photograph of the solid and concluded that it had a lattice of low symmetry. The suggestion that the tetragonal symmetry of pure hydrogen peroxide degenerates progressively into monoclinic on addition of water (16) is unsubstantiated. The symmetry degeneration would entail formation of solid solutions contrary to definite experimental evidence (17). The same conclusion was already reached by Natta and Rigamonti, who failed to observe any shift in the positions of the peroxide lines in X-ray diffraction photographs of solid hydrogen peroxide containing 10 and 18% water. The extra features appearing on addition of water were assigned by them to the presence of the solid hydrate as a separate phase.

It is not difficult to visualize for that hydrate a highly organized structure which might be related to molecular aggregates of short lifetime existing in the liquid at low temperatures, and responsible for local density increases. The only requirement is the maximum engagement of the available donor and acceptor sites in hydrogen bonding. There is a total of six donor and eight acceptor sites per "molecule" of the compound, the water molecules contributing four of each kind and the peroxide molecule, two donors and four acceptors. With maximum possible engagement there will always remain two vacant acceptor sites.

The structure that we suggest here (Figs. 10 and 11) is based on the following assumptions: the unengaged acceptor sites are located on the peroxide oxygens; each peroxide molecule is surrounded by four water molecules; each water molecule is surrounded by

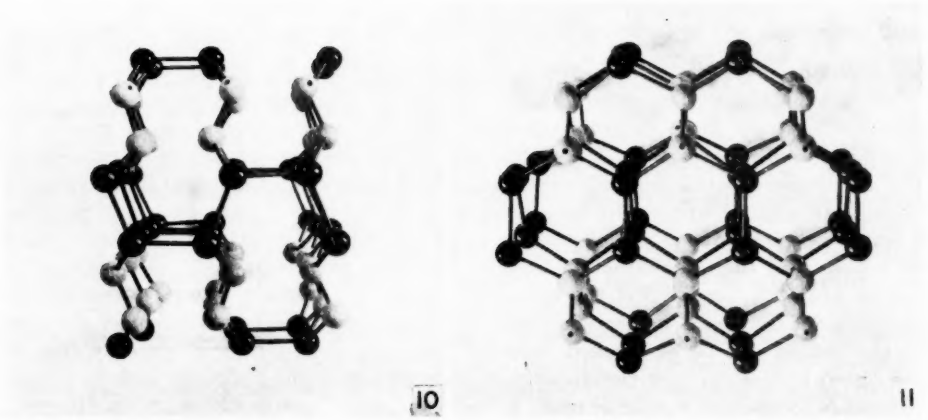

FIG. 10. Possible structure of the crystalline hydrate $H_2O_2.2H_2O$ viewed along the rows of peroxide molecules. (White balls, peroxide oxygens; black balls, water oxygens; hydrogen atoms not shown.)
FIG. 11. Same structure as in Fig. 10 viewed in a direction normal to the puckered water–peroxide sheets.

two water and two peroxide molecules; all hydrogen bonds are linear and of equal length; all bond angles are tetrahedral. The resulting structure is of orthorhombic symmetry with two $H_2O_2.2H_2O$ "molecules" per unit cell. Assuming 2.8 Å for the length of the hydrogen bond and 1.5 Å for the O–O distance in the peroxide molecule, the calculated density turns out to be close to the value 1.20 indicated in preliminary measurements at the melting point of the hydrate, −52° C. The structure can, in fact, be looked upon as an extreme case of the substitution process proposed by Abrahams, Collin, and Lipscomb (16). Alternate molecules in the infinite chains of pure peroxide are replaced by pairs of water molecules of appropriate orientations. The original helical peroxide chains are transformed into puckered sheets of water and peroxide molecules held in parallel stacks through hydrogen bonds normal to the sheets.

Although we assumed tetrahedral angles, this is not a necessary requirement. Even with bond angles close to their values in the free molecules the symmetry of the lattice could be preserved and the distortion would be slight. In fact, the distance between the unengaged acceptor sites of nearest peroxide oxygens would then become slightly larger than 2.8 Å, which is perhaps nearer the expected separation. Bond angle distortion in a peroxide molecule can easily take place through twisting about the O–O bond. Indeed, spectroscopic evidence indicates that the restoring force for that deformation is rather small (4); also, a recent infrared investigation of the crystalline dihydrate at low temperature leads to the conclusion that the peroxide molecule is somewhat distorted in that compound (14).

There are other ways in which the hydrogen bonds in solid $H_2O_2.2H_2O$ can be arranged into three-dimensional networks similar to the one just described. The oxygen atoms of some of such structures are roughly in the same relationship to each other as the silicon atoms in β-tridymite to those of β-cristobalite. They are all structures of equal or almost equal density, and probably also of very similar lattice energies. The similarity might account for the strong association in aqueous solutions of hydrogen peroxide, since aggregates of high local density may be formed in several, more or less equivalent ways.

COMPARISON OF THE HYDROGEN AND DEUTERIUM SYSTEMS

The pair of binary systems H_2O–H_2O_2 and D_2O–D_2O_2 offer a particularly favorable situation for investigating the effects of isotopic substitution on the thermodynamic properties of highly associated liquids. Obviously, one cannot expect any detailed information from mere determinations of bulk properties. Comparative studies of hydrogen-bonded crystals by Ubbelohde and his co-workers (18–20) have established that deuterium substitution leads to a measurable lengthening of the short bonds (shorter than about 2.65 Å) whereas for longer bonds, as in the present case, the effect is either a small contraction or is not observable at all. No such observations have been made on liquids, but the same situation may be presumed to obtain.

It is generally agreed that the zero-point energy is the main factor responsible for bond-energy difference in isotopic compounds, although the contribution of thermal energy should not be overlooked entirely. Since the extent of hydrogen bonding in associated liquids varies with temperature, comparison of the hydrogen and deuterium systems of compounds should be made at the appropriate "corresponding temperatures". We may illustrate this point by considering the effect of deuterium substitution on the temperature of maximum density of liquid water. In D_2O the temperature interval between the melting point and the maximum density (3.8° to 11.2° C.) is nearly double that for H_2O (0° to 4.1°). This anomaly in both liquids is due to persistence above the melting point of some of the residual "open structure" of ice, a structure resulting from the strongly directional character of the hydrogen bonds. Bending of these bonds is achieved mainly through rocking or "libration" of the individual water molecules about their center of gravity. Since the moments of inertia of D_2O are roughly double (1.90 times) those of H_2O, the thermal energy required for the process should therefore be double, as observed. The amount of residual ice structure must be approximately the same in water at 4.1° and in heavy water at 11.2°. This is in agreement with our observations on the effect of deuterium peroxide and deuterated alcohols on the temperature of maximum density of heavy water. As may be seen in Fig. 9 the curves for the various isotopic pairs are nearly parallel.

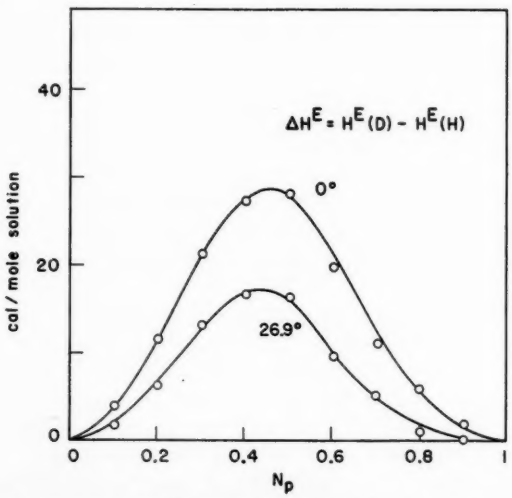

FIG. 12. Differences in the heats of mixing of the isotopic water–peroxide mixtures.

For the pure components comparison of the melting point (21), heat capacity, and heat of vaporization (1) denotes a slightly greater association of the deuterium compounds. By simple analogy we would expect correspondingly higher values of the excess functions of mixing for the deuterium system, and this is true of C^E_p and V^E. Quite unexpectedly, however, this trend is reversed in the case of H^E, the values for the deuterium compounds being significantly smaller (by nearly 10% at 25°) than for the hydrogen compounds (Fig. 12). If a temperature correction is applied to bring the two systems to the same "corresponding residual-structure states" as suggested above, namely by raising the temperature of the D_2O–D_2O_2 system by some 7°, then the two V^E curves (Fig. 4) are brought into near coincidence and the difference at the maximum in the two H^E curves is reduced by about one-third. The rest might be interpreted as an indication of weakening of the hydrogen bond on deuterium substitution. Before a more precise appraisal of the relative importance of the configurational and the other factors involved can be achieved more experimental data will be necessary, in particular on the temperature dependence of the heat capacity of the two isotopic systems. We are planning to complete such measurements at a variety of temperatures over the range 0° to 75° at all concentrations.

ACKNOWLEDGMENTS

We are indebted to the National Research Council for financial assistance, to the Shawinigan Chemical Co. for a fellowship, and to Dr. L. C. Leitch for the gift of samples of deuterated alcohols.

RÉSUMÉ

A partir de données récentes sur les propriétés volumiques et thermiques des solutions de peroxyde d'hydrogène et d'eau on a calculé les fonctions d'excès de ce système binaire. On a repris les mesures de densité des solutions de péroxyde de deutérium et d'eau lourde et on a étudié l'effet de divers composés deutérés sur la température de densité maximum de l'eau lourde. De cette étude il appert que les molécules de peroxyde d'hydrogène s'insèrent facilement dans la structure de l'eau et disloquent les traces de réseau cristallin qui y persistent encore au-dessus du point de fusion.

On propose une structure cristalline pour le composé $H_2O_2.2H_2O$.

REFERENCES

1. GIGUÈRE, P. A., MORISSETTE, B. G., OLMOS, A. W., and KNOP, O. Can. J. Chem. **33**, 804 (1955).
2. JESSUP, R. S. J. Research Natl. Bur. Standards, **55**, 317 (1955).
3. GIGUÈRE, P. A., MORISSETTE, B. G., and OLMOS, A. W. Can. J. Chem. **33**, 657 (1955).
4. SCHUMB, W. C., SATTERFIELD, C. N., and WENTWORTH, R. L. Hydrogen peroxide. Reinhold Publishing Corp., New York. 1955.
5. GIGUÈRE, P. A. and GEOFFRION, P. Can. J. Research, B, **28**, 599 (1950).
6. VOZNESENSKAJA, O. M. and ZASLAVSKIJ, I. I. J. Gen. Chem. U.S.S.R. **16**, 1189 (1946).
7. PHIBBS, M. K. and GIGUÈRE, P. A. Can. J. Chem. **29**, 173 (1951).
8. SCATCHARD, G., KAVANAGH, G. M., and TICKNOR, L. B. J. Am. Chem. Soc. **74**, 3715 (1952).
9. GIGUÈRE, P. A. and MAASS, O. Can. J. Research, B, **18**, 181 (1940).
10. FREDENHAGEN, K. Grundlagen für den Aufbau einer Theorie der Zweistoffsysteme. Akademie-Verlag, Berlin. 1950.
11. MITCHELL, A. G. and WYNNE-JONES, W. F. K. Discussions Faraday Soc. No. **15**, 161 (1953).
12. BAIN, O. Ph. D. Thesis, Laval University, Quebec, Que. 1953.
13. TAYLOR, R. C. and CROSS, P. C. J. Chem. Phys. **24**, 41 (1956).
14. HARVEY, K. B. Ph. D. Thesis, Laval University, Quebec, Que. 1956.
15. NATTA, G. and RIGAMONTI, R. Gazz. chim. ital. **66**, 762 (1936).
16. ABRAHAMS, S. C., COLLIN, R. L., and LIPSCOMB, W. N. Acta Cryst. **4**, 15 (1951).
17. FOLEY, W. T. and GIGUÈRE, P. A. Can. J. Chem. **29**, 123 (1951).
18. GALLAGHER, K. J., UBBELOHDE, A. R., and WOODWARD, I. Proc. Roy. Soc. (London), A, **222**, 195 (1954).
19. UBBELOHDE, A. R. and GALLAGHER, K. J. Acta Cryst. **8**, 71 (1955).
20. GALLAGHER, K. J., UBBELOHDE, A. R., and WOODWARD, I. Acta Cryst. **8**, 561 (1955).
21. GIGUÈRE, P. A. and SECCO, E. A. Can. J. Chem. **32**, 550 (1954).

INFLUENCE OF CALCIUM IONS ON THE MYOSIN-CATALYZED HYDROLYSIS OF ADENOSINE TRIPHOSPHATE[1]

G. E. Pelletier and Ludovic Ouellet

ABSTRACT

The activation of the myosin-catalyzed hydrolysis of adenosine triphosphate by calcium ions has been studied at pH 7.5 over a range of temperature extending from 3° to 25° C. There is evidence that the activation is due to the equilibrium formation of a complex between adenosine triphosphate and calcium ions.

From such a reaction mechanism, values of equilibrium constants are reported for the binding of adenosine triphosphate to the myosin in the presence and in the absence of calcium ions, together with stability constants for the calcium complexes of both the adenosine triphosphate and the myosin – adenosine triphosphate. The influence of hydrogen-ion concentrations on these constants is indicated.

INTRODUCTION

In the presence of myosin, a muscle protein, adenosine triphosphate (ATP) is hydrolyzed to adenosine diphosphate (ADP) and inorganic phosphate. This reaction has already been studied and related to the process of muscular contraction by Szent-Gyorgyi (1) and Engelhardt and Liubimova (2).

Various aspects of the kinetics of this reaction have been reported by Mommaerts (3, 4) including the influence of pH, magnesium, and ADP on the rate of the reaction at 27° C.

The influence of temperature on both the over-all rate and the enzyme substrate interaction constant has been reported previously (5). Pressure and ionic strength effects were studied by Laidler and Beardell (6).

This paper reports on the activation of the reaction by calcium ions at pH 7.5 over a range of temperatures. The reaction is interesting from this particular point of view as it proceeds both in the presence and in the absence of calcium ions (4).

Treatment of the Data

In the formation of enzyme–substrate–modifier complexes, the modifier (activator or inhibitor) is usually treated as being bound to an enzyme active site. If instead the modifier were bound in the complex to the substrate only, a general reaction mechanism for such a system could be represented by the following equations:

$$[1] \qquad S + M \overset{K_1}{\rightleftharpoons} SM,$$

$$[2] \qquad E + S \overset{K_2}{\rightleftharpoons} ES \overset{k_0}{\rightarrow} E + \text{Products},$$

$$[3] \qquad E + SM \overset{K_3}{\rightleftharpoons} ESM,$$

$$[4] \qquad ES + M \overset{K_4}{\rightleftharpoons} ESM \overset{k_r}{\rightarrow} E + \text{Products}.$$

In this scheme S is a substrate molecule, E and M are enzyme and modifier molecules that form with S the binary complexes ES and SM, and the ternary complex ESM. Only the complexes ES and ESM dissociate into products. The rate constants k_0 and

[1]*Manuscript received January 29, 1958.*
Contribution from the Department of Chemistry, University of Ottawa, Ottawa, Canada. Grateful acknowledgment is made to the National Research Council of Canada for financial assistance.

k_r are first-order rate constants for the breakdown of ES and ESM into enzyme and products of the reaction. All other constants are considered to be equilibrium constants.

The rapid equilibrium hypothesis yields an expression which is adequate to describe the experimental results in the kinetic behavior of the myosin – ATP – calcium ions system. As pointed out by Schwert (7), this observation does not eliminate the possibility that steady-state conditions prevail. Evidence along these lines arises from other considerations (8).

Under equilibrium conditions the rate of formation of products v in the above system can be written as

$$[5] \qquad v = \frac{k_r[E]_0}{1+(1/K_2K_4[M][S])+(1/K_4[M])} + \frac{k_0[E]_0}{1+(1/K_2[S])+K_4[M]}.$$

The different equilibrium constants can be evaluated through a proper choice of experimental conditions.

If $[M] = 0$ or $K_4[M] \gg 1$, equation [5] reduces to well-known Michaelis–Menten equations (9). K_2 and K_3 can then be obtained from plots of $1/v$ against $1/[S]$ (10).

If $K_2[S] \gg 1$ the equation can be rearranged to

$$[6] \qquad v-v_0 = \frac{(k_r-k_0)[E]_0}{1+(1/K_4[M])}$$

where $v_0 = k_0[E]_0$. In this case a plot of $1/(v-v_0)$ against $1/[M]$ gives K_4.

K_1 can be obtained from the thermodynamic relation

$$[7] \qquad K_1K_3 = K_2K_4.$$

If specific binding of the modifier on the enzyme did occur, equation [1] would become

$$[8] \qquad E + M \overset{K_1'}{\rightleftharpoons} EM$$

and equation [3],

$$[9] \qquad EM + S \overset{K_3'}{\rightleftharpoons} EMS.$$

Assuming equilibrium conditions, a simple expression can be derived for a system involving equations [8], [9], [2], and [4] (11). Although the expression obtained is different from equation [5], it reduces to simple Michaelis–Menten relations for both $[M] = 0$ and $K_4[M] \gg 1$, and to equation [6] for the cases where $K_2[S]$ or $K_3[S] \gg 1$. The interpretation of the constants is of course different. Evidence for the first mechanism proposed will be presented later in this paper.

EXPERIMENTAL PART

Reagents

The dipotassium salt of adenosine triphosphate (Pabst Laboratories, Milwaukee, Wis.) was used throughout these experiments. Tris(hydroxymethyl)aminomethane (THAM) (Fisher purified grade) and potassium chloride (Fisher certified reagent) were recrystallized from glass-distilled water. Calcium chloride was a certified reagent (Fisher). Acetic acid was Merck reagent grade.

Rabbit back-muscle myosin of the Weber-Edsall type was prepared according to a procedure described by Botts and Morales (12). Myosin concentrations were determined by a micro-Kjeldahl nitrogen-determination method. The myosin had a specific activity

of 5.1×10^{-6} moles of ATP hydrolyzed per second per gram of protein, at pH 7.5, in 0.6 *M* potassium chloride and 0.01 *M* calcium chloride, at 25° C.

Procedure

All reactions were carried out in buffered solutions containing 0.6 mole of potassium chloride and 0.1 mole of THAM per liter adjusted at the proper pH with acetic acid using a Beckman model G pH meter. These buffers were so adjusted at a series of temperatures, since the pH of THAM-buffered solutions varies considerably with temperature.

The solutions were kept in a constant-temperature bath (±0.1° C.) for 15 minutes, then mixed. At measured intervals of time, samples were pipetted into equal volumes of 20% trichloroacetic acid, thus precipitating the myosin which was removed by filtration through a dry filter paper. Phosphate concentrations in the filtrate were determined colorimetrically by the Fiske – Subba Row method (13), using a model DU Beckman spectrophotometer.

The rate of the reaction was measured as the number of moles of inorganic orthophosphate produced per liter per second.

RESULTS AND DISCUSSION

At constant concentration of myosin, in the presence of 5×10^{-4} moles per liter of ATP, the rate was found to increase with the concentration of calcium chloride according to equation [6]. At concentrations of calcium chloride higher than 0.01 *M* an already reported (4) lowering of the rate has been observed. Fig. 1 shows the results of a series of experiments at pH 7.5 and three temperatures. For the determination of the constants, the rates at zero concentration of calcium ion v_0 were subtracted from the rates obtained in the presence of calcium ions v, and the reciprocal of these values was plotted against the reciprocal of the calcium-ion concentrations. From these plots values for the constant K_4 for the binding of the calcium ions on the myosin–ATP complex were determined for each temperature. The apparent heat of reactions, $-\mathrm{R}\ d\ln K_4/d(1/T)$, was −3.5 kcal. per mole of calcium ions. The change in entropy was +3.0 e.u.

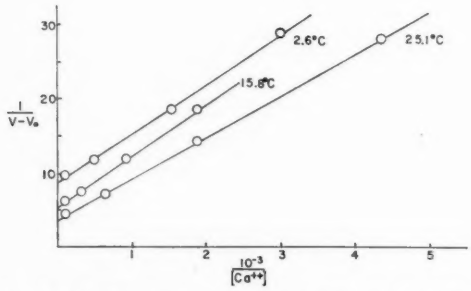

FIG. 1. Determination of K_4 in liters per mole by plotting $1/(v-v_0)$ against the reciprocal of the calcium-ion concentration in moles per liter at pH 7.5.

The pH of the solution had little effect on this constant. At 25° C. in the presence of 0.75 g. of myosin per liter K_4 was found to be 7.5×10^2 liters per mole at pH 7.5 and 8.0×10^2 liters per mole at pH 8.5. These values are consistent with data reported by Green and Mommaerts (4).

There is some evidence that the values of the experimentally determined constants

depend on the concentration of enzyme. Fig. 2 shows the effect of the enzyme concentration on the constant K_4 at 25° C. Assuming that the only effect of the enzyme is to decrease somewhat the concentration of the calcium ion in solution by non-specific binding, extrapolation to zero concentration of enzyme should give the constant K_4 independent of enzyme concentration. The extrapolated value of K_4 at 25° C. is approximately 1.5×10^3 liters per mole.

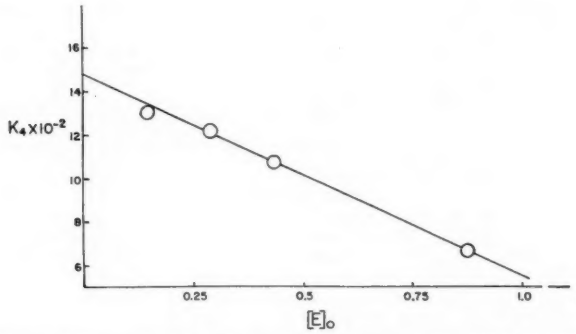

FIG. 2. Variation of the constant K_4 with enzyme concentration at 25° C. [ATP] = 5×10^{-4} M at pH 7.5.

It is interesting to note at this point that the stability constant of ATP Ca^{-2} is given by Smith and Alberty (14) as 1970 ± 280 at 25° C. and an ionic strength of 0.2. The agreement between this value and the above extrapolated value of K_4, although it could be a pure coincidence, supports the assumption made at the beginning of this paper that the activator calcium ion is bound to the ATP molecule in the ternary myosin–ATP–calcium complex. This would not of course exclude non-specific binding of calcium ions on the protein. The variation of K_4 with enzyme concentration would indeed suggest that calcium ions are bound to a considerable extent on the protein.

The constants K_2 and K_3 for the formation of the enzyme–substrate complex in the absence and in the presence of calcium ions were determined at pH 7.5 over a range of temperatures. Fig. 3 shows the results of these experiments as log K against $1/T$. The data from this figure suggest $\Delta H = +9$ kcal. per mole and $\Delta S^\circ = 50$ e.u. The presence of calcium ions apparently does not affect to any great extent the binding of ATP on myosin. The interpretation of the above enthalpy and entropy values is complicated by contributions from hydrogen-ion concentration effects. Raising the pH from 7.0 to 9.3 lowers the value for the constant K_3 from 9.2×10^4 to 1.2×10^4 liters per mole at 25° C. (Fig. 4). A detailed description of K_3 as a function of hydrogen-ion concentration is made difficult by the fact that at high pH the enzyme is deactivated rapidly as shown by a sharp drop in the activity–pH curve around pH 9.5.

From equation [7] and the fact that $K_2 \cong K_3$, one finds that $K_1 \cong K_4$. This would imply that the calcium ion is bound just as readily to the substrate in the enzyme–substrate complex as it is to the substrate alone. As in the case of K_4 the value obtained for the constant K_1 is very close to that reported for the ATP calcium-ion stability constant (14). In an ATP – calcium ion system, there exists independently of any mechanism an equilibrium between the ATP–calcium complex and the ATP and calcium ions. The fact that this equilibrium constant has within experimental error the same value as the constant obtained in these experiments for K_1 supports the idea that K_1

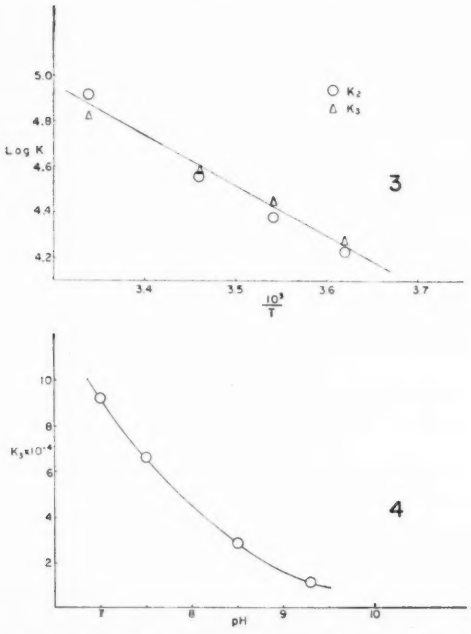

FIG. 3. Variation of the equilibrium constants for the formation of the myosin–ATP complex in the absence of calcium ions (○) and in 0.01 *M* calcium chloride solution (△).
FIG. 4. Influence of the pH on K_3 at 25° C.

actually is the equilibrium constant for the binding of calcium ions on ATP rather than the equilibrium constant for the binding of calcium ions on myosin. On the other hand, this might not be unequivocal evidence for the mechanism suggested here. As pointed out previously, the present treatment of data (equation [6]) would still describe the system if the calcium ions were bound to the active site of the enzyme.

As the variation of K_2 with temperature follows that of K_3, K_1 includes the same thermodynamic quantities as K_4, that is $\Delta H = -3.5$ kcal. per mole, $\Delta S° = +3$ e.u. These values are quite different from those reported by Smith and Alberty (14) for orthophosphate, where the formation of the calcium phosphate complex is mostly due to an increase of entropy. The behavior of ATP towards calcium ions however could be somewhat different from that of orthophosphate.

CONCLUSION

The data presented in this paper are consistent with the suggestion that the activation of the myosin-catalyzed hydrolysis of ATP by calcium ions is due to the formation of an ATP–calcium complex. The formation of such a complex would be slightly exothermic and accompanied by a small increase in entropy.

RÉSUMÉ

L'influence de la concentration des ions calcium sur le taux d'hydrolyse de l'adénosine triphosphate à été étudiée à des températures allant de 3° à 25° C. Il existe des indications que l'"activation" du système dépend de la formation d'un complexe ATP–calcium, en

état d'équilibre. Utilisant ce mécanisme, on a déterminé des constantes d'équilibre se rapportant à la formation du complexe myosine–ATP en la présence et en l'absence d'ions calcium, de même que les constantes de formation à l'équilibre des complexes des ions calcium avec l'adénosine triphosphate et l'intermédiaire myosine – adénosine triphosphate. L'influence de la concentration des ions hydrogène est mentionnée.

REFERENCES

1. SZENT-GYORGYI, A. Chemistry of muscular contraction. Academic Press, Inc., New York. 1951.
2. ENGELHARDT, V. A. and LIUBIMOVA, M. N. Nature, **144**, 668 (1939).
3. GREEN, I. and MOMMAERTS, W. F. H. M. J. Biol. Chem. **208**, 833 (1954).
4. GREEN, I. and MOMMAERTS, W. F. H. M. J. Biol. Chem. **202**, 541 (1953).
5. OUELLET, L., LAIDLER, K. J., and MORALES, M. F. Arch. Biochem. and Biophys. **39**, 37 (1952).
6. LAIDLER, K. J. and BEARDELL, A. J. Arch. Biochem. and Biophys. **55**, 138 (1955).
7. SCHWERT, G. W. Federation Proc. **13**, 971 (1954.)
8. LAIDLER, K. J. Discussions Faraday Soc. **20**, 83 (1955).
9. MICHAELIS, L. and MENTEN, M. L. Biochem. Z. **49**, 333 (1913).
10. LINEWEAVER, J. and BURK, D. J. Am. Chem. Soc. **56**, 658 (1934).
11. ALBERTY, R. A. J. Am. Chem. Soc. **75**, 1928 (1953).
12. BOTTS, J. and MORALES, M. F. J. Cellular Comp. Physiol. **37**, 27 (1951).
13. FISKE, C. H. and SUBBA ROW, J. J. Biol. Chem. **81**, 629 (1929).
14. SMITH, R. M. and ALBERTY, R. A. J. Am. Chem. Soc. **78**, 2376 (1956).

LYCODINE, A NEW ALKALOID OF LYCOPODIUM ANNOTINUM[1]

F. A. L. Anet and C. R. Eves

ABSTRACT

A new alkaloid, lycodine, $C_{17}H_{24}N_2$, m.p. 118°, has been isolated from *Lycopodium annotinum*. Lycodine is a tetracyclic diacidic base containing a secondary nitrogen atom, a 2,3-disubstituted pyridine ring, and a C-methyl group. The 2,3-disubstitution is in the form of a saturated six-membered ring.

The alkaloids of *Lycopodium annotinum* L. have been studied by several groups of workers in Canada and in Europe (1, 2, 3, 4, 5). The structure of annotinine, $C_{16}H_{21}O_3N$, which is the main alkaloid of this species, is now known (6, 7) and is of a quite novel type. It therefore becomes of interest to study the chemical structure of the minor alkaloids of this plant.

During the process of developing suitable methods for the separation of the many minor alkaloids which have been reported to occur in this *Lycopodium* species, we noticed that certain fractions possessed ultraviolet absorption characteristic of a pyridine chromophore, more or less submerged behind general absorption. This paper describes the isolation, characterization, and partial determination of the structure of a new alkaloid, lycodine, which was responsible for this characteristic absorption.

Lycodine was concentrated by countercurrent distribution of the alkaloid mother liquors from the crystallization of annotinine. Two successive countercurrent distributions were carried out, first in six large separatory funnels with the system chloroform–buffer of pH 6 and then in a 60-tube Craig machine with the system chloroform–buffer of pH 5.2. From these countercurrent distributions an alkaloid fraction was obtained which had the correct ultraviolet absorption. By chromatography of this fraction on activated alumina pure crystalline lycodine was obtained.

Lycodine, m.p. 118°, $[\alpha]_D$ −10°, had the formula $C_{17}H_{24}N_2$ and gave a characteristic dipicrate, m.p. 229°–233° (decomp.), which was sparingly soluble in methanol. Titration of the base in 50% methanol showed that the pK_a's of the base were 3.97 and 8.08. One C-methyl group was found to be present by the Kuhn–Roth method. The ultraviolet spectra of the base in neutral and in acid solutions are shown in Fig. 1, and correspond to an unconjugated pyridine chromophore in the base and salt forms respectively. A fuller discussion of these spectra will be left till after consideration of other results (see below).

The infrared spectrum of the base (in Nujol) is shown in Fig. 2; the sharp band at 3270 cm.$^{-1}$ must be due to a N—H group (8). As often happens (8) this band is of very low intensity in the spectrum (Fig. 2) of the carbon tetrachloride solution of the compound. The presence of a pyridine ring is confirmed by the band (9) at 1580 cm.$^{-1}$ (in Nujol) and that of a C-methyl group by a band (10) at 1382 cm.$^{-1}$ (in CCl_4). Acetylation of lycodine with acetic anhydride gave a N-acetyl derivative, isolated as the monopicrate. Titration of the picrate showed that the acetylated base had only one basic center (pK_a 4.95). Hydrolysis of N-acetyl lycodine gave back lycodine, thus confirming the presence of a secondary nitrogen atom in the alkaloid.

In order to determine the substitution on the pyridine ring we examined the NMR spectrum (Fig. 3) of lycodine. Under moderately high resolution there are three peaks of

[1]*Manuscript received February 6, 1958.*
Contribution from the Department of Chemistry, University of Ottawa, Ottawa, Canada.

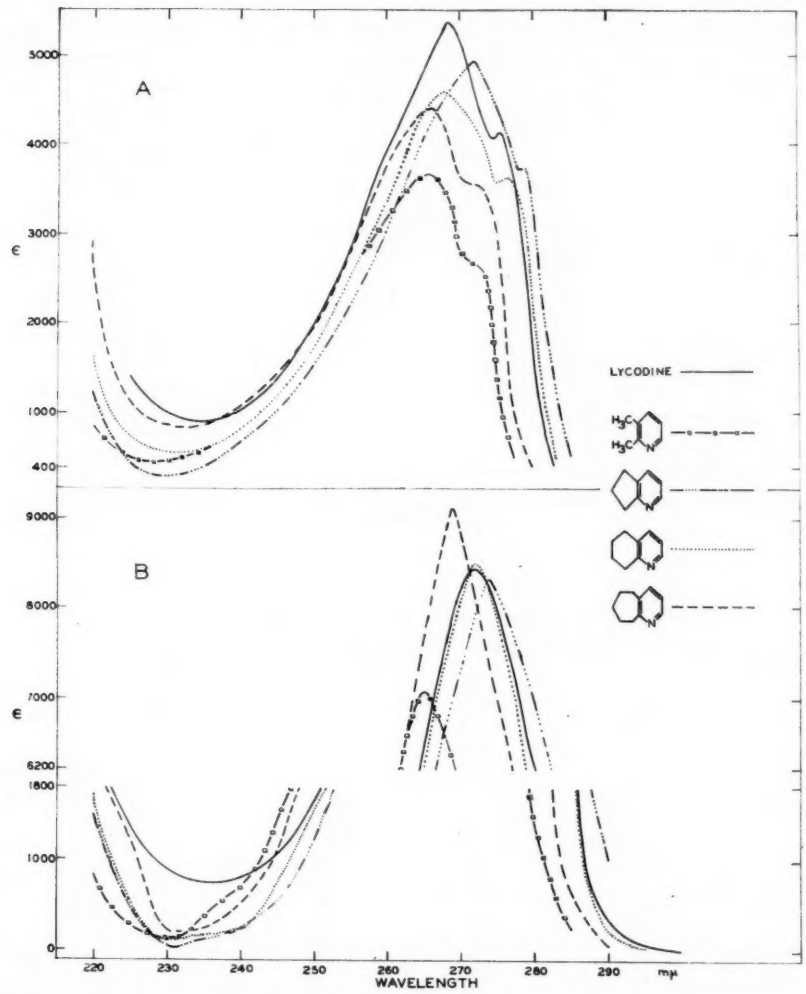

FIG. 1. Comparison of ultraviolet absorption spectra of lycodine and of 2,3-disubstituted pyridines (14). A, free bases; B, salts.

equal area at low field. These are probably due to protons on the pyridine ring (11). The sharp peak at highest field has three times the area of any of the peaks at lowest field and must correspond to the C-methyl group already found. It may be observed that the low value (61% of theoretical) found in the Kuhn–Roth estimation and the fact that the C-methyl peak in the NMR spectrum is unsplit both suggest that the methyl group is attached to a quaternary carbon atom. The other peaks in the spectrum correspond to the remaining protons in the molecule.

The spectrum of the low field part is shown at higher resolution above the main spectrum in Fig. 3. Each peak is split into four peaks, not always very well resolved.

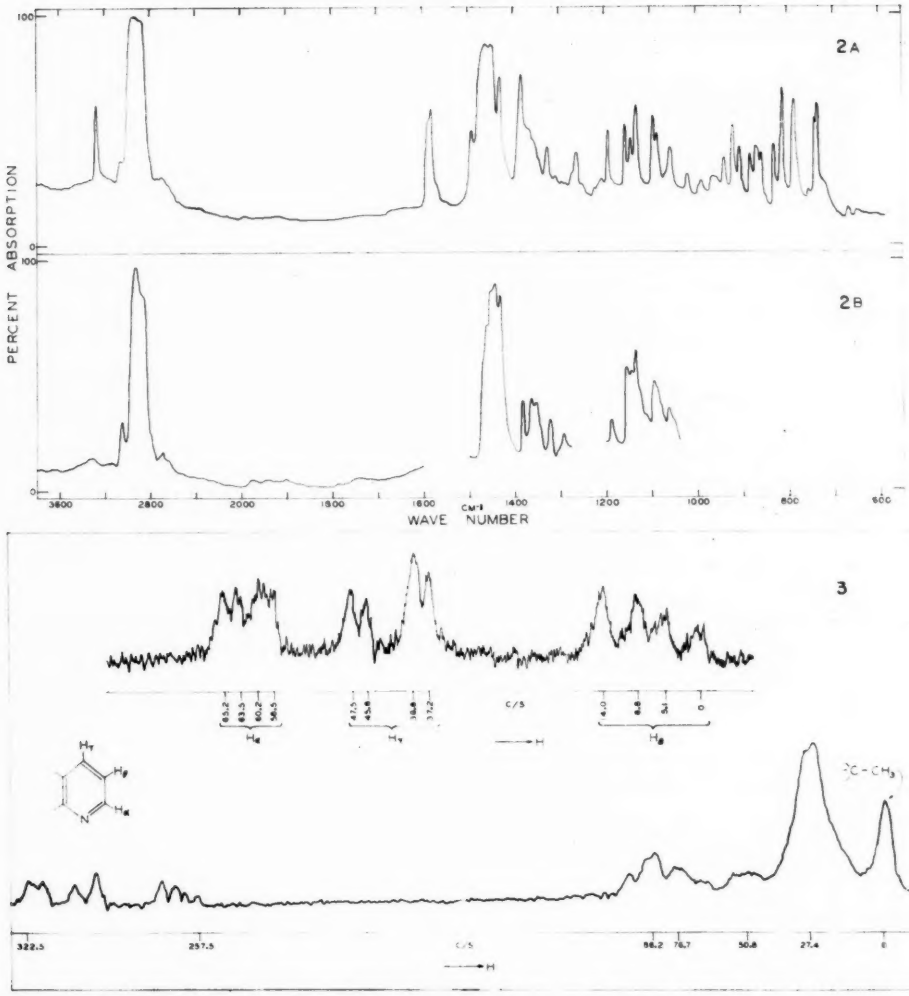

FIG. 2. Infrared absorption spectra of lycodine. A, Nujol mull; B, CCl_4 solution (1 mm. path length, 31 mg. per ml.).

FIG. 3. Nuclear magnetic resonance spectrum of lycodine. The upper curve represents the peaks at left of lower curve at higher resolution.

Bernstein, Pople, and Schneider (11, 12, 13) have recently examined the spectra of pyridine and various substituted pyridines and discussed the effect of chemical shifts and coupling constants on the spectra. From their analysis it can be seen that lycodine must be a 2,3-disubstituted pyridine, and in fact the spectrum of lycodine is very similar to that of 2,3-lutidine except for a difference in the relative chemical shift of the γ proton. The three peaks at low field may be assigned, from left to right, to the α, γ, and β protons of the pyridine ring.

The relative chemical shifts and coupling constants of the pyridine protons of lycodine

compared with those of 2,3-lutidine and pyridine are given in Table I. The observed intensities and energies of the signals from the pyridine protons of lycodine are in satisfactory agreement (Table II) with those calculated from the above parameters by the method of Bernstein, Schneider, and Pople (11). This confirms that the three peaks at low field indeed originate from the protons on the pyridine ring, and not from any other

TABLE I

CHEMICAL SHIFTS AND COUPLING CONSTANTS FOR LYCODINE AND SOME PYRIDINE DERIVATIVES (in c./sec.)

	Lycodine*	2,3-Lutidine† (11)	Pyridine† (13)
Chemical shifts			
$H\beta-H\alpha$	54.6	55.1	60.6
$H\gamma-H\alpha$	20.4	43.4	45.6
$H\gamma-H\beta$	34.2	11.7	15.0
Coupling constants			
$H\alpha.H\beta$	4.6	5.0	5.5
$H\beta.H\gamma$	8.6	7.35	7.5
$H\alpha.H\gamma$	2.3	1.3	1.9

**As a concentrated solution in carbon tetrachloride.*

†As pure liquids. (The effect of carbon tetrachloride on the chemical shift of these spectra is small even at infinite dilution, and is mainly on the α proton (13).)

TABLE II

OBSERVED AND CALCULATED SPECTRA FOR LYCODINE

Line	Origin of transition	Energy (c./sec.)		Relative intensity	
		Calc.	Obs.	Calc.	Obs.
1	β	0	0	0.77	0.65
2	β	5.1	5.1	0.75	0.76
3	β	8.6	8.8	1.23	1.17
4	β	13.8	14.0	1.25	1.41
5	γ	37.0	37.2	1.23	1.24
6	γ	38.5	38.8	1.25	1.54
7	γ	45.8	45.6	0.77	0.69
8	γ	47.3	47.5	0.75	0.89
9	α	58.5	58.5	1	1.85
10	α	60.3	60.2	1	
11	α	63.7	63.5	1	0.83
12	α	65.4	65.2	1	0.96

protons. The reason for the abnormal chemical shift of the γ proton of lycodine may be due to the nearness of the secondary nitrogen atom. Although, as will be shown later (see below), the secondary nitrogen atom is most probably separated from the pyridine ring by more than one carbon atom, it may still be fairly close in space to the γ proton. The abnormal chemical shift is not due to the fact that in lycodine, as will also be shown below, the 2,3-substitution is in the form of a saturated six-membered ring, since 5,6,7,8-tetrahydroquinoline gave a NMR spectrum closely similar to that of 2,3-lutidine.

We may be certain, therefore, of the presence of a 2,3-disubstituted pyridine ring in lycodine. Recently Godar and Mariella (14) have recorded the ultraviolet absorption spectra of 2,3-lutidine, 2,3-trimethylene-, 2,3-tetramethylene-, and 2,3-pentamethylene-pyridine both as free bases and as salts. Their data have been replotted in Fig. 1 using a linear ϵ scale, instead of the original log scale, which facilitates the comparison of these

curves with those of lycodine. It is clear that lycodine shows the greatest similarity to 2,3-tetramethylenepyridine (5,6,7,8-tetrahydroquinoline) and therefore that lycodine has in fact a saturated six-membered ring fused 2,3 to the pyridine ring.

The pK_a's (3.97 and 8.08) of lycodine are appreciably different from those of nicotine (3.35 and 7.70) determined under identical conditions. The difference in pK_a's of the non-pyridine nitrogen atoms may be due to the secondary nature of the nitrogen atom in one case and the tertiary nature in the other. The difference in the pK_a's of the pyridine nitrogen atoms, however, cannot be due to such an effect, but is readily understood if the saturated nitrogen atom is further (i.e. at least β) from the pyridine ring in the case of lycodine than in the case of nicotine.

Lycodine does not seem to contain unsaturation apart from the pyridine ring, as far as is shown by U.V., I.R., and NMR spectra. Therefore lycodine contains four rings, and the facts known about its constitution may be summarized by the following partial structure:

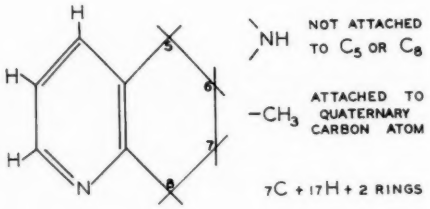

Finally, it may be mentioned that there appears to be a close similarity between lycodine and the *Lycopodium* alkaloid, β-obscurine, $C_{17}H_{24}ON_2$, which has been shown by Marion and Moore (15) to have an α-pyridone chromophore. Although the empirical formula of β-obscurine is correct for it to be the α-pyridone analogue of lycodine, the relationship between the two alkaloids cannot be so simple, for the basic nitrogen atom of β-obscurine appears to be tertiary, as the alkaloid could not be acetylated.

EXPERIMENTAL

Ultraviolet spectra were measured in methanol on a Beckman DK-2 spectrophotometer. Determinations of pK_a values were made by electrometric titrations in 50% aqueous methanol on 10–15-mg. samples. The infrared spectra of Fig. 2 (A) and (B) were measured on a Perkin-Elmer double-beam spectrometer, model 21B, with sodium chloride optics. Other infrared spectra were measured on a Perkin-Elmer single-beam double-pass instrument. The NMR spectra of compounds, as concentrated carbon tetrachloride solutions, were recorded (11) with a Varian V-4300 NMR spectrometer, equipped with field stabilizer, at a fixed frequency of 40 Mc./sec., with spinning sample tubes. Signal separations were measured by the side-band technique in the usual manner.

Isolation of Lycodine

From preliminary countercurrent distribution experiments with buffer of pH 6 and chloroform it was observed that most of the alkaloids have a high partition coefficient (conc. in buffer/conc. in $CHCl_3$) with this system, but that annotinine, lycopodine, acetyl acrifoline (alkaloid L.12), and lycodine have low partition coefficients. Alkaloids with a partition coefficient close to unity are present to only a minor extent in the batches of alkaloids used. Annotine (alkaloid L.11), which has such a partition coefficient (16), is

not present to a significant extent (16) in the crude alkaloid mixture which was available to us. On the basis of the above results the lycodine was concentrated in several stages.

(*a*) *Countercurrent distribution* (*large scale*).—The mother liquors from the crystallization of annotinine (approx. 40 g. of crude alkaloid) were first partitioned by countercurrent distribution between chloroform and concentrated citrate–phosphate buffer, pH 6 (600 ml. in each phase), using six 2-liter separatory funnels. The extraction scheme used was that of Bush and Densen (17). At each transfer the pH of the buffer was checked and corrected to pH 6, if necessary. Of the six chloroform phases (C-1 to C-6) and the six buffer phases (B-1 to B-6) obtained, the four containing lycodine (C-1 to C-4) were mixed and concentrated for the next step. The remaining fractions were retained for the separation of other alkaloids.

(*b*) *Countercurrent distribution* (*Craig machine*).—The chloroform fractions, C-1 to C-4, concentrated to 120 ml., were placed in the initial three tubes (40 ml. each) of a 60-tube Craig countercurrent machine (18) and partitioned through 60 transfers between chloroform and citrate–phosphate buffer, pH 5.2 (40 ml. in each phase). Examination of the fractions by their ultraviolet absorption disclosed the presence of lycodine in tubes 30 to 40. The alkaloids contained in both phases of these 11 tubes were then isolated in the usual manner. Paper chromatography (19) of the material by the descending technique with Whatman No. 1 paper buffered to pH 2.5, with *n*-butanol saturated with water as solvent, showed the presence of alkaloids after spraying with Dragendorff's reagent.

(*c*) *Absorption chromatography on activated alumina.*—The alkaloid mixture (2.6 g.) from tubes 30 to 40 of the Craig machine was then chromatographed on activated alumina, using *n*-pentane–benzene (1:1). The first alkaloid eluted from the column was the known alkaloid, lycopodine, followed by lycodine. A third alkaloid component, as yet uncharacterized, followed lycodine from the column upon elution wth benzene. The fractions containing lycodine were again detected by their ultraviolet absorption and by paper chromatography.

Characterization of Lycodine

Initially, lycodine was isolated as the dipicrate, which crystallized easily from methanol solution in characteristic radiating clusters of prisms, m.p. 229°–233° (decomp.). Calc. for $C_{17}H_{24}N_2.2C_6H_3O_7N_3$: C, 48.74; H, 4.23; N, 15.68%. Found: C, 48.20, 48.47; H, 4.02, 4.03; N, 15.91, 15.64%.

Lycodine dipicrate was converted to the base which was distilled at 100°–110° (air bath) (0.18 mm. Hg) to give a colorless distillate which crystallized spontaneously. The lycodine so obtained has m.p. 118°, $[\alpha]_D$ −10°±2° (*c*, 1.01 in ethanol). Calc. for $C_{17}H_{24}N_2$: C, 79.64; H, 9.43; N, 10.93; C—Me, 5.85%; M.W., 256.4. Found: C, 79.50, 79.46; H, 9.44, 9.38; N, 11.16; C—Me, 3.56%; M.W. (Rast), 246. Titration of lycodine in 50% aqueous methanol gave an equivalent weight of 255.8 (based on the strongly basic nitrogen) and pK_a's, 3.97 and 8.08.

Later, it was found that lycodine could be crystallized from *n*-pentane when seeded. This method was used to crystallize the base from the alumina fractions above, purification of the alkaloid in a number of instances being effected by means of recrystallizations of lycodine dipicrate. In all, about 400 mg. of lycodine was obtained. Attempts to obtain the monopicrate, diperchlorate, dihydrochloride, dihydroiodide, di-*p*-tolulene sulphonate, or the distyphnate in a crystalline state were unsuccessful. From the position of lycodine in the countercurrent distribution mentioned above, the distribution coefficient of the alkaloid in the system chloroform–buffer of pH 5.2 was calculated to be 1.4 (conc. in buffer/conc. in $CHCl_3$).

Acetylation of Lycodine

Lycodine (39.5 mg.) was refluxed in an excess of acetic anhydride under nitrogen for 2 hours. The solution was cooled and methanol added to react with the remaining acetic anhydride. After removal of the methyl acetate by distillation the residue was acidified with 5% hydrochloric acid and washed with ether. The aqueous solution was then made basic with sodium hydroxide solution and extracted with ether to obtain the base. N-Acetyl lycodine was isolated as the monopicrate, which crystallized from water as yellow needles, m.p. 180°–182.5° (decomp.). Calc. for $C_{19}H_{26}ON_2.C_6H_3O_7N_3$: C, 56.92; H, 5.54; N, 13.28%. Found: C, 56.58; H, 5.39; N, 13.69%. The free base was not obtained crystalline. The infrared absorption spectrum (in Nujol) of N-acetyl lycodine contained a band at 1661 cm.$^{-1}$ characteristic of an amide carbonyl, which band was not present in the spectrum of lycodine. By means of descending paper chromatography using Whatman No. 1 paper buffered at pH 3, and *n*-butanol saturated with water as the moving phase, lycodine (R_f, 0.35) was easily distinguished from N-acetyl lycodine (R_f, 0.65).

Hydrolysis of N-Acetyl Lycodine

N-Acetyl lycodine obtained from the monopicrate was refluxed in conc. hydrochloric acid for 6 hours. After cooling, the solution was rendered basic with sodium hydroxide solution and extracted with ether. The ether extractions were each washed with water and dried over anhydrous sodium sulphate before being evaporated to dryness. The residue was distilled around 125° (air bath) (0.8 mm. Hg) and the clear distillate crystallized on standing. These crystals had m.p. 118° either alone or mixed with lycodine.

Attempted Acetylation of β-Obscurine

β-Obscurine (*ca.* 1 mg.) was subjected to the same reaction conditions as used for the acetylation of lycodine. After removal of the remaining acetic anhydride, the product gave only one spot which corresponded to that of β-obscurine when it was paper chromatographed. The same result was obtained when β-obscurine was acetylated with acetic anhydride, using anhydrous sodium acetate as catalyst, for double the length of time. The neutral fraction of the product did not contain any substance having an α-pyridone chromophore.

ACKNOWLEDGMENTS

We are greatly indebted to Dr. Léo Marion, of the National Research Council, for providing us with the mother liquors from the crystallization of annotinine, to Dr. H. J. Bernstein, of the National Research Council, for taking the NMR spectra and for discussion of the results, to Dr. E. M. Godar and Dr. R. P. Mariella, of Loyola University, Chicago, Illinois, for generously providing us with a sample of tetrahydroquinoline, to Dr. D. B. McLean, of McMaster University, for a gift of obscurine, and to Mr. R. Lauzon and Dr. R. N. Jones, of the National Research Council, for the infrared spectra taken on the double-beam instrument. We wish to thank the National Research Council for a grant in aid of this work. One of the authors (C. R. E.) wishes to thank the Commissioner, Royal Canadian Mounted Police, whose kind permission and support enabled him to take part in this work.

REFERENCES

1. MARION, L. and MANSKE, R. H. F. Can. J. Research, B, **21**, 92 (1943).
2. MANSKE, R. H. F. and MARION, L. J. Am. Chem. Soc. **69**, 2126 (1947).
3. BERTHO, A. and STOLL, A. Ber. **85**, 663 (1952).

4. ACHMATOWICZ, O. and RODEWALD, W. Roczniki Chem. **29**, 509 (1955).
5. PERRY, G. S. and MACLEAN, D. B. Can. J. Chem. **34**, 1189 (1956).
6. PRZYBYLSKA, M. and MARION, L. Can. J. Chem. **35**, 1075 (1957).
7. WIESNER, K., AYER, W. A., FOWLER, L. R., and VALENTA, Z. Chem. & Ind. 564 (1957) and previous papers.
8. MARION, L., RAMSAY, D. A., and JONES, R. N. J. Am. Chem. Soc. **73**, 305 (1951).
9. BELLAMY, L. J. The infra-red spectra of complex molecules. Methuen & Co. Ltd., London. 1954. p. 234.
10. BELLAMY, L. J. The infra-red spectra of complex molecules. Methuen & Co. Ltd., London. 1954. p. 13.
11. BERNSTEIN, H. J., POPLE, J. A., and SCHNEIDER, W. G. Can. J. Chem. **35**, 65 (1957).
12. POPLE, J. A., SCHNEIDER, W. G., and BERNSTEIN, H. J. Can. J. Chem. **35**, 1060 (1957).
13. SCHNEIDER, W. G., BERNSTEIN, H. J., and POPLE, J. A. Can. J. Chem. **35**, 1487 (1957).
14. GODAR, E. and MARIELLA, R. P. J. Am. Chem. Soc. **79**, 1402 (1957).
15. MOORE, B. P. and MARION, L. Can. J. Chem. **31**, 952 (1953).
16. ANET, F. A. L. and KHAN, N. H. Unpublished results.
17. BUSH, M. T. and DENSEN, P. M. Anal. Chem. **20**, 121 (1948).
18. CRAIG, L. C. and POST, O. Anal. Chem. **21**, 500 (1949).
19. BRINDLE, H., CARLESS, J. E., and WOODHEAD, H. B. J. Pharm. and Pharmacol. **3**, 793 (1951).

THE VAPOR PRESSURE OF LITHIUM IN THE REDUCTION OF LITHIUM OXIDE BY SILICON[1]

W. MORRIS[2] AND L. M. PIDGEON

ABSTRACT

The vapor pressure of lithium over the system lithium oxide – calcium oxide – silicon has been measured using the gas entrainment method at temperatures between 970° C. and 1025° C. The experimental results are summarized in the form $4 \log P = 43.1 - (6.69/T) \times 10^4$, where P is in atmospheres and T in ° A. The reaction, as usually written,

$$2Li_2O + 2CaO + Si = 4Li(g) + 2CaO.SiO_2,$$

does not describe the process completely.

INTRODUCTION

The classical method of producing alkali metals involves electrolysis of fused chlorides, preferably a mixture of chlorides in order to utilize a low-melting-point eutectic. Lithium is so produced using LiCl–KCl mixtures. In this case, however, certain inherent disadvantages of electrolytic processes are intensified. Lithium is at the head of the electromotive series; hence, any metallic impurities present in the bath would be deposited at the cathode and find their way into the final product. The purity of the metal is dependent on the purity of the charge material.

These characteristics, together with the low electrochemical equivalent of lithium (6.94 lb. of Li per 500 amp-days of power) and the reactivity of the metal, justify the search for alternative methods in the form of thermal reduction techniques. The relative volatility of lithium metal should permit its evolution in the gaseous state from a reaction mixture consisting of the oxide and a suitable reducing agent.

Such a method has been successfully applied to magnesium, where calcined dolomite is reacted with silicon (as ferrosilicon) in the solid state, the reaction occurring being described as

$$2CaO.MgO(s) + Si(s) = 2Mg(g) + 2CaO.SiO_2(s). \quad [1]$$

Kroll and Schlechten (1) examined a number of reducing agents and decided that a reaction similar to that for magnesium was feasible and, in fact, preferable to others. For this purpose, these authors calcined mixtures of Li_2CO_3–CaO, which were subsequently briquetted with FeSi to provide the charge for their experiments. In a manner analogous to the magnesium-forming reaction, lime was added so that a calcium silicate rather than a lithium silicate would form according to the postulated reaction

$$2Li_2O(s) + 2CaO(s) + Si(s) = 4Li(g) + 2CaO.SiO_2(s). \quad [2]$$

These authors described the general procedures adopted and were not concerned with the measurement of the pressures of lithium over the system.

This paper describes measurements of the equilibrium pressures of lithium over a mixture of calcined $Li_2CO_3.CaO$ and silicon. The magnitude of this pressure is the effective driving force of the reaction, and directly controls the feasibility of a practical reduction process of this type.

[1]*Manuscript received December 23, 1957.*
Contribution from the Metallurgical Engineering Laboratory, University of Toronto, Toronto, Ontario, based on a thesis by W. Morris submitted in partial fulfillment of the requirements for the degree of Doctor of Philosophy to the Graduate School of the University of Toronto.
[2]*Now with Dow Chemical of Canada Limited, Toronto.*

EXPERIMENTAL

From preliminary experiments, it was found that the reaction pressure of lithium in the reduction process was in the order of 5 mm. Hg at 1000° C. As a result, the entrainment method was adopted, similar to that used by Pidgeon and King (2) and later by Ellingsgaeter and Rosenqvist (3) in their examination of reaction [1].

Purified argon was employed as the carrier gas, which was saturated with lithium vapor. The metal vapors were carried downstream to a point where conditions were appropriate for condensation.

Owing to the reactivity of lithium metal, the reaction tube adopted was a clean 30-inch length of black iron pipe (1 inch diameter) enclosed by a heat-resisting nickel–chromium tube. Insert condensers were troublesome, and it was decided to utilize the downstream portion of the iron reaction tube itself as condenser. At the end of an experimental run the tube was cut in two, separating the condensing section from the charge zone. The condensed product could not be weighed directly because of the rapid formation of lithium nitride in the atmosphere. As a result, the deposit was dissolved in hot distilled water, and the amount of lithium collected determined by polarographic means (4).

Clean steel wool placed at the extreme downstream section of the charge prevented the contamination of the condensing section of the reaction tube by fine particles entrapped in the gas stream. Vapor-phase condensation of the lithium vapor similar to the formation of "blue powder" in the thermal reduction of ZnO was eliminated by inserting a second piece of clean steel wool slightly downstream from the point where the bulk of the condensation occurred. This vapor-phase condensation phenomenon is caused by the "cold blanket" of carrier gas on the walls of the condenser. Steel wool serves to eliminate this phenomenon and also acts as a dust trap.

The reaction zone was equipped with baffles which maintained a 3-inch zone constant to ±1° C.

CHARGE MATERIAL

Li_2O was produced by thermal dissociation of reagent grade Li_2CO_3–CaO mixtures in vacuum according to the procedures described by Kroll and Schlechten (1). The calcined product, originally containing 60% CaO and 40% Li_2CO_3, was mixed with a 20% addition of 100% −100 mesh ferrosilicon analyzing 79% Si, and subsequently briquetted to provide particles ⅓ inch in average dimension. The mixture for reduction analyzed 7.0% Li and 16.9% Si.

PROCEDURE

Reduction briquettes were charged to the reaction tube and heated to the required temperature. After the passage of a given amount of argon, sufficient to bring about 5–10% reduction (i.e., approximately 0.3 g. Li collected), the reaction tube was removed from the furnace and cooled in argon. When the tube had cooled sufficiently, it was subsequently sectioned, and the product in the condensing section was dissolved and analyzed.

From the volume of argon used, corrected to N.T.P., and the amount of lithium collected, the reaction pressure of lithium over the system was calculated.

RESULTS

A series of experiments at a temperature of 993° C. and flow rates varying from 2.0 to 8.0 cc. per second was performed. The results are shown in Table I and plotted in Fig. 1.

From the graph (Fig. 1), it can be seen that the extrapolation to zero flow rate yields

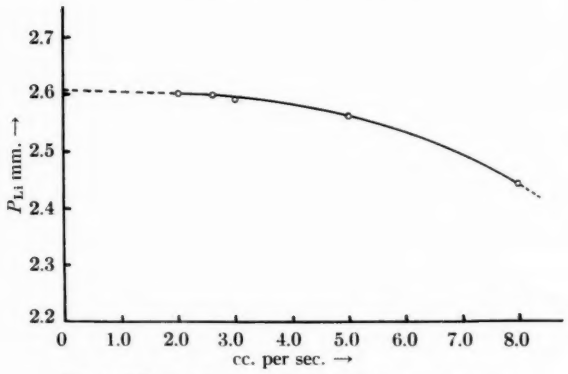

FIG. 1. Effect of flow rate on apparent vapor pressure.

TABLE I

Rate (cc./sec.)	P_{Li} mm. Hg)
2.0	2.60
2.6	2.60
3.0	2.59
5.0	2.56
8.0	2.44

a value of the vapor pressure essentially the same as the value at a flow rate of 2.6 cc. per second. At flow rates above 2.6 cc. per second saturation of the argon carrier gas was not established. This is shown by the lower values of the apparent vapor pressures at these higher rates.

The flow rate of 2.6 cc. per second is large enough to overcome thermal-diffusion effects, and small enough to establish saturation. At very low flow rates, it was observed that the iron reaction tube was bright-annealed by the lithium vapors upstream from the reaction zone, caused by the back-diffusion of lithium in the gas stream. At the saturation rates, this bright-annealing effect was not observed.

Saturation experiments were also performed at 972° C. and results similar to those at 993° C. were obtained.

EFFECT OF TEMPERATURE

At temperatures below 970° C., consistent results could not be obtained; at temperatures above 1025° C., the charge showed definite evidence of the formation of a liquid phase. Successful measurements were therefore restricted to this range of temperature.

TABLE II

P_{Li} (mm.)	log K_p (atm.)	° C.	° A.	$1/T$° K.
1.8	−10.5020	972	1245	8.032×10^{-4}
2.3	−10.0764	982	1255	7.968
2.6	− 9.8632	993	1266	7.899
2.9	− 9.6736	996	1269	7.880
3.5	− 9.3468	1005	1278	7.825
4.1	− 9.0720	1011	1284	7.788
4.5	− 8.9104	1012	1285	7.782
4.9	− 8.7624	1016	1289	7.758
6.6	− 8.2452	1025	1298	7.704

Table II summarizes the results obtained. The values quoted for the measured vapor pressure are estimated to have a probable error of 5% and represent the average of several determinations at the various temperatures.

Fig. 2 is a plot of $4 \log_{10} P_{Li}$ against $1/T°$ K.

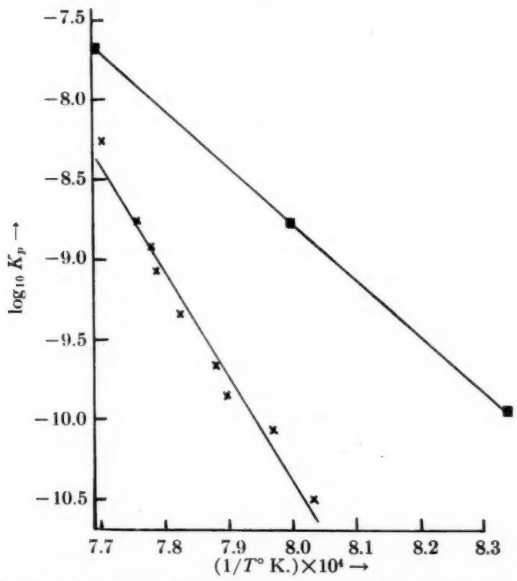

FIG. 2. Calculated and observed equilibrium constants plotted against reciprocal temperature.
■—Calculated. ×—Observed.

DISCUSSION

The reaction [2] as proposed by Kroll and Schlechten (1) served as a basis for the calculations. Experiments were performed in which the reaction was completed *in vacuo*. X-Ray diffractometer investigations on the solid residue revealed the presence of dicalcium silicate, excess CaO, and excess FeSi. The diffractometer traces also showed the presence of other compounds which could not be identified, suggesting that equation [2] is not the only reaction occurring.

The presence of the diatomic species of lithium vapor (Li_2), at a total pressure $P_{(Li+Li_2)}$ equal to 40 or 50 mm. Hg, would account for approximately 7% of the vapor phase at these temperatures (5). However, at the pressures of lithium involved in this research (in the order of 2–6 mm. Hg), the diatomic species can be shown to play a negligible role.

Assuming that the major reaction is reaction [2], equilibrium constants were computed and plotted against $1/T°$ K., both from the experimental values and from the calculated values for the reaction. The experimental values are shown in Table II and

TABLE III

P_{Li} (mm.)	log K_p (atm.)	° K.
2.46	−9.956	1200
4.94	−8.744	1250
9.25	−7.656	1300

plotted in Fig. 2. The calculated values are shown in Table III and are also plotted in Fig. 2.

For these calculations, the solids as predicted by reaction [2] were assumed to be present as pure, distinct phases; thus, their activities were equated to unity and the lithium vapors present were assumed ideal; hence, the equilibrium constant was written in the form

$$K_p = (P_{Li})^4.$$

The thermodynamic data used for the calculated values of the equilibrium constant were taken from Kubaschewski and Evans (6), Coughlin (7), and Kelley (8).

A statistical analysis of the experimental points gives the equation of the straight line in Fig. 2 in the form

$$\log_{10}K_p = 43.1 - (6.69\times10^4/T) \qquad [3]$$

corresponding to a heat of reaction of 306,000 cal. The calculated value for the heat of reaction utilizing the values shown in Table III is 164,000 cal.

The discrepancy between the calculated and the observed values is greater than either the experimental error or the uncertainty of the thermodynamic data used. The discrepancy must lie, then, in the assumption of unit activities or be due to the fact that the reaction cited (equation [2]) is an oversimplification.

It is quite probable that the formation of a lithium silicate should be accounted for, since in a series of experiments above 1025° C. the charge showed distinct evidence of the formation of a liquid phase. The melting point of pure Li_2SiO_4 is approximately 1025° C. A further possibility is the formation of the double silicate of Ca and Li.

In general, it can be stated that, if any side reaction occurs that effectively ties up any lithium, an increase in the heat of reaction would be observed.

CONCLUSIONS

1. The values of the pressure of lithium encountered in the reduction reaction are of sufficient magnitude to warrant a commercial thermal reduction process.

2. The experimental values are summarized in the form $\log_{10}P = 43.1 - (6.69/T)\times10^4$, where P is in atmospheres and T in ° K.

3. The reaction occurring, written in the form

$$2Li_2O + 2CaO + Si = 4Li + 2CaO.SiO_2,$$

is an oversimplification.

ACKNOWLEDGMENTS

The authors acknowledge financial assistance for this research in the form of an International Nickel Co. Fellowship to one of them. Reduction briquettes were supplied by courtesy of the Dominion Magnesium Limited, Haley, Ontario.

REFERENCES

1. KROLL, W. J. and SCHLECHTEN, A. W. A.I.M.M.E., Tech. Publ. No. 2179 (1947); Trans. A.I.M.M.E. **182**, 266 (1944).
2. PIDGEON, L. M. and KING, J. A. Discussions Faraday Soc. No. 4, 197 (1948).
3. ELLINGSGAETER, B. and ROSENQVIST, T. J. Metals (Aug.), 1111 (1956).
4. CLARK, W. E. J. Am. Chem. Soc. **75**, 6042 (1953).
5. DOUGLAS, T. B., EPSTEIN, L. F., DEVER, J. L., and HANLAND, W. H. J. Am. Chem. Soc. **77**, 2144 (1955).
6. KUBASCHEWSKI, O. and EVANS, E. LL. Metallurgical thermochemistry. John Wiley & Sons, Inc., New York. 1956.
7. COUGHLIN, J. P. Contribution to the data on theoretical metallurgy. III. Heats and free energy of formation of inorganic oxides. Bureau of Mines (U.S.A.), Bull. 542 (1954).
8. KELLEY, K. K. III. Free energies of vaporization and vapour pressures of inorganic substances. Bureau of Mines (U.S.A.), Bull. 383 (1935).

SUR LES RÉACTIONS DES POLYESTERS AVEC LE TÉTRACHLORURE DE TITANE

I. LA RÉACTION DE L'OXALATE DE DIÉTHYLE AVEC LE TÉTRACHLORURE DE TITANE[1]

RÉAL AUBIN[2] ET ROLAND RIVEST

SOMMAIRE

On montre dans ce mémoire que l'oxalate de diéthyle réagit avec le tétrachlorure de titane pour donner un composé d'addition moléculaire: le diéthyl oxalate-1,2 tétrachlorure de titane IV. On examine quelques propriétés de ce complexe de coordination et on propose pour ce composé la structure d'un chélate monomérique de configuration *cis*.

INTRODUCTION

Les réactions des polyesters avec le tétrachlorure de titane ont été peu étudiées; Demarçay (1) paraît en avoir donné la première description et depuis, seulement deux autres réactions (2, 3) ont été signalées. Des travaux parallèles conduits par Hieber et Reindl (4) sur le tétrachlorure d'étain et l'analyse récente menée par Archambault (5) sur les réactions acide–base du titane avec certains composés électrodotiques nous ont incités à entreprendre une étude systématique et comparée des réactions des polyesters avec le tétrachlorure de titane.

L'atome tétravalent du titane possède dans plusieurs composés connus un nombre de coordination (6). Dans le tétrachlorure, il peut donc recevoir deux doublets additionnels d'électrons venant d'une substance électrodotique appropriée. Il adopte alors une configuration octaédrique très stable de type d^2sp^3. Les diesters sont des polydentates présentant plusieurs possibilités de réaction avec le tétrachlorure de titane. Ils peuvent donner des chélates où les liaisons chimiques diester–tétrachlorure peuvent être en position *cis* ou *trans* selon la stéréochimie du diester impliqué dans la formation du composé. Il est aussi possible qu'un empêchement stérique s'oppose à la cyclisation et dans ce cas, le produit obtenu pourrait être soit un polymère, soit un composé d'addition simple.

Dans le but de vérifier ces différentes possibilités nous avons entrepris l'étude des trois types de diesters suivants:

(*a*) Les diesters à constitution $R-O-\overset{\overset{O}{\|}}{C}-(CH_2)_n-\overset{\overset{O}{\|}}{C}-O-R$, où "R" et "*n*" peuvent varier. Exemple: l'oxalate de diéthyle.

(*b*) Les polyesters du type $R-\overset{\overset{O}{\|}}{C}-O-(CH_2)_n-O-\overset{\overset{O}{\|}}{C}-R$. Exemple: le diacétate d'éthylène.

(*c*) Les polyesters aromatiques $Ar(COOR)_2$, tels l'isophthalate de diméthyle.

Comme premier terme de notre investigation, la réaction de l'oxalate de diéthyle sur le tétrachlorure de titane semblait particulièrement bien adaptée à notre projet puisque la description de Demarçay (1) et les brefs commentaires de Wurtz (7) n'avaient guère précisé la structure et les propriétés générales du complexe issu de cette réaction.

[1]*Manuscrit reçu le 27 janvier 1958.*
Contribution du Département de Chimie de l'Université de Montréal, Montréal, Qué.
[2]*Boursier de l'Office des Recherches scientifiques de la Province de Québec.*

PARTIE EXPÉRIMENTALE

Purification des produits chimiques

On utilise pour cette réaction le tétrachlorure "purifié" de la compagnie Fisher Scientific. On met en œuvre une méthode de purification achevée en appliquant le mode opératoire de Gilchrist et de ses collaborateurs (8). On obtient ainsi un produit de haute pureté sans traces de chlore ni de vanadium.

L'oxalate de diéthyle est également un produit "purifié" de Fisher Scientific. Le diester est desséché sur du sulfate de sodium anhydre et soumis à une distillation fractionnée sous pression réduite. La fraction médiane est conservée sur le sulfate de sodium anhydre.

Au cours de l'addition des deux substances concernées dans cette réaction, le tétrachlorure de carbone tient lieu de solvant usuel. Il reçoit un traitement identique à celui de l'oxalate de diéthyle sauf en ce qui a trait à la pression, lors de la distillation fractionnée.

Mode opératoire

Comme le tétrachlorure de titane réagit violemment avec certains polyesters, nous diluons les réactifs dans le tétrachlorure de carbone.

Le tétrachlorure de carbone (100 ml.) est placé dans un ballon de 250 ml. Un courant d'azote sec chasse l'air humide et prévient l'hydrolyse au cours des opérations subséquentes. Une quantité mesurée du réactif qui doit être en excès est alors ajoutée à l'aide d'une seringue graduée à aiguille de Téflon. L'agitation du mélange est provoquée par un agitateur magnétique. Une portion mesurée de l'autre réactif est alors ajoutée lentement à l'aide d'une autre seringue graduée à aiguille de Téflon. Une coloration jaune apparaît aussitôt. Bien que l'addition s'opère à température normale, la chaleur de réaction n'augmente pas trop la température du système, si l'addition est assez lente, l'agitation suffisante et les dilutions dans CCl_4 assez poussées. Bientôt le complexe précipite sous forme finement cristallisée.

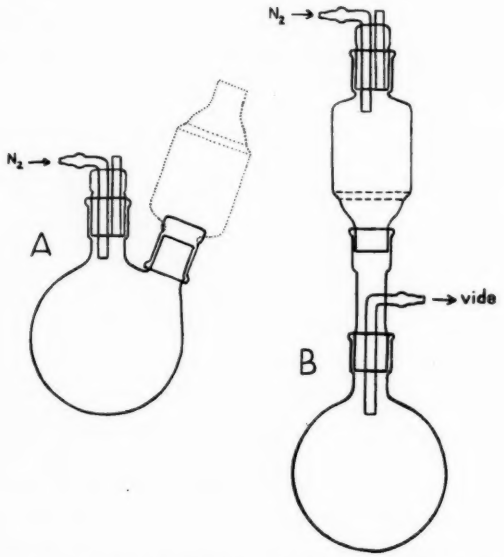

FIG. 1. Appareils utilisés: pour l'addition des réactifs (A); pour l'extraction, la purification et le séchage du complexe formé (B).

Le tout est transféré quantitativement sur un filtre de porosité moyenne. On maintient une atmosphère d'azote dans l'appareil et le précipité est lavé une dizaine de fois avec des portions de 20 ml. de CCl_4 pour le débarrasser de l'excès de réactif très soluble dans le tétrachlorure de carbone.

Le complexe cristallisé et lavé est séché durant quelques heures sous une pression inférieure à 1 mm. de mercure et à température ordinaire. Le produit est conservé dans un récipient scellé ou dans un dessiccateur renfermant du pentoxyde de phosphore.

Le schéma des appareils utilisés pour ces opérations est donné dans la figure 1.

Méthodes d'analyse

Le point de fusion (p.f.) est corrigé; il a été déterminé dans un appareil de Thiele.

Le poids moléculaire a été évalué par ébullioscopie dans le benzène anhydre chez Huffman Microanalytical Laboratories, Wheatridge, Colorado.

La détermination gravimétrique du chlore a été conduite selon le protocole analytique décrit par Vogel (9). Le titane a été déterminé gravimétriquement sous forme de TiO_2.

Les spectres infrarouges ont été déterminés à l'aide d'un spectromètre "Perkin-Elmer", modèle 112, à simple faisceau et parcours double.

RÉSULTATS ET DISCUSSION

Structure du produit de la réaction

Les travaux de Sisler et de ses collaborateurs (10) ont montré que le rapport de l'addition moléculaire dans ce genre de réaction se trouve parfois être 1:2 ou 1:1 selon qu'il y a, ou non, excès de réactif électrodotique. Nous avons voulu préciser la valeur de ce rapport dans la réaction d'addition de l'oxalate de diéthyle avec le tétrachlorure de titane; dans ce dessein, nous avons effectué plusieurs additions de l'oxalate de diéthyle dans des concentrations relatives variables par rapport au tétrachlorure de titane. C'est ainsi que nous avons utilisé l'oxalate de diéthyle en excès sur le tétrachlorure de titane, les deux réactifs en proportions équivalentes et finalement, l'oxalate de diéthyle avec un excès de tétrachlorure de titane. Le tableau I résume les résultats obtenus dans les dosages du titane et du chlore des différents composés d'addition réalisés. On voit clairement que le rapport de l'addition moléculaire demeure toujours et seulement 1:1, quelles que

TABLEAU I

TABLEAU COMPARATIF DES VALEURS (%) DE Ti ET DE Cl DANS LES COMPOSÉS THÉORIQUES 1:1 ET 1:2 ET DANS LES COMPOSÉS FORMÉS EXPÉRIMENTALEMENT

Valeurs calculées	% Ti	% Cl	Valeurs trouvées	% Ti	% Cl
$1TiCl_4.1(COOC_2H_5)_2$	14.26	42.22	Addition avec TiCl en excès	14.48	40.40
			Addition sans excès de réactif	14.49	41.27
$1TiCl_4.2(COOC_2H_5)_2$	9.93	29.41	Addition avec $(COOC_2H_5)_2$ en excès	14.48	41.38

soient les concentrations respectives de l'oxalate de diéthyle et du tétrachlorure de titane. En aucun cas, nous n'avons pu obtenir le rapport d'addition 1:2, soit $TiCl_4.2(COOC_2H_5)_2$.

Une détermination du poids moléculaire par ébullioscopie dans le benzène rigoureusement anhydre, non seulement justifie la formule brute $TiCl_4.(COOC_2H_5)_2$ pour le complexe formé, mais, également, met en évidence le caractère monomérique de la structure moléculaire recherchée; le poids moléculaire théorique 335.9 g. coïncide assez bien avec le poids moléculaire trouvé 364.

La structure cyclique ou chélatée du présent complexe de coordination est déduite

des mesures dans l'infrarouge, des vibrations du groupe C=O de la molécule du diester. Des mesures effectuées sur l'oxalate de diéthyle pur montrent une bande C=O à 1770 cm^{-1} et à 1745 cm^{-1}. Il est vrai que Randall et ses collaborateurs (11) ne mentionnent pour l'oxalate de diéthyle qu'une seule bande C=O à 1757 cm^{-1} mais, d'autre part, nos résultats rejoignent bien les mesures plus récentes de Bender (12): 1771 cm^{-1} et 1747 cm^{-1}.

L'existence d'une structure cyclique exige ici des modifications de ces deux valeurs de bande C=O; en effet, si l'on retrouve dans le complexe l'une ou l'autre de ces valeurs inchangée, alors seulement on pourra penser que l'un des groupes C=O est demeuré libre. Mais, dans ces conditions, on se demande comment les exigences du nombre de coordination maximum du titane IV pourraient être sauvegardées, le caractère monomérique du complexe et la valeur 1:1 du rapport d'addition demeurant acquis. Si, par ailleurs, les deux valeurs de bande C=O sont modifiées en passant du diester pur au complexe, il faut attribuer cette modification à une variation de la distance C=O et, pour autant, à une liaison quelconque de l'atome d'oxygène de chaque groupe C=O avec un autre atome. Puisque les deux groupes C=O habitent déjà la même molécule et que le ou les atomes liants ne peuvent se trouver que sur une seule autre molécule, on doit nécessairement envisager une structure cyclique.

Or le spectre infrarouge du complexe (émulsion dans le nujol, prisme NaCl) révèle un déplacement marqué des deux bandes C=O vers une plus grande longueur d'onde; les valeurs obtenues pour le diester pur sont disparues et remplacées par deux nouvelles bandes à 1698 cm^{-1} et à 1675 cm^{-1}, soit un décalage moyen de 71 cm^{-1} par rapport aux valeurs des bandes C=O libres. Il est donc normal de déduire une liaison nouvelle dans chacun des groupes C=O et partant, une structure cyclique.

Gordy (13) a d'ailleurs montré que la chélation du groupe C=O se traduit possiblement par un effet dans le sens que nous avons observé et Bryant et ses collaborateurs (14) ont noté que l'importance du déplacement de la bande C=O est reliée à la nature des atomes du cycle résultant et dépend aussi des substituants greffés sur le cycle.

On peut donc raisonnablement proposer une structure chélatée pour le produit de l'addition de l'oxalate de diéthyle avec le tétrachlorure de titane.

La configuration *cis* ou 1,2 doit enfin être préférée à la forme *trans* ou 1,6. On considère avec Martell et Calvin (15) qu'il est stériquement impossible pour les oxygènes de l'oxalate d'occuper deux coins opposés 1,6 de l'octaèdre du titane IV. En effet, la distance entre les deux atomes d'oxygène concernés serait très voisine de 2.73 Å pour la forme *cis* de l'oxalate de diéthyle tandis que la distance entre deux coins opposés 1,6 de l'octaèdre du titane dépasse 4.3 Å. Par contre, la distance entre deux coins voisins 1,2 de l'octaèdre du titane est de l'ordre de 3.0 Å; ces dernières positions sont donc nettement favorisées du point de vue stérique.

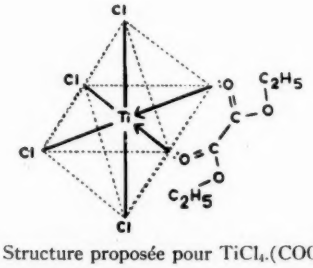

FIG. 2. Structure proposée pour $TiCl_4.(COOC_2H_5)_2$.

Dans l'évaluation de la distance entre les deux atomes d'oxygène de l'oxalate de diéthyle, il n'y a pas d'objection à postuler la forme *cis* pour le diester pur à l'état liquide car les recherches de Jatkar et Phansalkar (16) justifient l'hypothèse d'une rotation libre des deux groupes estérifiés autour de la liaison CO—CO.

Nous proposons donc la structure représentée dans la figure 2 pour le diéthyl oxalate-1,2 tétrachlorure de titane IV.

Quelques propriétés du complexe $TiCl_4.(COOC_2H_5)_2$

Le point de fusion de ce composé (p.f.) est 104–105° C.; la fusion est probablement accompagnée de décomposition partielle du complexe.

L'analyse élémentaire donne pour $TiCl_4.(COOC_2H_5)_2$:

	% Ti	% Cl
Valeurs calculées	14.26	42.22
Valeurs trouvées	14.48	41.72

Le complexe d'addition est un solide jaune pâle finement cristallisé, à odeur d'acide chlorhydrique. Il est extrêmement hygroscopique et s'hydrolyse rapidement en présence d'humidité. Quand le composé est chauffé, il donne d'abord un liquide jaune clair, puis une pâte brun foncé et finalement un résidu blanc identifié comme TiO_2. Conservé dans un récipient scellé et sous atmosphère d'azote sec, le composé conserve son état initial pendant plusieurs mois.

Nous avons étudié avec une attention particulière la solubilité de $TiCl_4.(COOC_2H_5)_2$ dans une gamme de solvants organiques usuels. Chacun de ces solvants a été séché au préalable selon le procédé le plus approprié à chaque cas. Le tableau II résume les résultats quantitatifs obtenus.

TABLEAU II

SOLUBILITÉ DE $TiCl_4.(COOC_2H_5)_2$ À TEMPÉRATURE ORDINAIRE

Nom du solvant	Formule du solvant	Solubilité en g./100 ml.
Chlorure de *n*-butyle	$CH_3—(CH_2)_2—CH_2Cl$	26.4
Dichlorure d'éthylène	$ClCH=CHCl$	49.0
Chloroforme	$CHCl_3$	64.4
Tétrachlorure de carbone	CCl_4	0.3
n-Hexane	$CH_3—(CH_2)_4—CH_3$	Insoluble
Cyclohexane	C_6H_{12}	Insoluble
Sulfure de carbone	CS_2	1.1
Éther	$C_2H_5OC_2H_5$	5.9
Dioxane	$C_4H_8O_2$	1.8
Acétone	CH_3COCH_3	87.8
Oxalate de diéthyle	$(COOC_2H_5)_2$	50.3
Acétate d'éthyle	$CH_3COOC_2H_5$	97.3
Benzène	C_6H_6	61.6
Toluène	$C_6H_5CH_3$	32.6
Xylène	$C_6H_4(CH_3)_2$	5.5
Chlorobenzène	C_6H_5Cl	43.2

On voit que le complexe est tout à fait insoluble dans les hydrocarbures saturés. Les dérivés halogénés les plus polaires sont de meilleurs solvants; si la solubilité est peu élevée dans les éthers, elle est très convenable dans les esters. Enfin, une substitution sur le noyau benzénique semble diminuer l'efficacité du solvant.

$TiCl_4.(COOC_2H_5)_2$ s'hydrolyse instantanément dans l'eau. Ce composé est soluble dans les alcools mais il réagit avec ces derniers. Il réagit aussi avec les amines et les amides.

La réaction d'addition de l'oxalate de diéthyle sur le tétrachlorure de titane réalisée dans le cyclohexane donne comme rendement de réaction: 95%.

REMERCIEMENTS

Nous tenons à adresser nos remerciements au Conseil National de Recherches du Canada pour l'aide financière accordée sous forme de subvention (R.R.) et à l'Office des Recherches scientifiques de la province de Québec pour la bourse d'études accordée (R.A.). Nous remercions aussi M. le Professeur Sandorfy et Mlle Chenon de leur collaboration dans l'étude des spectres.

BIBLIOGRAPHIE

1. DEMARÇAY, E. Bull. soc. chim. France, [2], **20**, 127 (1873).
2. SCAGLIARINI, G. et TARTARINI, G. Atti accad. nazl. Lincei, [6], **4**, 318 (1926).
3. HERTEL, E. et DEMMER, A. Ann. **499**, 134 (1932).
4. HIEBER, W. et REINDL, E. Z. Elektrochem. **46**, 559 (1940).
5. ARCHAMBAULT, J. Mémoire de maîtrise. Université de Montréal, Montréal, Québec. 1956. p. 20.
6. LEWIS, G. N. J. Franklin Inst. **226**, 293 (1938).
7. WURTZ, A. D. Dictionnaire de chimie pure et appliquée. Vol. III. Librairie Hachette & Cie, Paris. 1878. p. 425.
8. CLABAUGH, W. S., LESLIE, R. T. et GILCHRIST, R. J. Research Natl. Bur. Standards, **55**, 261 (1955).
9. VOGEL, A. I. A text-book of quantitative inorganic analysis. 2nd ed. Longmans, Green and Co., London. 1953. p. 399.
10. HAMILTON, P. M., MCBETH, R., BEKEBREDE, W. et SISLER, H. H. J. Am. Chem. Soc. **75**, 2881 (1953).
11. RANDALL, H. M., FUSON, N., FOWLER, R. G. et DAUGL, J. R. Infrared determination of organic structures. D. Van Nostrand Co., Inc., New York. 1949. p. 21.
12. BENDER, M. L. J. Am. Chem. Soc. **75**, 5986 (1953).
13. GORDY, W. J. Chem. Phys. **8**, 516 (1940).
14. BRYANT, B. E., PARIAUD, J.-C. et FERNÉLIUS, W. C. J. Org. Chem. **19**, 1889 (1954).
15. MARTELL, A. E. et CALVIN, M. Chemistry of the metal chelate compounds. Prentice-Hall, Inc., New York. 1956. p. 258.
16. JATKAR, S. K. K. et PHANSALKAR, V. K. J. Univ. Poona, Sci. Technol. No. **4**, 45 (1953).

HYDROGENOLYSIS OF CARBOHYDRATES

V. ISOMERIZATION OF METHYL β-L-ARABOPYRANOSIDE[1]

A. S. PERLIN, E. VON RUDLOFF, AND A. P. TULLOCH[2]

ABSTRACT

Treatment of methyl β-L-arabopyranoside under hydrogenolytic conditions with copper chromium oxide catalyst induces extensive isomerization. Products formed include glycosides of D-ribose, D-xylose, D-lyxose, and L-lyxose which together represent about an 80–90% conversion of starting material. Isolation of these compounds shows that carbons 2, 3, and 4 undergo isomerization, but no evidence has been obtained of anomerization. These findings possibly explain the formation of an optically *inactive* mixture of *cis*- and *trans*-tetrahydropyran-3,4-diol under slightly more drastic reaction conditions.

INTRODUCTION

The hydrogenolysis of methyl β-L-arabopyranoside (I) at 250° C. using copper chromium oxide catalyst has yielded mainly a mixture of dihydro-arabinal and -xylal (*cis*- and *trans*-3,4-dihydroxytetrahydropyran) (1). These products appeared to have been formed by reductive cleavage of the glycosidic methoxyl group and of the 2- or 4-hydroxyl group giving, respectively, the *cis*-(*arabo*-) or *trans*-(*xylo*-)isomer. However, the mixture of compounds was optically inactive and hence not the expected L-diols II and III, and it was suggested that isomerization may have occurred (1). Reinvestigation of the reaction under conditions slightly milder than used earlier has now shown, in fact, that methyl β-L-arabopyranoside readily undergoes isomerization, yielding a mixture of pentosides.

At 200° C. very little tetrahydropyrandiol was formed from methyl arabinoside although about half of the pentoside had reacted. A portion of the crude product was hydrolyzed with dilute acid, and examination of the liberated sugars by paper chromatography and electrophoresis indicated the presence in the mixture of ribose, lyxose, and xylose, the latter two being clearly distinguishable only by paper electrophoresis. In addition, an unidentified reducing material (R_{rham} 0.9) and a non-reducing product (R_{rham} 0.4) were detected on the chromatograms as minor components. The mixture of methyl pentosides proved difficult to resolve by cellulose column chromatography (2). A series of fractions was obtained, some containing predominantly one or another sugar. From one of these fractions a small quantity of a crystalline glycoside was isolated and this was shown by specific rotation, mixed melting point, and X-ray powder diagram to be methyl α-D-lyxopyranoside (IV). Chromatographic separation of the mixture of sugars after hydrolysis afforded D-xylose (V), L-lyxose (VI), and D-ribose (VII). The first two were characterized as crystalline sugars and the latter as the *p*-toluenesulphonhydrazone (3) by specific rotations, mixed melting points, and X-ray diffraction diagrams or infrared absorption spectra. Visual examination of the mixture of free pentoses on paper chromatograms and electrophoretograms suggested that lyxose and ribose were formed in about equal amounts, that approximately twice as much xylose was produced, and that these pentoses together corresponded to perhaps 40% of the starting material, i.e., to about 90% conversion.

[1]*Manuscript received February 17, 1958.*
Contribution from the National Research Council of Canada, Prairie Regional Laboratory, Saskatoon, Saskatchewan.
Issued as N.R.C. No. 4702 and as Paper No. 253 on the Uses of Plant Products.
[2]*National Research Council of Canada Postdoctorate Fellow, 1956–57.*

Other instances of hydrogenolytic isomerization of carbohydrates have recently been found in this laboratory, i.e., the formation of dihydro-D-altral from methyl α-D-glucopyranoside (4) and of *O-iso*propylidene-L-idose from 1,2-*O-iso*propylidene-D-glucose (4a). These findings suggest, therefore, that isomerization may occur frequently and may constitute an important reaction quantitatively when carbohydrates are subjected to catalytic hydrogenation conditions. Isomerization of hexitol dianhydrides (5), cyclic alcohols (6), and inositol derivatives (7) under such conditions has been established, the reactions probably involving dehydrogenation to form intermediate ketones. It is reasonable to expect that the carbohydrate isomerizations take place by a similar mechanism.

The wide variety of products obtained from methyl arabinoside by isomerization shows that the reaction involves attack at carbons 2, 3, and 4, sometimes at one carbon individually, sometimes at more than one. Thus, the formation of methyl D-xyloside requires isomerization at carbon 4, and of methyl L-lyxoside at carbon 3. Carbons 3 and 4 are both attacked in the production of methyl D-riboside and carbons 2 and 4 in the production of methyl D-lyxoside. The 2-position is least affected by isomerization; little methyl D-lyxoside is produced as indicated by the isolation of virtually pure L-lyxose from the mixture of free sugars. Since each of the secondary hydroxyl groups is affected to some degree it is possible that D-arabinose, L-xylose, and L-ribose are also products of the reaction but have not been detected. However, there is as yet no evidence for isomerization at carbon 1; the configuration at carbon 1 is retained in methyl α-D-lyxoside, the one intact glycoside isolated. Also, it may be concluded that the L-lyxoside is present in the mixture as the β-glycoside, i.e., that anomerization has not occurred, for the α-D-isomer could not have been separated from methyl α-L-lyxoside by the isolation procedure used.

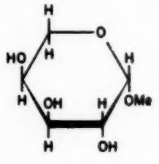

I

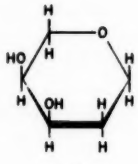

II

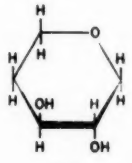

III

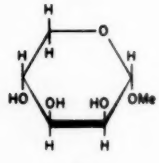

IV

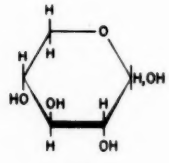

V

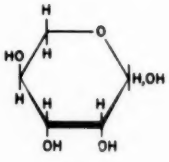

VI

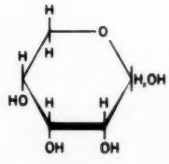

VII

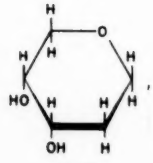

VIII

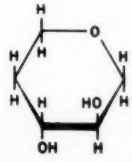

IX

The finding that extensive isomerization can accompany the hydrogenolysis of methyl β-L-arabopyranoside points to a reaction mechanism somewhat more complex than had been indicated earlier (1). Reductive cleavage of carbon–oxygen bonds at the glycosidic center and at position 2 or 4 should yield dihydro-L-arabinal (II) and -L-xylal (III), respectively (*cis*- and *trans*-L-diol). However, with the isomeric pentosides formed as intermediates, this sequence of reactions should yield the *cis*- and *trans*-D-isomer (VIII and IX, respectively), also, as indicated in the following table:

	Product obtained when secondary position attacked	
Glycoside	2-Position	4-Position
L-Arabinoside	*cis*-L	*trans*-L
D-Xyloside	*trans*-D	*trans*-L
D-Riboside	*cis*-D	*cis*-L
L-Lyxoside	*trans*-L	*cis*-L
D-Lyxoside	*trans*-D	*cis*-D

It is seen that all four isomeric diols are obtainable by hydrogenolysis of the mixture of glycosides. Formed in the proper proportions these products could have accounted for the observation that the mixture of diols isolated was optically inactive (1). Such a possibility is increased by the fact that the rotatory power of the *cis*- and *trans*-diols is of approximately the same magnitude (dihydro-D-xylal and dihydro-D-arabinal show $[\alpha]_D$ −45° (8) and −48° (8), respectively). According to these findings, it is possible also that hydrogenolysis does not involve both positions 2 and 4. The fact that *cis*- and *trans*-diol were produced led to the early suggestion that each of these positions is attacked. A mixture of all four isomers may be obtained, however, by reductive cleavage only of the 2-hydroxyl group and the glycosidic methoxyl. By contrast, if hydrogenolysis were to occur at position 4 rather than at 2 the product would be almost exclusively a mixture of L-isomers and hence strongly dextrorotatory. The present results do not completely resolve these questions. They show, however, that isomerization can occur, which possibly leads to the formation of optically inactive hydrogenolysis products.

EXPERIMENTAL

Melting points are corrected. Infrared spectra were prepared by the potassium bromide window technique (9).

Chromatographic Methods

Paper chromatograms were developed on Whatman No. 1 paper using the following solvents: (A) phenol saturated with water (10), (B) ethyl acetate–acetic acid–water (9:2:2, v/v) (11, 12), and (C) *n*-butanol–pyridine–benzene–water (5:4:1:3 v/v) (13). None of these solvents satisfactorily resolved a sugar mixture consisting of D-ribose, D-xylose, L-arabinose, and D-lyxose. Solvent A gave a partial separation of xylose and lyxose, solvent C a good separation of ribose, xylose (or lyxose), and arabinose.

Paper electrophoresis (14) was carried out in borate buffers (pH 8–10) with a Spinco apparatus, Model R, and Whatman No. 1 paper; the current and voltage applied were 4.5 ma. and 900 volts, respectively. At pH 9.7 lyxose and xylose were completely separated (respective distances traveled in 5 hours, 3.2 cm. and 5.5 cm.) but these in turn were not as clearly separated from ribose (3.7 cm.) and arabinose (4.9 cm.). Lyxose and xylose were also separable at pH 8.0 (3.7 cm. and 4.9 cm., respectively, in 7.5 hours), but now the relative speeds of ribose and arabinose were reversed (5.4 cm. and 3.9 cm.,

respectively; compare (14)). Conditions were not found for complete resolution of the mixture.

Cellulose column chromatography was carried out using as solvents: (D) *n*-butanol one-eighth saturated with water, and (E) benzene–ethanol–water (10:1:trace).

Isomerization of Methyl β-L-Arabopyranoside

Methyl β-L-arabopyranoside (10 g.) in ethanol (100 ml.) was treated with hydrogen in the presence of copper chromium oxide catalyst (1 g.) at 200° C. and 2000 p.s.i. initial pressure for 4 hours. After removal of the catalyst a crystalline solid (2.1 g.) separated out; it was found to be slightly impure methyl arabinoside for it yielded mainly arabinose (detected chromatographically) on acid hydrolysis. A sirupy product (7.6 g.) was then obtained by evaporating the solvent. The sirup (5.4 g.) in 0.2 *N* sulphuric acid (100 ml.) was hydrolyzed on the steam bath for 4 hours, the solution was then neutralized with barium carbonate, and the filtered solution concentrated to dryness (weight 4.3 g.). Examined by paper chromatography, the residue was found to contain two minor products, one having R_{rham} 0.9 (yellow color with *p*-anisidine hydrochloride spray (12)), the other having R_{rham} 0.41 (non-reducing, detected with silver nitrate spray (10)), and major components corresponding to ribose, xylose and/or lyxose, and arabinose.

Identification of the Reaction Products

The mixture of sugars (3.5 g.) obtained on hydrolysis of the reaction product was chromatographed on a column (25 inches × 2½ inches) of powdered cellulose using solvent D, 17 1-liter fractions were collected, and the sugars present in these were tentatively identified by paper chromatography and electrophoresis. Complete resolution of the sugar mixture was not obtained. Accordingly, those fractions found to consist chiefly of one or another sugar were selected and the products characterized as described below. The proportion of the pentoses present in each fraction was approximated visually from the intensity and area of the spots developed on the chromatograms and electrophoretograms with *p*-anisidine hydrochloride spray, a spray suited to the estimation of sugars (15). Related to the known weight of each fraction and the amount of arabinose separated earlier as the crystalline glycoside, these evaluations suggested that the ratio of arabinose–xylose–lyxose–ribose in the reaction mixture was about 5:2:1:1.

D-*Ribose.*—Fraction 8 contained only ribose. The sirup (124 mg.) obtained on removal of the solvent was treated with *p*-toluenesulphonhydrazide (120 mg.) in methanol (6 ml.) affording the corresponding hydrazone of D-ribose (93 mg.), m.p. 160°–162° C., after two recrystallizations from methanol; mixed melting point with D-ribose *p*-toluenesulphonhydrazone (m.p. 161°–163° C.) 160°–163° C., $[\alpha]_D$ 22.9° (45 minutes) → 12.5° (18 hours) (*c*, 1.0, moist pyridine). (Literature (3), $[\alpha]_D$ 42.0° (initial) → 14.0° (17 hours) (moist pyridine).) Calc. for $C_{12}H_{18}O_6N_2S$: C, 45.28%; H, 5.70%. Found: C, 45.46%; H, 5.71%. The identity of the compound was confirmed by comparison of its infrared absorption spectrum and X-ray powder diagram with those of an authentic specimen.

L-*Lyxose.*—Fraction 10 contained lyxose and a smaller proportion of xylose. On being seeded with L-lyxose the sirupy product (160 mg.) crystallized, and after recrystallization twice from ethanol – ethyl acetate and once from *n*-propanol had m.p. 104° – 106° C., undepressed on admixture with L-lyxose (m.p. 107°–108° C.), $[\alpha]_D$ 12.0° (equilibrium value) (*c*, 1.0, water). Calc. for $C_5H_{10}O_5$: C, 40.02%; H, 6.71%. Found: C, 39.89%; H, 6.71%. The X-ray powder diagram of the product and that of L-lyxose were indistinguishable.

D-*Xylose.*—Fraction 12 contained mainly xylose and a small percentage of lyxose. The sirup (170 mg.) was taken up in glacial acetic acid and crystallization promoted by

seeding with D-xylose. One recrystallization from ethanol gave a product (70 mg.) having m.p. 138°–141° C., undepressed on admixture with D-xylose, $[\alpha]_D$ 18.6° (equilibrium value) (*c*, 1.0, water). Calc. for $C_5H_{10}O_5$: C, 40.02%; H, 6.71%. Found: C, 39.80%; H, 6.71%. The infrared absorption spectrum of the compound was indistinguishable from that of D-xylose.

Methyl α-D-lyxopyranoside.—The mixture of glycosides obtained by isomerization of methyl arabinoside was chromatographed on a cellulose powder column using solvent E, a series of fractions being collected and examined chromatographically. One of these fractions, which on hydrolysis was found to contain mainly lyxose, yielded a crystalline product, m.p. 106°–107° C. after recrystallization from acetone–ether, undepressed by admixture with methyl α-D-lyxopyranoside, $[\alpha]_D$ 59.0° (*c*, 1.0, water). Calc. for $C_6H_{12}O_5$: C, 43.90%; H, 7.37%. Found: C, 44.00%; H, 7.37%. The X-ray powder diagram of the compound and that of methyl α-D-lyxopyranoside were indistinguishable.

ACKNOWLEDGMENTS

The technical assistance of Mr. M. Granat is gratefully acknowledged. The authors also thank Mr. J. A. Baignée for microanalyses, Mr. T. M. Mallard for X-ray diffraction diagrams, and Mr. G. B. Rennie for infrared absorption analyses.

REFERENCES

1. Bauer, H. F. and Stuetz, D. E. J. Am. Chem. Soc. **78**, 4097 (1956).
2. Hough, L., Jones, J. K. N., and Wadman, W. H. J. Chem. Soc. 2511 (1949).
3. Easterby, D. G., Hough, L., and Jones, J. K. N. J. Chem. Soc. 3416 (1951).
4. Rudloff, E. von and Tulloch, A. P. Can. J. Chem. **35**, 1504 (1957).
4a. Gorin, P. A. J. and Perlin, A. S. Can. J. Chem. **36**, 661 (1958).
5. Fletcher, H. G., Jr. and Goepp, R. M., Jr. J. Am. Chem. Soc. **67**, 1042 (1945).
6. Wicker, R. J. J. Chem. Soc. 2165 (1956).
7. Angyal, S. J. and McHugh, D. J. J. Chem. Soc. 3682 (1957).
8. Fletcher, H. G., Jr. and Hudson, C. S. J. Am. Chem. Soc. **71**, 3682 (1949).
9. Schiedt, U. and Reinwein, H. Z. Naturforsch. **7b**, 270 (1952).
10. Partridge, S. M. Nature, **158**, 270 (1946).
11. Jermyn, M. A. and Isherwood, F. A. Biochem. J. **44**, 402 (1949).
12. Hough, L., Jones, J. K. N., and Wadman, W. H. J. Chem. Soc. 1702 (1950).
13. De Whalley, H. C. S., Albon, N., and Gross, D. Analyst, **76**, 287 (1951).
14. Consden, R. and Stanier, W. M. Nature, **169**, 783 (1952).
15. Pridham, J. B. Anal. Chem. **28**, 1967 (1956).

THE CHEMISTRY OF PEAT

II. THE TRITERPENES OF PEAT MOSS (SPHAGNUM)[1]

D. A. J. IVES[2] AND A. N. O'NEILL

ABSTRACT

By further chromatographic fractionation of the unsaponifiable matter from an extract of peat moss (*Sphagnum*) three crystalline triterpenes have been isolated. They have been identified as α-amyrin, taraxerone, and taraxerol by their physical and chemical properties.

In the preceding paper (5) the method of separating the crude unsaponifiable material present in peat moss was described. Two sterols were isolated and identified. This paper deals with some of the other compounds isolated during the chromatography of the crude extract. The fraction of unsaponifiable material eluted from the alumina column with benzene represented approximately five per cent of the total. This material consisted of a light yellow oil which crystallized on standing. Attempts to purify it by crystallization from methanol or ethanol failed. However, if the material was taken up in light petroleum, a yellow sirup was dissolved leaving a white crystalline mass, which after filtration could be readily recrystallized from chloroform–methanol solution. The crystals melted at 238°–239° and had a specific rotation of +12°. The material gave a crystalline derivative with 2,4-dinitrophenylhydrazine and showed a marked peak in the infrared at 1705 cm.$^{-1}$, indicative of a carbonyl group. The infrared spectrum of this ketone from peat moss also showed the presence of a double bond by a band at 816 cm.$^{-1}$ and the position of the band indicated a trisubstituted double bond in a six-membered ring. The high melting point and comparatively few functional groups, in addition to a positive Liebermann–Burchard reaction, indicated that the compound could be a triterpene, possibly of the allobetulin series. This hypothesis was reached since derivatives of allobetulin have been found in lignite (8), a decomposition product of peat. However, analysis showed the presence of only one oxygen function, the carbonyl group, whereas allobetulin itself has two, one being an ether function. A search of the literature showed that the ketone was possibly taraxerone (I), previously isolated from *Taraxacum officinale* (3) and *Alnus glutinosa* L. (1), and further chemical evidence confirmed this. The ketone was reduced with lithium aluminum hydride to give the alcohol (II, R = H), which had the physical constants of taraxerol. This was confirmed by the preparation of the acetate in the usual way (II, R = Ac). This acetate was treated with hydrochloric acid in acetic acid (1) and the resulting product crystallized from chloroform–methanol to give β-amyrin acetate (III, R = Ac), identified by melting point and rotation and the melting point and rotation of the derived alcohol (III, R = H) β-amyrin. This rearrangement has been shown to involve the migration of a methyl group from C_{13} to C_{14} with the concomitant movement of the double bond from the 14,15-position to the 12,13-position. The process is concerted and there are no intermediates. It is also irreversible and the yield of β-amyrin is virtually 100%. The rearrangement is typical of taraxerol and some of its derivatives, and treatment of taraxerone under the same conditions afforded β-amyrone (I). Reduction by the Wolff–Kishner procedure afforded the unsaturated hydrocarbon taraxerene (VI), recently

[1]*Manuscript received February 26, 1958.*
Contribution from the National Research Council of Canada, Atlantic Regional Laboratory, Halifax, Nova Scotia.
Issued as N.R.C. No. 4717.
[2]*National Research Council of Canada Postdoctorate Fellow 1955–1957.*

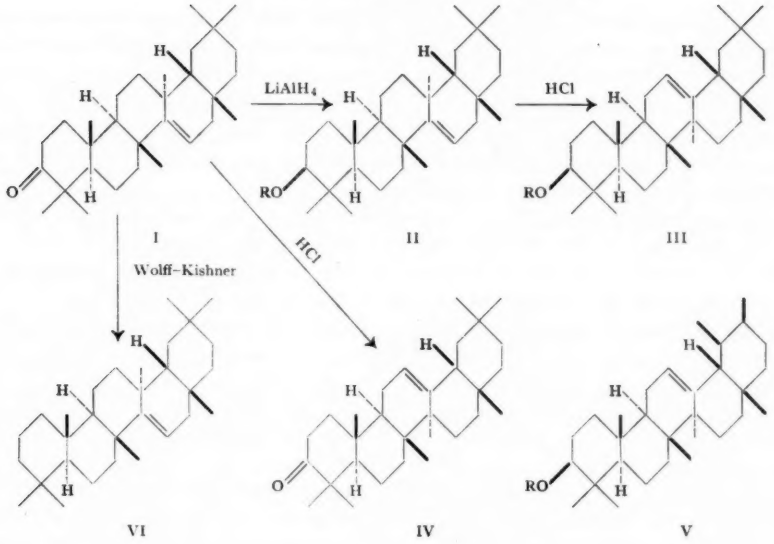

isolated from a lichen by Bruun (2). The amount of taraxerone present in the unsaponifiable extract was approximately two per cent.

The ether fraction of the crude chromatogram gave, in its earlier subfractions, a highly crystalline colorless solid. The amounts however were small, at 50–100 mg. per extraction. The material was only very slightly soluble in ethanol and ether, and could be readily recrystallized from benzene and chloroform. The same compound was also obtained from the fraction of the unsaponifiable material insoluble in light petroleum, extracted before chromatography of the crude unsaponifiable fraction. If this mixture was chromatographed roughly on alumina, elution with benzene afforded taraxerone and elution with chloroform–methanol (5:1) gave the insoluble compound. On recrystallization from chloroform–methanol this material had a melting point of 278°–279°, characterized by a change of crystalline form between 200° and 220°. The specific rotation was 0°. The infrared absorption spectrum showed the presence of a secondary hydroxyl group by bands at 3571 and 1035 cm.$^{-1}$ and the presence of a trisubstituted double bond from a band at 816 cm.$^{-1}$. The spectrum had many of the characteristics of taraxerone and the alcohol corresponded in physical constants and infrared spectrum to taraxerol (see Table I).

The material was shown to be identical with the reduced taraxerone by melting point

TABLE I

	Skimmiol (10)		Taraxerol (6)		Taraxerol*	
	M.p.	$[\alpha]_D$	M.p.	$[\alpha]_D$	M.p.	$[\alpha]_D$
Alcohol	279°–281°	+ 3°	282°–283°	+ 3°	278°–279°	0°
Acetate	298°–299°	+14°	304°–305°	+ 9°	300°–301°	+ 9°
Benzoate	287°–289°	+36°	292°–293°	+37°		
Ketone	241°–243°	+12°	240°–241°	+12°	238°–239°	+12°
Unsaturated hydrocarbon			237°–238° (2)	+ 1°	236°–238°	+ 1°

Data from Brooks, C. J. W. J. Chem. Soc. 1675 (1955).
**Constants found for materials from peat moss.*

and mixed melting point. Oxidation of the alcohol with chromium trioxide in pyridine gave taraxerone, as proved by melting point, mixed melting point, and specific rotation. The amount of taraxerol present in the extract was difficult to estimate owing to its insolubility, but it was approximately 1.5% of the unsaponifiable material or 0.02% by weight of the dried moss. It is probable that some was lost on the chromatographic column. The final proof of the identity of the material was provided by a mixed melting point with a genuine specimen of taraxerol.

The third triterpene isolated from the unsaponifiable extract was α-amyrin (V, R = H). This was not found in the preliminary extractions of the moss, possibly owing to the fact that it requires fairly careful chromatography to separate it from the sterols. However, on working up the ether–methanol fraction from the chromatography of 450 g. of unsaponifiable material, approximately 3.5 g. of α-amyrin were obtained. Chromatography of the acetylated material after the low-melting lignoceryl alcohol had been removed as previously described afforded α-amyrin acetate in the petrol–benzene (4:1) fraction and the steroid acetates in the petrol–benzene (2:1) fraction. The identity of the material was proved by the melting point and rotation of the alcohol, the derived acetate, and the derived benzoate (V, R = Ac and R = Bz respectively). The compound also had an infrared spectrum identical with that published for α-amyrin by Cole (4). A mixed melting point with an authentic specimen of α-amyrin was undepressed.

EXPERIMENTAL

All rotations were measured in a 1 dm. tube with a Rudolph polarimeter. Melting points were observed on a Kofler micromelting-point apparatus and are corrected. The infrared spectra were determined in carbon disulphide solution with a Baird double-beam infrared spectrophotometer, model 4-55. Light petroleum refers to the fraction with boiling point 35°–36°. For the method of obtaining the unsaponifiable fraction of the peat moss, see Part I (5).

Isolation of Taraxerone

The benzene fraction (1 g.) from the chromatography of the crude unsaponifiable extract was extracted with light petroleum and the white crystalline residue filtered off. Recrystallized from chloroform–methanol, it gave taraxerone (500 mg.), m.p. 238°–239°, $[\alpha]_D^{24}$ +12° (c = 1.34 in chloroform). Anal. Calc. for $C_{30}H_{48}O$: C, 84.84; H, 11.39. Found: C, 84.92; H, 11.31. The material gave a purple color in the Liebermann–Burchard test. The yellow 2,4-dinitrophenylhydrazone had m.p. 260°–262°.

Reduction of Taraxerone

Taraxerone (300 mg.) was dissolved in ether (50 ml.) and lithium aluminum hydride (500 mg.) added. The mixture was refluxed for 3 hours. The excess lithium aluminum hydride was decomposed with ethyl acetate and the ether layer washed with dilute acid and water and evaporated to dryness. The resulting product was crystallized from chloroform–methanol to give taraxerol, m.p. 279°–280°, $[\alpha]_D^{24}$ 0° (c = 1.2 in chloroform). For the constants recorded in the literature see Table I.

Acetylation

Taraxerol (200 mg.) was dissolved in pyridine (10 ml.) and acetic anhydride (3 ml.) added. The mixture was heated on the steam bath for 1 hour, then diluted with benzene and washed with dilute alkali, dilute acid, and water, and evaporated to dryness. The crude product, dissolved in benzene, was filtered through alumina and, after removal of the solvent, the material was crystallized from chloroform–methanol to give the

derived acetate with m.p. 300°–301°, $[\alpha]_D^{25}$ +9° (c = 1.56 in chloroform). Anal. Calc. for $C_{32}H_{52}O_2$: C, 81.99; H, 11.18. Found: C, 81.99; H, 11.00.

Rearrangement of Taraxerol Acetate

Taraxerol acetate (300 mg.) was suspended in acetic acid (30 ml.) and heated to 90°. Concentrated hydrochloric acid (1 ml.) was added and the mixture heated for 15 minutes on the steam bath, in which time all the taraxerol acetate went into solution. The acetic acid was distilled off under reduced pressure and the resulting product crystallized from chloroform–methanol to give β-amyrin acetate (200 mg.), m.p. 239°–240°, $[\alpha]_D^{25}$ +79° (c = 1.15 in chloroform). The values recorded in the literature for the constants are m.p. 241°, $[\alpha]_D$ +82° (11).

The β-amyrin acetate was hydrolyzed in the usual manner to give β-amyrin. Crystallized from aqueous ethanol this had m.p. 195°–196°, $[\alpha]_D^{24}$ +88° (c = 1.34 in chloroform). The values recorded in the literature for the constants are m.p. 197°, $[\alpha]_D$ +89° (11).

The rearrangement when repeated on taraxerone gave β-amyrone, with m.p. 174°–176°, $[\alpha]_D^{24}$ +109° (c = 1.41 in chloroform). The values recorded in the literature for the constants are m.p. 178° $[\alpha]_D$ +107° (7).

Wolff–Kishner Reduction of Taraxerone

Taraxerone (200 mg.) was added to a solution of sodium (500 mg.) in ethanol (5 ml.). Hydrazine hydrate (100%, 1 ml.) was added and the mixture heated in a sealed tube at 180° overnight. The mixture was diluted with benzene, washed with dilute acid and water, and evaporated to dryness. The crude product, dissolved in benzene, was filtered through alumina. After evaporation of the solvent, the resulting product was crystallized from chloroform–methanol to give taraxerene, m.p. 236°–238°, $[\alpha]_D^{24}$ +1° (c = 1.42 in chloroform). The values for the constants reported in the literature are m.p. 237°–238°, $[\alpha]_D$ +1° (2). The infrared absorption spectrum of the material showed no absorption at 1705 cm.$^{-1}$, which would indicate a carbonyl function, and no absorption at 3600 cm.$^{-1}$, which would indicate a hydroxyl group. This proved that the reduction was complete.

Isolation of Taraxerol from Peat Moss

The petrol-insoluble portion of the unsaponifiable material was dissolved in benzene and chromatographed on alumina. Elution with benzene afforded taraxerone (300 mg.), identified by its infrared spectrum. Elution with chloroform–methanol (4:1) afforded taraxerol (400 mg.), recrystallized from chloroform–methanol to give m.p. 278°–279°, $[\alpha]_D^{24}$ 0° (c = 1.17 in chloroform). The melting point was undepressed on admixture with a specimen obtained from the lithium aluminum hydride reduction of taraxerone, and also undepressed on admixture with a genuine specimen of taraxerol of like melting point. Anal. Calc. for $C_{30}H_{50}O$: C, 84.44; H, 11.81. Found: C, 84.77; H, 11.53.

Oxidation of Taraxerol

Taraxerol (500 mg.) was dissolved in pyridine (10 ml.) and the solution added to a suspension of chromium trioxide (1 g.) in pyridine (10 ml.). The mixture was allowed to stand overnight at room temperature, then diluted with water, and sulphur dioxide passed through to destroy the excess chromium trioxide. The mixture was extracted with benzene, and the benzene extract washed free of acid and evaporated to dryness. The crude product was dissolved in benzene and the solution filtered through alumina. After evaporation of the solvent, the resulting material was crystallized from chloroform–methanol to give taraxerone, identical in m.p., specific rotation, and infrared spectrum

with that isolated directly from the unsaponifiable material. This method of oxidation had to be used, since oxidation with chromium trioxide in acetic acid solution led to an impure product, which probably contained β-amyrone, owing to the acid rearrangement of taraxerone.

Isolation of α-Amyrin

The unsaponifiable material (450 g.) from the benzene–ethanol extract of 22 kg. of *Sphagnum* was chromatographed on a 60×4 in. column of alumina using the same solvents as described previously. After the ether–methanol fraction had been treated with urea to remove the lignoceryl alcohol, the residue (50 g.) was acetylated and the mixed acetates chromatographed on alumina. Elution with petrol–benzene (7:3) gave a white crystalline solid (3.5 g.), which on recrystallization from aqueous ethanol had m.p. 224°–225°, $[\alpha]_D^{25}$ +78° (c = 1.26 in chloroform). Anal. Calc. for $C_{32}H_{52}O_2$: C, 81.99; H, 11.18. Found: C, 82.69; H, 11.23. Vesterberg (11) reports m.p. 225°–226° and $[\alpha]_D$ +79° for α-amyrin acetate.

Hydrolysis

α-Amyrin acetate (500 mg.) was dissolved in dioxane (15 ml.) and methanol (20 ml.). Potassium hydroxide (1 g.) in water (3 ml.) was added and the solution heated under reflux for 1 hour. The solution was diluted with water and extracted with benzene, and the extract washed well with dilute acid and water and evaporated to dryness. The product was crystallized from methanol to give m.p. 183°–184°, undepressed on admixture with a genuine sample of α-amyrin, $[\alpha]_D^{25}$ +85° (c = 0.58 in chloroform). Anal. Calc. for $C_{30}H_{50}O$: C, 84.44; H, 11.81. Found: C, 84.56; H, 11.43. The values recorded in the literature for the constants are m.p. 186°, $[\alpha]_D$ +84° (11).

Benzoylation

α-Amyrin (250 mg.) was dissolved in pyridine (5 ml.) and benzoyl chloride (0.25 ml.) added. The mixture was heated on the steam bath for 50 minutes. The solution was diluted with benzene and washed well with dilute alkali, dilute acid, and water. It was then evaporated to dryness. The crude benzoate was dissolved in benzene and the solution filtered through alumina. After evaporation of the solvent the product was crystallized from chloroform–methanol to give α-amyrin benzoate m.p. 191°–193°, $[\alpha]_D^{25}$ +95° (c = 0.86 in chloroform). Anal. Calc. for $C_{37}H_{54}O_2$: C, 83.72; H, 10.25. Found: C, 83.81; H, 9.92. The values recorded in the literature for the constants are m.p. 193°–194°, $[\alpha]_D$ +95° (9).

ACKNOWLEDGMENT

The authors wish to thank Professor F. S. Spring, F.R.S., of the Royal Technical College, Glasgow, for his generous gifts of taraxerol and α-amyrin.

REFERENCES

1. Beaton, J. M., Spring, F. S., Stevenson, R., and Stewart, J. L. J. Chem. Soc. 2131 (1955).
2. Bruun, T. Acta Chem. Scand. **8**, 1291 (1954).
3. Burrows, S. and Simpson, J. C. E. J. Chem. Soc. 2042 (1938).
4. Cole, A. R. H. J. Chem. Soc. 3807 (1954).
5. Ives, D. A. J. and O'Neill, A. N. Can. J. Chem. **36**, 434 (1958).
6. Koller, E., Hiestand, A., Dietrich, P., and Jeger, O. Helv. Chim. Acta, **33**, 1050 (1950).
7. Rollett, A. Monatsh. **43**, 413 (1923).
8. Ruhemann, S. and Raud, H. Brennstoff-Chem. **13**, 341 (1932).
9. Ruzicka, L. and Wirz, W. Helv. Chim. Acta, **22**, 948 (1939).
10. Takeda, K. J. Pharm. Soc. Japan, **61**, 117 (1942).
11. Vesterberg, K. A. Ann. **428**, 243 (1922).

THE EFFECT OF WATER REMOVAL ON THE CRYSTALLINITY OF CELLULOSE[1]

M. KOURIS,[2] H. RUCK,[3] AND S. G. MASON

ABSTRACT

The effect of various modes of drying upon the crystallinity of cellulose has been determined by X-ray diffraction.

No change in the crystallinity index was observed when previously undried pure cellulose fibers from softwood were dried from water under a wide range of conditions, but a lower value was obtained when they were dried from benzene to which the fibers were accommodated by a series of solvent exchanges. Heat of wetting determinations on the same samples indicated changes in the accessibility with different drying methods. Qualitative variations in the degree of intrafiber bonding were also detected by a differential staining method. The X-ray measurements suggested that drying from water either produces no change in lateral order or that such changes are too small to be detectable by X-rays.

The crystallinity of cellulose prepared by dry-milling whole fibers was studied. The crystallinity was substantially reduced in a Wiley mill and obliterated in a ball mill. X-Ray diffraction showed that wetting with water and then drying restored the crystallinity, while similar treatment with other liquids yielded less definite results. However, by following the destruction of the lattice with progressive periods of milling, it was concluded that alcohols reform this lattice to a limited extent depending, among other factors, upon the swelling capacity.

INTRODUCTION

The formation of intermolecular bonds between adjacent cellulose chains by the removal of water is of considerable importance, particularly in connection with technical applications of cellulose, e.g. in textiles and in paper, and has been the subject of numerous investigations. It is now reasonably well established that most of the bonds, which can be either intra- or inter-fiber, depending upon whether or not the cellulose chains are in the same fiber, are due to hydrogen bridges (1) between hydroxyl groups of adjoining chains. As a consequence, the number of available hydroxyl groups, and therefore the accessibility of the fibers, would be reduced if additional hydrogen bridge bonds are formed.

The decrease in accessibility with evaporation-drying has been amply verified by Jayme (2, 3) and Purves *et al.* (4), the former by noting the decreased swelling capacity of dried fibers and the latter by applying the thallous-ethylation method.

Since the drying of cellulose is an irreversible process, any lateral order established by hydrogen-bonding may be expected to increase with repeated wetting and drying of the fibers, and cause a sharpening of the X-ray diffraction pattern of the crystalline portion. In this connection, it has been shown that the capacity of the fibers to reabsorb and retain the water decreases with the severity of drying conditions (3). Recently, it has been observed that freezing the wet fibers before air-drying the thawed material adversely affected the interfiber bonding of paper (5, 6). This effect was attributed to partial dehydration of the fibers as a result of freezing.

The mobility, and hence the alignment of the molecular chains in the amorphous regions of wet cellulose fibers, may be expected to be greatly reduced by freezing the water and removing it by sublimation- or freeze-drying, or by replacing the water by

[1]*Manuscript received February 19, 1958.*
Contribution from Physical Chemistry Division, Pulp and Paper Research Institute of Canada, and Department of Chemistry, McGill University, Montreal, Quebec.
[2]*Holder of the Courtaulds (Canada) Limited Fellowship 1955–57.*
[3]*Present address: Industrial Cellulose Research Limited, Hawkesbury, Ontario.*

a non-polar liquid before drying (6). Fibers dried by this means would be expected to have a higher accessibility than fibers dried by evaporation of liquid water. Although little work has been done on the accessibility of freeze-dried fibers, solvent-exchanged fibers show an increase in reactivity towards various reagents. Thus Siggia *et al.* (7) found an increased accessibility of cotton linters to HIO_4 solution, while Conrad and Scroggie (8) found the same effect towards HCl–$FeCl_3$ attack. A similar trend was observed by Brown and Purves (9) in their nitration experiments on cotton linters. In addition, several workers have shown that a reduction in interfiber bonding, during freeze-drying from water or evaporation-drying from a non-swelling liquid, may be responsible for adversely affecting paper strength. Van den Akker (5), Broughton and Wang (10), and Marchessault, Lodge, and Mason (6) demonstrated that the strength of paper handsheets dried by such methods was considerably less than the strength of normally air-dried sheets. From this it can be seen that the method of drying influences the physical properties of cellulose fibers. In turn these properties may be assumed to be closely related to the degree of hydrogen-bonding, and in turn to the lateral order introduced in the fibers by the drying operation.

In the investigation to be described the effect of different drying conditions on the crystallinity of cellulose fibers was determined by an X-ray diffraction method using the crystallinity index parameter introduced by Ant-Wuorinen (11). This parameter may be considered to be a relative (but not absolute) measure of the fraction of crystalline material. Heat of wetting determinations and a differential staining procedure were also applied to the fibers.

As the crystallinity index of whole fibers proved to be insensitive to drying, attempts were made to magnify the effects by first reducing the crystallinity by mechanical attrition and then wetting with various liquids and drying.

The almost complete destruction of crystallinity of dried cellulose I fibers by ball-milling has been shown by Hess (12) and by Hermans (13), using X-ray diffraction. These workers also showed that wetting the pulverized material resulted in partial recrystallization accompanied by a lattice modification to cellulose II. In the present investigation similar behavior was observed upon rewetting cellulose whose crystallinity had been drastically reduced by dry-grinding fibers in both a Wiley and a ball mill. However, no lattice modifications were observed on wetting. In the case of the Wiley-milled material, recrystallization was observed to occur upon exposure to water vapor of high relative humidity.

The recrystallization of mechanically degraded fibers by non-aqueous liquids has received little attention. Investigating the sorption of vapors by cellulose fibers, Kanamaru and Chao (14), Lauer (15), and Stamm and Tarkow (16) found that the sorptive capacity of cotton for the normal alcohols decreased regularly with increasing molecular weight of the homologous series. From the sparse data available, it is now generally accepted that the penetration and appreciable swelling of cellulosic material can occur only with polar liquids. Furthermore, to encourage rearrangement of the fibers and increase lateral order the swelling medium must be capable of promoting hydrogen-bonding. In this connection, it has been shown that the strength of paper handsheets made by drying from benzene was considerably less than that of handsheets dried from ethanol (10).

In the experiments described below, the variations in the crystallinity index of the mechanically degraded cellulose treated with various organic liquids appeared to parallel their sorption capacity by cellulose.

EXPERIMENTAL

1. Materials

Cellulose Fibers

Softwood dissolving-grade sulphite pulp which had never been previously dried was kindly supplied by Fraser Companies Ltd., Campbellton, N.B., together with the following analytical data:

Viscosity	25.4 cp.
Resin	0.37%
Pentosan	2.42%
Rayon yield	93.7%
10% Caustic insoluble	89.3%

Dried samples were prepared as follows:

Sample F-1.—Oven dried at 105° C.

Sample F-2.—Dried at room temperature. The drying was conducted in two stages. The pulp was first placed in a vacuum desiccator containing concentrated sulphuric acid. After about two days, when the moisture content was reduced to approximately 15%, the pulp was transferred to a desiccator containing phosphorus pentoxide and again evacuated for several days.

Sample F-3.—Cyclic wetting and oven drying. After oven drying at 105° C., the pulp was suspended in water at room temperature for 24 hours, the excess water removed under mild suction, and the pulp again dried at 105° C. This operation was repeated until the sample had been exposed to 10 complete drying cycles.

Sample F-4.—Cyclic wetting and room temperature drying. This sample was subjected to 10 wetting and drying cycles the same as for F-3, except that each drying stage was carried out at room temperature as for F-2.

Sample F-5.—Freeze-drying from water. The water-wet pulp was initially frozen at −78° C. by immersion in acetone/Dry Ice. The ice was then removed by sublimation under vacuum in a laboratory-model freeze-drier.

Sample F-6.—Freeze-drying from benzene. The water-wet pulp was suspended in 200 cc. of acetone which had previously been distilled over activated alumina to remove traces of water. The acetone was replaced several times by a fresh batch until titration of an aliquot with Karl Fischer reagent indicated the absence of water. The pulp was then suspended in 300 cc. of dry benzene, and allowed to stand for 24 hours in a stoppered flask. After a further immersion of 24 hours in a fresh batch of benzene, the latter was decanted and the pulp frozen at −78° C. The benzene (m.p. 5.3° C.) was removed by sublimation under vacuum as for F-5. It was noted that on rewetting the sample with water a strong odor of benzene was detectable. It has been shown that up to 1.5% benzene can be retained in this way (17).

Sample F-7.—Freezing in liquid nitrogen. The adverse effect of ice formation on the bonding properties of fibers has been attributed to a partial dehydration of the fibers at low temperature (6). To determine the effect of this partial dehydration on the crystallinity of cellulose, water-wet pulp was suspended in liquid nitrogen (−195.8° C.) until it had frozen solidly. It was then allowed to thaw at room temperature and finally dried as for F-2. The physical state of the dried pulp depended upon the method of drying. Evaporation of liquid water allowed the capillary forces of water to exert their influence in promoting interfiber bonding, and the fibers tended to be densely packed.

Cyclic wetting and drying produced a bulkier pulp in which the fibers were more easily separated. Pulp which had been dried either by freeze-drying, or from a non-swelling liquid such as benzene, was even less highly bonded than when cyclically dried by evaporation of water.

Wiley-Milled Cellulose

A portion of the same batch of virgin pulp used in the preceding preparation was dried at 105° C. and subsequently milled for 90 minutes in a laboratory attrition mill. An intermediate model Wiley mill was used for this purpose, with a clearance of 7.5×10^{-3} cm. between the stationary and revolving blades. Small quantities of the milled material, which was fine enough to pass a 60-mesh screen, were immersed in pure liquids, having various swelling capacities, for 24 hours at room temperature and then dried as listed in Table I.

TABLE I

TREATMENT OF WILEY-MILLED SAMPLES

Sample	
M-1	Original milled sample
M-2	M-1 immersed in water, 24 hours R.T., dried at 105° C.
M-3	Treatment for M-2 repeated 10 times
M-4	M-1 immersed in ethanol, 24 hours R.T., dried at 105° C.
M-5	Treatment for M-4 repeated 10 times
M-6	M-1 immersed in acetone, 24 hours R.T., dried at 105° C.
M-7	Treatment for M-6 repeated 10 times
M-8	M-1 exposed in a vacuum desiccator to water vapor at 93.3% R.H. for 48 hours, dried at 105° C.

Ball-Milled Cellulose

A series of ball-milled samples of dissolving grade "Rayaceta" wood pulp were kindly supplied by Dr. J. A. Howsmon of the American Viscose Corporation, Marcus Hook, Pa. The dry material had been milled for various times up to 153 hours under the following conditions:

Initial treatment of pulp	Wiley Mill, 20-mesh screen
Ball-mill charge	1200 g. steel balls, 40 g. pulp
Mill speed	47 r.p.m.

To follow the destructive action of ball-milling on the crystallinity of cellulose the samples milled for progressive periods were subjected to X-ray measurements. These samples are denoted by the letter H, followed by the number of hours milled.

In addition, small quantities of sample H-153, which was completely pulverized, were subjected to various wetting and drying treatments as outlined in Table II. Except for sample B-4, the wetting and drying procedures were as for the Wiley-milled material.

The differently treated samples prepared from both sets of milled materials remained powdery and to the eye were unchanged from the untreated material.

2. EXPERIMENTAL METHODS AND RESULTS

X-Ray Measurements

General

A transmission technique based on that of Hermans (18) was adopted for the X-ray measurements, except that air scattering was used as a reference for the incident X-ray

TABLE II

TREATMENT OF BALL-MILLED SAMPLES

Sample	
B-1	Original ball-milled sample H-153 (milled for 153 hours)
B-2	B-1 immersed in water, 24 hours R.T., dried at 105° C.
B-3	Treatment for B-2 repeated 10 times
B-4	B-1 treated as described for cellulose fibers (sample F-6) with benzene removed at 105° C.
B-5	B-1 immersed in benzene, 24 hours R.T., dried at 105° C.
B-6	B-1 immersed in ethanol, 24 hours R.T., dried at 105° C.
B-7	Treatment for B-6 repeated 10 times
B-8	B-1 immersed in acetone, 24 hours R.T., dried at 105° C.
B-9	Treatment for B-8 repeated 10 times
B-10	B-1 immersed in methanol, 24 hours R.T., dried at 105° C.
B-11	B-1 immersed in propanol, 24 hours R.T., dried at 105° C.
B-12	B-1 immersed in butanol, 24 hours R.T., dried at 105° C.

intensity instead of a Goppel (19) camera, and the samples were mounted in the form of compressed pellets which were supported in a holder during an exposure. In addition, a nickel foil was used for X-ray absorption measurements.

Fig. 1 shows the disposition of the various parts of the camera and collimating system. The nickel-filtered copper radiation was delivered by a Muller MC-50 tube. A 9×12 cm. flat film camera, manufactured commercially by R. Seifert & Co., Hamburg, Germany, was used. Its collimator was replaced by a four-pinhole system and a removable nickel foil was incorporated as shown in Fig. 1. Details of construction are to be published separately.

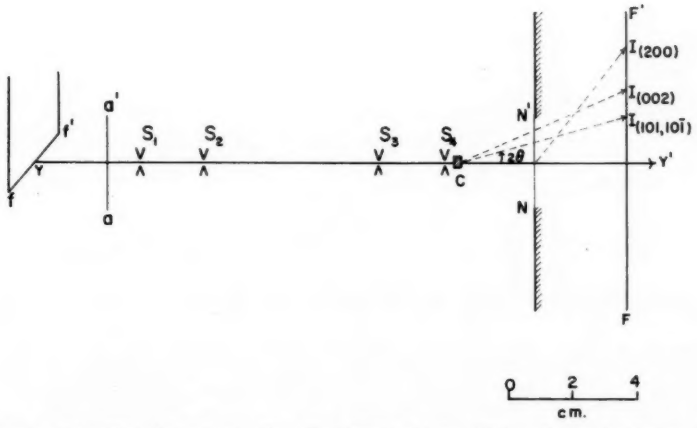

FIG. 1. Camera and collimating system. ff′ = Focal spot of tube. YY′ = Path of primary beam. aa′ = Nickel filter. S_1S_4 = Pinhole apertures, 1 mm. S_2S_3 = Pinhole apertures, 0.7 mm. C = Sample. NN′ = Nickel foil, 0.021 mm. thick, supported on metal frame. FF′ = Film. $I_{(200)}$ = Nickel interference. $I_{(101,10\bar{1})}$, I_{002} = Cellulose A_4 and A_1 interference respectively.

Mounted pellets were prepared from whole fibers by separating them with two dissecting needles until the resulting material was a mass of loosely tangled individual fibers. A weight of 3 mg, ±3% of the loose fibers was placed in a metal sample holder and compressed into a pellet by a specially-constructed press, care being taken to ensure isotropic packing in the plane of the holder. Pellets of the milled cellulose were formed in the

same manner but with no previous scraping. For an exposure to the X-ray beam, the loaded pellet holder was mounted on the collimator. The dimensions and densities of the pellets are given in Table III.

TABLE III

DIMENSIONS AND DENSITIES OF PELLETS

Pellets	Diameter, mm.	Thickness (t), mm.	Density (ρ), g./cm.^{3}
Cellulose fibers	3.0	1.7	0.25
Wiley-milled cellulose	3.0	0.5	0.85
Ball-milled cellulose	3.0	0.4	1.06

All exposures were made at room temperature and at the prevailing relative humidity, which was in the region of 50%. Ilford-B film was used throughout.

Measurements of Intensity

To determine the intensities of X-ray diffraction lines on a film, a continuous recording microdensitometer, manufactured by A. Krüss, Hamburg, Germany, was used. The sensitivity of the galvanometer was adjusted to give zero deflection in the unexposed region, and a full-scale deflection of 80 mm. when no light was transmitted through the film. Fig. 2 is a reproduction of a photometer trace of a diffraction pattern of wood

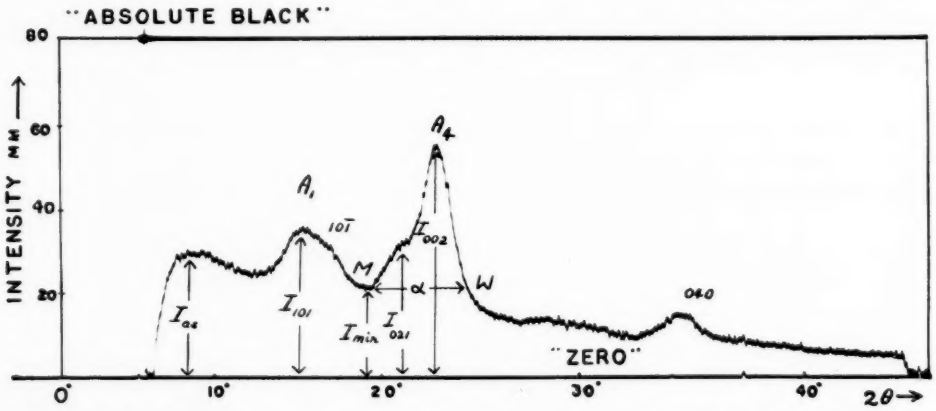

FIG. 2. Radial photometer trace of an X-ray diffraction pattern of wood pulp. I_{aa} = Maximum intensity of air scattering. I_{101} = Intensity of (101) peak. I_{min} = Intensity of minimum point M. I_{021} = Intensity of (021) peak. I_{002} = Intensity of (002) peak. α = Width MW of peak (002) in radians. A_1, A_4 = Herzog designation of peaks (101) and (002), respectively.

pulp. The traces of the extreme positions of the galvanometer deflections are shown as the "zero" and "absolute black" lines. The height in mm., above the "zero" line, of any point on the trace is a measure of its intensity. The Herzog (20) designations and Miller (21) indices (*hkl*) of the principal planes of cellulose corresponding to the various peaks are included in Fig. 2. The maximum intensity of air scattering, I_{aa}, occurs at an angle $2\theta = 7° 30'$.

Measurements of Absorption

Since sample F-6 contained entrapped benzene, measurements were made to determine

any change in its X-ray absorption coefficient, using sample F-1 as a standard. In making absorption measurements the sample was alternately placed in position and removed, and two exposures at the same intensity were made of the nickel foil NN′ (Fig. 1). From the difference in intensity of the (200) nickel interference the absorption $\mu_m\rho t$ of the sample was calculated using (see Ref. 18):

$$\ln(I_{Ni})_{air} - \ln(I_{Ni})_{cell.} = \mu_m\rho t, \quad [1]$$

where

$(I_{Ni})_{cell.}$, $(I_{Ni})_{air}$ = intensity of (200) nickel interference with and without sample in position respectively,
μ_m = mass absorption coefficient of the sample (cm.²/g.),
ρ = packing density in the sample (g./cm.³),
t = thickness of the sample in cm.

The resulting values of $\mu_m\rho t$ for samples F-1 and F-6, 0.383 and 0.363 respectively, agreed within experimental error indicating equal absorption coefficients. Hence, no correction was applied to the observed peak height of sample F-6; in Hermans' experiments such corrections were necessary (22).

Determination of Crystallinity Index

(*i*) *Cellulose Fibers*

Following the method of calculation used by Ant-Wuorinen (11), the per cent crystallinity index, X, is given by the following equation, which is readily derived from Ant-Wuorinen's equations:

$$X = \{1 - [80\alpha/(I_{002} - I_{min})]\} \times 100, \quad [2]$$

where, as illustrated in Fig. 2,

I_{002} = height of A_4 peak in mm.,
I_{min} = height of minimum point M above "zero" line in mm.,
α = width (MW) of peak A_4 in radians.

TABLE IV

PROCEDURE FOR IRRADIATION OF SAMPLES

Series	Samples	Pellets per sample	Exposures per pellet	Anode voltage, kv.	Anode current, ma.	Time of each exposure, min.
1	F-1 to F-7	4	1	30	20	65
2	M-1 to M-8	1	3	30	≈20	45, 80, 100
3	B-1 to B-12	1	3	30	≈20	45, 80, 100
4	H-0 to H-153	1	1	30	≈20	80

The conditions of irradiation for Series I, Table IV, produced a maximum intensity of air scattering, I_{as}, of 30 mm. and α was found to be independent of the intensity of irradiation. The results of the X-ray measurements for cellulose fibers are shown in Table V. Sample M-1 has been included for comparison.

(*ii*) *Milled Cellulose Samples*

For every sample in Series 2 and 3, Table IV, I_{as} was plotted against the corresponding values of I_{101}, I_{002}, and I_{min} obtained from the photometer trace as in Fig. 2. Excellent

TABLE V

X-RAY AND HEAT OF WETTING DATA FOR CELLULOSE FIBERS

Sample No.	Treatment	A_1 I_{101}, mm.	A_4 I_{002}, mm.	I_{min}, mm.	α, radians	X, %	Heat of wetting, cal./g.
F-1	Oven-dried at 105° C.	32.8 (1.1)†	48.8 (2.1)	21.9 (0.63)	0.0989	70.6 (1.05)	13.06
F-2	Drying at room temperature over P_2O_5	33.2 (1.03)	49.0 (2.2)	21.7 (0.97)	0.0989	71.0 (1.2)	13.90
F-3	Sample F-1, rewetted at room temperature and dried at 105° C. (10 times)	32.0 (1.3)	49.1 (2.3)	20.0 (0.53)	0.0989	72.8 (1.5)	11.80
F-4	Sample F-2, rewetted and dried at room temperature over P_2O_5 (10 times)	32.7 (1.06)	48.0 (2.4)	21.8 (1.4)	0.0989	69.8 (1.4)	12.98
F-5	Original wet sample freeze-dried	33.6 (1.2)	48.2 (2.2)	22.5 (1.1)	0.0989	69.2 (1.4)	13.68
F-6	Original wet sample solvent-exchanged to and freeze-dried from benzene	32.1 (1.05)	44.2 (1.7)	22.5 (0.76)	0.0989	63.5 (1.3)*	11.98
F-7	Original wet sample, immersed in liquid nitrogen, allowed to melt, and dried at room temperature over P_2O_5	31.2 (1.0)	44.3 (1.9)	20.3 (0.65)	0.0989	67.0 (2.0)	13.46
M-1	Original wet sample dried at 105° C. and Wiley-milled	28.0	28.0	21.5	0.0817	0.00	17.40

Repeated 6 months later with same result.
†*Quantities in parentheses denote standard deviations from the associated mean values.*

TABLE VI

X-RAY DATA FOR WILEY-MILLED CELLULOSE

Sample No.	Treatment	A_1 I_{101}, mm.	A_4 I_{002}, mm.	I_{min}, mm.	α, radians	X, %	K_{002}
M-1	Original milled sample	28.0	28.0	21.5	0.0817	0.00	0.934
M-2	M-1 water-wetted and dried	30.0	37.0	21.0	0.0989	50.5	1.230
M-3	M-1 water-wetted and dried (10 times)	30.3	40.0	19.5	0.0989	61.4	1.330
M-4	M-1 immersed in ethanol and dried	27.8	32.0	20.5	0.0946	33.8	1.065
M-5	M-1 immersed in ethanol and dried (10 times)	27.8	28.5	18.5	0.0903	28.7	0.956
M-6	M-1 immersed in acetone and dried	29.4	29.5	22.5	0.0946	—ve	0.975
M-7	M-1 immersed in acetone and dried (10 times)	29.4	30.0	21.5	0.0903	15.0	1.018
M-8	M-1 exposed to water vapor at 93.3% R.H. and dried	30.0	36.5	20.5	0.0989	50.5	1.200

straight lines of the type shown in Fig. 3 were obtained. The lines passed through the origin and the linearity was maintained up to an optical density of film blackening of 0.9. The values at I_{as} = 30 mm. were obtained from the respective graphs and X determined from Equation [2]. The same procedure was applied to samples exhibiting no interferences associated with crystallinity, except that the maximum intensity of the "amorphous" halo, I_{AmH}, was measured. Furthermore, the absence of the peaks A_4 and A_1 eliminated the minimum point M between them, and α could not be measured.

The results of the X-ray measurements on the Wiley- and ball-milled cellulose are recorded in Tables VI and VII, respectively.

For Series 4, Table IV, the values of I_{101}, I_{021}, I_{002}, I_{min}, and I_{AmH}, measured at the I_{as} of the exposure, were reduced to an I_{as} = 30 mm. by multiplying by the factor 30/measured I_{as}. The results of the X-ray experiments on the samples milled for progressive periods are recorded in Table VIII. It is interesting to note that it took more than 100 hours of ball-milling to render the photometer tracing uniform. Ellefsen *et al.* (23) report that no change was observed after 6 hours of milling in their recent experiments.

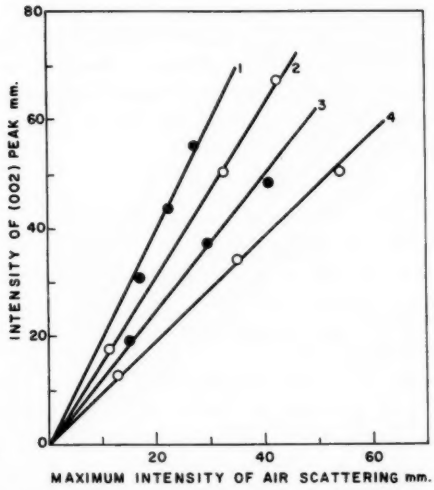

FIG. 3. Variation of intensity of (002) peak with crystallinity of cellulose and maximum intensity of air scattering. 1 = Dewaxed cotton linters. 2 = Sample F-7. 3 = Sample M-2. 4 = Sample M-1.

TABLE VII

X-RAY DATA FOR BALL-MILLED CELLULOSE

Sample No.	Treatment	A_1 I_{101}, mm.	A_4 I_{002}, mm.	I_{min}, mm.	α, radians	I_{AmH},* mm.	X, %	K_{002}
B-1	Original milled sample					28.5		
B-2	B-1 water-wetted and dried	28.0	34.0	23.0	0.0989		28.0	1.115
B-3	B-1 water-wetted and dried (10 times)	27.5	35.0	21.0	0.0946		45.9	1.170
B-4	B-1 water-wetted and dried from benzene	26.0	31.5	22.5	0.0989		12.0	1.040
B-5	B-1 immersed in benzene and dried					28.5		
B-6	B-1 immersed in ethanol and dried					26.0		
B-7	B-1 immersed in ethanol and dried (10 times)					29.0		
B-8	B-1 immersed in acetone and dried					28.0		
B-9	B-1 immersed in acetone and dried (10 times)					28.5		
B-10	B-1 immersed in methanol and dried					28.5		
B-11	B-1 immersed in propanol and dried					29.5		
B-12	B-1 immersed in butanol and dried					27.5		

*I_{AmH} = *maximum intensity of "amorphous" halo.*

TABLE VIII

X-RAY DATA FOR CELLULOSE BALL-MILLED FOR PROGRESSIVE PERIODS

Sample (hours of milling)	A_1 I_{101}, mm.	I_{021}, mm.	A_4 I_{002}, mm.	I_{AmH}, mm.	I_{min}, mm.	α, radians	X, %
H-0	32.2	29.2	45.1		22.1	0.0946	67.1
H-16	30.0	27.3	35.0		21.3	0.0946	44.8
H-32	31.0	28.4	32.3		23.7	0.0946	12.0
H-48	26.8	24.5	24.8		21.5	0.0903	
H-68	25.7	24.0	23.0		21.2	0.0860	
H-80	26.2		23.4	25.6	23.4	0.0860	
H-96	25.8			26.1	24.2		
H-114	25.7			26.2	24.8		
H-132	26.8			28.7	26.8		
H-153				28.5	25.6		

Value of K_{hkl} and Crystallinity

The ratio of a cellulose interference, I_{hkl}, and the intensity of a reference line of the Goppel (19) camera used by Hermans (18) yields a value independent of the energy of irradiation. A similar result is obtained if the Goppel interference is replaced by the maximum intensity of air scattering, I_{as}, occurring at an angle $2\theta = 7° 30'$.

Thus

$$I_{hkl}/I_{as} = K_{hkl}. \qquad [3]$$

Any variation of I_{as} with atmospheric pressure was neglected.

The air scattering peak did not contain any appreciable contribution from the cellulose. This was established by means of diffraction patterns of cellulose obtained with a Kiessig small-angle vacuum camera, both with and without a vacuum. Under vacuum the scattered intensity at $7° 30'$ was negligible, a circumstance which made it possible to use air scattering for standardization.

In Table VI it is seen that in certain cases, although the diffraction pattern showed the unmistakable presence of A_1 and A_4 peaks, X failed to represent the state of crystallinity of samples subjected to severe mechanical degradation. In addition, the difficulty in measuring α caused by the broadening of the minimum between A_1 and A_4 peaks introduces an error of (0.16 to 0.20) X, when X is in the range 20 to 30%. Since the A_4 peak is more sensitive to crystallinity changes than A_1, the value of K_{002} may provide a parameter which is less susceptible to error and which is capable of continuously representing the state of crystallinity of cellulose. Assuming approximately equal size distribution of crystallites, I_{002} for a given I_{as} will be greater for a more crystalline than for a less crystalline sample.

In Tables VI and VII, K_{002} was determined from the slope of the straight lines obtained by plotting I_{as} vs. I_{002}. Fig. 3 shows the plot of I_{002} vs. I_{as} of four cellulose samples of different degrees of crystallinity. Dewaxed cotton linters, a cellulose of high crystallinity which is estimated from various methods to amount to 70% (22), was included for comparison. I_{002}, X at $I_{as} = 30$, and K_{002} are given in Table IX. Fig. 3 and Table IX show that K_{002} decreases together with X, and in addition, gives a positive value in the case of sample M-1 where X indicates somewhat misleadingly the total destruction of crystallinity.

TABLE IX

VARIATION OF I_{002}, X, AND K_{002} WITH DEGREE OF CRYSTALLINITY

No.	Sample	A_4 I_{002}, mm.	X, %	K_{002}
1	Dewaxed cotton linters	58.5	79.8	1.950
2	F-7	44.3	67.0	1.535
3	M-2	37.0	50.5	1.230
4	M-1	28.0	0.0	0.934

Heats of Wetting

Heats of wetting by liquid water were measured for samples F-1 to F-7 and M-1 using a Bunsen isothermal calorimeter with diphenyl ether as the working substance (24). The apparatus was kept in a thermostat maintained at $26.90 \pm 0.003°$ C. The results of these experiments are given in Table V.

Differential Staining

Differential staining of fibers provides a visual and qualitative means of demonstrating variations in the density of amorphous cellulose and the degree of fibrillation

(25). Samples F-1 to F-7 were dyed with a solution of equal parts of Benzo-Fast Yellow A and Benzo Brilliant Blue 6BS. The dyes were obtained from Bayer, Farbenfabriken, Leverkusen, Germany. The technique used by Jayme (26) was followed in its entirety. The results of the differential staining experiments are shown in Table X.

TABLE X

DIFFERENTIAL STAINING

Sample No.	Sample preparation	Color after staining
1	Sample F-2 (at room temperature over P_2O_5)	Pale green
2	Sample F-4 (10 times as No. 1)	Pale green
3	Wet (virgin) pulp	Yellowish
4	Sample F-3 (10 times as No. 8)	Blue
5	Sample F-5 (freeze-dried)	Greenish yellow
6	Sample F-7 (wet sample in liquid N dried as No. 1)	Greenish yellow
7	Sample F-6 (solvent exchanged)	Yellowish
8	Sample F-1 (dried once at 105°)	Blue to blue-green

Viscosity

To follow the effect of mechanical degradation on the degree of polymerization (D.P.), viscosity measurements were made on samples F-1 and M-1 and H-0 to H-153. The viscosity pipette procedure described in Tappi, method T-230 sm-50, was followed in its entirety.

The intrinsic viscosities were calculated from Schulz and Blaschke's (27) equation:

$$\eta_{sp}/c = [\eta](1+k'\eta_{sp}), \qquad [4]$$

where

η_{sp} = specific viscosity,
c = concentration of cellulose in g./dl.,
k' = $2.303k$,
k = 0.13 (Martin's (28) constant),
$[\eta]$ = intrinsic viscosity in dl./g.

The degree of polymerization was calculated from the equation in Ref. (29):

$$\text{D.P.} = 156[\eta]. \qquad [5]$$

The intrinsic viscosities and D.P. values are recorded in Table XI.

TABLE XI

VARIATION OF D.P. OF CELLULOSE WITH MECHANICAL TREATMENT

Sample No.	$[\eta]$, dl./g.	D.P.
F-1	2.70	422
M-1	2.49	389
H-0	4.83	755
H-16	2.68	418
H-32	2.57	402
H-48	2.41	376
H-68	2.24	350
H-80	2.08	325
H-96	1.94	303
H-114	1.79	279
H-132	1.62	253
H-153	1.53	239

DISCUSSION

Cellulose Fibers

From Table V it is seen that drying cellulose fibers under different conditions produced little change in the crystallinity index, X. Although the diffraction pattern of fibers dried by evaporation of water and freeze-drying remained unaltered, the heats of wetting varied with the method of drying. Only in sample F-6 (the results of which were duplicated) could a change in X be detected. On immersing sample F-6 in water at room temperature for 24 hours and then drying for 24 hours, it was found that X increased to 67.6% so that the increase in X due to drying from water must be considered to be real.

The results obtained for samples F-1 to F-4 and F-7 suggest that any relative changes in crystallinity, arising from variations in intrafiber bonding with the method of drying, were small compared with other changes tending to decrease the accessibility, as indicated, by the heats of wetting. Since the quantity of heat evolved when cellulose is wetted with water is believed to be primarily due to an interaction of the water molecules with free hydroxyl groups of the cellulose, it may be taken as a measure of the accessibility of these hydroxyl groups (30). On this assumption, it may be inferred that in conformity with previous findings, the vitrified regions (2) and junction points (31) established with a first drying in samples F-1 and F-2 increase with repeated wetting–drying cycles (samples F-3 and F-4) as well as with the temperature of drying. The formation of impenetrable vitreous regions and junction points would then immobilize and prevent the interaction of any available hydroxyl groups with the water molecules without necessarily increasing lateral order.

Freezing the fibers as in sample F-7 may have reduced their hydrophilic (32) character and produced the same effect on the accessibility as drying at a temperature between 105° C. and room temperature. In freeze-drying cellulose fibers the plasticizing action of water is reduced and the mobility of the molecular chains curtailed. In addition, previous work has shown that freeze-drying decreases interfiber bonding especially in the absence of hemicellulosic material (5, 6). Since benzene is a poor swelling and a poor hydrogen-bonding medium, it may be reasonable to conclude that the degree of alignment of the molecular chains in the amorphous region during drying from benzene is less than with water. Hence, any additional crystallization produced in this manner in drying from water will be absent with benzene-dried fibers. Fibers dried in this manner would be expected to have a lower X (as was found for sample F-6) and a higher value of heat of wetting than fibers dried by evaporation of water. However, since sample F-6 contained trapped benzene, the heat of wetting of 11.98 cal./g. is of doubtful validity.

An attempt was made to determine X by taking a diffraction diagram of wet (virgin) fibers, but it proved unsuccessful because it was not possible to make a quantitative separation of the X-ray scattering due to water from that due to cellulose.

Table X shows the effect of different drying procedures on the staining of cellulose fibers. The color differences resulting from the staining procedure depend upon the dyeing properties of the different components of the dyes. The main component of the yellow dye has a greater affinity for cellulose than either component of the blue dye, but the blue dye is composed of smaller molecules than the yellow dye. Hence, the blue dye can enter a capillary network into which the yellow dye, in spite of its greater affinity for cellulose, is not admitted (26). A cellulose structure having fine capillaries will be dyed blue to blue-green, while a structure in which the molecular chains are less highly bonded would stain yellow.

As could be seen under the microscope, in the virgin as well as the solvent-exchanged sample, intrafiber bonding was least and a yellow color resulted. In contrast, the highly bonded fibers resulting from the evaporation of water acquired a similar blue to blue-green color exhibited by the oven-dried sample. The color of the freeze-dried sample further indicated that drying by sublimation of water reduced intrafiber bonding to a smaller extent than drying by solvent exchange.

The variations in color became more distinct when the stained fibers were viewed in bulk. The most striking differences in color were again exhibited by the undried (virgin) and solvent-exchanged samples No. 3 and 7, respectively. Fibers dried by room-temperature evaporation of water stained pale green (No. 1) and the color did not intensify when the fibers were stained after having been wetted, and dried 10 times (No. 2). Fibers dried by evaporation of water at 105° C. stained pale blue (No. 8), while fibers which had been wetted at room temperature and dried at 105° C. exhibited a more intense blue color upon staining (No. 4). Freeze-drying (No. 5) or treatment with liquid nitrogen (No. 6) resulted in greenish-yellow fibers upon staining.

From these results it could be inferred that intrafiber bonding was least in the undried (virgin) pulp sample and greatest in sample F-3 (No. 4). Further work is in hand to measure the reflection spectra between 400 and 700 mμ of the differentially stained pulps. Preliminary measurements have indicated that a quantitative method of measuring the degree of vitrification can be worked out.

Milled Cellulose

From Tables V, VI, and VII it is seen that Wiley-milling increased the heat of wetting of cellulose fibers and reduced X to zero, while ball-milling completely destroyed the crystallinity. Figs. 4, 5, and 6 are reproductions of photometer traces of X-ray diffraction patterns of F-1, M-1 and M-2, B-1, B-2 and B-4, and B-1 (in the dry and wet state), respectively. By comparing Fig. 4(*b*) with 4(*a*), the following points may be noted:

(1) Wiley-milling reduced the intensity of the A_1 and A_4 peaks.

(2) The grinding action preferentially destroyed the $A_4(002)$ planes, reducing the A_4 peak intensity to 57% of its value in F-1, while the A_1 peak suffered a reduction of only 20%.

(3) The width α in M-1, a measure of the crystallite size, was also reduced.

In contrast, the X-ray diffraction pattern of B-1 showed only a diffuse halo, which

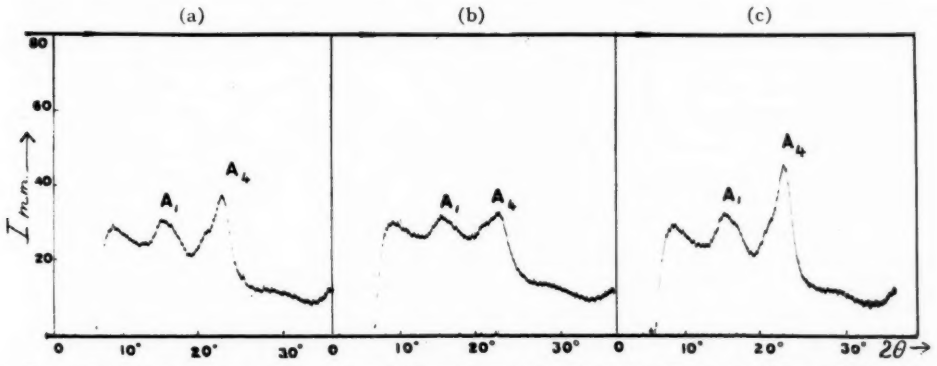

FIG. 4. Radial photometer traces of X-ray diffraction patterns of cellulose fibers and Wiley-milled cellulose. (*a*) Sample M-2. (*b*) Sample M-1. (*c*) Sample F-1.

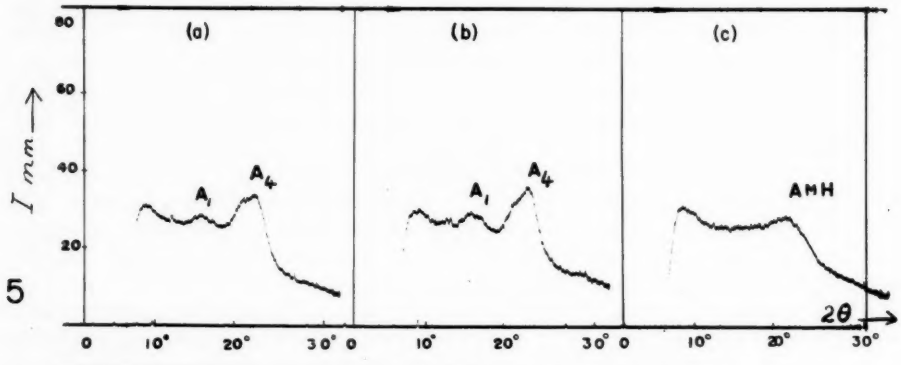

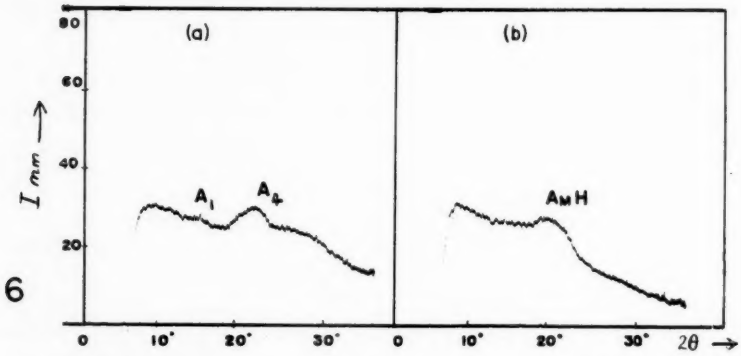

FIG. 5. Radial photometer traces of X-ray diffraction patterns of ball-milled cellulose. (*a*) Sample B-4. (*b*) Sample B-2. (*c*) Sample B-1.

FIG. 6. Radial photometer traces of X-ray diffraction patterns of dry and wet ball-milled cellulose. (*a*) Sample B-1—wet. (*b*) Sample B-1—dry.

can be seen in Fig. 5(*a*) as a broad maximum in the region previously occupied by the (021) peak.

Treatment of the milled material with water resulted in the following behavior:

(1) Partial restoration of crystallinity, Figs. 4(*c*) and 5(*b*).

(2) Exposure of the Wiley-milled product to water vapor at 93.3% R.H. resulted in the same degree of recrystallization as for M-2.

(3) Repeated wetting and drying (samples M-3 and B-3) further increased X.

(4) Recrystallization of B-1 occurred in the wet state, Figs. 6(*a*) and 6(*b*).

(5) Displacing the water from the wetted ball-milled sample with benzene and drying from the non-polar solvent resulted in a smaller degree of recrystallization than with B-2, Fig. 5(*c*).

(6) No modification to cellulose II occurred, but a slight shift was observed in the position of the A_4 peak of the treated ball-milled samples.

Treatment of the Wiley-milled samples with organic liquids gave smaller X values than with water. Because of the large error associated with such small values of X, the state of crystallinity can be better appreciated by referring to the K_{002} values. It is seen that a single wetting with ethanol gave, as expected from its greater swelling power, a larger K_{002} value than acetone. Anomalously, a lower K_{002} value was obtained

for repeated wetting and drying from ethanol than for a similar treatment using acetone, but this may have been due to contamination of the acetone with water. In contrast, treatment of the ball-milled samples with organic liquids produced no detectable X-ray interferences associated with crystallinity.

The increase in the heat of wetting of sample M-1 may be readily explained by an increase in the number of available hydroxyl groups. The disruption of the hydrogen-bonded crystalline lattice and the reduction in the degree of polymerization of the fibers with grinding (Table XI) exposed hitherto unavailable hydroxyl groups which could then react with the water molecules. Although a reduction in the size of the crystallites may be expected to produce an increase in the width α of the A_4 peak in sample M-1, the observed decrease may be attributed to a change in the distribution of the crystallite size with the larger crystallites surviving the destruction action better than the smaller ones. The progressive decrease in α with milling, observed in Table VIII, is at present inexplicable.

In order to explain the recrystallization of the milled material with water it may be assumed that mechanical degradation, in destroying the crystalline regions, also ruptures the junctions restraining normal swelling of the fibers. The plasticizing action of water, by conferring mobility on the chains, allows their realignment and the surface tension of water during drying promotes hydrogen-bonding, which increases the lateral order. Repeated wetting and drying may be expected to further extend the process of realignment and a higher degree of lateral order may be attained.

The identical results obtained for samples M-2 and M-8 may indicate that removal of the water in the earlier stages of drying contributes little to recrystallization. Upon addition of water beyond the range of "bound" water the rapid rise in the sorption isotherm in the high humidity regions cannot be explained by assuming formation of new sorption sites by swelling. In the opinion of various workers, water in the high relative humidity regions is adsorbed as multilayers (33), or by capillary condensation (34), or by solution of the non-crystalline cellulose (35).

Such water will condense within the structure with heat effects associated with normal condensation (36, 37). However, since only imbibed water can affect the intrinsic properties of the fibers and promote their rearrangement, it is reasonable to assume that recrystallization of M-8 had occurred in the range of 60–70% R.H.

Broughton and Wang (10), investigating the strength of handsheets dried from non-aqueous liquids, observed a similar behavior. Upon conditioning butanol-dried handsheets to water vapor of 85% R.H., the strength attained was found to be as great as that of a sheet initially formed from water. These authors did not discount the possibility of an increase in bonding occurring only at the onset of capillary condensation. According to Barkas (38), such condensation begins at a relative humidity of 65–70%.

By comparing values of α for the undegraded and milled material, it may be inferred that the mending action of water reproduced the same distribution of crystallite size existing before degradation. The low X and K_{002} values obtained for sample B-4 fall within expectation. Here, as in sample F-6, the mobility of the chains in benzene was greatly curtailed and there was little tendency for hydrogen-bonding, and hence on drying resulted in a low degree of lateral order. These results further confirm previous findings that drying from benzene is much less effective in bond formation in fibers than drying by sublimation of water (10).

The results obtained for samples M-4 to M-7 indicate that the amount of recrystallization occurring on drying increases with the swelling capacity of the liquid. As expected,

ethanol produced a higher lateral order than acetone, but less than for water. From the results of the ball-milled samples treated separately with benzene and acetone, it is concluded that no recrystallization is possible with these liquids. The almost complete absence of order in the ball-milled samples, and the smaller swelling capacities for cellulose of the alcohols with respect to water, may be responsible for the failure of these media to produce any detectable recrystallization. Here, it may be assumed that the relatively weaker swelling medium is unable to align the molecular chains without the initial presence of well-defined crystallites to act as anchoring points.

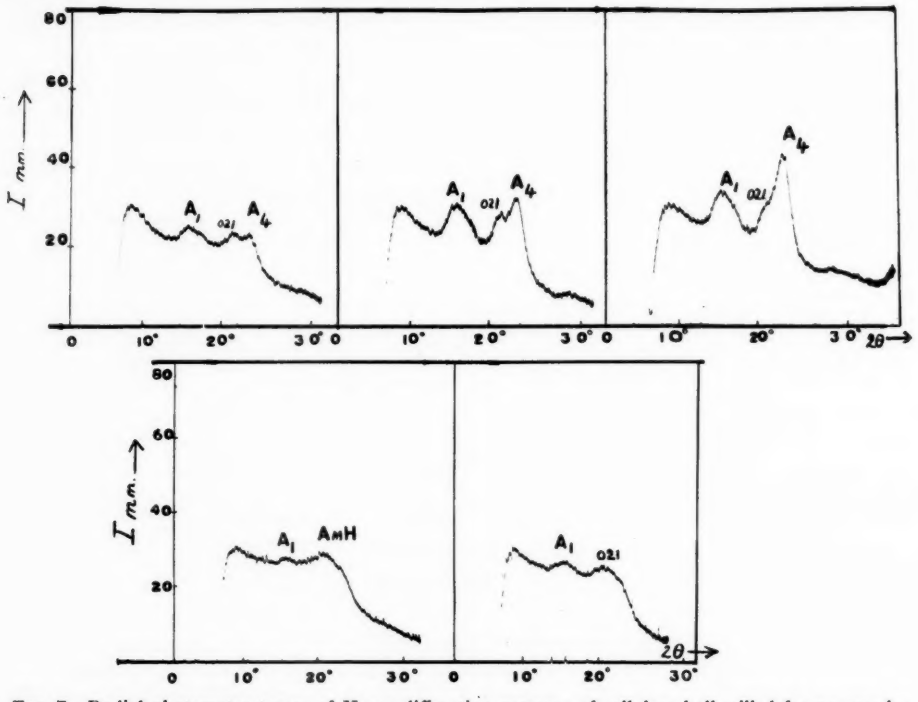

FIG. 7. Radial photometer traces of X-ray diffraction patterns of cellulose ball-milled for progressive periods. *Top*—Left: Sample H-68. Center: Sample H-32. Right: Sample H-0. *Bottom*—Left: Sample H-132. Right: Sample H-96.

Although in this case the presence of nuclei of ordered regions appears necessary for recrystallization, a further conclusion may be drawn from the variations in the intensity of the amorphous halo I_{AmH}, for the alcohol-treated samples. Fig. 7 is a reproduction of photometer traces of X-ray diffraction patterns of H-0, H-32, H-68, H-96, and H-132. From the traces and Table VIII, the following observations were made:

(1) The A_4 peak diminished steadily and disappeared after 80 hours of milling.

(2) The (021) peak also diminished and disappeared between 68 and 80 hours of milling, being replaced by an amorphous halo.

(3) The position of the maximum intensity of the amorphous halo coincided with the position of the (021) peak it replaced.

(4) The intensity of the amorphous halo increased and finally levelled out after 132 hours of milling.

(5) The A_1 peak resisted initial degradation and began to suffer only after 32 hours of milling.

(6) Table VIII shows that the intensity of I_{min} increased with decreasing crystallinity and hence may be taken as a measure of the amorphous content.

(7) The increasing intensity of I_{min} helped to maintain constant the intensity of the A_1 peak which merged with the background after 132 hours of milling.

Fig. 8 shows a plot of the intensity of the (021) peak against time of milling. The curve has a minimum region where the transition from the (021) peak to the amorphous halo takes place. The intensity of the (021) peak decreases gradually with milling until, after 70 hours, the intensity of the amorphous halo predominates, and increases with continued milling. After approximately 130 hours, it reaches its final value of 28.5 mm. This stage appears to mark the limiting effect of the grinding process, for although the sample probably is not completely amorphous, the intensity of the "amorphous" halo remains constant with further milling.

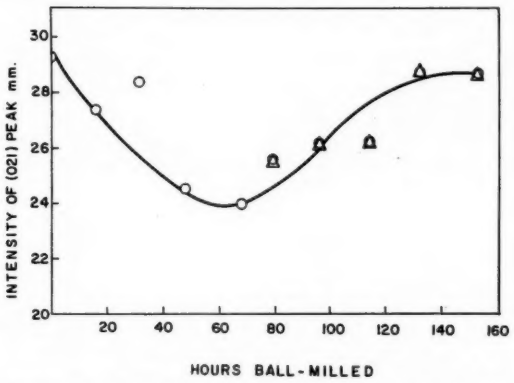

FIG. 8. Variation in intensity of (021) peak with time of ball-milling. Circles: I_{021}. Triangles: I_{AmH}.

The variations in I_{AmH} may be taken to herald the beginnings of the (021) lattice planes of cellulose I, and the I_{AmH} values for the ethanol- and methanol-treated samples may be considered to be I_{021} values on the left of the transition region in Fig. 8. It is evident that propanol and butanol are hindered (sterically or otherwise) from penetrating the degraded cellulosic structure; no (021) lattice planes are formed. Although the evidence is inconclusive, the formation of the (021) lattice planes under these conditions should not be discounted.

ACKNOWLEDGMENTS

The authors are indebted to Dr. R. M. Screaton for measuring the heats of wetting.

REFERENCES

1. CORTE, H. and SCHASCHEK, H. Das Papier, **9**, 519 (1955).
2. JAYME, G. Cellulosechemie, **21**, 73 (1943).
3. JAYME, G. Papier-Fabr. **42**, 187 (1944).
4. ASSAF, A. G., HAAS, R. H., and PURVES, C. B. J. Am. Chem. Soc. **66**, 66 (1944).
5. VAN DEN AKKER, J. A. Tappi, **35**, 13 (1952).
6. MARCHESSAULT, R. H., LODGE, W. C., and MASON, S. G. Svensk Papperstidn. **59**, 859 (1956).
7. GOLDFINGER, G., MARK, H., and SIGGIA, S. Ind. Eng. Chem. **35**, 1083 (1943).
8. CONRAD, C. G. and SCROGGIE, A. G. Ind. Eng. Chem. **37**, 592 (1945).
9. BROWN, R. K. and PURVES, C. B. Pulp & Paper Mag. Can. **48** (6), 100 (1947).

10. BROUGHTON, G. and WANG, J. P. Tappi, **38**, 412 (1955).
11. ANT-WUORINEN, O. Paperi ja Puu, **37**, 335 (1955).
12. HESS, K., KIESSIG, H., and GUNDERMANN, J. Z. physik. Chem. **49**, 64 (1941).
13. HERMANS, P. H. and WEIDINGER, A. J. Am. Chem. Soc. **68**, 2547 (1946).
14. KANAMARU, K. and CHAO, J. Kolloid-Z. **84**, 85 (1938).
15. LAUER, K. Kolloid-Z. **107**, 86 (1944).
16. STAMM, A. J. and TARKOW, H. J. Phys. & Colloid Chem. **54**, 745 (1950).
17. MARCHESSAULT, R. H., MCKNIGHT, T. S., and MASON, S. G. Pulp Paper Mag. Can. **59** (2), 81 (1958).
18. HERMANS, P. H. and WEIDINGER, A. J. Appl. Phys. **19**, 491 (1948).
19. GOPPEL, J. M. and ARLMAN, J. J. Appl. Sci. Research, A, **1**, 3 (1947).
20. MARK, H. Physik und Chemie der Cellulose. Julius Springer, Berlin. 1932. p. 140.
21. CLARK, G. L. Applied X-rays. McGraw-Hill Book Co., Inc., New York. 1955. Chap. 13.
22. HERMANS, P. H. and WEIDINGER, A. J. Polymer Sci. **4**, 135 (1949).
23. ELLEFSEN, O., LUND, E. W., TØNNESEN, B. A., and OIEN, K. Norsk Skogsind. **11**, 284, 349 (1957).
24. SCREATON, R. M. and MASON, S. G. Svensk Papperstidn. **60**, 379 (1957).
25. SIMONS, F. L. Tappi, **33**, 312 (1950).
26. JAYME, G. and HARDERS-STEINHÄUSER, M. Das Papier, **9**, 507 (1955).
27. SCHULZ, G. V. and BLASCHKE, F. J. prakt. Chem. **158**, 130 (1941).
28. DAVIS, W. E. and ELLIOTT, J. H. *In* Ott, E. and Spurlin, H. M. Cellulose and cellulose derivatives. Interscience Publishers, Inc., New York. 1955. Part III, p. 1217.
29. IMMERGUT, E. H., RANBY, B. G., and MARK, H. F. Ind. Eng. Chem. **45**, 2482 (1953).
30. REES, H. W. J. Textile Inst. **39**, T351 (1948).
31. HERMANS, P. H. Physics and chemistry of cellulose fibers. Elsevier Publishing Co., Inc., New York. 1949. p. 189.
32. KLENKOVA, N. I. J. Appl. Chem. (U.S.S.R.), **27**, 401 (1954). English translation.
33. BRUNAUER, S., EMMETT, P. H., and TELLER, E. J. Am. Chem. Soc. **60**, 309 (1938).
34. PRESTON, J. M., NIMKAR, M. V., and GUNDAVDS, S. P. J. Textile Inst. **42**, T79 (1951).
35. HERMANS, P. H. Physics and chemistry of cellulose fibers. Elsevier Publishing Co., Inc., New York. 1949. Part II, Chaps. 2 and 6; Part III, Chap. 8.
36. SMITH, S. E. J. Am. Chem. Soc. **69**, 646 (1947).
37. MAGNE, F. C., PORTAS, H. J., and WAKEHAM, H. J. Am. Chem. Soc. **69**, 1896 (1947).
38. BARKAS, W. W. The mechanical properties of wood and their relation to moisture. Interscience Publishers, Inc., New York. 1953. pp. 54–56.

ÉTARD REACTION

II. POLYCYCLIC AROMATIC AND HETEROCYCLIC COMPOUNDS[1]

OWEN H. WHEELER

ABSTRACT

Polycyclic aromatic compounds can, in a number of cases, be oxidized with chromyl chloride, whereas heterocyclic compounds are unaffected.

The Étard oxidation of a number of substituted toluenes to substituted benzaldehydes with chromyl chloride was reported in a previous publication (1). The reaction should be extendable to methyl-substituted polycyclic aromatics and possibly to heterocyclic compounds. The only such reference in the literature is the statement, without experimental details, that some substituted polycyclic aromatics are oxidized to traces of quinones (2).

In the case of many of the polycyclic aromatic compounds studied (see Table I) products could be isolated by chromatography from the tarry residues formed in the reaction.

TABLE I

Reactant	Product	Yield, %
Anthracene	Anthraquinone	12
Naphthalene	—	—
2-Methylnaphthalene	—	—
9-Methylanthracene	Anthraquinone	70
2-Methylanthracene	2-Methylanthraquinone	42
	Anthraquinone-2-aldehyde	25
9-Methylphenanthrene	9-Phenanthraldehyde	30
	Phenanthraquinone	18
9,10-Dihydroanthracene	Anthraquinone	32, 62[a]
9,10-Dihydrophenanthrene	Phenanthraquinone	35
Fluorene	Fluorenone	35
2-Picoline	—	—
2-Picoline-N-oxide	—	—
3-Methylthiophene	—	—

[a]*Time of reaction reduced to 6 hours.*

Anthracene gave 12% anthraquinone as well as a small amount of uncrystallizable oil, but naphthalene gave only traces of a dark red oil. 2-Methylnaphthalene also gave only small quantities of a yellow oil. However, 9-methylanthracene gave anthraquinone in good yield (70%). The only previous observation of the removal of a methyl group by this reagent is the conversion of isopropylbenzene to acetophenone (2, 3). The oxidation of 2-methylanthracene took place at two positions giving 2-methylanthraquinone (42%) and anthraquinone-2-aldehyde (25%). No 2-anthraldehyde was isolated and it is to be expected that the 9,10 positions would be more reactive. 9-Methylphenanthrene also gave two products: 9-phenanthraldehyde (30%) and 9,10-phenanthraquinone (18%), again with displacement of a methyl group.

Considering the high reactivity of the 9,10 positions of anthracene and phenanthrene, it should be possible to oxidize their 9,10-dihydro derivatives, and 9,10-dihydroanthracene and 9,10-dihydrophenanthrene readily gave anthraquinone and phenanthraquinone,

[1]*Manuscript received February 17, 1958.*
Contribution from the Department of Chemistry, Dalhousie University, Halifax, N.S. For Part I of this series see Can. J. Chem. **36**, *667 (1958).*

respectively. In the latter case the yield was considerably improved by reducing the reaction time, suggesting that the yields in other cases might be improved by using shorter periods of reaction. Fluorene was also converted readily into fluorenone.

2-Picoline and 2-picoline-N-oxide both formed solid complexes with chromyl chloride, but on decomposition no aldehydic products could be isolated. Continuous ether extraction of the basified aqueous extracts gave some recovered starting material and the reaction complexes must have been salts between the base and the Lewis acid, chromyl chloride. Similarly, 3-methylthiophene gave no oxidized product and was recovered unchanged. This heterocyclic could also act as a Lewis base towards chromyl chloride and complexing on the heteroatom would prevent further reaction on the methyl group.

Details of only some typical oxidations are given in the experimental section but in the other cases the identity of the isolated products was checked by mixed melting-point determinations.

EXPERIMENTAL

Many of the compounds used were commercially available samples.

2-Methylanthracene.—2-Methylanthraquinone (10 g.) in xylene (100 ml.) was refluxed with aqueous ammonia (300 ml.) and zinc dust (100 g.) added in portions during 6 hours (4). The organic layer was evaporated and the residue in benzene chromatographed on alumina using benzene–hexane mixtures as eluent. 2-Methylanthracene (5.5 g.), m.p. 206° from ethanol (lit. m.p. 207° (5)), was eluted first, followed by 2-methylanthrone (3.5 g.), m.p. *ca.* 75°. Reduction with sodium hydroxide and zinc dust gave no reaction and phosphorus and hydriodic acid gave only 2-methyloxanthranol.

9-Methylphenanthrene.—9-Phenanthraldehyde (6) was converted to its hydrazone, m.p. 102°, from ethanol. The hydrazone (16 g.) was heated with sodium (3 g.) in ethylene glycol (100 ml.) to 200° for 18 hours (7). The reaction mixture was diluted with water and extracted with ether. The residue left when the ether was evaporated was chromatographed as above and gave 9-methylphenanthrene (1.9 g.), m.p. 93–94°, from ethanol (lit. m.p. 91–92.5° (8)).

9,10-Dihydrophenanthrene was prepared by catalytic hydrogenation of purified phenanthrene (9).

2-Picoline-N-oxide resulted from peracetic acid oxidation of 2-picoline (10).

Oxidation of 9-methylanthracene.—9-Methylanthracene (0.95 g.) in carbon tetrachloride (80 ml.) was treated dropwise with chromyl chloride (1.70 g., 10% excess) in carbon tetrachloride (20 ml.) with stirring at 20–25°. The reaction was stirred for a total of 2 hours and allowed to stand overnight. The mixture was worked up by pouring into excess ice-cold aqueous sodium sulphite. The residue left after evaporation of the solvent was taken up in benzene and chromatographed on alumina using hexane, hexane–benzene mixtures, and benzene as successive eluents. The product (720 mg.) had m.p. 286°, undepressed on admixture with anthraquinone.

Oxidation of 2-methylanthracene (300 mg.) gave on chromatography 2-methylanthraquinone (145 mg.), followed by anthraquinone-2-aldehyde (95 mg.), m.p. 182–184° (lit. m.p. 188–189° (11)).

Oxidation of 9-methylphenanthrene (810 mg.) gave 9-phenanthraldehyde (260 mg.), m.p. 95–97° (lit. m.p. 100–101° (6)), and 9,10-phenanthraquinone (155 mg.), m.p. 196° (lit. m.p. 198° (12)).

ACKNOWLEDGMENTS

Dr. H. Estrada and Dr. J. Romo kindly supplied samples of 9,10-dihydroanthracene and 9-methylanthracene.

REFERENCES

1. WHEELER, O. H. Can. J. Chem. **36**, 667 (1958).
2. LAW, H. D. and PERKIN, F. M. J. Chem. Soc. **93**, 1663 (1908).
3. WHEELER, O. H. Unpublished observations.
4. BORNSTEIN, A. Ber. **15**, 1821 (1882).
5. FISCHER, F. J. prakt. Chem. **79**, 555 (1909).
6. HINKEL, L. E., AYLING, E. E., and BEYNON, J. H. J. Chem. Soc. 339 (1936).
7. FIESER, L. F. and HARTWELL, J. L. J. Am. Chem. Soc. **60**, 2555 (1938).
8. BRADSCHER, C. K. and TESS, R. W. H. J. Am. Chem. Soc. **61**, 2184 (1939).
9. DURLAND, J. R. and ADKINS, H. J. Am. Chem. Soc. **60**, 1501 (1938).
10. BOEKELHEIDE, V. and LINN, W. J. J. Am. Chem. Soc. **76**, 1286 (1954).
11. RUGGLI, P. and DISLER, A. Helv. Chim. Acta, **10**, 938 (1927).
12. SCHOLL, R. and SCHWARZER, G. Ber. **55**, 324 (1922).

MOLECULAR SIZE AND CONFIGURATION OF CELLULOSE TRINITRATE IN SOLUTION[1]

M. M. Huque,[2] D. A. I. Goring, and S. G. Mason

ABSTRACT

Viscosity and light-scattering measurements were made on several fractions and two unfractionated samples of cellulose trinitrate. The samples were prepared from bleached ramie, unbleached ramie, and cotton linters. The solvents were acetone and ethyl acetate. Viscosity was measured in a multishear viscometer designed for the purpose. Light-scattering measurements were made in a Brice-Phoenix Light-scattering Photometer modified to accommodate a cell which could be ultracentrifuged.

The range of molecular weight investigated was from 6.5×10^5 to 25.0×10^5. The relationship between the z-average mean-square radius of gyration, $\overline{s_z^2}$, and the z-average molecular weight was approximately linear in both solvents. The ratio of $(\overline{s_0^2})_z/\overline{M}_z$ (where $(\overline{s_0^2})_z$ is the value of $\overline{s_z^2}$ in the unperturbed state) was found constant in acetone but to increase with $\overline{M}_z$ in ethyl acetate. This indicated that, whereas in acetone random coil configuration was attained, a configurational transition occurred in ethyl acetate in the molecular weight range investigated.

The value of the exponent a in the relationship between intrinsic viscosity and molecular weight was found to be lower than unity but approximately equal in both solvents.

The significance of the experimental data is discussed.

INTRODUCTION

Recent studies of the solution properties of cellulose trinitrate (designated CTN hereafter) have revealed certain unusual characteristics of the macromolecule. For example, Hunt *et al.* (1) and Holtzer *et al.* (2) showed that for CTN the ratio of the mean-square radius of gyration to the molecular weight increased with increasing molecular weight and reached a constant value at a M.W. of about 400,000. This is much higher than the value of 30,000 found for some vinyl polymers (3). This behavior was considered to arise from the unusual stiffness of the cellulose chain which attained a Gaussian configuration only at relatively high molecular weights. Holtzer *et al.* failed to observe an expected decrease in the exponent of the intrinsic viscosity – molecular weight relationship; but because of experimental difficulties these authors regarded their data for M.W.'s higher than 1.5×10^6 as unreliable. Such a decrease in the exponent has been reported by Badger and Blaker (4) and by Münster (5). There are, therefore, some anomalies and contradictions in the published data, particularly for high molecular weight material.

Apart from interest in the behavior of cellulose derivatives in solution, there is a more practical aspect of this work. Timell (6) has shown that with careful nitration the cellulose chain is made soluble without degradation. Trinitration, followed by fractionation and measurement of intrinsic viscosity, can be used to find the size distribution in any given sample of cellulose. Timell (7) has found that undegraded celluloses from a variety of sources all have rather high molecular weights ($>10^6$). In order to compute reliable values of molecular weight from intrinsic viscosities, the configurational behavior of the molecule should be understood.

The purpose of the present work was to study the configuration of high molecular weight CTN in a good (ethyl acetate) and a poor (acetone) solvent. Viscosity and light-

[1]*Manuscript received January 20, 1958.*
Contribution from the Physical Chemistry Division, Pulp and Paper Research Institute of Canada, and the Chemistry Department, McGill University, Montreal, Que.
[2]*Colombo Plan Scholar from Dacca, Pakistan.*

scattering methods were used and the results interpreted in the light of modern theories of the solution properties of polymers.

EXPERIMENTAL PART

Materials

Cellulose Nitrate

Cellulose trinitrates prepared from unbleached raw ramie, bleached ramie, and cotton linters (designated respectively by H, M, and T) were used in this investigation. The method of nitration has been described by Timell (6). The nitrogen contents are given in Table I.

TABLE I

ANALYTICAL DATA OF CELLULOSE NITRATES

Source	Nitrogen* content, % N	Degree of substitution	Base molecular weight
Unbleached raw ramie (H)	13.68	2.90	288
Bleached ramie (M)	13.80	2.93	290
Cotton linters (T)	13.57	2.88	285

**Complete nitration to cellulose trinitrate would correspond to 14.14% N with a base molecular weight of 297.*

Fractionation

The samples were fractionated by adding water to an acetone solution following the method of Mitchell (8). The exact quantities of water necessary for precipitation were ascertained from exploratory fractionations. Fractionation data for samples M and H are given in Tables II and III respectively.

TABLE II

FRACTIONATION DATA ON SAMPLE M

Fraction	Water added, cc.	Weight, g.	Yield, %
M-1	31.0	1.190	28.4
M-2A*	4.8	0.723	17.0
M-2B*	5.2	0.524	12.3
M-3	12.1	0.578	13.8
M-4		0.880	19.5
Undissolved material		0.320	7.1
Loss			1.9

**Fractions M-2A and M-2B had nearly identical intrinsic viscosities and were blended by dissolving in acetone and precipitating by addition of water. The blended sample is referred to as M-2 hereafter.*

For sample M, 4.5 g. was soaked in an acetone–water mixture (91: 9) for 24 hours and then stirred vigorously for 6 hours to yield a 0.1% solution; solutions of higher concentration were too viscous for convenient handling. The solution was then centrifuged at 500*g* for 20 minutes to remove any undissolved material. The decanted solution was placed in a 25° C. bath and distilled water added to it dropwise with vigorous stirring.

TABLE III

FRACTIONATION DATA ON SAMPLE H

Fraction	Water added, cc.	Weight, g.	Yield, %
H-1	34.0	0.369	18.5
H-2	10.3	0.548	27.4
H-3	40.0	0.397	19.8
H-4	—	0.265	13.3
H-5	—	0.340	17.0
Undissolved material		0.020	1.0
Loss			3.0

When the previously determined quantity of water had been added, the system was allowed to stand for 1 hour in the bath while the stirring was continued. The precipitate was separated by centrifuging for 20 minutes at 500*g*. The precipitate in the centrifuge cups was gel-like in appearance. It was found that addition of methanol facilitated removal of the precipitate from the cups. Excess liquid was squeezed out of the solid, which was then vacuum-dried at about 45° C. This procedure was repeated to yield four fractions (M-1, M-2A, M-2B, and M-3).

The solution remaining after separation of M-3 was evaporated to dryness to yield M-4.

Sample H was fractionated in essentially the same way from a 0.1% solution of 2 g. in acetone. The solution left after separation of the third fraction was evaporated to about one-quarter of its original volume by blowing air through it and stirring. The resulting suspension was centrifuged to take out the fourth fraction. The final fraction was obtained as before by evaporating the remaining liquid to dryness.

All fractions were stored over fused calcium chloride in a refrigerator.

Sample T, also, was fractionated after the method of Mitchell (8). Ten fractions were obtained, of which only T-6 and T-8 were used in this study. These fractions were chosen in order to extend the range to a somewhat lower molecular weight than values found for the fractions of M and H.

Finally a fraction, P, from an exploratory fractionation of bleached ramie nitrate was used to fill the gap of molecular weights between M-2 and M-3.

In the fractionation of samples M and H the solutions developed a cloudiness which increased as the fractionation proceeded. Repeated centrifugations did not remove the cloudiness. The effect seemed greater in sample H, possibly because of its lower nitrogen content. Evidently part of the precipitate remained suspended as colloidal material. It is possible that the non-sedimentable aggregates from one cycle were precipitated on the next addition of water.

Solvents

Reagent grade acetone was used for fractionation. For viscosity and light-scattering measurements reagent grade solvents were redistilled. Boiling ranges for acetone and ethyl acetate were 56.3–56.8° C. and 77–77.3° C. respectively.

Preparation of Solutions

Solutions were made up by shaking CTN in solvent for 24 hours in a wrist-action shaker. This was followed by centrifugation in stainless-steel tubes at 24,000*g* for 30 minutes to remove any undissolved material. Three-fourths of the liquid in the centrifuge

tubes was decanted into a glass-stoppered flask. This served as stock solution from which solutions were made for viscosity and light-scattering measurements. A calibrated 10-cc. hypodermic syringe was used for transfer of liquids.

It was thought possible that CTN might form aggregates on repeated cycles of dissolution, recovery (by precipitation or evaporation), and re-solution, and thus yield erroneous results from the light-scattering measurements. Such cycles were inevitable in fractionation and recovery. A careful series of experiments on approximately 0.2% solution of bleached ramie nitrate in both acetone and ethyl acetate showed, however, that the light-scattering dissymmetry did not change when such cycles were repeated. This indicated absence of significant aggregate formation.

Viscosity Measurements

Since the viscosity of solutions of high DP cellulose nitrate is shear-dependent, a standard shear rate of 500 sec.$^{-1}$ was adopted following the convention of Newman *et al.* and others (9, 10). A modified form of the suspended-level dilution capillary viscometer of Schurz and Immergut (11) was used. The viscometer had four bulbs, which enabled measurements to be made at different rates of shear calculable from the expression (12)

$$G_i = 8V_i/3\pi r^3 t_i, \quad [1]$$

where G_i = mean rate of shear corresponding to bulb i,
V_i = volume of bulb i,
t_i = efflux time of V_i,
r = radius of viscometer capillary.

Efflux times were measured at 25.00±0.01° C. to 0.1 second for each of the four bulbs for pure solvent and over a range of concentrations of the solutions obtained by progressive dilution of the solution first introduced in the viscometer. Efflux times for five or six concentrations were measured on each sample. Kinetic energy corrections (amounting to 0.2 to 3 per cent) were applied in the usual way (13) and values of the specific viscosity, η_{sp}, at shear rates calculated from Eq. [1] were obtained.

The concentration, c, of the initial solution was determined in a duplicate measurement by evaporation and weighing. The solid from 10 cc. of the solution was dried in vacuum to constant weight in a weighed aluminum cup. In determining the concentration of ethyl acetate solutions, filtered ethyl alcohol was added during evaporation to aid in the complete removal of ethyl acetate (1).

From these data, plots of log (η_{sp}/c) against log G for different concentrations were obtained. Fig. 1 shows an example. From these plots the values of η_{sp}/c for G = 500 sec.$^{-1}$ were obtained by interpolation. A plot of η_{sp}/c vs. c was then made as shown in Fig. 2. Linear extrapolation to zero concentration gave the intrinsic viscosity, $[\eta]_{500}$. In a similar manner intrinsic viscosities were obtained for a range of G values between 300 and 700 sec.$^{-1}$.

The Huggins' interaction constant (14), k'_{500}, was calculated from the slope of the η_{sp}/c vs. c line at 500 sec.$^{-1}$ using the equation

$$\eta_{sp}/c = [\eta] + k'[\eta]^2 c. \quad [2]$$

For some solutions at very low concentrations the plot η_{sp}/c vs. c deviated from linearity and showed marked upward curvature. This effect has been observed by others (15, 16)

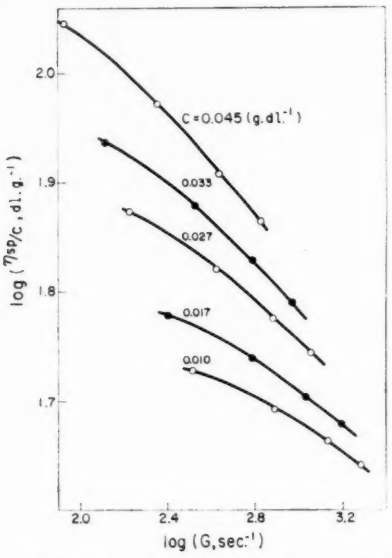

FIG. 1. Log of reduced viscosity vs. log of rate of shear at different concentrations for fraction H-2 in acetone.

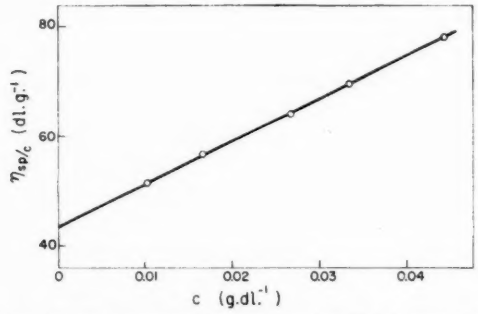

FIG. 2. Reduced viscosity vs. concentration for fraction H-2 in acetone at a shear rate of 500 sec.$^{-1}$.

and was shown by Öhrn (15) to be due to adsorption of polymer on the walls of the capillary. Extrapolation of the η_{sp}/c vs. c line to $c = 0$ was always carried out from concentrations at which the effect was negligible.

Light Scattering

Apparatus

Light-scattering measurements were made in a Brice-Phoenix photometer. The instrument was modified to accommodate cells of the type described by Dandliker and Kraut (17) in which the solution is clarified by ultracentrifugation *in situ*. This course was found necessary after attempts to remove stray dust from the solutions by conventional means such as centrifugation (outside the measuring cell) and filtration proved unsatisfactory. Despite elaborate care, the solution, clarified by centrifuging, became contaminated with dust in the transfer to the measuring cell; when ultrafine sintered-glass filters were used, the solute was retained by adsorption on the filter.

Details of the modification of the photometer are expected to be reported in a separate paper (18). After modification the intensity emitted by a dilute solution of fluorescein was constant to $\pm 1\%$ from angles of 30° to 135°. Negligible background scattering was found with toluene and acetone. Calibration with Ludox (19) was checked by measuring the excess turbidity of a 0.50% solution of Cornell standard polystyrene in toluene. The value found was 3.26×10^{-3} cm.$^{-1}$ and is in good agreement with the National Bureau of Standards' value (20) of 3.30×10^{-3} cm.$^{-1}$. The Rayleigh ratio of redistilled and filtered benzene was found to be 49.6×10^{-6} cm.$^{-1}$, also in good agreement with Maron and Lou's (21) value of 49.7×10^{-6} cm.$^{-1}$.

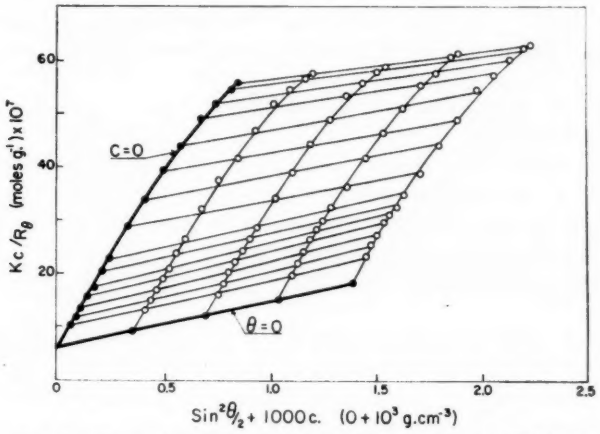

FIG. 3. Zimm plot of light-scattering data for fraction M-2 in acetone.

Zimm plots, an example of which is shown in Fig. 3, were obtained from the light-scattering data in the usual way by plotting Kc/R_θ vs. $\sin^2\theta/2 + kc$, where

K = $2\pi^2 n_s^2 (dn/dc)^2 / N\lambda^4$,
n_s = refractive index of solvent,
dn/dc = refractive index increment,
λ = wave length in vacuum,
θ = angle between scattered and transmitted beam,
R_θ = Rayleigh ratio at angle θ,
k = an assigned constant,
N = Avogadro's number,
c = concentration in grams per cc.

The weight-average molecular weight, $\overline{M_w}$, was obtained from the intercept from

[3] $$\overline{M_w} = 1/(Kc/R_\theta)_{c,\theta=0}$$

and the z-average radius of gyration, $\sqrt{\overline{s_z^2}}$, was computed from the initial slope of the $c = 0$ line by means of the expression

[4] $$\frac{\text{initial slope}}{\text{intercept}} = \frac{16\pi^2}{3} \cdot \overline{s_z^2} \cdot (n/\lambda)^2,$$

where n is the refractive index of the solution. The concentration dependence of the intensity can be written as

[5] $$Kc/R_\theta = [1/MP(\theta)]+2A_2c$$

where $P(\theta) = (R_\theta^\circ/R_\theta)$. R_θ° is the Rayleigh ratio if there is no intraparticle interference. A_2 is the second virial coefficient and is computed from the slope of the $(Kc/R_\theta)_{\theta=0}$ vs. c line in the Zimm plot (22).

Refractive Index Measurements

The increment of refractive index dn/dc of the solution over that of the solvent was measured by means of a Brice-Phoenix differential refractometer for $\lambda = 4358$ Å at 25° C. The instrument was calibrated with sucrose solutions of different concentrations using sodium light ($\lambda = 5890$ Å). The calibration was checked by measurement of Δn for a 4% aqueous KCl solution. The measured value was within 0.4% of the value calculated from data obtained from the International Critical Tables.

RESULTS

Viscosity and Light Scattering

The experimental results from viscosity and light-scattering measurements are listed in two tables. Table IV contains the results in acetone solution while the contents of Table V are for ethyl acetate solutions. The quantities given for each sample are the weight-average molecular weight, $\overline{M_w}$, z-average root-mean-square radius of gyration, $\sqrt{\overline{s_z^2}}$, the second virial coefficient, A_2, the intrinsic viscosity, $[\eta]_{500}$, and the Huggins' interaction constant, k'_{500}.

In order to derive the configurational parameters from the light-scattering data, certain assumptions about the molecular weight distribution were necessary since polydispersity is inevitable even in carefully fractionated material (1, 2). A suitable distribution is one

TABLE IV

RESULTS OF VISCOSITY AND LIGHT-SCATTERING MEASUREMENTS IN ACETONE

Sample	$[\eta]_{500}$, dl. g.$^{-1}$	k'_{500}	$\overline{M_w}\times10^{-5}$	$\sqrt{\overline{s_z^2}}$, Å	$A_2 \times 10^4$, mole cc. g.$^{-2}$
T-8	12.1	0.83	6.5	869	7.3
T-6	15.6	0.95	8.4	958	7.4
M-3	18.9	0.62	9.9	1060	3.2
P	20.5	0.55	11.4	1150	4.1
M	22.1	0.52	15.3	1440	4.9
M-2	26.0	0.56	16.9	1480	4.6
M-1	36.8	0.33	22.8	1610	3.8
H	43.4	0.39	23.8	1670	5.1
H-2	43.6	0.41	25.0	1730	3.8

TABLE V

RESULTS OF VISCOSITY AND LIGHT-SCATTERING MEASUREMENTS IN ETHYL ACETATE

Sample	$[\eta]_{500}$, dl. g.$^{-1}$	k'_{500}	$\overline{M_w}\times10^{-5}$	$\sqrt{\overline{s_z^2}}$, Å	$A_2 \times 10^4$, mole cc. g.$^{-2}$	$[\eta]_0$ dl. g.$^{-1}$
T-8	16.9	0.58	6.8	972	7.3	16.9
T-6	20.4	0.74	7.8	1097	7.8	20.4
M-3	24.6	0.52	9.8	1430	3.1	24.6
P	—	—	—	—	—	—
M	32.4	0.50	16.1	1520	6.6	32.9
M-2	32.8	0.55	15.9	1630	4.4	34.4
M-1	44.6	0.35	23.2	2100	4.8	46.5
H	—	—	—	—	—	—
H-2	58.6	0.27	25.0	2190	3.6	61.3

in which the z-average, weight-average, and number-average molecular weights, represented respectively by $\overline{M}_z$, $\overline{M}_w$, and $\overline{M}_n$, are related in the proportion 3:2:1. Such a distribution has been used by others (2, 22) and was assumed by Hunt *et al.* (1) for their high molecular weight samples. This proportionality will be assumed in computing $\overline{M}_z$ and $\overline{M}_n$ from the values of $\overline{M}_w$ obtained from light scattering.

The initial concentrations of solutions employed for light-scattering measurements varied from 0.12 to 0.35 g./dl. depending on the molecular weight. At the lowest concentration the solvent scattering intensity was 50% of the scattering intensity from solution. The initial concentration range in viscometry was 0.035 to 0.085 g./dl. depending on the molecular weight. The lowest concentration in viscometric measurements was a fifth or sixth of the initial concentration.

The refractive index increments, dn/dc, at 25° C. used for the calculation of K were 0.104 cc. g.$^{-1}$ and 0.105 cc. g.$^{-1}$ for ethyl acetate and acetone solution respectively. These were the mean values from solutions of bleached and unbleached (raw) ramie nitrate. The corresponding K values were 1.85×10^7 and 1.84×10^7 respectively for ethyl acetate and acetone.

Shear Dependence of Viscosity

Shear dependence of intrinsic viscosity in the range of rate of shear between 300 and 700 sec.$^{-1}$ was estimated. For the complete range of molecular weight studied [η] was found to be independent of G in acetone solution. A typical plot of η_{sp}/c vs. c for different G is shown in Fig. 4.

In ethyl acetate solution, on the other hand, [η] showed slight dependence on the rate of shear for the higher molecular weight samples. An example is shown in Fig. 5, where the values for H-2 have been plotted. The magnitude of the dependence decreased with decreasing molecular weight and below [η] = 30 the dependence was no longer observed. Similar results for the shear dependence in ethyl acetate solution were obtained by Timell (10).

In those cases where such dependence was noticed, [η] values at different G were linearly related to the rate of shear. Fig. 6 shows the variation of [η] with G for samples M, M-2, M-1, and H-2. Extrapolation of these lines gave values of the intrinsic viscosity at zero rate of shear, $[\eta]_0$ which have been included in Table V.

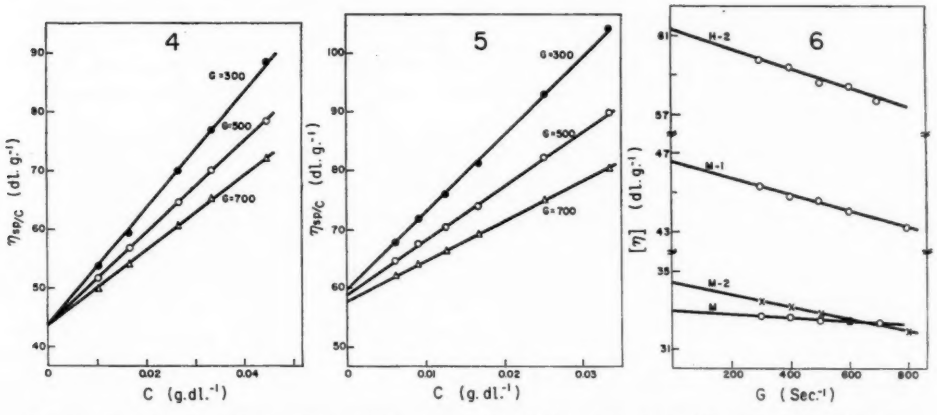

FIG. 4. Reduced viscosity vs. concentration for fraction H-2 in acetone at different rates of shear.
FIG. 5. Reduced viscosity vs. concentration for fraction H-2 in ethyl acetate at different rates of shear.
FIG. 6. Intrinsic viscosity vs. rate of shear for samples M, M-1, M-2, and H-2 in ethyl acetate.

These results show a small or no dependence of $[\eta]$ on G in the range of shear studied. As clearly shown in Figs. 4 and 5 marked shear dependence of η_{sp}/c occurs at finite concentration. This shear dependence is probably due to molecular interaction, which will increase as concentration increases, rather than to deformation or orientation of isolated molecules. A similar result has been noted recently by Nawab and Mason (23) for suspensions of model filaments. In the present work the reservation must be made that the range of shear was small, and a more marked variation of $[\eta]$ with G may have been detected had measurements been made at much lower shear rates.

Anomalous Light Scattering

Early in the work certain persistent irregularities were noted in the light-scattering measurements. In all samples the graph of Kc/R_θ vs. $\sin^2\theta/2+kc$ at $\theta = 0$ curved downwards after a certain concentration was reached and in some cases passed through a maximum. Fig. 7 is a Zimm plot showing this effect. The concentration, c_c, at which the curvature became noticeable decreased approximately linearly with increasing molecular weight. The curvature started at such low concentration with the very high molecular weight fraction H-1 in acetone solution that determination of $\overline{M_w}$ by extrapolation was not possible. The effect was also observed in solutions which were centrifuged for 1 hour or more instead of the usual 30 minutes, so that the effect was not caused by the presence of debris.

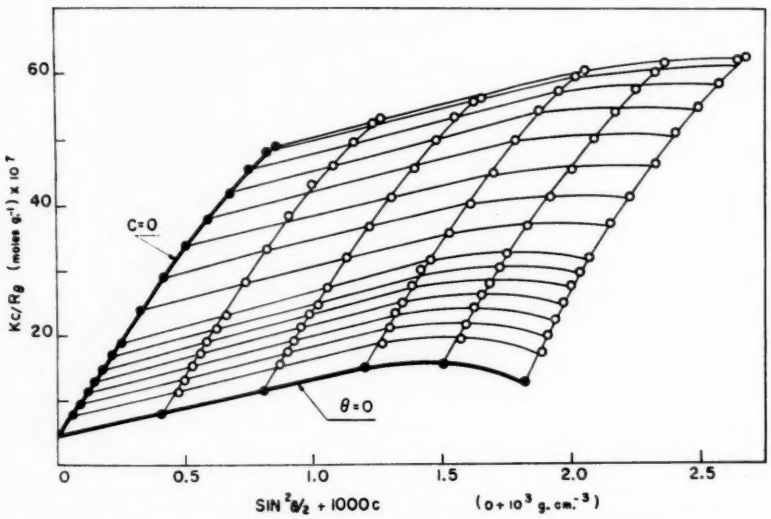

FIG. 7. Zimm plot of light-scattering data for fraction M-1 in acetone showing deviation from linearity of $(Kc/R_\theta)_{\theta=0}$ vs. c line at high concentration.

At about the same concentration at which the deviation from linearity of Zimm plots occurred, a curious optical phenomenon was noted. If the solution was centrifuged for 30 minutes at 55,000g, placed in the light-scattering apparatus and the scattered beam observed in a mirror held at low angles, quite clear vertical striations, i.e., vertical bands of scattering substance, could be seen. They were observed in nearly all samples provided that the concentration was sufficiently high.

Striations occurred only on high-speed centrifugation; none could be seen in a fresh, uncentrifuged solution. Thus the phenomenon was associated in some way with ultracentrifugation. If a centrifuged solution was allowed to stand, the striations gradually disappeared over a period of several hours, indicating that the process was reversible. In some solutions the discontinuities were not stationary but appeared to drift gradually.

The effect of striations on the scattering intensity was relatively small. A variation of intensity by about $\pm 5\%$ was found in successive measurements. No clear trend of increase or decrease in scattering intensity was noted on standing. Also the polarization of the transmitted or scattered light was unaffected.

Similar behavior for high molecular weight nitrocellulose has been reported by Holtzer *et al.* (2). These authors found that prolonged centrifugation at high speed caused the effect to disappear. However, in the present work striations were observed in a sample centrifuged at 55,000*g* for 5 hours. Also, a number of experiments were made which showed that their origin was not a trivial one, e.g. concentration or density gradients produced by sedimentation.

It is proposed to publish a separate account of deviations from linearity in Zimm-type plots and of striations.

DISCUSSION

Variation of Radius of Gyration with Molecular Weight

The radius of gyration is a characteristic dimension of the molecule in solution and, as expected, increased with increasing molecular weight (Tables IV and V). Also, for a given sample, $\sqrt{\overline{s^2}}$ was higher in ethyl acetate than in acetone, thus indicating greater extension in the former solvent.

In both solvents the relationship between $\overline{s_z^2}$ and $\overline{M_z}$ was approximately linear as shown in Figs. 8 and 9. In acetone the line passed through the origin and is expressed by the equation

$$\overline{s_z^2} = 0.80 \times \overline{M_z}. \qquad [6]$$

For ethyl acetate the relationship is

$$\overline{s_z^2} = 1.33\overline{M_z} - 3.55. \qquad [7]$$

If the data for CTN in ethyl acetate obtained by Hunt *et al.* (1) are included in Fig. 9, it is seen that below a molecular weight of about 800,000 the graph curves towards the origin. Similarly in Fig. 8 the data of Holtzer *et al.* (2) suggest a breakdown in the linearity at low molecular weight. Recently Notley and Debye (24) have noted a similar trend in the relationship between molecular dimensions and weights of polystyrene.

Configurational Change with Molecular Weight

The deviation from linearity in Figs. 8 and 9 could be expected if a transition to non-Gaussian behavior occurred at low molecular weight. Such configurational changes have been treated theoretically by Benoit and Doty (25) in terms of a stiffness parameter, the persistence length, q. The persistence length was defined originally by Porod and Kratky (26, 27) as the mean value of the projection of an infinitely long chain along the direction of the first element in the chain. The expression deduced by Benoit and Doty is

$$\overline{s_0^2} = q^2[(x/3) - 1 + (2/x) - 2(1 - e^{-x})/x^2] \qquad [8]$$

where $\sqrt{\overline{s_0^2}}$ is the unperturbed radius of gyration (described later) and x is the number of units of length q in the fully extended molecule. The value of x is given by

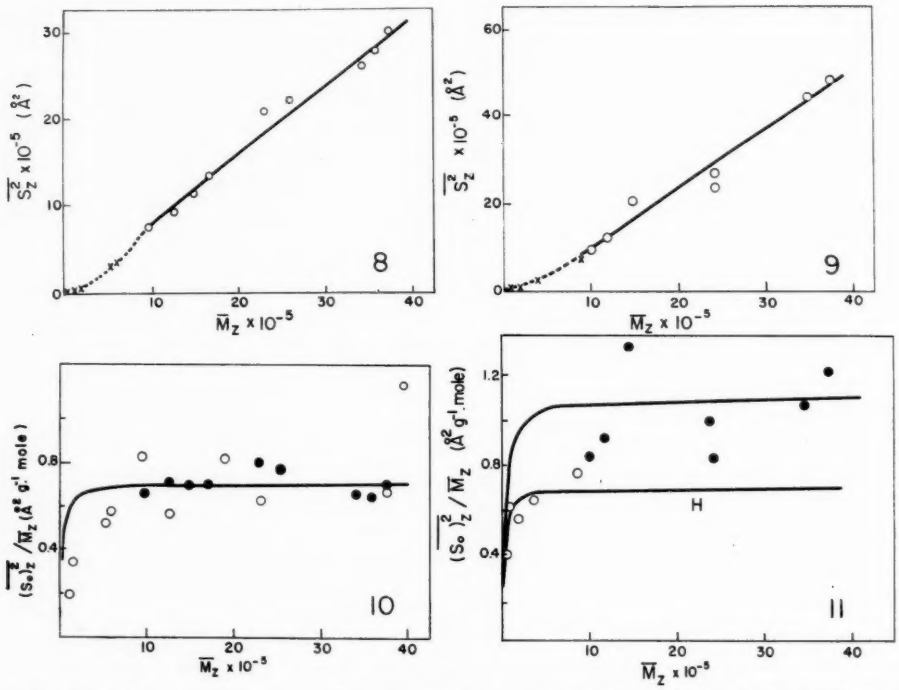

FIG. 8. Z-Average mean-square radius of gyration vs. z-average molecular weight of the CTN samples in acetone. ○—Present work. ×—Holtzer *et al.* (2).

FIG. 9. Z-Average mean-square radius of gyration vs. z-average molecular weight of the CTN samples in ethyl acetate. ○—Present work. ×—Hunt *et al.* (1).

FIG. 10. Dependence of $(\overline{s_0^2})_z/\overline{M}_z$ on $\overline{M}_z$ for the CTN samples in acetone. The solid curve is the theoretical one based on Eq. [8]. ●—Present work. ○—Holtzer *et al.* (2).

FIG. 11. Dependence of $(\overline{s_0^2})_z/\overline{M}_z$ on $\overline{M}_z$ for CTN samples in ethyl acetate. The upper solid curve is the theoretical one based on Eq. [8]. The solid curve H is the one proposed by Hunt *et al.* (1). ●—Present work. ○—Hunt *et al.* (1).

$$[9] \qquad x = r_{max}/q = [(DP)/q].L$$
$$= (\overline{M}/M_0).(L/q),$$

r_{max} being the length of the fully extended chain and L being the length of one monomer unit which was taken as 5.15 Å. Here $\overline{M}$ is the average molecular weight and M_0 is the monomer molecular weight.

For large x (i.e., large $\overline{M}$) Eq. [8] reduces to

$$[10] \qquad \overline{s_0^2}/r_{max} = q/3,$$

which for a Gaussian coil corresponds to $(\overline{s_0^2}/\overline{M})$ being constant. For smaller x, the other terms decrease the value of $\overline{s_0^2}/\overline{M}$, indicating an approach to the rod-like configuration.

After the manner of Hunt *et al.* (1), the experimentally determined values of $(\overline{s_0^2})_z/\overline{M}_z$ may be plotted against $\overline{M}_z$ and compared with the theoretical curve deduced from Eq. [8]. The unperturbed radius of gyration was obtained from the relationship

$$[11] \qquad \sqrt{s_z^2} = \alpha\sqrt{(\overline{s_0^2})_z},$$

where the expansion factor, α, was calculated from the second virial coefficient by the method of Orofino and Flory (28). As found by Hunt *et al.* for CTN in ethyl acetate, α was near unity for all samples in both solvents (1.03–1.09) and showed a very slight increase with increasing molecular weight. The persistence length, q, required in Eq. [8], was calculated by means of Eq. [10], from $(\overline{s_0^2})_z$ and $\overline{M}_z$ for the two highest molecular weight samples. Averages of the values of q were 115 Å and 200 Å in acetone and ethyl acetate, respectively. Hunt *et al.* (1) used a q value of 117 Å derived from the data on their three highest molecular weight samples.

In Figs. 10 and 11 $(\overline{s_0^2})_z/\overline{M}_z$ is plotted against $\overline{M}_z$ for acetone and ethyl acetate, respectively. Values of $(\overline{s_0^2})_z$ and $\overline{M}_z$ are given in Table VI. The data of Holtzer *et al.* (2) for CTN in acetone are included in Fig. 10 and the data of Hunt *et al.* (1) for CTN in ethyl acetate are included in Fig. 11.

TABLE VI

MOLECULAR AND HYDRODYNAMIC PARAMETERS

	In acetone			In ethyl acetate		
Sample	$\overline{M}_z \times 10^{-6}$	$(\overline{s_0^2})_z \times 10^{-6}$, Å²	$\Phi' \times 10^{-22}$	$\overline{M}_z \times 10^{-6}$	$(\overline{s_0^2})_z \times 10^{-6}$, Å²	$\Phi' \times 10^{-22}$
T-8	0.98	0.66	2.34	1.01	0.85	2.95
T-6	1.26	0.80	2.90	1.17	1.08	2.83
M-3	1.49	1.04	3.05	1.47	1.98	1.96
P	1.71	1.21	2.97	—	—	—
M	2.30	1.85	2.21	2.42	2.01	3.52
M-2	2.54	1.93	2.62	2.39	2.47	2.86
M-1	3.42	2.27	3.91	3.48	4.07	2.64
H	3.57	2.32	4.32	—	—	—
H-2	3.75	2.63	4.11	3.75	4.59	3.28

As predicted by theory, the combined data in both cases show increase of $(\overline{s_0^2})_z/\overline{M}_z$ with $\overline{M}_z$. In the case of acetone, the results from the present investigation lie in the region of constant $(\overline{s_0^2})_z/\overline{M}_z$ while at lower molecular weight the data of Holtzer *et al.* (2) show decrease in $(\overline{s_0^2})_z/\overline{M}_z$. Their results indicated that at $\overline{M}_z$ values above 10^6 the molecule behaves like a Gaussian coil. For ethyl acetate, except for one point, $(\overline{s_0^2})_z/\overline{M}_z$ increases with $\overline{M}_z$ over the complete range of molecular weights. This suggests that in the molecular weight range studied, CTN does not attain the random coil configuration in ethyl acetate. Curve *H* in Fig. 11 is the theoretical one given by Hunt *et al.*, which is based on a persistence length of 117 Å computed from the results for their three highest molecular weight samples. The points from the present investigation are well above their theoretical line. This discrepancy indicates that Hunt *et al.* (1) did not use a high enough value of $\overline{M}_z$ in computing q. It must also be noted that because of increasing trend of $(\overline{s_0^2})_z/\overline{M}_z$ with $\overline{M}_z$, the value of q computed for samples M-1 and H-2 may also be erroneously low.

The higher value of the persistence length in ethyl acetate was unexpected since, to a first approximation, q must depend only on orientation and steric factors in the chain itself. It is possible, however, that the greater solvation in ethyl acetate may cause an added inflexibility due to more extensive packing of solvent molecules around the polymer in the better solvent.

The values of x calculated from $\overline{M}_w$ by means of Eq. [9] ranged from 60 to 370. Peterlin (29) has shown that such values of x lead to perceptible downward curvature in the usual

graph of the angular distribution of light scattering intensity at zero concentration. For example, in the case of samples M-2 and M-1 (Figs. 3 and 7) the theoretical envelope for the Porod chain was deduced from the data of Peterlin (29). The envelope was assumed to deviate from the linear graph (tangential at the origin), which is expected for a completely flexible polymer with $\overline{M_z}$: $\overline{M_w}$: $\overline{M_n}$ = 3:2:1. For both sample M-2 and M-1, the theoretical curve was found to coincide almost exactly with the experimentally determined points. However no systematic analysis of the light-scattering envelopes was attempted because measurements at high angles were not precise enough.

Variation of Intrinsic Viscosity with Molecular Weight

The intrinsic viscosity is a measure of the effective hydrodynamic volume of a solute and, as expected, $[\eta]_{500}$ increased with $\overline{M_w}$. The values of the constants $\boldsymbol{K}$ and a in the intrinsic viscosity – molecular weight relationship

$$[\eta] = \boldsymbol{K}\overline{M_w}^{a} \qquad [12]$$

were obtained from plots of log $[\eta]_{500}$ vs. log $\overline{M_w}$ shown in Figs. 12 and 13 respectively for acetone and ethyl acetate solution. The values are given in Table VII along with the more recent values obtained by other workers. If $[\eta]_0$ at $G = 0$ (obtained as described previously) is used, a increases from 0.83 to 0.86 in ethyl acetate. Similar adjustment leaves a unchanged for acetone solutions since $[\eta]$ was found to be independent of G.

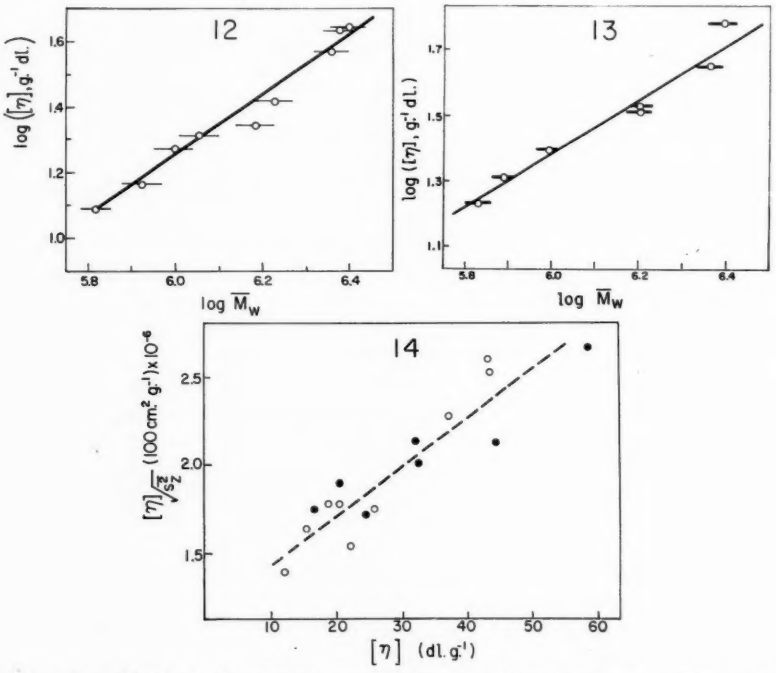

FIG. 12. Log of intrinsic viscosity at a rate of shear of 500 sec.$^{-1}$ vs. log of molecular weight for the samples in acetone.

FIG. 13. Log of intrinsic viscosity of the samples in ethyl acetate at a rate of shear of 500 sec.$^{-1}$ vs. molecular weight.

FIG. 14. Ratio of intrinsic viscosity to root-mean-square z-average radius of gyration vs. intrinsic viscosity in acetone and ethyl acetate. ●—Ethyl acetate. ○—Acetone.

TABLE VII

VALUES OF a AND K

Investigator	Solvent	Range of method, $M \times 10^{-4}$		G (sec.$^{-1}$) for $[\eta]$	a	K	Ref.
Holtzer *et al.*	Acetone	7.7–264	Light scattering	0	0.99	1.73×10^{-5}	(3)
Holtzer *et al.**	Acetone	64–264	Light scattering	0	0.91	5.37×10^{-6}	(3)
Present†	Acetone	65–250	Light scattering	500	0.91	5.96×10^{-5}	
Newman *et al.*	Ethyl acetate	9.3–150	Ultracentrifuge	500	0.99	4.82×10^{-5}	(14)
Hunt *et al.*	Ethyl acetate	4.1–57.3	Light scattering	0	1.01	2.50×10^{-5}	(4)
Present	Ethyl acetate	68–250	Light scattering	500	0.83	2.60×10^{-4}	
Present	Ethyl acetate	68–250	Light scattering	0	0.86	1.66×10^{-4}	

**Values of a and K are derived from the six highest molecular weight samples.*
†The standard error in a was 0.08 in all cases.

The intrinsic viscosity of CTN has been shown to vary considerably with small changes in the nitrogen content of the sample (30, 31, 32). The intrinsic viscosity was corrected by the method of Lindsley and Frank (30) to a hypothetical value, $[\eta]^T$ corresponding to 14.14% nitrogen. The results are shown in Table VIII: $[\eta]^T$ is considerably higher than the corresponding $[\eta]$ value given in Tables IV and V. Plots of log $[\eta]^T_{500}$ vs. log $\overline{M_w}$ yield $a = 0.77$ in ethyl acetate and $a = 0.87$ in acetone. With $[\eta]^T_0$ (i.e. $[\eta]^T$ at zero rate of shear) the value of a becomes 0.82 in ethyl acetate.

TABLE VIII

VALUES OF INTRINSIC VISCOSITIES AFTER CORRECTION FOR NITROGEN CONTENT

Sample	In acetone	In ethyl acetate		% Nitrogen
	$[\eta]^T_{500}$, dl. g.$^{-1}$	$[\eta]^T_{500}$, dl. g.$^{-1}$	$[\eta]^T_0$, dl. g.$^{-1}$	
T-8	14.5	20.3	20.3	13.58
T-6	18.7	24.4	24.4	13.58
M-3	20.9	27.2	27.2	13.84
P	23.4	—	—	13.74
M	24.6	36.1	36.7	13.81
M-2	28.8	36.3	40.1	13.83
M-1	40.4	49.0	51.1	13.85
H	50.4	—	—	13.68
H-2	49.4	66.5	69.5	13.76

The value of a is influenced by two factors: (i) the configuration of the molecule and (ii) its permeability to solvent. Any increase in molecular extension would cause an increase in a whereas a change from the free-draining to the solvated (solvent immobilizing) state would cause a to decrease.

As shown in Table VII, a was lower than unity in both solvents in contrast to the results of Holtzer *et al.* (2), Hunt *et al.* (1), and Newman *et al.* (9). The lower value of a in the high molecular weight range is in conformity with the theory of Kirkwood and Riseman (32) and the data of Badger and Blaker (4) and Münster (5). Also, it is supported by the agreement between the present data and those for the six highest molecular weight samples of Holtzer *et al.* (2). Further, the low value of a is accentuated by the correction of the $[\eta]$ values for variation in nitrogen content. Thus the data support in a general way the assumption of a more coiled configuration at high molecular weights as demonstrated by the light-scattering results.

Within experimental error a was equal in both acetone and ethyl acetate in the molecular weight range studied. This applies to the work of others (2, 1, 9) as well, and is

contrary to the behavior of other polymers (e.g., polystyrene (33)) in good and bad solvents. This seeming anomaly may be due to the increased solvation in the good solvent which will decrease a by contributing to the solvent immobilizing character and compensating for extension effects. The low a in ethyl acetate may also be related to the configurational behavior discussed above. The data in Figs. 10 and 11 show that, while the configuration in acetone was constant in the present range, it changed continuously in ethyl acetate. For ethyl acetate, therefore, it is unlikely that the value of the exponent can be assigned with certainty to any model and a should remain an empirical quantity determined for various ranges of M.

The Hydrodynamic Parameter Φ

It was of interest to compute the universal hydrodynamic parameter Φ introduced by Flory (34). Following the notations of Hunt *et al.* (1) the intrinsic viscosity may be related to the chain dimensions by the equation

$$[\eta] = \Phi'(\overline{s_0^2}/\overline{M})^{3/2}\overline{M}^{1/2}\alpha^3. \qquad [13]$$

The prime is appended to Φ to indicate use of the radius of gyration instead of the end-to-end distance as customarily used (34). Values of Φ' for CTN samples in both solvents calculated according to the procedure of Hunt *et al.* are given in Table VI.

As shown in Table VI, Φ' increases with molecular weight in acetone. This is contrary to the conclusion of Holtzer, Benoit, and Doty (2) whose results suggest that Φ' is constant and approximately equal to 2.8×10^{22} in agreement with the values for our lower molecular weights. In ethyl acetate, on the other hand, Φ' is seen to be virtually constant with a mean of $2.86(\pm0.33)\times10^{22}$, which is in good agreement with the values for the two highest molecular weight samples of Hunt *et al.* (1) and close to the constant experimental value of 3.2×10^{22} obtained for the synthetic polymers.

The data can be further analyzed if Eq. [13] is written as

$$\Phi' = k[\eta]\overline{M}_z/(\overline{s_z^2})^{3/2} \qquad [14]$$

or

$$\Phi' = k.[1/(\overline{s_z^2}/\overline{M_z})].[\eta]/\sqrt{\overline{s_z^2}}, \qquad [15]$$

where k is a constant for each solvent derived after the manner of Hunt *et al.* (1) and depends on the polydispersity. For a random coil $\overline{s_z^2}/\overline{M_z}$ is constant (α is taken as unity) according to Benoit and Doty (25) and Hunt *et al.* (1). Also, Kunst (35) has shown that $[\eta]$ is directly proportional to $\sqrt{\overline{s_z^2}}$ for polyisobutylene in different solvents. Similar direct proportionality between $[\eta]$ and $\sqrt{\overline{s_z^2}}$ can be derived from results on polystyrene (36), polymethylmethacrylate (37), and polyvinyl acetate (38), all of which have been shown to obey random flight statistics. Therefore, Φ' is constant for these polymers. In the case of CTN, $[\eta]/\sqrt{\overline{s_z^2}}$ increases with intrinsic viscosity in ethyl acetate and acetone in the range investigated, as shown in Fig. 14. Since $\overline{s_z^2}/\overline{M_z}$ is constant in acetone, Φ' will increase with increasing $\overline{M}$; whereas the increase of $\overline{s_z^2}/\overline{M_z}$ with $\overline{M}$ in ethyl acetate apparently just compensates the increase in $[\eta]/\sqrt{\overline{s_z^2}}$, leaving Φ' constant. The change of $[\eta]/\sqrt{\overline{s_z^2}}$ might be expected in ethyl acetate for which a configurational transition occurs throughout the range studied. In acetone, however, the light-scattering data suggest that a random coil configuration was attained. The increase of $[\eta]/\sqrt{\overline{s_z^2}}$ may, therefore, be related to a decreasing degree of free-draining as the molecular weight increases.

Interaction Constants

The Huggins' interaction constant, k', is an empirical quantity, but its value has been used as an indication of molecular branching (39). It was, therefore, of interest to consider the variation of k' for change of solvent and shear rate. A typical set of results is shown in Table IX. The value of k' is higher in the poor solvent, acetone, which is in agreement with the findings of Alfrey *et al.* (40) for polymethylmethacrylate in different solvents. It may also be noted that k' decreases with increasing rate of shear, in agreement with the results of Masson and Goring (41) on carrageenin—a polygalactose sulphate—and Conrad *et al.* (42) on cellulose in cuprammonium and cupriethylenediamine. In consideration of the dependence of k' on such variables as solvent and rate of shear, one must be cautious in using k' as a criterion for detecting branching, especially in the case of solutions showing non-Newtonian viscosity behavior.

TABLE IX

HUGGINS' INTERACTION CONSTANT, k', FOR FRACTION H-2 IN TWO SOLVENTS AT DIFFERENT SHEAR RATES

G (sec.$^{-1}$)	In acetone	In ethyl acetate
300	0.514	0.366
400	0.450	0.310
500	0.407	0.274
600	0.364	0.232
700	0.330	0.206

The variation of k'_{500} and A_2, the second virial coefficient in light scattering, with molecular weight is shown in Fig. 15 for both solvents. The graphs are irregular, but there is a significant decrease in k'_{500} with increase in $\overline{M}$ for both solvents. This is contrary to Huggins' (14) suggestion that it should be independent of molecular weight. Similar dependence of k'_{500} on molecular weight was found by Timell (43) for CTN in ethyl acetate and Alfrey *et al.* (40) for polymethylmethacrylate in different solvents.

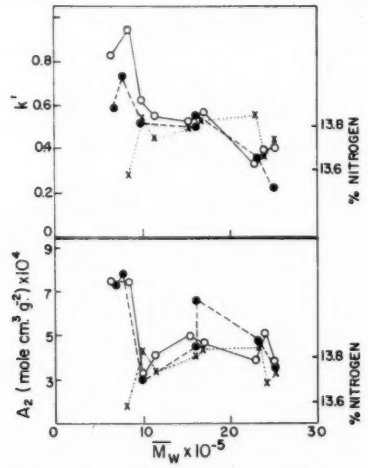

FIG. 15. The second virial coefficient, A_2, and the Huggins' interaction constant, k', vs. molecular weight of the samples in acetone and ethyl acetate. Nitrogen content of the samples have also been included in the graph. ●—Ethyl acetate. ○—Acetone. ×—Nitrogen content.

The second virial coefficient, A_2, for a polymer–solvent system should decrease slowly with increasing molecular weight. For the same polymer the value of A_2 is dependent on the nature of the solvent, being higher in a good solvent. These two general characteristics of A_2 which have been observed in the case of other polymers are not found for CTN solutions. Holtzer *et al.* (2) found negligible and irregular change of A_2 with molecular weight. In ethyl acetate, for low molecular weight fractions, Hunt *et al.* (1) obtained values of A_2 which were practically the same as found by Holtzer *et al.* except the lowest molecular weight sample for which the value was slightly higher. In the present investigation, values of A_2 were found to be the same, within experimental error, in both solvents; a slight decrease in A_2 with increase of $\overline{M}_w$ can, however, be detected.

An obvious feature of Fig. 15 is the irregularity of the data. Similar irregular results for the Huggins' constant have been reported by other workers (40, 42, 43). Irregularities in both k'_{500} and A_2 show the same trend in the two different solvents, indicating that this behavior is due to the samples rather than to experimental error. The nitrogen contents of the samples have been included in Fig. 15. Except for two points, it is seen that there is a rough correlation between the nitrogen content and the fluctuations in k'_{500} (44) and A_2. A more detailed study would be required to elucidate more clearly the source of these irregularities.

ACKNOWLEDGMENTS

The authors wish to thank Dr. T. E. Timell for kindly supplying the ramie and fractionated cotton nitrates, and Dr. R. F. Robertson for use of a Spinco preparative ultracentrifuge.

REFERENCES

1. Hunt, M. L., Newman, S., Scheraga, H. A., and Flory, P. J. J. Phys. Chem. **60**, 1278 (1956).
2. Holtzer, A. M., Benoit, H., and Doty, P. J. Phys. Chem. **58**, 624 (1954).
3. Newman, S. and Flory, P. J. J. Polymer Sci. **10**, 121 (1953).
4. Badger, R. M. and Blaker, R. H. J. Phys. & Colloid Chem. **53**, 1056 (1949).
5. Münster, A. J. Polymer Sci. **8**, 633 (1952).
6. Timell, T. E. Ind. Eng. Chem. **47**, 2166 (1955).
7. Timell, T. E. Svensk Papperstidn. **60**, 836 (1957).
8. Mitchell, R. L. Ind. Eng. Chem. **45**, 2526 (1953).
9. Newman, S., Loeb, L., and Conrad, C. M. J. Polymer Sci. **10**, 463 (1953).
10. Timell, T. E. Svensk Papperstidn. **57**, 777 (1954).
11. Schurz, J. and Immergut, E. H. J. Polymer Sci. **9**, 281 (1952).
12. Kroeplin, H. Kolloid-Z. **47**, 294 (1929).
13. Daniels, F., Mathews, J. H., and Williams, J. W. Experimental physical chemistry. 4th ed. McGraw-Hill Book Company, Inc., New York. 1949. p. 434.
14. Huggins, M. L. J. Am. Chem. Soc. **64**, 2716 (1942).
15. Öhrn, O. E. J. Polymer Sci. **17**, 137 (1955).
16. Takeda, M. and Eno, R. J. Phys. Chem. **60**, 1202 (1956).
17. Dandliker, W. B. and Kraut, J. J. Am. Chem. Soc. **78**, 2380 (1956).
18. Huque, M. M. and Goring, D. A. I. Forthcoming publication.
19. Goring, D. A. I., Senez, M., Melanson, B., and Huque, M. M. J. Colloid Sci. **12**, 412 (1957).
20. Kushner, L. M. J. Opt. Soc. Am. **44**, 155 (1954).
21. Maron, S. H. and Lou, R. H. J. Polymer Sci. **14**, 273 (1954).
22. Zimm, B. H. J. Chem. Phys. **16**, 1093, 1099 (1948).
23. Nawab, M. A. and Mason, S. G. Forthcoming publication.
24. Notley, N. T. and Debye, P. J. Polymer Sci. **24**, 275 (1957).
25. Benoit, H. and Doty, P. J. Phys. Chem. **57**, 958 (1953).
26. Kratky, O. and Porod, G. Rec. trav. chim. **68**, 1106 (1949).
27. Porod, G. Monatsh. **80**, 251 (1949).
28. Orofino, T. A. and Flory, P. J. J. Chem. Phys. **26**, 1067 (1957).
29. Peterlin, A. Nature, **171**, 259 (1953).
30. Lindsley, C. H. and Frank, M. B. Ind. Eng. Chem. **45**, 2491 (1953).
31. Wannow, H. A. Kolloid-Z. **102**, 29 (1943).
32. Kirkwood, J. G. and Riseman, J. J. Chem. Phys. **16**, 565 (1948).

33. BAWN, C. E. H., FREEMAN, R. E. J., and KAMALIDDIN, A. R. Trans. Faraday Soc. **46**, 1107 (1950).
34. FLORY, P. J. Principles of polymer chemistry. Cornell University Press, Ithaca, N.Y. 1953.
35. KUNST, E. D. Rec. trav. chim. **69**, 125 (1950).
36. OUTER, P., CARR, C. I., and ZIMM, B. H. J. Chem. Phys. **18**, 830 (1950).
37. BISCHOFF, J. and DESREUX, V. Bull. soc. chim. Belges, **61**, 10 (1952).
38. SCHULTZ, A. R. J. Am. Chem. Soc. **76**, 3422 (1954).
39. CRAGG, L. H. and BIGELOW, C. C. J. Polymer Sci. **14**, 177 (1955).
40. ALFREY, T., GOLDBERG, A. I., and PRICE, J. A. J. Colloid Sci. **5**, 251 (1950).
41. MASSON, C. R. and GORING, D. A. I. Can. J. Chem. **33**, 895 (1955).
42. CONRAD, C. M., TRIPP, V. W., and MARES, T. J. Phys. & Colloid Chem. **55**, 1474 (1951).
43. TIMELL, T. E. Svensk Papperstidn. **57**, 913 (1954).
44. IMMERGUT, E. H., RÄNBY, B. G., and MARK, H. F. Ind. Eng. Chem. **45**, 2483 (1953).

PHOTOÖXIDATION OF BUTENE-1 AND ISOBUTENE BY NITROGEN DIOXIDE[1]

S. SATO[2] AND R. J. CVETANOVIĆ

ABSTRACT

Reactions of oxygen atoms, produced by photolysis of nitrogen dioxide at 3660 Å, with butene-1 and isobutene have been studied at room temperature. In the case of butene-1, α-butene oxide and *n*-butanal have been identified as the major products, and methyl ethyl ketone, propanal, acetaldehyde, and ethyl nitrate as minor products. With isobutene, isobutanal was recovered as the major product and acetone, methyl ethyl ketone, methyl nitrate, and nitromethane as minor products. The absence of isobutene oxide in the recovered products from the isobutene reaction is due to its rapid reaction with nitrogen dioxide.

The following values were obtained for the relative reaction rates of oxygen atoms with nitrogen dioxide (k_2), butene-1 (k_{4a}), and isobutene (k_{4b}): $k_2/k_{4a} = 1.9$, $k_2/k_{4b} = 0.34$, $k_{4b}/k_{4a} = 5.5$.

INTRODUCTION

The photochemical reaction between nitrogen dioxide and olefins has been studied especially from the point of view of its relation to "smog" formation in polluted atmosphere (1), but little information has been obtained about the reaction mechanism and the type of products formed. In a previous communication (2) the authors have reported a long wave length threshold for the photochemical reaction between nitrogen dioxide and butene-1. The reaction occurs at 4047 Å and shorter wave lengths, with the formation of α-butene oxide and *n*-butanal as the main products, but does not occur at 4358 Å and longer wave lengths. It has, therefore, been assumed that even at 4047 Å nitrogen dioxide decomposes and forms free oxygen atoms in their ground electronic state,

$$NO_2 + h\nu = NO + O(^3P). \qquad (1)$$

The photolysis of nitrogen dioxide itself has been extensively investigated (3). In the absence of foreign gases reaction (1) is followed by

$$O + NO_2 = NO + O_2. \qquad (2)$$

When an olefin is added, nitrogen dioxide and the olefin compete for the oxygen atoms formed in reaction (1).

Reactions of oxygen atoms, produced by the mercury-photosensitized decomposition of nitrous oxide, have been studied in this laboratory for some time. In the case of olefins (4), studied at pressures between about 50 and 600 mm., oxygen atoms add to the olefinic double bond, and isomeric epoxides, aldehydes, and ketones are formed as the main products when the olefins consist of more than three carbon atoms. Propylene and ethylene require a collisional stabilization of the addition products formed.

In this paper, results of a study of the photochemical reaction of nitrogen dioxide with butene-1 and isobutene at 3660 Å are reported. At this wave length oxygen atoms produced in reaction (1) are in their ground state.

EXPERIMENTAL

Nitrogen dioxide was obtained from Matheson Co., Inc., and was further purified by repeated bulb-to-bulb distillation *in vacuo* at Dry Ice temperature. The middle third was

[1]*Manuscript received February 13, 1958.*
Contribution from the Division of Applied Chemistry, National Research Council, Ottawa, Canada.
Issued as N.R.C. No. 4728.
[2]*National Research Council Postdoctorate Fellow 1956–58.*

retained and stored at liquid nitrogen temperature. The color of the solid was pure white. Butene-1 and isobutene were Phillips reagent grade products, and were purified by repeated bulb-to-bulb distillation *in vacuo*. Nitrogen gas was supplied by Linde Air Products Co., and was used without further purification.

Because of rapid reaction of nitrogen dioxide with mercury it was necessary to use a mercury-free apparatus. Stopcocks were lubricated with Myvacene-S (Dow Corning) which was not attacked by nitrogen dioxide. Pressures were measured by means of a Bourdon gauge and the compensating pressures were read on a mercury or a silicon oil manometer. The reaction cell consisted of a 300 ml. quartz cylindrical vessel with an all-glass circulating pump supported on teflon bearings and a trap for condensing the reactants attached to it. The light from a medium-pressure mercury arc (Hanovia S 500) was used with Corning glass filter 7-60 so that essentially only the monochromatic light of 3660 Å entered the reaction cell. The cell and the attachments were screened from the diffuse light in the room.

The products formed were fractionated on a LeRoy still (5). Unreacted butene was pumped off at −120° C. and the remainder was transferred into a sampling tube containing a few drops of mercury to remove the unreacted nitrogen dioxide. This tube had been previously evacuated on a second, mercury-containing, high-vacuum apparatus. After the completion of the reaction between nitrogen dioxide and mercury, the tube was evacuated again at liquid nitrogen temperature. Subsequently the products were analyzed by gas–liquid chromatography (GLC) using a 7 ft. dinonyl-phthalate-on-glass-beads column (6, 4) and helium as the carrier gas. To confirm the identity of the compounds separated by GLC, use was made of infrared and mass spectroscopy. The quantitative estimate of the products was based on GLC peak areas.

RESULTS AND DISCUSSION

Thermal Reaction

Nitrogen dioxide attacks olefins thermally and forms addition products (7). Under the conditions employed in this work, however, the thermal reaction was much slower than the photochemical reaction. Moreover, it was found that no products formed in the thermal reaction, with the exception of nitric oxide, were recorded by the GLC. The thermal reaction between nitrogen dioxide and butene was, therefore, ignored in the present work.

Photochemical Reaction

The amounts of the main products formed* at various irradiation times and constant light intensity in the reaction of 3 mm. nitrogen dioxide with 3 mm. and 30 mm. butene-1 are shown in Fig. 1(*a*), and with 3 mm. isobutene in Fig. 1(*b*). The products formed increase almost linearly with the irradiation time up to 30 minutes and the primary processes of these reactions were subsequently studied within this time interval.

The main products formed in the case of butene-1 are the same as found previously for this reaction with the use of O atoms produced by mercury-photosensitized decomposition of nitrous oxide (4). In the case of isobutene, however, isobutene oxide, one of the two main products of the reaction (4), was usually not observed (Fig. 1*b*). This was shown to be due to its rapid reaction with excess nitrogen dioxide. A sample of isobutene oxide was kindly supplied by Dr. A. M. Eastham of these laboratories and its removal

**In the presence of large excess of unreacted NO_2 no attempt could be made to analyze for NO, formed in reactions (1) and (2), and for O_2, formed in reaction (2). A knowledge of the amounts of these products, however, is not essential for the present study.*

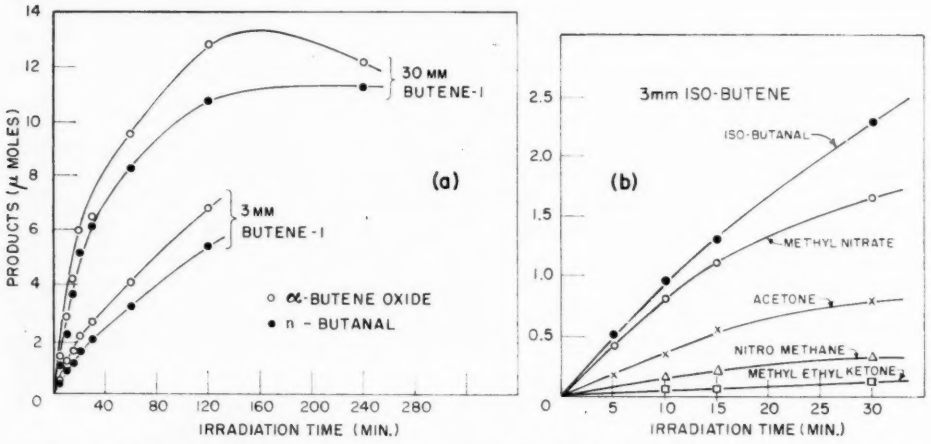

FIG. 1. Yield of the principal products as a function of irradiation time in the photoöxidation of (*a*) butene-1 and (*b*) isobutene.

in the presence of nitrogen dioxide and under conditions employed in the present experiments was demonstrated. The much greater reactivity of isobutene oxide relative to that of the 1,2-epoxides of *n*-olefins has been observed before (8).

Typical chromatograms of the reaction products are shown in Fig. 2. In the case of butene-1 (Fig. 2, A), the main products are α-butene oxide and *n*-butanal, and the minor products are methyl ethyl ketone, propanal, acetaldehyde, ethyl nitrate, and two unidentified compounds (compounds *a* and *b*). In the case of isobutene (Fig. 2, B) isobutanal appears as the only major product since isobutene oxide is removed by excess

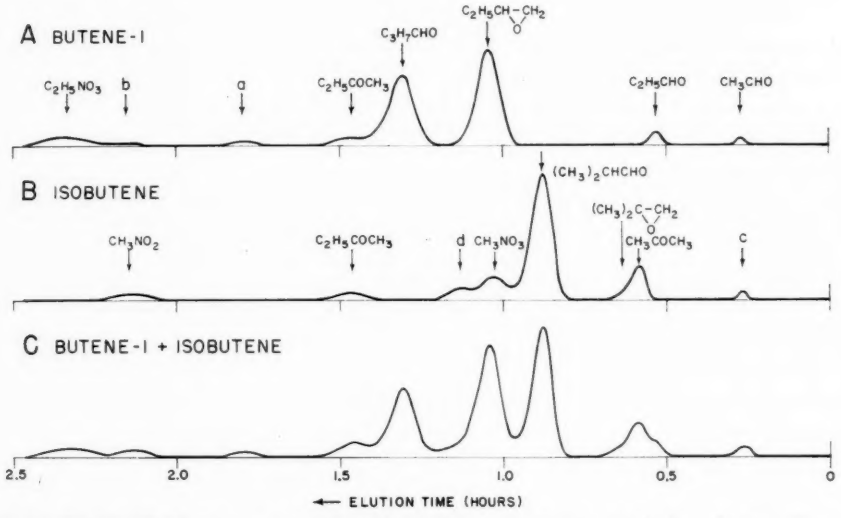

FIG. 2. Typical GLC peaks: A, photoöxidation of butene-1; B, photoöxidation of isobutene; and C, photoöxidation of mixtures of butene-1 and isobutene. (Column temperature 25° C.)

nitrogen dioxide; acetone, methyl nitrate, methyl ethyl ketone, nitromethane, and two unknown compounds (compounds *c* and *d*) are minor products. It was shown that these minor products were not formed in the thermal reaction of isobutene oxide and nitrogen dioxide.

Fig. 2, C shows the chromatogram of the products of a simultaneous photoöxidation of butene-1 and isobutene. No new products are observed but only those obtained in the reactions of the two butenes separately. This is in agreement with the previous conclusion (4) that the principal reactions under consideration do not involve a free-radical mechanism.

Effect of Pressure

Figs. 3(*a*) and 3(*b*) show the effect of pressure on the photochemical reactions of nitrogen dioxide with butene-1 and isobutene, respectively, at a constant irradiation time of 30 minutes. In both cases 1 mm. each of nitrogen dioxide and the olefin and various amounts of nitrogen were used. There is a pressure effect of the type observed previously (4) for propylene but in the present case it is confined to the pressures below about 30 mm. The lifetimes of the "hot" addition products formed appear to be an order of magnitude longer

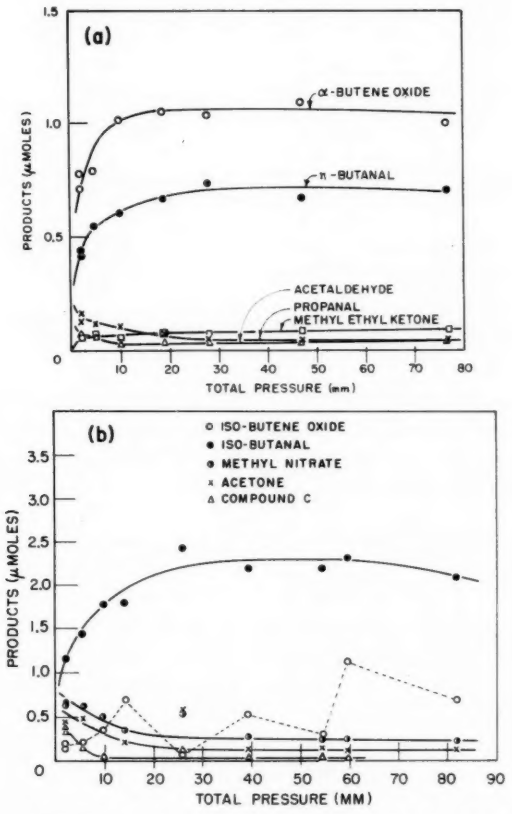

FIG. 3. Pressure effects in the photoöxidation of (*a*) butene-1 and (*b*) isobutene.

than in the case of propylene and the collisional stabilization, therefore, takes place at much smaller pressures. At pressures higher than about 70 mm. the rates of formation of the major products seem to show a tendency to decrease again. This is probably due to the additional consumption of oxygen atoms in the three-body reaction

$$O + NO_2 + M = NO_3 + M. \qquad (3)$$

No analogous decline was observed when O atoms were generated by the mercury-photosensitized decomposition of nitrous oxide (4).

In the case of butene-1 throughout the investigated pressure range the ratio of *n*-butanal to α-butene oxide was 0.40 ± 0.02 to 0.60 ± 0.02. In the case of isobutene only small and irregular quantities of isobutene oxide were recovered, for reasons already discussed. In the nitrous oxide work (4) the respective ratios of the aldehyde to the epoxide formed for the case of butene-1 and isobutene were 0.43 to 0.57 and 0.42 to 0.58.

Relative Reaction Rates of Oxygen Atoms with Nitrogen Dioxide, Butene-1, and Isobutene

Oxygen atoms are believed (4) to react with terminal monoölefins according to the following scheme:

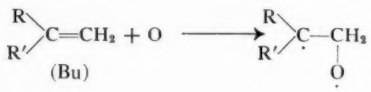

(4)

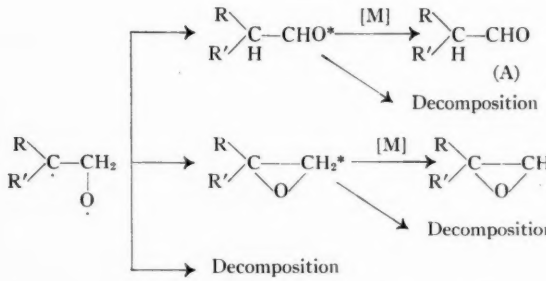

(5)
(6)
(7)
(8)
(9)

At a pressure of, for example, 40 to 50 mm. reactions (6) and (8) need not be considered. At small conversions and on applying the usual steady-state treatment to the remaining reactions and writing Bu for the butene and A for the aldehyde formed in reaction (5), the following relationship is obtained:

[1] $$\frac{\alpha\phi I[NO_2]}{R_A} = 1+\frac{k_2\,[NO_2]}{k_4\,[Bu]}\left(1+\frac{k_3}{k_2}[M]\right),$$

where $\phi I[NO_2]$ is the rate of light absorption by nitrogen dioxide (at small I and $[NO_2]$), R_A the rate of formation of the aldehyde A produced in reaction (5), and α the ratio of molecules of A formed to the number of oxygen atoms consumed in reaction (4). At constant $[NO_2]$, [M], irradiation time, and light intensity (I) a plot of reciprocal GLC peak areas of the compound A against $[NO_2]/[Bu]$ is linear. The slope-to-intercept ratio is

[2] $$m = \frac{k_2}{k_4}\left(1+\frac{k_3}{k_2}[M]\right).$$

Also

[3] $$k_{4a}/k_{4b} = m_b/m_a,$$

where the suffixes *a* and *b* refer to the butene-1 and the isobutene reaction, respectively.

The composition of the main products recovered after 15 minutes irradiation of NO_2–butene-1 mixtures at a total pressure of 50 mm. and at constant NO_2 but variable $[NO_2]/[Bu]$ ratios is shown in Table I, and for the NO_2–isobutene mixtures at a total pressure of 40 mm. in Table II.

TABLE I

YIELD OF THE PRINCIPAL PRODUCTS IN THE PHOTOÖXIDATION OF BUTENE-1 AS A FUNCTION OF THE $[NO_2]/[Bu\text{-}1]$ RATIO

(Irradiation time 15 min.)

Bu-1, mm.	NO_2, mm.	N_2, mm.	$[NO_2]/[Bu\text{-}1]$	GLC peak areas (cm.²)				
				n-BuA	α-BuO	PrA	MEK	AcA
28.9	3.1	11.3	0.11	12.9	16.2	0.3	1.5	0.3
19.4	3.1	27.6	0.16	12.6	16.0	0.5	1.0	0.4
12.9	3.1	36.7	0.24	11.2	15.9	0.6	1.3	0.4
9.2	3.1	37.0	0.34	10.8	14.3	0.5	1.1	0.5
7.1	3.1	39.2	0.44	8.4	11.9	0.5	1.0	0.5
6.0	3.1	40.7	0.52	8.1	11.1	0.4	0.8	0.4
5.0	3.1	41.3	0.62	7.4	9.4	0.5	0.8	0.4
4.5	3.1	42.4	0.69	6.0	8.1	0.4	0.8	0.3
3.9	3.1	43.2	0.79	6.6	9.1	0.4	0.6	0.3
3.3	3.0	43.3	0.91	5.9	6.2	n.d.	0.5	0.5
3.0	3.1	44.0	1.03	5.2	7.5	0.3	0.5	0.3

Bu-1 = *butene;* *n*-BuA = *n-butanal;* α-BuO = *α-butene oxide;* PrA = *propanal;* MEK = *methyl ethyl ketone;* AcA = *acetaldehyde;* *n.d.* = *not determined.*

TABLE II

YIELD OF THE PRINCIPAL PRODUCTS IN THE PHOTOÖXIDATION OF ISOBUTENE AS A FUNCTION OF THE $[NO_2]/[ISOBUTENE]$ RATIO

(Irradiation time 15 min.)

i-Bu, mm.	NO_2, mm.	N_2, mm.	$\frac{[NO_2]}{[i\text{-Bu}]}$	GLC peak areas (cm.²)							
				i-BuA	CH_3NO_3	Acetone	*i*-BuO	MEK	CH_3NO_2	Cpd. *c*	Cpd. *d*
29.2	3.1	6.7	0.11	19.2	2.5	1.7	0	0.8	1.8	0.1	1.5
9.1	3.1	26.0	0.34	17.9	2.2	2.7	0	0.8	1.0	0.2	1.4
4.8	3.1	28.0	0.65	16.2	n.d.	2.6	n.d.	n.d.	n.d.	n.d.	n.d.
3.0	3.1	33.3	1.03	12.8	2.4	2.4	0	0.3	1.0	0.3	1.4
2.0	3.1	34.3	1.6	13.4	2.5	2.5	0	0.5	0.8	0.3	1.0
1.6	3.1	34.4	2.0	11.8	2.6	1.8	0	0.4	1.0	0.3	1.2
1.5	3.1	35.6	2.1	11.7	2.1	2.0	0	0.6	0.8	0.3	1.5
1.2	3.1	38.2	2.6	11.0	1.9	1.5	0.1	0.4	0.7	0.4	1.1
0.98	3.1	38.0	3.2	9.4	1.6	1.2	0.6	0.3	1.0	0.3	1.0
0.85	3.1	39.1	3.7	8.0	1.4	1.2	0.2	0.3	0.7	0.3	1.0
0.75	3.1	39.6	4.2	7.7	2.1	1.9	0	0.2	0.5	0.2	0.7

i-Bu = *isobutene;* *i*-BuA = *isobutanal;* *i*-BuO = *isobutene oxide;* MEK = *methyl ethyl ketone;* *n.d.* = *not determined.*

The reciprocal peak areas of *n*-butanal and isobutanal, respectively, are plotted against $[NO_2]/[Bu]$ in Figs. 4(*a*) and 4(*b*). There is an appreciable scatter of experimental values and the least mean squares treatment gives $m_a = 2.1$ and $m_b = 0.38$. These quantities are approximately equal to k_2/k_{4a} and k_2/k_{4b}, respectively, since at pressures of 40 to 50 mm. the expression in the bracket in Eq. [2] does not differ much from unity. According to Ford and Endow (9), $k_3[M]/k_2 = 47.6\ [M]$ (where [M] is in mole/l.) so that the corrected values are

$$k_2/k_{4a} = 1.9, \text{ and } k_2/k_{4b} = 0.34.$$

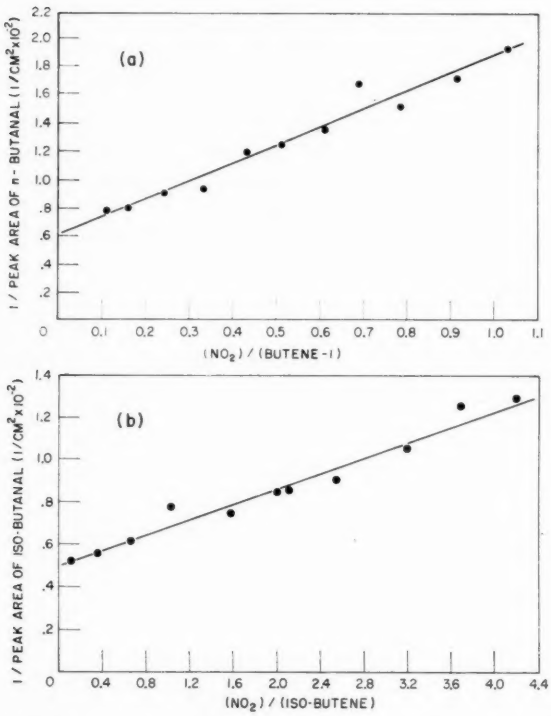

FIG. 4. (*a*) Reciprocal GLC peak areas of *n*-butanal as a function of the $[NO_2]/[\text{butene-1}]$ ratio (*b*) Reciprocal MLC peak areas of isobutanal as a function of the $[NO_2]/[\text{isobutene}]$ ratio.

The ratio of the rate constants of the reactions of oxygen atoms with butene-1 and isobutene is, therefore,

$$k_{4b}/k_{4a} = 5.5.$$

By photolyzing nitrogen dioxide in the presence of mixtures of butene-1 and isobutene, this ratio of the rate constants can be also evaluated from the relationship

$$\frac{k_{4b}}{k_{4a}} = \frac{[R_A]_b}{[R_A]_a}\frac{\alpha_a}{\alpha_b}\frac{[\text{butene-1}]}{[\text{isobutene}]}. \qquad [4]$$

Table III shows the amounts of *n*-butanal and isobutanal formed with various mixtures of butene-1 and isobutene. The two aldehydes have essentially the same molar GLC responses, as is shown in Fig. 5. Since it has also been found before (4) that $\alpha_a/\alpha_b \simeq 1$, the relative rate constant in Eq. [4] is obtained simply by multiplying the ratio of the GLC peak areas of the two aldehydes by the inverse ratio of the concentrations of the butenes. The values obtained are given in the last column of Table III. The mean value of about 5.8 agrees well with the above value of 5.5. There is, however, a considerable scatter from the mean value and perhaps also a systematic drift with the ratio of the two olefins: a decrease with decreasing isobutene to butene-1 ratio extrapolating to a limit of about 4.5 as the amount of isobutene tends to zero. In view of this and of the

TABLE III

YIELD OF ALDEHYDES IN THE PHOTOÖXIDATION OF MIXTURES OF BUTENE-1 AND ISOBUTENE

NO_2, mm.	*i*-Bu, mm.	Bu-1, mm.	N_2, mm.	Irradiation time, min.	GLC peak areas (cm.²)		k_{4b}/k_{4a}
					n-BuA	*i*-BuA	
3.1	0.98	3.95	31.0	15	6.8	10.1	5.9
3.2	0.81	4.97	32.3	15	7.9	6.9	5.4
3.1	1.26	3.48	31.8	15	3.9	9.1	6.4
6.2	1.00	4.10	32.1	10	6.4	9.1	5.7
3.1	0.99	4.02	31.6	15	4.8	6.8	5.8
						Average	5.8

i-Bu = *isobutene;* Bu-1 = *butene-1;* *n*-BuA = *n-butanal;* *i*-BuA = *isobutanal.*

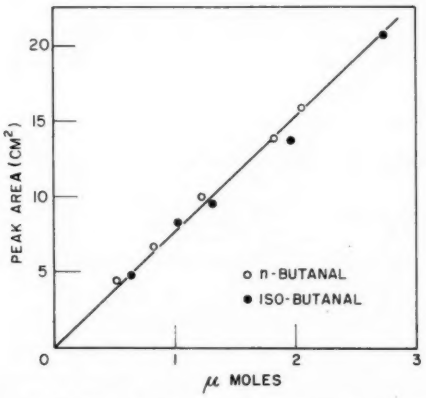

FIG. 5. GLC molar responses of *n*-butanal and isobutanal.

scatter of points in the plots in Figs. 4(*a*) and 4(*b*), it is felt that there is probably an experimental uncertainty of the order of 20 to 30 per cent in the relative rate constants determined in the present work. Previously (4) a value of 4.2 was obtained for k_{4b}/k_{4a}, which within the estimated experimental uncertainties agrees with the present value.

Formation of Minor Products

The complexity of the reactions and the incomplete analytical information preclude a detailed explanation of the method of formation of minor products.

Small amounts of methyl ethyl ketone were found in the case of both butene-1 and isobutene. The formation of this compound has been explained before (4) by addition of a small amount of oxygen atoms to the "more-substituted" carbon atom in the two butenes followed by migration of H or CH_3.

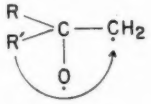

This migration is probably largely intramolecular, although the formation of nitromethane in the isobutene system suggests the presence of some free methyl radicals.

Most of the minor products increase at lower pressures, as is shown in Figs. 3(*a*) and

3(*b*). This is in agreement with an increasing importance of reactions (6) and (8) at lower pressures. However, even at higher pressures certain amounts of minor products are still formed, suggesting also the occurrence of some pressure-independent decomposition (reaction (9)).

Finally, it should be mentioned that under certain conditions in the presence of molecular oxygen propanal and acetone are formed as major products in the reactions of butene-1 and isobutene, respectively, besides the C_4 epoxides and aldehydes which are normally the only major products in these reactions. While these effects require further investigation, it is possible that oxygen produced in reaction (2) may contribute to some extent to the formation of propanal and acetone even when only nitrogen is used as diluent.

ACKNOWLEDGMENTS

The authors wish to thank Dr. E. C. Horswill for a sample of ethyl nitrate, Dr. A. W. Tickner for mass spectrometer analyses, and the Analytical Section of this Division for infrared analyses.

REFERENCES

1. THOMAS, M. D. Ind. Eng. Chem. **48**, 1522 (1956); FORD, H. W. and ENDOW, N. J. Chem. Phys. **27**, 1277 (1957).
2. SATO, S. and CVETANOVIĆ, R. J. Can. J. Chem. **36**, 279 (1958).
3. NOYES, W. A., Jr. and LEIGHTON, P. A. The photochemistry of gases. Reinhold Publishing Corp., New York. 1941. p. 400.
4. CVETANOVIĆ, R. J. J. Chem. Phys. **25**, 376 (1956); Can. J. Chem. **36**, 623 (1958).
5. LEROY, D. J. Can. J. Research, B, **28**, 492 (1950).
6. CALLEAR, A. B. and CVETANOVIĆ, R. J. Can. J. Chem. **33**, 1256 (1955).
7. LEVY, N. and SCAIFE, C. W. J. Chem. Soc. 1093 (1946); BROWN, J. F., Jr. J. Am. Chem. Soc. **79**, 2480 (1957).
8. ELTEKOW, A. Ber. **16**, 395 (1883); PRITCHARD, J. G. and LONG, F. A. J. Am. Chem. Soc. **78**, 2667 (1956).
9. FORD, H. W. and ENDOW, N. J. Chem. Phys. **27**, 1156 (1957).

CHEMICAL EFFECTS OF THE $Br^{81}(\gamma, \alpha)As^{77}$ REACTION IN BROMIDES[1]

D. H. Nelson and K. J. McCallum

ABSTRACT

An investigation has been made of the chemical forms of the arsenic produced when solid bromides, following irradiation with high-energy gamma rays, are dissolved in aqueous solution. The As^{77} is found to appear in both the pentavalent and the trivalent forms, the ratio AsV/AsIII increasing with an increase in the number of moles of water present in the hydrated solid. For the monohydrate of lithium bromide, the ratio depends upon the pH of the solution in which the solid is dissolved.

INTRODUCTION

When bromine atoms are exposed to high-energy gamma rays, one of the nuclear reactions which occurs involves the ejection of alpha particles, with the formation of As^{77}, a beta-emitting nuclide with a half-life of 39 hours (1). The present work is concerned with the chemical forms assumed by the radioactive arsenic when bromides which have been irradiated with gamma rays from a betatron are dissolved in aqueous solutions.

The As^{77} nuclide decays with the emission of a beta particle with 0.68 Mev. maximum energy to form stable Se^{77}. From the known masses of Br^{81} and Se^{77} (2), and the energy of the beta particles, the threshold energy for the $Br^{81}(\gamma, \alpha)As^{77}$ reaction can be calculated to be about 7 Mev. When betatron gamma rays of 23 Mev. peak energy are used to bring about this nuclear reaction, the maximum recoil energy imparted to the As^{77} nucleus is about 0.9 Mev.

Taylor and Haslam (3) have determined the activation and cross section curves for this reaction. From their results it can be calculated that for an irradiation dose of 10,000 roentgens with betatron gamma rays of 23 Mev. peak energy, the As^{77} produced in a 30 g. sample of KBr should have an initial decay rate equivalent to 200 disintegrations per second. This is sufficiently high to make the separation and measurement of the chemical forms of the As^{77} feasible by the carrier technique.

EXPERIMENTAL AND RESULTS

All of the bromide salts used were of reagent grade and were dried before use. The hydrated salts were prepared by the evaporation of solutions of the bromides, and drying the residue over the corresponding anhydrous salt. The water content of the hydrates so prepared did not differ by more than 2% from the theoretical quantity.

Sixty-gram samples of the bromides were exposed to radiation from a betatron operating at a peak energy of 23 Mev. for a period of 10 minutes. The intensity at the position of irradiation varied from about 1000 to 2000 roentgens per minute in different experiments. A number of different radioactive species resulted from this treatment. To determine the total amount of As^{77} produced in an irradiation a chemical separation was necessary before counting. The following procedures were used.

A weighed amount of the irradiated sample, approximately 30 g., was mixed with 40 mg. of powdered arsenic metal and the mixture was dissolved in 200 ml. of cold 6 *M* nitric acid. When the initial evolution of free bromine had ceased, the solution was then made

[1]*Manuscript received February 14, 1958.*
Contribution from the Department of Chemistry, University of Saskatchewan, Saskatoon, Saskatchewan. From a thesis submitted by D. H. Nelson in partial fulfillment of the requirements for the degree of Master of Arts.

basic with ammonia, and the arsenate precipitated as $MgNH_4AsO_4.6H_2O$. The precipitate was separated by filtration, dissolved and reprecipitated twice more. The precipitate was then mounted on filter paper, washed with a small amount of alcohol, and dried under a heat lamp. It was counted with a mica-window end-on counter under conditions of standard geometry. The weight of arsenate present in the precipitate was then determined volumetrically. The observed counts were corrected for decay. Self-scattering and self-absorption corrections were found to be negligible for the thicknesses of precipitate that were used.

The separation procedure was sufficient to separate all other radioactive nuclides present from the As^{77}, as was shown by half-life determinations on the precipitate. The measurements permitted a calculation of the total activity of the As^{77} produced per gram of bromide during the particular irradiation.

Measurements were made to determine the fraction of the As^{77} present as arsenite (AsIII) and as arsenate (AsV). A known weight of the irradiated sample, approximately 30 g., was dissolved in 100 ml. of solution containing known amounts of arsenite and arsenate carriers. After time for complete dissolution and equilibration, the arsenate fraction was removed by precipitation as $MgNH_4AsO_4.6H_2O$. This precipitate was separated by filtration, dissolved, reprecipitated, and prepared for counting in the manner previously described.

The filtrate containing the arsenite fraction was acidified to pH 2 with HCl, and the AsIII precipitated as As_2S_3 with hydrogen sulphide. The precipitate was filtered, dissolved in ammonium sulphide, and reprecipitated by acidification. The precipitate was removed and dissolved with HCl and $KClO_3$, which oxidized the arsenic to the pentavalent state. The arsenic was then precipitated and counted as $MgNH_4AsO_4.6H_2O$.

In all cases, the sum of the amounts of the As^{77} found in the AsIII and AsV fractions was equal to the total As^{77} content within experimental error. Attempts were made to detect As^{77} present as arsine by bubbling arsine through a freshly prepared solution of the irradiated bromide and then absorbing the gas on a filter paper impregnated with mercuric chloride solution. The paper was then counted but no detectable amounts of radioactivity were observed.

Experiments were carried out on the exchange of arsenic between arsenite and arsenate in the presence of high concentrations of bromide ion. Labeled arsenate ion was prepared using radioactive As^{76} produced by the (n, γ) reaction on sodium cacodylate (4). This was added to 100 ml. of a solution containing 30 g. of potassium bromide and a known amount of arsenite carrier. The solution was allowed to stand for 2 hours, and then the arsenite and arsenate fractions were separated and counted. The results indicated that at both high and low values of the pH, less than one per cent exchange had occurred.

The results obtained when irradiated samples of some bromides and bromide hydrates were dissolved in water are given in Table I. Lithium, sodium, potassium, and ammonium bromides each gave approximately 10% of the As^{77} activity in the AsV fraction, and the remainder appeared as AsIII. The monohydrate of lithium bromide gave 55% in the AsV fraction while the dihydrates of lithium and sodium bromides gave approximately 95% of the As^{77} in the AsV fraction.

The effect upon the distribution of As^{77} of the pH of the solution in which the irradiated solids were dissolved was determined. A Beckman pH meter, model N-2, was used to determine the pH values. The addition of large quantities of the solid bromides to the solutions tended to decrease the pH values. An attempt was made to keep the pH constant by the gradual addition of NaOH solution as the solid was dissolved. Table II

TABLE I

PERCENTAGE OF $As^{77}V$ FOLLOWING SOLUTION IN WATER

Compound	% $As^{77}V$
LiBr	11±1
NaBr	9±1
KBr	10±1
NH_4Br	11±1
$LiBr.H_2O$	55±2
$LiBr.2H_2O$	91±3
$NaBr.2H_2O$	92±3

TABLE II

EFFECT OF pH ON PERCENTAGE OF $As^{77}V$

Compound	pH	% $As^{77}V$
NaBr	3.0– 3.2	8±1
	10.5–10.9	9±1
	10.8–11.2	8±1
LiBr	3.0– 3.2	10±1
	10.0–10.2	9±1
	10.6–11.2	9±1
	11.0–11.6	8±1
$LiBr.H_2O$	0.5	51±1
	2.5– 2.8	55±1
	9.2– 9.6	57±2
	10.5–10.9	68±1
	10.7–11.2	72±2
	10.9–11.2	73±2
	11.1–11.6	60±2
	11.2–12.0	53±2
	12.0–13.0	54±2
$LiBr.2H_2O$	4.0– 4.2	90±3
	10.7–11.2	92±2
	13.0–14.0	96±2

gives the pH range observed during the solution of the solid, and the percentage of As^{77} appearing in the AsV fraction.

The results show that in basic solutions, anhydrous sodium and lithium bromides and the dihydrate of lithium bromide give essentially the same distribution as they do in neutral solutions. The monohydrate of lithium bromide, however, shows a peculiar behavior in that the percentage of As^{77} appearing as AsV increases to a maximum at about pH 11, and then decreases at higher pH values.

DISCUSSION

The results in Table I indicate that the distribution of As^{77} between the trivalent and pentavalent states is markedly dependent upon the amount of water contained in the crystal. For 0, 1, or 2 moles of water per mole of bromide, the percentage of As^{77} appearing as AsV is about 10, 53, and 95 respectively. An increase in the amount of water favors the formation of the more highly oxidized form. This is probably to be correlated with the corresponding increase in the percentage of oxygen in the solid.

The results given in Table II indicate that for the anhydrous salts and for the dihydrate of lithium bromide, the same results are obtained when the solids are dissolved in solutions of high pH as when they are dissolved in water. For the anhydrous bromides and the dihydrate the results can be explained by assuming that two types of As^{77}-containing

species may be present, the first reacting with water to form AsIII and the second to form AsV, the ratio of the second to the first increasing when the water content of the solid is increased from 0 to 2 moles per mole of bromide. The valence state formed on solution appears to be independent of pH.

Although the percentage of the As^{77} appearing as AsV for lithium monohydrate is intermediate between the values found for the anhydrous salts and the dihydrate, the results of Table II cannot be explained by assuming that here the same two As^{77}-containing species are present in the solid, but in intermediate proportions. The maximum in the percentage of the As^{77} appearing as AsV which occurs at about pH 11 requires the presence of at least one species in the solid whose reactions on solution depend upon the pH of the solution in a rather complicated way. This species appears to be absent or present in only small proportions when the irradiated solid is the anhydrous bromide or the dihydrate.

There is no evidence concerning the exact identity of any of the species which have been postulated to occur in the irradiated solid. The two species assumed to be present in the irradiated anhydrous bromides and in the dihydrate could contain arsenic in the trivalent and pentavalent states respectively and undergo hydrolysis upon solution to form arsenite and arsenate. The third type of species, present in addition to the other two in irradiated bromide monohydrates, could represent an intermediate type formed only at intermediate water content. If there is only one species of this intermediate type, to explain the results of Table II, one would have to assume that it undergoes three competing reactions in solution. The first would involve a reaction with water to form AsIII, the second a reaction with hydroxyl ion to form AsV, and the third a reaction of higher order with respect to hydroxyl ion to form AsIII. Other schemes to explain the results of Table II can be devised if one assumes more than one species of this intermediate type.

The results obtained are not sufficient to allow any definite conclusions to be drawn as to the chemical forms of the As^{77} in these irradiated bromides. It can be stated, however, that As^{77} is present in more than one chemical form, and that for lithium bromide monohydrate, reactions on solution involving hydroxyl ions can occur.

ACKNOWLEDGMENT

Grateful acknowledgment is made to the National Research Council for financial support.

REFERENCES

1. ERDOS, P., JORDAN, P., SCHMEUKER, J., and STOLL, P. Helv. Phys. Acta, **27**, 127 (1954).
2. COLLINS, T. L., JOHNSON, W. H., and NIER, A. O. Phys. Rev. **94**, 398 (1954).
3. TAYLOR, J. G. V. and HASLAM, R. N. H. Phys. Rev. **87**, 1138 (1952).
4. WESTERVELT, D. Phys. Rev. **92**, 531 (1953).

REACTION OF DEUTERIUM ATOMS WITH ETHANE—MECHANISM OF METHANE EXCHANGE[1]

R. Berisford[2] and D. J. Le Roy

ABSTRACT

The reaction of deuterium atoms with ethane has been studied at 25° C. by the method of mercury ($^3P_1$) photosensitization. Methane formation takes place by the addition of D atoms to methyl radicals in the presence of a third body. From the dependence of methane exchange on third-body concentration the lifetime of the excited methane molecule is estimated to be of the order of 10^{-9} sec. The lifetime of the excited ethane molecule formed by the addition of a D atom to an ethyl radical is estimated to be considerably less than 10^{-9} sec.

INTRODUCTION

The reaction between ethane and atomic hydrogen (or deuterium) has been studied under a number of different conditions and the literature has been discussed extensively by Steacie (1). There is little doubt that the primary reaction in every case is

$$H \text{ (or D)} + C_2H_6 = C_2H_5 + H_2 \text{ (or HD)}. \quad [1]$$

Methane is the main product formed at the low pressures used in the discharge tube method of Wood and Bonhoeffer (1) and the hot filament method of Berlie and Le Roy (2). It is also an important product when the H (or D) atoms are produced by mercury photosensitization, even when the initial quenching is by ethane:

$$Hg(^3P_1) + H_2 = Hg(^1S_0) + 2H, \quad [2]$$

$$Hg(^3P_1) + C_2H_6 = Hg(^1S_0) + H + C_2H_5. \quad [3]$$

Presumably, the methane arises from methyl radicals formed in the atomic cracking reaction,

$$H + C_2H_5 = 2CH_3, \quad [4]$$

followed by

$$H + CH_3 = CH_4, \quad [5]$$

$$CH_3 + H_2 = CH_4 + H, \quad [6]$$

or

$$CH_3 + C_2H_6 = CH_4 + C_2H_5. \quad [7]$$

The primary purpose of the present investigation was the elucidation of the mechanism of methane formation, particular emphasis being placed on the role of inert gases on the extent of deuterization of the methane.

EXPERIMENTAL

Reagents

Heavy water (99.83%), obtained from Atomic Energy of Canada Limited, was used to produce deuterium by the method described by Kirshenbaum (3). Ethane, obtained from the Ohio Chemical and Manufacturing Company, was subjected to numerous trap-to-trap distillations in which only the intermediate portions were retained. Carbon dioxide, obtained from commercial Dry Ice, and propane (Ohio) were treated in the same way. The four deuterated methanes, CH_3D, CH_2D_2, CHD_3, and CD_4, were obtained

[1]*Manuscript received January 30, 1958.*
Contribution from the Department of Chemistry, University of Toronto, Toronto, Ontario.
[2]*Present address: E. I. Du Pont de Nemours & Co., Inc., Newport Experimental Station, Newport, Delaware.*

from Merck & Co., Ltd., Montreal. Their purity was said to be not less than 98.0, 96.0, 96.9, and 99.4%, respectively. We were unable to detect any foreign bands in their individual infrared spectra.

Reaction System

The total volume of the reaction system was 2780 cm.^{3}, and included a buffer volume, an all-glass circulating pump, and a cylindrical quartz cell 10 cm. long and 5 cm. in diameter. Resonance radiation was provided by a 4-watt U-shaped General Electric germicidal lamp. The mercury vapor concentration in the reaction cell was the equilibrium vapor pressure at room temperature. The ethane was measured accurately in a small calibrated volume before condensing it into the reaction system.

Analysis of Products

The non-condensable products, consisting of the various hydrogens and methanes, were passed through a trap containing silica gel cooled with liquid air. This removed all of the methanes and most of the hydrogens. The methanes were finally separated in a pure state by treating the desorbed gas with copper oxide at 250° C. and then passing it through a liquid-air trap.

The condensable gases were fractionated on a low-temperature still (4). A few of the ethane fractions were subjected to infrared and mass spectrographic analysis.

Infrared analyses of the methanes formed in the reaction were made with a Perkin-Elmer Model 12-C spectrometer with sodium chloride optics, modified as described previously (5). No CH_4 was found but each of the other four methanes was present. The fundamental vibration frequencies used are given in Table I.

TABLE I

INFRARED ABSORPTION OF DEUTERATED METHANES, VALUES OF q $(=(1/P)\log I_0/I_t)$ IN MM.$^{-1}$†

cm.$^{-1}$	996	1034	1090	1156	1235	1299	1306
CH_3D	0.00	0.00	0.0045	0.0294	0.0100	0.0046	0.0227
CH_2D_2	0.00	0.0226	0.0367	0.0083	0.0215	0.0078	0.0072
CHD_3	0.0236	0.0449	0.0062	0.0034	0.0036	0.0114	0.0092
CD_4	*	*	0.00	0.00	0.00	0.00	0.00

*See text.
†For path length of 67 cm., slit width 0.250 mm.

Because of the small moments of inertia there was a considerable amount of overlapping of the bands, but of more significance was their susceptibility to pressure broadening. The observed extinction coefficient of any particular methane at one of its principal absorption frequencies was strongly dependent on the amounts of other methanes present, even when there was no overlapping of bands. This difficulty was overcome by deliberately broadening the rotational structure by the addition of large amounts of carbon dioxide. An example of the effect of carbon dioxide on optical density ($D = \log I_0/I_t$) is shown in Fig. 1. Calibration curves were obtained and analyses made using a standard pressure of 400 mm. of carbon dioxide in the absorption cell.

Under these conditions linear plots of D vs. P, the pressure in mm., were obtained for the individual methanes (except in the case of CD_4) and the values of q in the expression $D = qP$ are given in Table I; q has the units mm.$^{-1}$ and applies to the particular

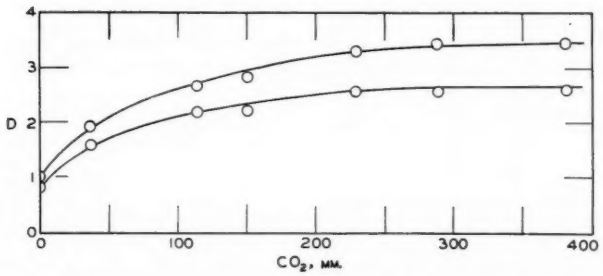

FIG. 1. Effect of carbon dioxide on the optical density, $D = \log I_0/I_t$, at 1306 cm.$^{-1}$ (upper curve) and 1235 cm.$^{-1}$ (lower curve) for a sample containing the four deuterated methanes.

optical cell used, which had a path length of 67 cm. The values of q, which are underlined in Table I, are for frequencies at which maxima occur; the remaining values indicate the magnitude of overlapping. Since D was not proportional to P for CD_4, the concentration of CD_4 in a mixture was obtained from the empirical curve of D vs. P after correcting the observed optical density at 996 cm.$^{-1}$ for the contribution due to CHD_3. The concentrations of CHD_3, CH_2D_2, and CH_3D were obtained by solving equations of the form $D = \sum q_i P_i$ for each of the appropriate frequencies.

Analytical results on three synthetic mixtures are given in Table II. Mass spectrographic analysis on sample No. 2 was done through the kindness of Dr. A. W. Tickner, Division of Applied Chemistry, National Research Council, Ottawa.

TABLE II

ANALYSIS OF SYNTHETIC MIXTURES OF THE DEUTERATED METHANES

Sample	Method	% CH_3D	% CH_2D_2	% CHD_3	% CD_4
1	Synthesis	28	30	32	10
	Infrared anal.	31	31	30	8
2	Synthesis	27.9	21.7	18.7	31.7
	Infrared anal.	29.2	21.4	19.5	29.9
	Mass spec. anal.*	30±3	22±3	21±1	24±1
3	Synthesis		37.9	52.7	9.4
	Infrared anal.		41.3	48.1	10.6

**Analysis report included 0+5% CH_4.*

RESULTS AND DISCUSSION

The effect of the inert gas carbon dioxide on the relative yields of the deuterated methanes is shown in Table III. A comparison of the ethane consumed with the total methanes formed shows that these are the most important products. In a few instances analyses were made for higher products: 0.066 mm. of propane and 0.0040 mm. of butane were formed in experiment No. 6; 0.063 mm. of propane, 0.007 mm. of butane, and 0.006 mm. of hexane were formed in experiment No. 8. A mass spectrographic analysis of the residual ethane from experiment No. 12 showed that 0.36 mm. of C_2H_5D and 0.09 mm. of $C_2H_4D_2$ were formed.

It is evident from Table III that variations in the initial pressure of deuterium have

TABLE III

EFFECT OF CARBON DIOXIDE ON RELATIVE YIELDS OF THE DEUTERATED METHANES

No.	mm. $(C_2H_6)_0$	mm. $-\Delta(C_2H_6)$	mm. $(D_2)_0$	mm. (CO_2)	mm. (Methane)	% CH_3D	% CH_2D_2	% CHD_3	% CD_4
6	4.59	1.14	30.5	0	1.88	16.8	27.6	30.2	25.4
8	4.61	1.04	55.0	0	1.75	14.1	31.4	30.3	24.2
10	4.67	0.91	30.1	54.0	1.61	27.4	32.9	16.3	23.4
11	4.67	0.99	49.6	50.6	1.69	27.9	33.2	20.6	17.6
9	4.62	0.80	21.0	100.9	1.54	33.8	36.4	12.8	17.0
18	4.67	—	19.6	146.0	1.58	39.4	37.7	18.8	4.2
12	4.68	0.60	32.2	199.5	0.89	44.0	51.0	5.0	0.0

little or no effect either on the amount of total methane or on its isotopic composition. This suggests that the methyl radicals formed in [4′] do not, under the conditions of our experiments, form methane by the analogue of [6]:

$$D + C_2H_5 = CH_3 + CH_2D. \qquad [4']$$

This is further borne out by the fact that the analogue of [6] would yield only CH_3D and CH_2D_2 unless some source of CHD_2 and CD_3 radicals was provided. Reaction [7] can be eliminated since no CH_4 was produced, a fact which gives further support to the elimination of [6], since the rate constants reported for [6] and [7] are such that in the present experiments the abstraction by CH_3 radicals of D atoms from D_2 and of H atoms from C_2H_6 would proceed at approximately the same rate (6, 7).

The results in Table III show that high pressures of carbon dioxide cause an increase in the proportions of CH_3D and CH_2D_2 and a decrease in the proportions of CHD_3 and CD_4. It is evident, therefore, that reactions analogous to [5] require a third body. The following detailed mechanism is suggested:

$$D + CH_3 = CH_3D^*, \qquad [8]$$

$$CH_3D^* = CH_2D + H, \qquad [9]$$

$$CH_3D^* + M = CH_3D + M. \qquad [10]$$

Similar reactions involving $CH_2D_2^*$, CHD_3^*, and CD_4^* are assumed to occur. Defining α_1, α_2, α_3, and α_4 as the rate constants for the bimolecular formation, β_1, β_2, β_3, and β_4 for unimolecular decomposition, and γ_1, γ_2, γ_3, and γ_4 for bimolecular stabilization of these four excited molecules, expressions can be derived for the rates of formation of each of the stable deuterated methanes in terms of [4′]. The rate of [4′] will, of course, be equal to one half the total rate of formation of methane. Unimolecular decompositions of excited molecules yielding D atoms need not be taken into account, and the rate of formation of CD_4 will be given simply by $\alpha_4(D)(CD_3)$. Writing $\beta_i/\gamma_i = p_i$ and noting that the latter has the same units as M, the calculated percentage yields are as follows:

(i) $$\% CH_3D = 50[M/(p_1+M)],$$

(ii) $$\% CH_2D_2 = 50[(2p_1+M)/(p_1+M)].[M/(p_2+M)],$$

(iii) $$\% CHD_3 = 50[(2p_1+M)/(p_1+M)].[p_2/(p_2+M)].[M/(p_3+M)],$$

(iv) $$\% CD_4 = 50[(2p_1+M)/(p_1+M)].[p_2/(p_2+M)].[p_3/(p_3+M)].$$

If it is assumed that $\gamma_1 = \gamma_2 = \gamma_3 = Z$, in which Z is the collision frequency per unit concentration for the deactivating reactions, then the natural lifetimes, τ_1, τ_2, τ_3 of the activated species CH_3D^*, $CH_2D_2^*$, CHD_3^*, will be given by $\tau_1 = 1/(p_1Z)$, $\tau_2 = 1/(p_2Z)$,

$\tau_3 = 1/(p_3 Z)$. Lifetimes calculated in this way will apply, of course, only to decompositions which yield H atoms. The value of Z used, 4.3×10^{-10}, was based on that for a collision between CO_2 and CH_2D_2*, assuming a mean collision diameter of 4.42 Å, estimated from viscosity data. Taking into account reduced masses and mean collision diameters, M is given by the expression $M = (CO_2)+1.25(C_2H_6)+1.20(D_2)$; however, better correlation was obtained when the coefficient of the D_2 concentration was set at 0.6.

Since analytical errors in the determination of small percentages of CH_3D are emphasized when reciprocals are taken, the "best" value of p_1 was obtained by plotting equation (i) for various assumed values of p_1, as shown in Fig. 2. It was estimated that p_1 was approximately 60 mm. Using this value, equation (ii) was plotted for various assumed values of p_2, as shown in Fig. 3; p_2 was estimated to be approximately 85 mm. In a similar way p_3 was estimated to be approximately 50 mm. The uncertainty in p_3 was somewhat greater than that in p_2 and p_1, possibly because the analysis for CD_4 was dependent on that for CHD_3, as mentioned previously. Agreement between theory and

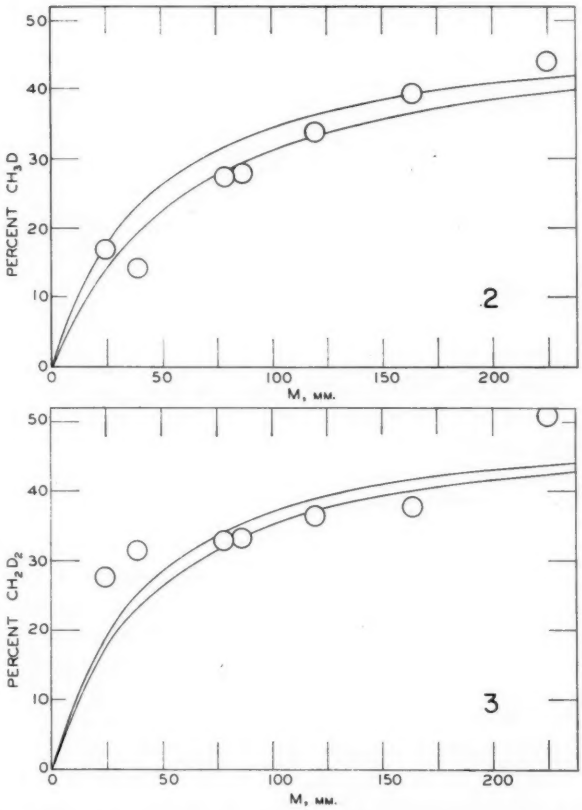

FIG. 2. Effect of third-body concentration on the proportion of CH_3D in the total methanes. Upper curve, equation (i) with $p_1 = 45$ mm.; lower curve, $p_1 = 60$ mm.

FIG. 3. Effect of third-body concentration on the proportion of CH_2D_2 in the total methanes. Upper curve, equation (ii) with $p_1 = 60$ mm., $p_2 = 85$ mm.; lower curve, $p_1 = 60$ mm., $p_2 = 95$ mm.

experiment was not improved by postulating pressure-independent exchange reactions of the type $D + CH_3 = CH_2D + H$.

In view of the limited accuracy of the determination of the individual deuterated methanes there is no justification for assigning different lifetimes to the three activated molecules. About all that can be said is that the lifetimes are of the order of 10^{-9} sec., corresponding to a p of the order of 70 mm.

It is possible to obtain a simple expression for the percentage of deuterium in the total methanes on the assumption that $p_1 = p_2 = p_3 = p$. For $p = 70$ mm. this expression agrees reasonably well with the experimental results, the average deviation being less than 4%. This would, of course, have been the only criterion of the mechanism if the methane fraction had simply been burned and the deuterium content of the water determined, but it also has some merit in the present instance since values for the individual methanes are, to some extent, interdependent.

In order to further substantiate the mechanism it is necessary to take into account the H atoms liberated in reactions such as [9]. Since no CH_4 was found the H atoms must be consumed in one or more of reactions [1], [4], and [11]:

$$H + D_2 = HD + D \qquad [11]$$

Glasstone, Laidler, and Eyring (8) have calculated that at 300° K., k_{11} will be 1.5/7.3 times the rate constant for the conversion of para to ortho hydrogen. Using the data of Geib and Harteck (8, 9) for the para–ortho conversion, k_{11} would be 2×10^7 cm.^{3} mole^{-1} sec.$^{-1}$; using the expression $10^{13.7}\ e^{-7500/RT}$, as suggested by Trotman-Dickenson (10), k_{11} would be 3.3×10^7. At the same temperature k_1 is 3.7×10^7 (2). Thus k_{11} and k_1 are of similar magnitude. Furthermore, the concentration of D_2 was from 4 to 10 times that of C_2H_6. An additional factor accounting for the absence of CH_4 is the fact that one quarter of the total atom consumption is due to reaction [1], in which the substitution of an H for a D atom would not affect the relative amounts of the deuterated methanes.

The consumption of H atoms by [4] would result in less-extensive deuterization than predicted by the mechanism. The magnitude of the decrease depends on the ratio $k_4(H)/k_{4'}(D)$ and would be more important at low values of M. By assuming a reasonable magnitude for this ratio it was concluded that the true lifetime would probably be greater than 0.5×10^{-9} sec. It is unfortunate that the experimental accuracy did not permit the use of such criteria as plotting $(CHD_3)/(CD_4)$ vs. M.

Lavrovskaia, Mardaleishvili, and Voevodskii (11, 12) have suggested a mechanism for the exchange of radicals which, in the case of CH_3, would correspond to the reaction

$$CH_3 + D_2 = CH_3D + HD \qquad [12]$$

While their results are not directly comparable to ours because they did not investigate the deuterium content of their methane, their conclusion that deuterium atoms play no role in radical exchange must be taken with reservation in view of the dependence of deuterization on third-body concentration, clearly demonstrated in the present work.

The argument that reactions such as [8], [9], and [10] cannot account, in many cases, for the amount of deuterium found in the products hinges on the relative rates of [11] and of the primary reaction of the D atoms (reaction [1] in the present instance). If the former is greater than the latter there is no difficulty in accounting for the extent of deuterization; if the rates are comparable then the extent of deuterization could increase with D_2, as found by Lavrovskaia, Mardaleishvili, and Voevodskii, even if reactions analogous to [12] did not occur.

It is of interest to compare the present results with the possible lifetime of $C_2H_5D^*$, formed in the reaction

$$D + C_2H_5 = C_2H_5D^*. \qquad [13]$$

This reaction undoubtedly precedes [4′], but the lifetime of the excited molecule must be much less than 10^{-9} sec., as shown by the following considerations.

From quenching data for D_2 (13) and CO_2 (14) the observed rates of formation of methane were corrected for quenching by CO_2. The corrected rates showed no dependence on M and hence the formation of deuterized ethane must be attributed to reactions which are independent of pressure in the range used, presumably to the combination of methyl radicals. The lifetime of $C_2H_5D^*$ formed in [13] would be expected to be much less than that of the excited methanes, in spite of the increased number of degrees of freedom, since its energy content would be about 14 kcal. per mole greater than that required for breaking the C—C bond.

The authors wish to express their thanks to the National Research Council for supporting this research.

REFERENCES

1. STEACIE, E. W. R. Atomic and free radical reactions. Reinhold Publishing Corp., New York. 1954.
2. BERLIE, M. R. and LE ROY, D. J. Discussions Faraday Soc. **14**, 50 (1953).
3. KIRSHENBAUM, I. Physical properties and analysis of heavy water. McGraw-Hill Book Company, Inc., New York. 1951.
4. LE ROY, D. J. Can. J. Research, B, **28**, 492 (1950).
5. SEFTON, V. B. and LE ROY, D. J. Can. J. Chem. **34**, 41 (1956).
6. WHITTLE, E. and STEACIE, E. W. R. J. Chem. Phys. **21**, 993 (1953).
7. TROTMAN-DICKENSON, A. F., BIRCHARD, J. R., and STEACIE, E. W. R. J. Chem. Phys. **19**, 163 (1951).
8. GLASSTONE, S., LAIDLER, K. J., and EYRING, H. The theory of rate processes. McGraw-Hill Book Company, Inc., New York. 1941.
9. GEIB, K. H. and HARTECK, P. Z. physik. Chem. (Bodenstein Festband), 849 (1931).
10. TROTMAN-DICKENSON, A. F. Gas kinetics. Butterworth Scientific Publications, London. 1955.
11. VOEVODSKII, V. V., LAVROVSKAIA, G. K., and MARDALEISHVILI, P. E. Doklady Akad. Nauk S.S.S.R., **81**, 215 (1951) (TT-358).
12. LAVROVSKAIA, G. K., MARDALEISHVILI, R. E., and VOEVODSKII, V. V. Voprosy Khimicheskoi Kinetiki, Kataliza i Reakstsionnoi Sposobnosti. Akad. Nauk S.S.S.R., Otdel. Khim. Nauk, 40 (1955) (TT-701).
13. EVANS, M. G. J. Chem. Phys. **2**, 445 (1934).
14. MITCHELL, A. C. G. and ZEMANSKY, M. W. Resonance radiation and excited atoms. Cambridge University Press, London. 1934.

THE MASS SPECTRA OF THREE DEUTERATED BUTANOLS[1]

W. H. McFadden, M. Lounsbury, and A. L. Wahrhaftig[2]

ABSTRACT

The mass spectra of 1,1-dideutero-1-butanol, 1,1,1,3,3-pentadeutero-2-butanol, and 1,1,1,2,3,3-hexadeutero-2-butanol have been obtained using 70-volt ionizing electrons. Comparison of the cracking patterns of the deuterated butanols with those of the undeuterated compounds confirms certain known features of the mass spectra of alcohols and reveals further information regarding the formation of several rearrangement ions. The strong tendency for alcohols to break at bonds beta to the hydroxyl group has been attributed to charge localization on the oxygen and this feature is used to explain the formation of many of the rearrangement ions. It is postulated that a hydrogen atom may be transferred to the electron-deficient oxygen and that the resulting structure distributes its excess energy and charge to give the activated complexes leading to the observed ions.

INTRODUCTION

The mass spectra of some deuterated ethanols (1), propanols (2, 3, 4), and butanols (5, 6) have been previously reported. In addition to being a valuable aid in kinetic studies the cracking patterns have given considerable information about the behavior of alcohols under electron bombardment. In the mass spectra of the four isomeric butanols rearrangement* ions occur at mass/charge ratio† $m/e = 33$ ($CH_3OH_2^+$) for *n*-butanol and isobutanol and at $m/e = 31$ (CH_2OH^+) for *sec*-butanol and *tert*-butanol (7). With the exception of a small amount of a mass 33 ion formed from *n*-propanol these ions are not observed in the mass spectra of other alcohols. However, many higher alcohols produce ions by loss of uncharged groups having mass 31 or 33, a notable example being formation of the abundant ion with mass 55 from 3-methyl-1-butanol. Inspection of the mass spectra of the alcohols reported by the American Petroleum Institute (7) suggests that these ions may be formed as primary daughter ions. In addition, many ions are apparently formed by loss of similar rearrangement groups such as H_3O, H_2O, CH_3OH, CH_3CH_2OH. It is clear that an activated complex in which a highly stable molecule such as H_2O or CH_3OH is partially formed will be energetically favored. It is also likely that there is some stabilization obtained by the partial formation of such radicals as OH_3 and CH_3OH_2.

From previous research (8), we had available three deuterated butanols: 1,1-dideutero-1-butanol, 1,1,1,3,3-pentadeutero-2-butanol, and 1,1,1,2,3,3-hexadeutero-2-butanol (hereafter referred to as *n*-butanol-d_2, *sec*-butanol-d_5, and *sec*-butanol-d_6 respectively). In order to investigate the formation and significance of the rearrangement ions the mass spectra of the three deuterated butanols have been obtained, along with those of the undeuterated compounds.

EXPERIMENTAL

Preparation of the three deuterated butanols has been described elsewhere (8). Originally they were collected as small "center-cut" samples from a distillation column operating with approximately eight theoretical plates. They were stored two years at Dry-Ice

[1]*Manuscript received March 4, 1958.*
Contribution from Chemistry and Metallurgy Division, Atomic Energy of Canada Limited, Chalk River, Ontario, Canada, and the Department of Chemistry, University of Utah, Salt Lake City, Utah. Presented in part at the 40th Annual Conference, Chemical Institute of Canada, Vancouver, British Columbia, June 3–5, 1957.
Issued as A.E.C.L. No. 582.
[2]*Department of Chemistry, University of Utah, Salt Lake City, Utah.*
**"Rearrangement ions" refers to ions formed from an activated complex in which the molecular configuration differs from that of the original molecule owing to intramolecular transfer of atoms or groups of atoms.*
†Since this paper makes no reference to doubly charged ions the word "mass" is frequently substituted for the expression "m/e".

temperature and about six months at room temperature. Before introduction into the mass spectrometer they were further purified by processing through a gas–liquid chromatographic column to remove traces of water and other impurities.

The mass spectra were obtained using a 90°-deflection, 6-in.-radius mass spectrometer similar to one described previously (9). The alcohols were allowed to diffuse into the ion source through a capillary leak under their own vapor pressure. The electron-accelerating potential was 70 volts and the electron current to the ionization chamber was 40 μa. The positive ions were accelerated into the analyzer tube by a potential of 2000 volts and the mass spectrum was scanned magnetically. The ion current arriving at the collector was amplified and recorded with a Speedomax Pen Recorder, Type G.

RESULTS

The mass spectra of *n*-butanol-d_0, *n*-butanol-d_2, *sec*-butanol-d_0, *sec*-butanol-d_5, and *sec*-butanol-d_6 are presented in Table I. The ion abundances, in terms of mole per cent (i.e. total ion current normalized to 100%), are the averages of two runs appropriately corrected for background contributions. The normal residual corrections were insignificant except at $m/e = 28$ where residual nitrogen contributed from 5 to 10% of that peak. However, when a sample was admitted to the mass spectrometer considerable enhancement of background was observed, which was shown to be due to the previous alcohol sample. This memory effect was reduced by mass analyzing the samples several weeks apart and by baking and flushing the mass spectrometer tube during the intervening period. Where necessary, corrections were made for the previous sample by measuring the height of a suitable ion-current peak and calculating the contribution of the contaminant to the rest of the spectrum. The maximum possible error introduced by this procedure was too small to affect the conclusions reported.

The mass spectra have not been corrected for carbon or oxygen isotopic contributions nor has any assay been made to determine the hydrogen–deuterium isotopic purity of the samples. From previous work (8) it is believed that the isotopic purity is better than 97%, and inspection of the mass spectra presented in Table I appears to confirm this. For example, the abundance ratio of the ions at $m/e = 48$ and 47 obtained from *sec*-butanol-d_5 shows the maximum possible isotopic impurity to be 3% on carbon 1. This value for the isotopic impurity would be reduced by any contribution of the ions CD_3COH^+ or CD_3CHO^+ at $m/e = 47$.

DISCUSSION

A. General

Many outstanding features of the mass spectra of alcohols have led to the conclusion that dissociation of the parent molecule–ion occurs with the ion in an electronic state in which the electron removed from the molecule is one of the non-bonding electrons of the oxygen atom. This generalization was first suggested by Cummings and Bleakney as a result of appearance-potential studies for the ions from methanol and ethanol (10). The apparent localization of charge on the oxygen causes the oxygen to behave as a trivalent atom, and as a consequence it attempts to form a bond with atoms that approach within bond-length distances. Thus, it attempts to form an additional bond with the carbon to which it is already attached and as a result the other three bonds of that carbon are weakened. Breaking of any one of these bonds, with or without transfer of the charge to the hydrocarbon fragment, gives rise to the principal ions formed by simple bond rupture. In addition to this, the trivalent oxygen also attempts to form bonds with atoms or

TABLE I

MASS SPECTRA OF DEUTERATED BUTANOLS

	n-Butanol, mole %		*sec*-Butanol, mole %		
m/e	d_0	d_2	d_0	d_5	d_6
14	0.21	0.17	0.24	0.12	0.11
15	0.88	0.51	1.07	0.36	0.29
16	0.27	0.42	0.19	0.51	0.41
17	1.15	0.79	0.08	0.96	0.55
18	4.90	3.03	0.34	2.77	1.11
19	0.58	0.23	1.57	0.17	0.22
20		0.27		0.70	0.11
21				0.64	1.14
22				0.06	0.26
27	7.41	6.02	5.03	1.34	0.98
28	6.67	6.85	4.67	4.63	4.50
29	4.45	3.68	4.61	3.80	2.30
30	0.44	2.83	0.24	2.58	4.91
31	14.9	1.25	7.72	3.65	2.60
32	0.28	1.56	0.11	4.45	4.39
33	1.27	13.8		2.06	4.14
34		0.36		0.18	0.56
35		1.32			
39	2.68	2.00	2.02	0.45	0.23
40	0.74	1.11	0.36	0.68	0.53
41	11.1	7.06	6.66	1.64	0.98
42	5.34	8.02	0.98	1.65	1.12
43	10.3	11.8	4.30	3.86	1.59
44	0.95	1.32	3.23	2.03	3.49
45	2.23	1.04	38.6	3.17	2.91
46	0.12	0.23	0.92	4.97	3.72
47		0.76		1.06	2.46
48				36.5	1.68
49				1.25	37.6
50					2.05
55	2.43	0.35	1.48	0.30	0.17
56	15.2	1.14	1.32	0.62	0.22
57	1.40	1.88	2.05	0.58	0.36
58	0.04	15.9	0.26	0.66	0.17
59	0.26	1.10	7.64	1.06	0.79
60		0.06	0.27	0.97	0.59
61		0.06		6.30	0.86
62				1.10	6.72
63				0.12	1.31
64				0.11	0.11
65					0.10
72	0.09	0.03	0.12		
73	0.30	0.10	0.67		
74	0.13(P)*	0.14	0.10(P)		
75		0.03			
76		0.11(P)			
77				0.08	0.06
78				0.51	0.27
79				0.10(P)	0.04
80					0.06(P)

*(P) = *parent ion.*

groups that come in its vicinity as a result of vibrations and internal rotations. The complexes thus formed can give rise to the various rearrangement ions observed in the mass spectra of alcohols.

These suggestions are consistent with the theory of mass spectra of polyatomic molecules presented by Rosenstock and co-workers (11, 12, 13). According to this theory, the

excited parent ion distributes its excess energy among its various degrees of freedom until a particular configuration, the activated complex, is formed. This complex then dissociates, forming a daughter ion. The redistribution of excess energy can lead to a number of different activated complexes and in addition the daughter ions can decompose to give secondary ion products. The mass spectrum is thus the result of several competing unimolecular reactions. Studies of mass spectra of polyatomic molecules show that the charge is selectively localized at various sites but it is not always possible to determine a priori where the most probable location may be. The determining factor is most generally the relative magnitudes of the ionization potentials of the two fragments but experimental data to illustrate this point for alcohols are scarce. Calculations of the mass spectra have been made using the theory of Rosenstock *et al.* for methyl, ethyl, isopropyl, and *n*-propyl alcohols (14, 15). For these calculations, charge localization on the oxygen was assumed for determinations of the principal reactions and the calculated results are in agreement with the experimental observations.

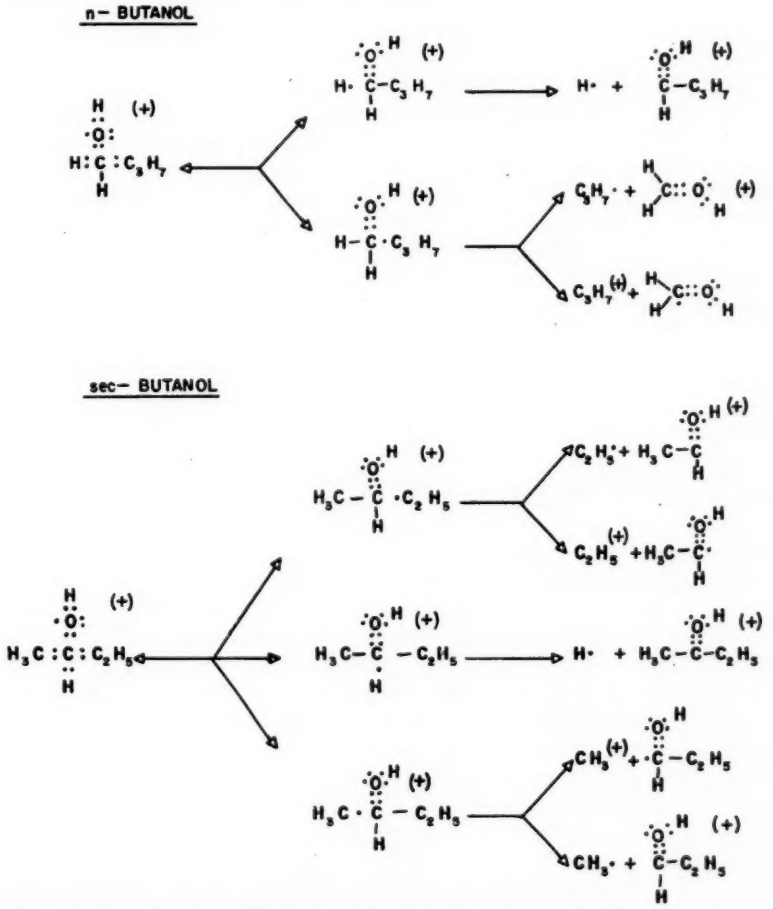

FIG. 1. Principal reactions leading to a simple bond break in *n*-butanol and *sec*-butanol.

B. Ions Formed by Simple Bond Rupture

The principal contribution of ions formed by a simple bond break to the mass spectra of alcohols arises from the rupture of bonds beta to the hydroxyl (i.e. the other bonds of the carbon to which the hydroxyl is attached). In Fig. 1 the ions formed by a simple bond break are shown for *n*-butanol and *sec*-butanol. An attempt has been made to show the important influence of charge localization by using the electron dot representation where appropriate. In Table II the data from which these reactions are deduced are shown. These data and previous experimental evidence (1, 2, 3, 4, 5, 6) indicate that this influence is not extended appreciably beyond bonds beta to the hydroxyl. During the period between ionization and decomposition the parent ion may resonate between the various structures illustrated and eventually dissociate to give the ions observed.

(*i*) *n-Butanol*

In the parent region the most abundant ion is that due to the loss of hydrogen. In Table II the mass spectrum of *n*-butanol-d_2 shows that this hydrogen is lost primarily from the carbon containing the hydroxyl for, when this carbon is deuterated, the largest ion in the parent region becomes the parent minus 2 mass units. This observation has

TABLE II

ABUNDANCES OF IONS FORMED BY A SIMPLE BOND BREAK

Ion	*n*-Butanol, mole %		*sec*-Butanol, mole %		
	d_0	d_2	d_0	d_5	d_6
Parent	0.13	0.11	0.10	0.10	0.06
P−1 (H)*	0.30	0.03	0.67	0.51	0.04
P−2 (D, H_2)	0.09	0.14	0.12	0.08	0.27
P−15 (CH_3)	0.26	0.06	7.64	0.11	0.10
P−18 (CD_3)	—	—	—	6.30	6.72
P−29 (CH_2CH_3)	2.23	0.76	38.6	—	—
P−31 (CD_2CH_3)	—	—	—	36.5	37.6
P−31 (CH_2OH)	10.3	—	—	—	—
P−33 (CD_2OH)	—	11.8	—	—	—
P−43 (C_3H_7)	14.9	13.8	—	—	—

**P refers to parent ion; P−1 refers to the parent ion minus 1 atomic mass unit (H), etc.*

been previously noted for deuterated ethanols (1) and isopropanols (2, 3, 4). Loss of $CH_3\cdot$ from *n*-butanol-d_0 can occur by a simple bond break only from a delta bond and significantly it is found that it contributes only 0.26% of the total ionization. Loss of $CH_3CH_2\cdot$ from *n*-butanol-d_0 can occur by a simple bond break of a gamma bond and contributes only 2.2% of the total. From *n*-butanol-d_2 loss of $CH_3\cdot$ or of $CH_3CH_2\cdot$ is considerably smaller (0.06% and 0.76% respectively), which may indicate that these processes occur only partly by simple rupture of gamma or delta bonds. On the other hand loss of a propyl radical to form the ion CH_2OH^+ or loss of $\cdot CH_2OH$ to form a propyl ion both contribute a considerable fraction of the total ionization of *n*-butanol and the data obtained from the mass spectrum of *n*-butanol-d_2 confirm the expectation that these ions are formed by a simple beta bond break.

(*ii*) *sec-Butanol*

The most abundant ion in the parent region is that due to loss of hydrogen, as was also noted for *n*-butanol. Again the data of Table II demonstrate that this hydrogen is

primarily from the carbon containing the hydroxyl. Loss of $CH_3\cdot$ from *sec*-butanol contributes 7.6% of the total ionization and could occur by breaking a carbon–carbon bond beta or gamma to the hydroxyl. In the d_5 and d_6 *sec*-butanols the beta methyl group is deuterated and the mass spectra show conclusively that the methyl group lost is almost entirely from the beta position. Loss of $CH_3CH_2\cdot$ may also occur as a result of a simple bond break beta to the hydroxyl and contributes 38% of the total ionization. The data of Table II indicate this to be the principal reaction with no significant indication of intramolecular rearrangements.

C. Ions Formed by Intramolecular Rearrangement

In addition to the tendency to break bonds beta to the hydroxyl, the mass spectra of alcohols show a number of important ions which are formed by intramolecular rearrangement. The existence of ions such as $CH_3OH_2^+$ from *n*-butanol indicates the possibility of an activated complex in which the rearranged group has been partly or wholly formed. It is further suggested that for certain reactions such an activated complex may lose the rearranged group as a neutral fragment by transfer of the charge to the hydrocarbon matrix. It is obvious that loss of the groups H_3O, CH_3OH_2, etc. might occur in two steps (e.g. loss of CH_3OH_2 could be the result of loss of $\cdot CH_2OH$ followed by loss of H_2) but in a homologous series no general relationship is observed between the relative abundance of the ion due to loss of $\cdot CH_2OH$ and that due to loss of CH_3OH_2. If the latter occurred principally as a two-step process one would expect the ratio (parent $-$ CH_3OH_2)/(parent $-$ $\cdot CH_2OH$) to be approximately constant. In actuality this ratio varies randomly over a range of 0.25 to 20 for the 11 alcohols cited in Table III. Alternatively it might be suggested that, since loss of H_2O gives the most abundant ion (15.2%) in the mass spectra of *n*-butanol, formation of the ion $C_3H_5^+$ could be due to loss of H_2O followed by loss of $\cdot CH_3$. However, loss of H_2O leads to the ion $C_4H_8^+$ and the most reasonable secondary step is then $C_4H_8^+ \rightarrow C_2H_4^+ + C_2H_4$. The other possibility, loss of $CH_3\cdot$ followed by loss of H_2O, seems unreasonable since the ion formed by loss of $CH_3\cdot$ at $m/e = 59$ requires breaking of a delta bond and is only 0.26% abundant.

It may reasonably be concluded that in some of the cases the CH_3OH_2 fragment is lost as a unit even though it is inherently unstable as a separate molecule. This postulate

TABLE III

RELATIVE ABUNDANCES[a] OF IONS FORMED BY LOSS OF CH_3O, CH_4O, AND CH_5O FOR BUTANOLS AND PENTANOLS

Alcohol	Minus CH_3O	Minus CH_4O	Minus CH_5O	Minus CH_3O / Minus CH_5O
1-Pentanol[b]	21.5	13.9	59.4	2.8
2-Pentanol[b]	0.81	0.72	16.0	20
3-Pentanol[b]	5.30	.43	3.00	0.57
2-Me-1-butanol[c]	*100.0*	88.2	24.5	0.25
3-Me-1-butanol[c]	30.7	12.8	*100.0*	3.3
2-Me-2-butanol[b]	1.98	1.67	32.6	16
3-Me-2-butanol[b]	1.06	0.49	9.49	9.0
2-Me-1-propanol[b]	*100.0*	57.5	57.2	0.57
2-Me-2-propanol[d]	12.1	2.7	18.3	1.5
1-Butanol[b]	60.3	31.4	61.7	1.0
2-Butanol[b]	10.5	1.77	10.8	1.0

[a] *Normalized to the most abundant ion equal to 100.*
[b] *Stanolind Oil and Gas Co., Tulsa, Oklahoma. See Ref. 7.*
[c] *University of California, Berkeley, California. See Ref. 7.*
[d] *Union Oil Co., Wilmington, California. See Ref 7.*

implies that both the rearrangement ion and the ion formed by loss of the rearranged group may result from the same activated complex. The appearance of the positive charge on either will be a statistical result of resonance between the various electronic configurations, and the ratio of the ion abundance of each species should be a function of the ionization potential of each fragment.

(*i*) *n-Butanol*

In order to explain the existence of the observed rearrangement ions it is suggested that an intramolecular rearrangement occurs whereby a hydrogen atom is transferred to the electron-deficient oxygen in the following fashion:

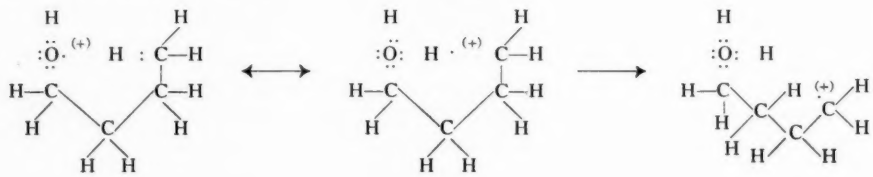

I II III

As a result of internal rotations and vibrations carbon-bonded hydrogen atoms will approach within bonding range of the oxygen and during this brief encounter establish equilibrium between structures I and II. As the molecule continues its internal motion the hydrogen may be transferred to the oxygen as shown. The resulting complex, III, would continue to distribute its excess energy and charge among the various degrees of freedom until a configuration was obtained which would lead to decomposition.

To demonstrate how a complex of this type can explain the formation of many of the rearrangement ions, specific examples are chosen for *n*-butanol. It is clear that the complex III could undergo a simple bond break to form the predominant ion $C_4H_8^+$ or the less predominant* H_2O^+. Comparison of the mass spectra of *n*-butanol-d_0 and *n*-butanol-d_2 (Table I) reveals that in the formation of H_2O^+ the hydrogen on carbon 1 is not involved to any significant extent (<7%). A similar comparison for the ion formed by loss of H_2O ($C_4H_8^+$) leads to the same conclusion, i.e. that the hydrogen lost with the hydroxyl does not come from carbon 1. The mass spectrum of 1-deutero-1-butanol tabulated by Eliel and Prosser (6) confirms this conclusion and in addition the mass spectrum of their compound, 2-deutero-1-butanol, indicates that the hydrogen on carbon 2 is also not involved. These observations agree with the fact that for the rearrangements proposed, transfer of the hydrogens from carbon 3 or 4 is sterically more favorable. An alternative suggestion (16) is that the hydrogen on carbon 2 is lost after the hydroxyl, thus forming the stable ethylenic structure, but the data of Eliel and Prosser eliminate this possibility so far as *n*-butanol is concerned.

The ion $CH_3OH_2^+$, which is observed for very few alcohols and is significant only for *n*-butanol and isobutanol, could be formed from complex III by transfer of the H_2O group to the terminal methyl or alternatively by transferring another hydrogen to carbon 1. In the mass spectrum of *n*-butanol-d_2 there is an rearrangement ion of 1.32% abundance at mass 35 ($CHD_2OH_2^+$). This value is in agreement with the value of 1.27% contributed by the corresponding rearrangement ion ($CH_3OH_2^+$) formed from *n*-butanol-d_0. Since

**Although care was taken to remove H_2O from the samples it is not known whether H_2O has contributed significantly to the ions at m/e = 18 in Table I. For example, the 2.4% increase observed at this mass from sec-butanol-d_5 is probably about 40% from CD_3 and 60% from an H_2O impurity.*

the position of the deuteriums has been retained in this ion it indicates that transfer of an additional hydrogen is the predominant mechanism. The data of Eliel and Prosser for 2-deutero-1-butanol indicate furthermore that approximately one-half of the time the extra hydrogen comes from the adjacent carbon, carbon 2. It is interesting to note that although the pentanols do not form the ion $CH_3OH_2^+$ to any significant extent, several show abundant ions due to loss of 33 mass units, and in the mass spectrum of 3-methyl-1-butanol (which is structurally similar to *n*-butanol) this ion is the largest peak. An important test of the mechanisms postulated here would be a study of deuterated forms of some of these pentanols.

Formation of the ion H_3O^+ could readily occur by transfer of a second hydrogen to the H_2O group on complex III. The data indicate that this hydrogen apparently comes from the adjacent carbon (carbon 1) about one-half of the time and a similar conclusion is reached regarding loss of H_3O to form the $C_4H_7^+$ ion. In the latter case there is at present no conclusive evidence to eliminate the possibility of two consecutive reactions contributing to this ion (e.g. loss of OH followed by loss H_2), but from the arguments presented earlier these would appear to be relatively unimportant.

(*ii*) *sec-Butanol*

The mass spectrum of *sec*-butanol contains a number of rearrangement ions similar to those observed from *n*-butanol but the data obtained from the deuterated analogues do not clearly indicate simple reaction mechanisms. Secondary butanol-d_0 produces the rearrangement ion CH_2OH^+ (7.7% abundance) at mass 31. Because of the possible contribution of the deuterated ethyl ions, $CD_2CH_3^+$ and $CH_2CD_3^+$, to the peaks observed at masses 31 and 32 the reaction mechanisms are not apparent but the data indicate that several patterns may be possible. For example, the appearance of the ion CD_2OH^+ (m/e = 33) in the mass spectrum of *sec*-butanol-d_5 indicates that approximately 25% of the time the hydrogen on the carbon containing the hydroxyl (carbon 2) is not involved. (The contributions of CDH_2OH^+ and $CDHOD^+$ to the mass 33 ion are relatively small.) In addition the peak observed at mass 32 from *sec*-butanol-d_6 could not be entirely due to the deuterated ethyl ion $CD_3CH_2^+$ and it is estimated that at least one-half of the observed abundance (4.4%) would be due to the ion $CDHOH^+$. This indicates that a significant number of events involve one of the hydrogens on carbon 4. The most plausible explanation of these observations seems to be that the ion CH_2OH^+ (or its deuterated analogues) arises from the daughter ions CH_3CHOH^+ (38%) and CH_3CH_2-$CHOH^+$ (7.6%), which may be in equilibrium with their various structures

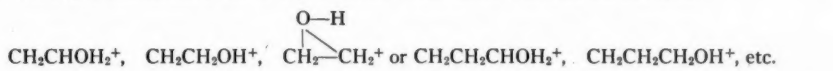

Such rearrangement ions could decompose to produce the various deuterated ions of CH_2OH^+ observed from *sec*-butanol-d_5 and *sec*-butanol-d_6. It is noteworthy that the equilibrium structures suggested might undergo a sufficient number of exchanges to give an ion with a deuterated hydroxyl. The ion abundance observed at mass 34 for both deuterated *sec*-butanols is too large to be explained as due to the C^{13} isotopic species or to a deuterated CH_3OH^+ analogue. In accordance with the foregoing postulates one may conclude that it is CD_2OD^+.

The formation of ions by loss of rearrangement groups such as CH_3OH_2, CH_2OH, cannot be deduced with any certainty because of the large expected contribution of secondary products from the abundant daughter ion CH_3CHOH^+. As indicated in Table I, the six ions with masses between 39 and 44 contribute 18% of the total ionization in the

mass spectra of *sec*-butanol-d_0. In the mass spectra of the deuterated *sec*-butanols this 18% ionization is divided quite evenly between nine ions so that one cannot reasonably determine probable reaction paths.

Ions formed by the possible loss of H_2O cannot be readily studied from the mass spectra of the two deuterated *sec*-butanols because of the excessive contribution due to the ion formed by loss of CD_3. The mechanism of the loss of H_3O to form $C_4H_7^+$ (or deuterated analogues) can be partially deduced. The data indicate that for about 60% of the events only the hydrogens from carbon 2 or carbon 4 are involved ($m/e = 59$, *sec*-butanol-d_5) while the ion at mass 60 in the spectrum of *sec*-butanol-d_6 indicates that one hydrogen from carbon 4 is involved in about 40% of the events. The formation of the hydronium ion apparently involves the hydrogens from carbon 4 less than 10% of the time ($m/e = 20$, *sec*-butanol-d_6) whereas the single hydrogen from carbon 2 can be involved about 40% ($m/e = 20$, *sec*-butanol-d_5). The appearance of the fully deuterated hydronium ion at $m/e = 22$ may indicate that H_3O^+ arises primarily from the daughter-ion structures suggested to explain the observations on the deuterated analogues of CH_2OH^+. It would seem that loss of a hydrogen and subsequent gain of three deuteriums by the oxygen would be quite unexpected except in terms of a relatively simple exchange equilibrium.

REFERENCES

1. Burr, J. G. J. Am. Chem. Soc. **79**, 751 (1957).
2. Condon, F. E. J. Am. Chem. Soc. **73**, 4675 (1951).
3. Condon, F. E., McMurray, H. L., and Thornton, V. J. Chem. Phys. **19**, 1010 (1951).
4. Friedman, L. and Turkevich, J. J. Am. Chem. Soc. **74**, 1666 (1952).
5. Eliel, E. L. and Prosser, T. J. Document number 4817, ADI Auxiliary Publications Project, Photoduplication Service, Library of Congress, Washington 25, D.C.
6. Eliel, E. L. and Prosser, T. J. J. Am. Chem. Soc. **78**, 4045 (1956).
7. Catalog of Mass Spectral Data, Am. Petroleum Inst., Research Project 44. Carnegie Institute of Technology, Pittsburgh, Pennsylvania. 1957.
8. McFadden, W. H. and Wahrhaftig, A. L. J. Am. Chem. Soc. **78**, 1572 (1956).
9. Graham, R. L., Harkness, A. L., and Thode, H. G. J. Sci. Instr. **24**, 119 (1947).
10. Cummings, C. S., II and Bleakney, W. Phys. Rev. **58**, 787 (1940).
11. Rosenstock, H. M., Wallenstein, M. B., Wahrhaftig, A. L., and Eyring, H. Proc. Natl. Acad. Sci. U.S. **38**, 667 (1952).
12. Rosenstock, H. M. Absolute rate theory for isolated systems and the mass spectra of polyatomic molecules. Doctoral thesis, University of Utah, Salt Lake City, Utah. 1952.
13. Wallenstein, M. B. The ionization and dissociation of molecules by electron impact. Doctoral thesis, University of Utah, Salt Lake City, Utah. 1951.
14. Collin, J. Bull. soc. roy. sci. Liège, 520 (1956).
15. Friedman, L., Long, F. A., and Wolfsberg, M. J. Chem. Phys. **27**, 613 (1957).
16. McLafferty, F. W. Private communication.

THE CONFIGURATION OF GLYCOSIDIC LINKAGES IN OLIGOSACCHARIDES

VI. DEGRADATION OF 4-*O*-METHYL-D-GLUCOPYRANURONOSYL-ALDOBIURONIC ACIDS TO 2-*O*-(4-*O*-METHYL-D-GLUCOPYRANOSYL)-GYCEROLS[1]

P. A. J. Gorin and A. S. Perlin

ABSTRACT

The configurations of glycosidic linkages in 4-*O*-methyl-D-glucopyranuronosyl-aldobiuronic acids can be determined by conversion to the derived 2-*O*-D-glucopyranosyl-glycerol hexamethyl ether, which is compared, by its infrared spectrum and specific rotation, with the sirupy hexamethyl ethers synthesized from 2-*O*-α- and 2-*O*-β-D-glucopyranosyl-glycerol. Thus, the configuration of 2-*O*-(4-*O*-methyl-D-glucopyranuronosyl)-D-xylose was shown to be α, since it was degraded to 2-*O*-α-D-glucopyranosyl-glycerol hexamethyl ether. The configuration of 4-*O*-(4-*O*-methyl-D-glucopyranuronosyl)-D-galactose was correlated with that of the former aldobiuronic acid, since both gave crystalline 2-*O*-α-(4-*O*-methyl-D-glucopyranosyl)-glycerol penta-*p*-nitrobenzoate.

INTRODUCTION

Parts II and IV of this series (1, 2) describe a method for determining the configuration of reducing disaccharides by degradation to one of the two possible anomeric 2-*O*-glycopyranosyl-glycerols. The present paper demonstrates the feasibility of this approach for the 4-*O*-methyl-D-glucopyranuronosyl-aldobiuronic acids, except those linked glycosidically to the primary hydroxyl group of the reducing end-unit. Two readily obtainable aldobiuronic acids, 2-*O*-(4-*O*-methyl-D-glucopyranuronosyl)-D-xylose (I) (3), from the wood of *Populus tacamahacca* Mill. (4), and 4-*O*-(4-*O*-methyl-D-glucopyranuronosyl)-D-galactose (II), from Mesquite gum (5), were examined and each found to contain the α-glycosidic linkage.

Isolated from the wood, 2-*O*-(4-*O*-methyl-D-glucopyranuronosyl)-D-xylose was converted to the D-xylitol derivative (III) by sodium borohydride reduction (6). The xylitol derivative was treated with diazomethane and the methyl ester formed was oxidized with 2.2 moles of lead tetraacetate (1) which preferentially oxidized the xylitol end-group to give 2-*O*-(4-*O*-methyl-D-glucopyranuronosyl)-L-glyceraldehyde methyl ester. Reduction of the glyceraldehyde derivative with sodium borohydride (6, 7) afforded after purification by cellulose column chromatography (8) 2-*O*-(4-*O*-methyl-D-glucopyranosyl)-glycerol (IV) ($[\alpha]_D$ +125°). All of the above-described intermediates were not crystalline. The last-named compound was methylated with sodium hydroxide – methyl sulphate to yield its hexamethyl ether ($[\alpha]_D$ +123°), which gave an infrared absorption spectrum indistinguishable from that of the sirupy hexamethyl ether ($[\alpha]_D$ +132°) prepared from the known 2-*O*-α-D-glucopyranosyl-glycerol (1). By contrast, the fully methylated sirupy derivative of the known anomeric β-glucosyl-glycerol (9, 10) showed $[\alpha]_D$ −5° and gave an infrared absorption spectrum distinctly different from that of the α-derivative. A crystalline derivative suitable for characterization of other α-(4-*O*-methyl-D-glucopyranuronosyl)-aldobiuronic acids was provided by the complete *p*-nitrobenzoylation of 2-*O*-α-(4-*O*-methyl-D-glucopyranosyl)-glycerol. This derivative may be prepared with perhaps as little as 10 mg. of the glycerol derivative and hence is more useful than the methyl ether for characterization of the α-anomer.

[1]*Manuscript received February 14, 1958.*
Contribution from the National Research Council of Canada, Prairie Regional Laboratory, Saskatoon, Saskatchewan.
Issued as N.R.C. No. 4730 and as Paper No. 254 on the Uses of Plant Products.

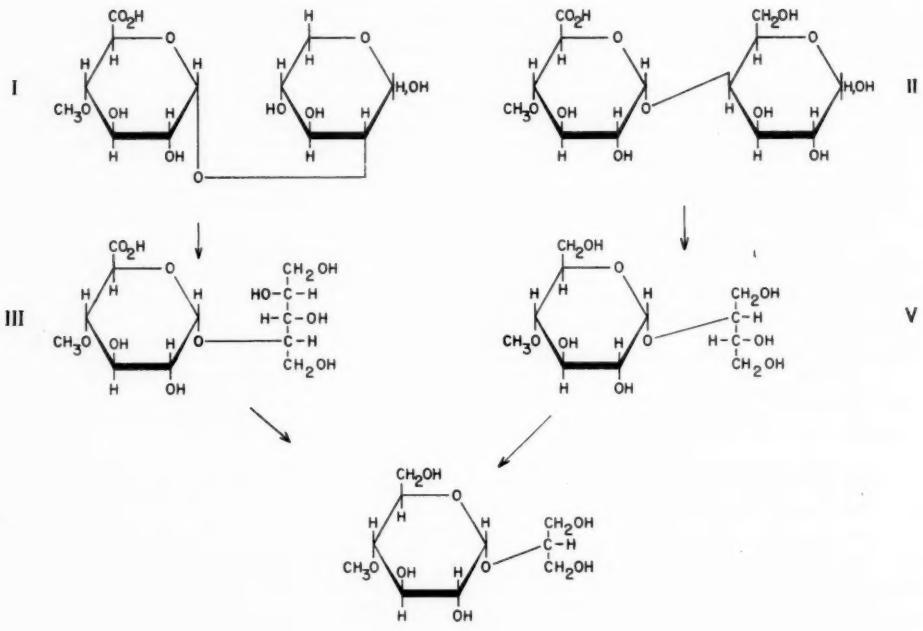

The aldobiuronic acid from Mesquite gum, 4-*O*-(4-*O*-methyl-D-glucopyranuronosyl)-D-galactose, was oxidized with 2 moles of lead tetraacetate. Reduction of the D-threose derivative with sodium borohydride afforded 2-*O*-(4-*O*-methyl-D-glucopyranuronosyl)-D-threitol (V), which was not crystalline. This compound was treated with diazomethane and the methyl ester was reduced with sodium borohydride. The material thus obtained proved to be a mixture containing the required sirupy 2-*O*-(4-*O*-methyl-D-glucopyranosyl)-D-threitol, which was obtained in poor yield after fractionation on a cellulose column. The comparatively low yield is probably due to the slow rate of lead tetraacetate oxidation of 4-substituted aldoses (10). The threitol portion was found to be cleaved preferentially by 1 mole of sodium periodate (11), since formaldehyde was formed in 98% yield. The resulting glyceraldehyde derivative was reduced to 2-*O*-(4-*O*-methyl-D-glucopyranosyl)-glycerol by sodium borohydride. Removal of trace amounts of impurity by fractionation on a cellulose column furnished a material having an $[\alpha]_D$ identical with that of the known α-anomer. Confirmation of the configuration was given by *p*-nitrobenzoylation of the glycerol derivative. The penta-*p*-nitrobenzoate formed was the α-anomer, since it had the same specific rotation, melting point, mixed melting point, and X-ray diffraction pattern as 2-*O*-α-(4-*O*-methyl-D-glucopyranosyl)-glycerol penta-*p*-nitrobenzoate derived from the disaccharide obtained from *P. tacamahacca*.

EXPERIMENTAL

Optical rotations were measured at 27° C. Paper chromatography was carried out on Whatman No. 1 filter paper using *n*-butanol–ethanol–water (40:11:19 v/v) as solvent

(12) and ammoniacal silver nitrate (13) and *p*-anisidine hydrochloride (14) spray reagents. Solutions were concentrated at 50° C. under reduced pressure. Infrared absorption spectra were prepared by the potassium bromide window technique (15).

2-O-α- and 2-O-β-D-Glucopyranosyl-glycerol Hexamethyl Ethers

2-*O*-α-D-Glucopyranosyl-glycerol (2.26 g.) was dissolved in water (50 cc.) containing sodium hydroxide (20 g.), and methyl sulphate (18 cc.) was added dropwise to the stirred solution. The mixture was left overnight and the procedure repeated four times. It was then heated to 100° C. for 1 hour to destroy excess reagent, cooled, and brought to neutrality with sulphuric acid. The solution was evaporated to a solid which was extracted with ethanol. The extract was filtered and evaporated to a crust which was dissolved in water and extracted continuously with chloroform. Evaporation of the chloroform after drying with magnesium sulphate yielded a sirup which was extracted with light petroleum (b.p. 50–60° C.) (16). The petrol solution yielded the required hexamethyl ether (1.21 g.) as a sirup which had $[\alpha]_D$ +137° (*c*, 1.2, $CHCl_3$), +132° (*c*, 1.3, 2,4-lutidine), and n_D^9 1.4548. Calculated for $C_9H_{12}O_2(OCH_3)_6$: —OCH_3, 55.0%. Found: —OCH_3, 55.7%.

2-*O*-β-D-Glucopyranosyl-glycerol (145 mg.), using the same procedure, yielded the sirupy hexamethyl ether (60 mg.) which had $[\alpha]_D$ −8° (*c*, 1.2, $CHCl_3$), −5° (*c*, 1.1, 2,4-lutidine), and n_D^9 1.4532. Calculated for $C_9H_{12}O_2(OCH_3)_6$: —OCH_3, 55.0%. Found: —OCH_3, 55.3%.

2-O-α-D-Glucopyranosyl-glycerol Hexamethyl Ether From 2-O-(4-O-Methyl-D-glucopyranuronosyl)-D-xylose

The aldobiuronic acid (3.0 g.) was dissolved in water (50 cc.) and neutralized with aqueous sodium hydroxide. Sodium borohydride (1.0 g.) was added and after 2 hours excess reagent was destroyed with acetic acid. Sodium ions were removed with Amberlite IR-120 and the solution was filtered and evaporated to dryness. Boric acid was removed by repeated evaporations with methanol, the residue containing sirupy 2-*O*-α-(4-*O*-methyl-D-glucopyranuronosyl)-D-xylitol which was converted to its methyl ester (2.4 g.) using methanolic diazomethane.

The methyl ester (2.4 g.) obtained on evaporation was oxidized with 2.2 moles of lead tetraacetate for 20 hours in acetic acid (200 cc.) containing water (5 cc.). Most of the lead was removed by addition of 10% oxalic acid in acetic acid (15 cc.). The precipitate was filtered off and the solution evaporated to dryness. The 2-*O*-α-(4-*O*-methyl-D-glucopyranuronosyl)-L-glyceraldehyde methyl ester (contained in the residue) was reduced to 2-*O*-α-(4-*O*-methyl-D-glucopyranosyl)-glycerol with sodium borohydride (1.0 g.) in water (50 cc.). After 18 hours the reaction mixture was worked up by the method described above. The sirupy product (1.79 g.) gave mainly a spot on a paper chromatogram with R_{rhamnose} 0.9 and small amounts of unidentified impurities. The mixture was fractionated on a cellulose column using *n*-butanol as solvent to yield a sirup having $[\alpha]_D$ +125° (*c*, 1.0, water) and which produced 4-*O*-methyl glucose and glycerol, identified chromatographically (17) (*p*-anisidine hydrochloride and ammoniacal silver nitrate sprays), on acid hydrolysis.

Methylation of a portion of the material (403 mg.) by the method described previously gave the hexamethyl ether (221 mg.) which had $[\alpha]_D$ +123° (*c*, 1.0, 2,4-lutidine), n_D^{10} 1.4552, and an infrared absorption spectrum indistinguishable from that of the known α-hexamethyl derivative, thus identifying it as the α-anomer. Calculated for $C_9H_{12}O_2(OCH_3)_6$: —OCH_3, 55.0%. Found: —OCH_3, 55.0%.

2-O-α(4-O-Methyl-D-glucopyranosyl)-glycerol Penta-p-nitrobenzoate

The glycerol derivative (85 mg.) was heated on a steam bath for 1 hour with *p*-nitrobenzoyl chloride (600 mg.) in pyridine (4 cc.) (18). The reaction mixture was added to excess aqueous sodium bicarbonate and stirring was continued overnight. The product was filtered off and recrystallized twice from ethyl acetate. Yield, 94 mg. The crystals had m.p. 207–209° C. and $[\alpha]_D$ +95° (*c*, 1.0, 2,4-lutidine). Calculated for $C_{45}H_{35}O_{23}N_5$: C, 53.31%; H, 3.48%. Found: C, 53.17%; H, 3.42%.

2-O-α-(4-O-Methyl-D-glucopyranosyl)-glycerol Penta-p-nitrobenzoate from 4-O-(4-O-Methyl-D-glucopyranuronosyl)-D-galactose

Partially degraded Mesquite gum (50 g.) was further hydrolyzed with strong acid by the method of Smith (5), and the aldobiuronic acids obtained by treatment of the mixed barium salts (16 g.) with Amberlite IR-120 were fractionated on a cellulose column using ethyl acetate – acetic acid – water (3:1:1 v/v) as solvent. The required 4-*O*-methyl-glucuronosyl-aldobiuronic acid (2.2 g.) was thus obtained.

The acid (0.88 g.) in methanol (200 cc.) was treated with excess ethereal diazomethane. The solution was evaporated to a sirup which was oxidized for 2½ hours with 2 moles of lead tetraacetate (2.11 g.) in acetic acid (200 cc.) and water (3 cc.). Lead was removed by addition of 10% oxalic acid in acetic acid (4.5 cc.); the solution was filtered and then evaporated to dryness.

Treatment of the methyl ester derivative contained in the residue with sodium borohydride (1.5 g.) in water (100 cc.) for 18 hours afforded the reduced material (0.52 g.) after the solution was worked up in the prescribed way. Two main spots were observed on the paper chromatogram using the silver nitrate spray. They had $R_{\text{galactose}}$ 2.0 and 2.3 respectively, and the mixture was fractionated on a cellulose column using *n*-butanol one-half saturated with water as solvent. The faster material isolated (125 mg.) gave $[\alpha]_D$ +80° (*c*, 2.0, water), and was considered to be the required 2-*O*-α-(4-*O*-methyl-D-glucopyranosyl)-D-threitol. It gave spots corresponding to 4-*O*-methyl glucose and threitol on a paper chromatogram (*p*-anisidine hydrochloride and ammoniacal silver nitrate sprays) on acid hydrolysis, and consumed 1.9 moles of sodium periodate in 20 hours. Also, when oxidized with 1 molar portions of sodium periodate and lead tetraacetate, 0.98 and 0.87 moles of formaldehyde, respectively, were formed, as estimated by the chromotropic acid method (19).

Therefore, the threitol derivative (101 mg.) was oxidized with 1 mole of sodium periodate in water (10 cc.). After 18 hours the solution was treated with Amberlite IR-120, and after removal of the resin, barium carbonate was added to remove iodic and periodic acids. The insoluble material was filtered off, the filtrate evaporated to dryness, and the residue extracted with methanol. The methanolic solution was treated with sodium borohydride (25 mg.) and after it had been left for 3 hours the required 2-*O*-α-(4-*O*-methyl-D-glucopyranosyl)-glycerol was isolated. Yield, 82 mg. Minor impurities were shown to be present on a paper chromatogram and these were removed by fractionating the product on a cellulose column using *n*-butanol as solvent. The pure glycerol derivative (60 mg.) had $[\alpha]_D$ +125° (*c*, 1.0, water).

A portion (45 mg.) was characterized by conversion to its penta-*p*-nitrobenzoate derivative. Yield, 65 mg., m.p. 208–210° C., and $[\alpha]_D$ +94° (*c*, 0.8, 2,4-lutidine) after two recrystallizations from ethyl acetate. It was indistinguishable from the penta-*p*-nitrobenzoate derived from 2-*O*-α-(4-*O*-methyl-D-glucopyranuronosyl)-D-xylose by comparison of X-ray diffraction patterns; no depression of the melting point on mixing was observed. Calculated for $C_{45}H_{35}O_{23}N_5$: C, 53.32%; H, 3.48%. Found: C, 53.28%; H, 3.19%.

ACKNOWLEDGMENTS

The authors wish to thank Dr. J. R. Nunn for a gift of 4-*O*-α-(4-*O*-methyl-D-glucopyranuronosyl)-D-galactose. Also thanks are due to Mr. J. A. Baignée for microanalytical work, Mr. T. M. Mallard for determination of X-ray diffraction patterns, Mrs. Agnes Birss (Epp) for infrared absorption data, and Mr. J. W. L. C. Christ and Miss Sheila Lubin for technical assistance.

REFERENCES

1. CHARLSON, A. J., GORIN, P. A. J., and PERLIN, A. S. Can. J. Chem. **34**, 1811 (1956).
2. CHARLSON, A. J., GORIN, P. A. J., and PERLIN, A. S. Can. J. Chem. **35**, 365 (1957).
3. JONES, J. K. N. and WISE, L. E. J. Chem. Soc. 3389 (1952).
4. GORIN, P. A. J. Can. J. Chem. **35**, 595 (1957).
5. SMITH, F. J. Chem. Soc. 2646 (1951).
6. WOLFROM, M. L. and WOOD, H. B. J. Am. Chem. Soc. **73**, 2933 (1951).
7. WOLFROM, M. L. and ANNO, K. J. Am Chem. Soc. **74**, 5583 (1952).
8. HOUGH, L., JONES, J. K. N., and WADMAN, W. H. J. Chem. Soc. 2511 (1949).
9. CARTER, N. M. Ber. **63**, 1684 (1930).
10. CHARLSON, A. J. and PERLIN, A. S. Can. J. Chem. **34**, 1200 (1956).
11. CRIEGEE, R. Sitzber. Ges. Beförder. ges. Naturw. Marburg, **69**, 25 (1934); Chem. Abstr. **29**, 6820 (1935).
12. HOUGH, L. Nature, **165**, 400 (1950).
13. PARTRIDGE, S. M. Nature, **158**, 270 (1946).
14. HOUGH, L., JONES, J. K. N., and WADMAN, W. H. J. Chem. Soc. 1702 (1950).
15. SCHIEDT, U. and REINWEIN, H. Z. Naturforsch. **7b**, 270 (1952).
16. BROWN, F. and JONES, J. K. N. J. Chem. Soc. 1344 (1947).
17. PARTRIDGE, S. M. Biochem. J. **42**, 238 (1948).
18. SHRINER, R. L. and FUSON, R. C. The systematic identification of organic compounds. 2nd ed. John Wiley & Sons, Inc., New York. 1940. p. 137.
19. LAMBERT, M. and NEISH, A. C. Can. J. Research, B, **28**, 83 (1950).

THE CONDUCTANCES OF AQUEOUS SOLUTIONS OF LITHIUM CHLORATE AT 25.00° C. AND AT 131.8° C.[1]

A. N. Campbell and W. G. Paterson[2]

ABSTRACT

The conductances, densities, and viscosities of aqueous solutions of lithium chlorate have been obtained over the complete range of concentration at 131.8° C. and up to saturation (and somewhat beyond) at 25.00° C. The curve of specific conductance versus concentration passes through a maximum which does not shift noticeably in composition with change in temperature. There are no minima on the curves of equivalent conductance versus concentration. The relative viscosity of the solutions decreases with rise in temperature; this is the reverse of the effect usually observed.

The experimental results have been compared with the calculated results, obtained by the use of the equations of Wishaw and Stokes and of Falkenhagen.

An extensive study of the conductances and viscosities of concentrated aqueous electrolytic solutions has been going on in this laboratory for several years. The salts suitable for this work are such as show a wide concentration range. The salts investigated have been: ammonium nitrate at 25°, 35°, 95°, and 180° C. (1, 2, 3, 4); silver nitrate at 25°, 35°, 95°, and 221.7° C. (1, 2, 3, 4); and lithium nitrate at 25° and 110° C. (5, 6).

The conductances of aqueous solutions of lithium chlorate over a wide range of concentration and at several temperatures are reported in the literature but, for various reasons, the work is either inadequate or erroneous. Kraus and Burgess (7) give data on conductance at a series of temperatures but they were primarily interested in the conductance of lithium chlorate on the addition of small amounts of water and their data are incomplete at 25° C. Accurate measurements have been made by Scatchard (8) and co-workers in the dilute range at 10° C. The investigations of Klotschko and Grigorjew (9) cover a wide range of concentrations at six different temperatures, one of which is 25° C. These authors prefer the specific to the equivalent conductance as a basis of theoretical interpretation. When their results are plotted against concentration, it becomes evident that there is a considerable scattering of points on the graph. Their results are too inaccurate to be of any value; for example, the specific conductance of their weakest solution at 25° C. yields a value of equivalent conductance greatly in excess of the limiting conductance as calculated from the sum of the limiting ionic conductances of lithium and chlorate ions. Further, when their curves of density or viscosity versus concentration are extrapolated to zero concentration, the values for the density or viscosity of pure water so obtained are considerably different from the accepted values.

EXPERIMENTAL PROCEDURE

Lithium chlorate was prepared and dried by the method of Campbell and Griffiths (10). Since lithium chlorate is exceedingly hygroscopic, it is not possible to make up solutions of defined concentration by weighing; all solutions must be analyzed. In view of the difficulties inherent in the direct determination of lithium or chlorate radical, the following simple and satisfactory procedure was adopted for arriving at lithium chlorate content. A weighed sample of solution was treated with excess concentrated sulphuric acid and evaporated to dryness in a Vycor dish; platinum cannot be used. The resulting

[1]*Manuscript received April 1, 1957.*
Contribution from the Chemistry Department of the University of Manitoba, Winnipeg, Manitoba.
[2]*Holder of N.R.C. Bursary, 1956–57.*

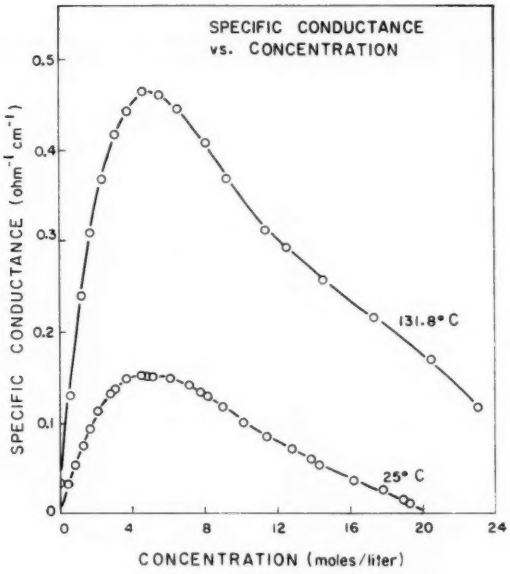

FIG. 1.

lithium sulphate was ignited to constant weight. The procedure was tested on sodium chlorate and it was found that an accuracy of 0.01% was attainable.

The density of each solution of lithium chlorate was determined and thus it was possible to plot a graph of weight per cent versus density of solution. Interpolation from this graph then became the analytical method used for the remainder of the research, with a consequent great saving of time.

Our technique of conductance measurements has been described previously (1, 2, 3, 4). In order, however, to keep down the voltage output of the audio-oscillator and avoid heating of the solution in the conductance cell, a simple triode-type amplifier was introduced in the telephone circuit.

For work at 131.8° C., where the vapor pressure of the solution exceeds 1 atm., the conductance cells were placed in a closed bomb; the technique has been described previously (4). The solvent water was distilled water having a specific conductance of less than 5×10^{-6} mhos and this is more than sufficiently low for work on concentrated solutions ($c > 0.01$ N).

The cell constants were obtained in the usual way. The standard potassium chloride solutions of Jones and Bradshaw (11) refer to 25° C. and it is not immediately obvious that cell constants obtained for 25° C. are good at other temperatures. Washburn (12), however, has shown how to calculate the cell constant at a temperature other than 25° C., from the value at 25° C. For cells constructed of Pyrex and platinum the change in cell constant is very slight. The correction for our cells for the change in temperature from 25° C. to 131.8° C. was about 0.03% and it was always applied.

Solutions were prepared from a concentrated stock solution, of known strength, by dilution with water. The exact concentration was then obtained from the density. Density was usually determined with a Weld pycnometer but for the anhydrous melt at

TABLE I

CONDUCTANCES (OBSERVED AND CALCULATED), DENSITIES, AND VISCOSITIES OF AQUEOUS SOLUTIONS OF LITHIUM CHLORATE AT 25.00° C.

Weight %	Molarity	Density, g./ml.	Relative viscosity, water = 1.000	Specific conductance, ohm^{-1} $cm.^{-1}$	Equivalent conductance, mhos	Λ_{calc} Wishaw–Stokes å = 5.3 Å	Wishaw–Stokes å = 5.5 Å	Falkenhagen å = 4.3 Å
0.1990	0.02188	0.9982	1.002	0.002044	93.31	93.34	93.41	93.22
0.9036	0.1002	1.0025	1.015	0.008495	84.78	85.09	85.29	84.92
4.519	0.5121	1.0243	1.067	0.03679	71.85	71.86	72.29	72.10
7.402	0.8532	1.0420	1.110	0.05662	66.36	66.17	66.66	66.84
10.60	1.247	1.0631	1.169	0.07677	61.58	60.73	61.26	61.86
13.68	1.640	1.0834	1.229	0.09379	57.19	56.30	56.83	57.81
17.24	2.113	1.1082	1.315	0.1108	52.45	51.34	51.86	53.23
23.01	2.928	1.1505	1.472	0.1337	45.67	44.30	44.77	46.69
24.27	3.115	1.1594	1.508	0.1374	44.11	42.94	43.40	45.42
28.39	3.742	1.1915	1.642	0.1495	39.94	38.56	38.49	41.32
33.38	4.549	1.2320	1.895	0.1546	33.90	32.58	32.97	35.47
35.49	4.908	1.2502	2.019	0.1556	31.69	30.27	30.63	33.18
36.90	5.157	1.2633	2.115	0.1556	30.17	28.69	29.04	31.60
42.58	6.199	1.3160	2.594	0.1511	24.38	22.71	22.97	25.57
47.61	7.185	1.3643	3.140	0.1420	19.76	18.27	18.49	20.99
50.36	7.762	1.3933	3.585	0.1346	17.35	15.78	15.96	18.33
51.68	8.047	1.4074	3.838	0.1312	16.30	14.63	14.80	17.10
55.71	8.947	1.4519	5.170	0.1189	13.29	10.63	10.74	12.65
60.88	10.19	1.5136	6.894	0.1031	10.11	7.723	7.752	9.441
65.82	11.49	1.5776	10.29	0.08639	7.521	5.005	5.043	6.304
70.43	12.80	1.6426	16.37	0.07189	5.618	3.035	3.055	3.953
74.09	13.93	1.7002	24.53	0.06010	4.313	1.964	1.973	2.632
75.06	14.27	1.7187	28.38	0.05644	3.955	1.681	1.690	2.271
80.66	16.15	1.8100	66.26	0.03928	2.432	0.6831	0.6850	0.9695
85.44	17.95	1.8989	166.5	0.02407	1.341	0.2577	0.2571	0.3862
88.17	19.03	1.9510	334.0	0.01644	0.8639	0.1241	0.1234	0.1920
89.03	19.33	1.9627	—	0.01487	0.7695	—	—	—

TABLE II

CONDUCTANCES (OBSERVED AND CALCULATED), DENSITIES, AND VISCOSITIES OF AQUEOUS SOLUTIONS OF LITHIUM CHLORATE AT 131.8° C.

Weight %	Molarity	Density, g./ml.	Relative viscosity, water = 1.000	Specific conductance, ohm^{-1} $cm.^{-1}$	Equivalent conductance, mhos	Λ_{calc} Wishaw–Stokes å = 3.2 Å Λ_0 = 403	Wishaw–Stokes å = 3.6 Å Λ_0 = 399	Falkenhagen å = 2.7 Å Λ_0 = 405
1.087	0.1131	0.9407	1.013	0.03438	304.02	304.62	303.76	304.29
4.987	0.5321	0.9645	1.047	0.1303	244.79	240.22	243.31	238.59
10.57	1.169	0.9994	1.110	0.2381	203.76	198.34	203.75	197.73
15.18	1.729	1.0294	1.165	0.3099	179.28	175.66	181.87	178.04
20.17	2.374	1.0641	1.257	0.3687	155.31	152.78	159.31	154.85
25.18	3.066	1.1006	1.323	0.4184	136.50	137.54	144.29	141.05
30.13	3.794	1.1382	1.408	0.4417	116.42	123.24	129.84	128.03
35.16	4.589	1.1799	1.519	0.4630	100.89	109.27	114.26	115.24
40.77	5.548	1.2302	1.686	0.4607	83.04	93.92	99.72	100.89
46.35	6.572	1.2818	1.903	0.4451	67.72	79.54	84.68	87.20
54.15	8.165	1.3630	2.364	0.4041	49.50	60.09	64.20	68.12
59.49	9.345	1.4201	2.838	0.3703	39.62	47.93	51.33	55.73
67.57	11.40	1.5251	4.263	0.3160	27.73	29.75	31.81	36.18
72.09	12.64	1.5855	5.477	0.2920	23.09	22.25	23.74	27.81
78.57	14.65	1.6860	8.836	0.2578	17.59	12.86	13.78	16.20
86.56	17.42	1.8197	17.48	0.2176	12.49	5.948	6.348	8.411
93.98	20.46	1.9681	43.38	0.1650	8.064	2.175	2.288	3.334
100.0	23.11	2.0889	113.0	0.1180	5.108	0.7684	0.7963	1.014

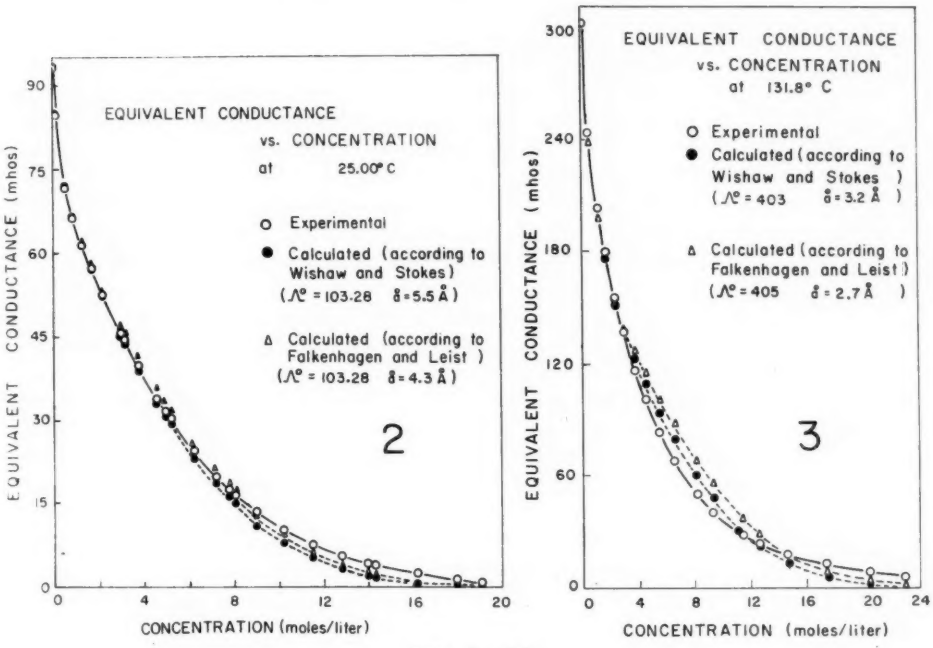

FIGS. 2 and 3.

131.8° C. a special type of filling and of pycnometer were used. This has also been described (4).

EXPERIMENTAL RESULTS

The experimental values of weight per cent, molarity, density, relative viscosity, specific conductance, and equivalent conductance, observed and calculated from the equations of Stokes and of Falkenhagen, are recorded in Tables I and II. The conductance measurements are limited to an accuracy of 0.1% and the density figures may be in error in the fourth decimal place. Plots of specific conductance and of equivalent conductance (observed and calculated) versus concentration at 25.00° C. and 131.8° C. are represented in Figs. 1 to 3. Fig. 4 is a plot of relative viscosity versus concentration at the two temperatures.

DISCUSSION OF RESULTS

The existence of maxima in the curves of specific conductance versus concentration is of interest, since it means that, for concentrations beyond that of the maximum, solutions containing more electrolyte have a lower conductance than solutions containing less electrolyte, that is, either the total number of ions is decreasing, or their mobility or both. For instance, the conductance at 131.8° C. of a 10 molar solution is the same as that of a 2 molar solution, despite a fivefold increase in electrolyte concentration. Such maxima are recorded only infrequently in the literature because of the lack of experimental investigations in the high concentration range.

The concentration corresponding to the maximum does not shift noticeably with

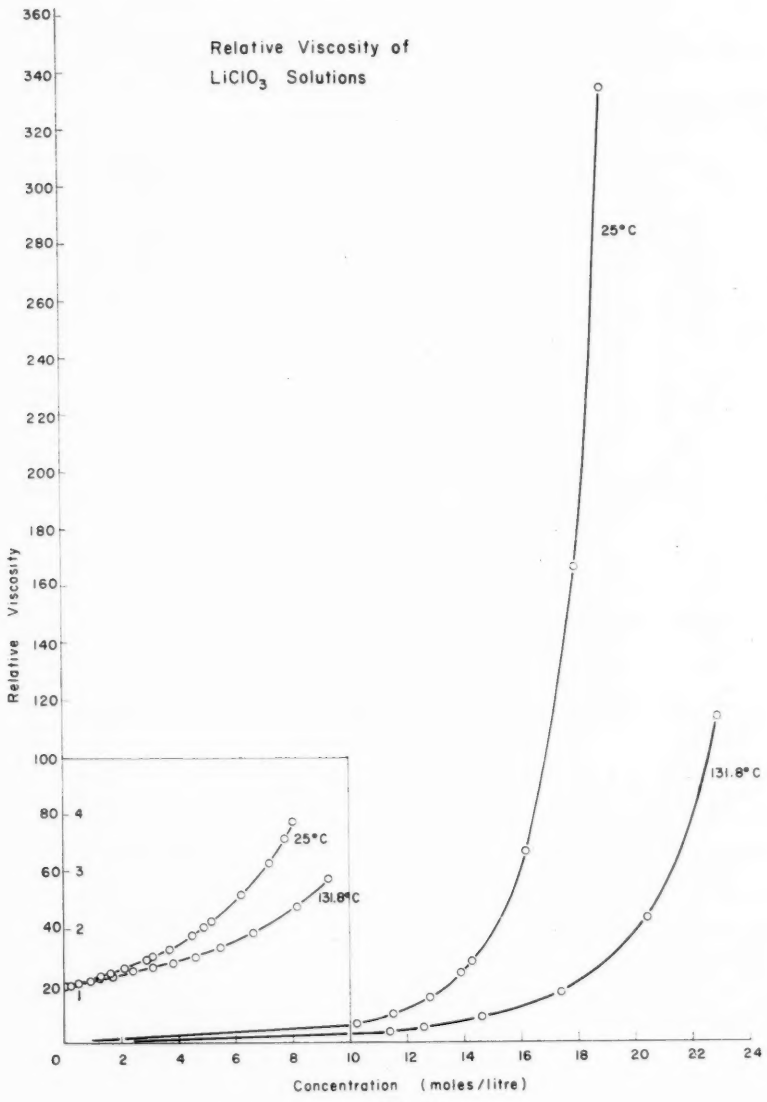

FIG. 4.

temperature, and this was observed by Klotschko and Grigorjew (9), who seek to connect this with the equilibrium diagram of the system lithium chlorate – water but there is, of course, no necessary connection whatever between the two. If it is assumed that strong electrolytes are completely ionized, no matter what the concentration, then the existence of the maximum points to a marked slowing down of the ions. Obviously, the electrical effects considered by the Debye–Hückel–Onsager theory will become very marked but the picture is complicated by changes in the hydration of the ions. At high concentrations,

all solvent molecules must be tightly held by ions; there will be little or no "free" water. This should produce, as it does, a very great increase in viscosity and this factor also tends to slow down the ions. The exact effect of viscosity on the motion of ions has not yet been formulated but it must be considerable, and is probably due in very concentrated solutions to interionic effects. Presumably, the effect is not measured simply by the bulk viscosity but there must be some connection.

The plots of equivalent conductance versus concentration (Figs. 2 and 3) show a progressive decrease in equivalent conductance with increasing concentration. At the higher temperature (131.8° C.) it was possible to cover the entire range of concentration up to anhydrous melt but no minimum is observed. Minima are found with electrolytes in solvents of relatively low dielectric constant and the meaning is discussed by Fuoss and Kraus (13). Their explanation is that non-conducting ion-pairs are first formed, followed, at high concentration, by conducting triple ions. It is apparent that, for all the salts investigated in this laboratory, no triple ions are formed. It is often contended that ion pairs cannot form in aqueous solution, because of the high dielectric constant of the medium but, in these very concentrated solutions, it becomes difficult to say what the medium is and therefore to state the dielectric constant. We think it unlikely that ion pairs will form in any lithium salt solution while there is still sufficient water present to preserve the very stable structure of the hydrated ion, but in very concentrated solutions, because of the proximity of the ions, formation of ion pairs must be considered probable. It should be pointed out that the last three figures of Table I refer to supersaturated solutions, which were easy to obtain.

The theory of extremely dilute solutions is well developed but there is no entirely satisfactory theory covering the conductance of concentrated solutions. The Debye–Hückel–Onsager theory has been extended by Fuoss and Onsager (14), by Wishaw and Stokes (15), and by Falkenhagen, Leist, and Kelbg (16). In every case, the extension consists in attributing to the ions a finite diameter, a, instead of considering them as mathematical points. In order to apply any of the above equations to more concentrated solutions, a viscosity correction must be used. Most authors, if they venture into this region at all, content themselves with dividing the calculated equivalent conductance by the relative viscosity. It has been suggested by Stokes (private communication) that it might be better to divide by some (fractional) power of the viscosity. Other workers, on the other hand, contend that because of the assumed complexity of concentrated solutions it is fruitless to pursue this line of investigation beyond, say, 0.1 N. It is our opinion, however, that solutions of moderate concentration are not so complicated in structure and that the Debye–Hückel–Onsager approach can be pursued further, if an appropriate viscosity correction can be found. It must be admitted that when the water content is reduced so low that there is not sufficient water present to hydrate the ions completely (notably in the present case of lithium chlorate) it is absurd to consider the ionic diameter as constant. It is therefore surprising that the equations of Wishaw and Stokes and of Falkenhagen to represent the general course of the equivalent conductance versus concentration curves rather well.

Papers proceeding from this laboratory have, since 1952, made extensive reference to the conductance equation of Wishaw and Stokes (15); no theoretical treatment is therefore necessary here. A somewhat similar equation is due to Falkenhagen and Leist (16); for uni-univalent electrolytes, the equation assumes the form:

$$\Lambda = \Lambda_0 \cdot \frac{\eta_0}{\eta} - \frac{e^2}{3\epsilon kT} \cdot \frac{\kappa}{1+\kappa a} \cdot \Lambda_0 \cdot \frac{\eta_0}{\eta} \cdot \frac{q}{(1+\sqrt{q})(1+\kappa a\sqrt{q})} - \frac{ne^2}{3\pi\eta_0} \cdot \frac{1000}{C\times 9\times 10^{11}} \cdot \frac{\kappa}{1+\kappa a} \cdot \frac{\eta_0}{\eta} \cdot$$

The symbols have their usual significance, except that $q = \frac{1}{2}$ for 1:1 electrolytes, n is the number of ions of a given type per cubic centimeter, and C is the concentration in moles per liter. We have used both the equations of Wishaw and Stokes and of Falkenhagen and Leist to calculate Λ for the concentrations used by us. These results are compared with our experimental results in Tables I and II and graphically in Figs. 2 and 3.

Quite recently, Professor Falkenhagen, in a private communication, has stated the most recent form of his conductance equation as:

[1] $$\Lambda = \Lambda_0 - \Lambda_I - \Lambda_{II} \qquad \text{(general formulation)}$$

where Λ_I represents the relaxation effect and Λ_{II} the electrophoretic effect:

[2] $$\Lambda_I = \frac{e^2\Lambda_0}{GD_0kT} \cdot \frac{(2-\sqrt{2})\kappa}{(1+\kappa a)(1+\frac{1}{2}\sqrt{2}\,.\,\kappa a+\frac{1}{6}\kappa^2a^2)},$$

[3] $$\Lambda_{II} = \frac{e^2L}{27\pi\times10^{11}\eta_0} \cdot \frac{\kappa}{1+\kappa a}.$$

The symbols have their usual significance except that L = Avogadro's number. We have used this equation to calculate Λ for lithium chlorate at 25.00° C. These results, for concentrations ranging from 0.0219 M to 6.199 M, are given in Table III. We have slightly altered å from 4.3 to 4.1 Å, for this purpose. The agreement is very good. Up to 0.5121

TABLE III

COMPARISON OF OBSERVED CONDUCTANCES AND THOSE CALCULATED BY FALKENHAGEN'S MOST RECENT EQUATION: LITHIUM CHLORATE SOLUTIONS AT 25.0° C.

Concentration,	$\Lambda_0 = 103.28$		å = 4.1 Å			
M	Λ_{exp}	Λ_I	Λ_{II}	Λ^*	Λ'	% Deviation
0.0219	93.31	2.545	7.436	93.36	93.17	−0.15
0.1002	84.78	3.923	13.301	86.06	84.79	0.12
0.5121	71.85	4.694	21.961	76.63	71.82	−0.04
0.8532	66.36	4.615	24.795	73.87	66.55	0.29
1.247	61.58	4.322	26.862	72.10	61.68	0.16
1.640	57.19	4.094	28.309	70.88	57.67	0.84
2.113	52.45	3.844	29.601	69.84	53.11	1.23
2.928	45.67	3.484	31.186	68.61	46.61	2.06
3.115	44.11	3.411	31.488	68.38	45.34	2.79
3.742	39.94	3.165	32.316	67.80	41.29	3.38
4.549	33.90	2.957	33.178	67.14	35.43	4.51
4.908	31.69	2.860	33.501	66.92	33.15	4.61
5.157	30.17	2.741	33.703	66.84	31.60	4.74
6.199	24.38	2.575	34.451	66.25	25.54	4.76

$\Lambda^* = \Lambda_{calc}$ uncorrected for viscosity.
$\Lambda' = \Lambda_{calc}$ corrected for viscosity.

M, the discrepancy is negligible. After this, the error of the calculated quantity becomes increasingly positive and amounts to 4.76% of the observed result at 6.199 M. Beyond 6 M, the difference between the results of the two Falkenhagen equations is negligible, so there is no point in carrying the new calculations beyond this. Neither have we calculated for 131.8° C., with the more recent equation, because our complete ignorance of the value of Λ_0 at 131.8° makes it impossible to impose a fair test. According to Falkenhagen himself, his most recent equation is on sound theoretical ground as long as $Ka << 1$. Beyond this point, a viscosity correction must be introduced. It has always been the fashion to divide the calculated conductance by the relative viscosity and, if this is done, the following equation results:

$$\Lambda_c = (\eta_0/\eta)\{\Lambda_0 - \Lambda_I - \Lambda_{II}\}.$$

Equations such as the above, however, must at best be described as "semi-empirical", since the exact form of the viscosity correction is not known. Falkenhagen and Leist (16) test the (original) equation by using the data for the conductance of lithium chloride solutions at 18° C. Using a value of å = 4.8 Å, they obtain very good agreement with the experimental data; at a concentration of 10 molar the experimental and calculated equivalent conductances differ by less than one mho. Some of the agreement may be fortuitous, since the equation is not really justified at such high concentrations, but it does indicate that dividing by the relative viscosity is at least an approximation to the truth. For our own results Stokes' suggestion of dividing by some power of the viscosity, other than one, can very well be met by using the power 1.05, that is, by dividing the calculated conductance by $(\eta/\eta_0)^{1.05}$; calculated and observed results then agree very well up to 6 *M*. Since, however, this is a purely empirical procedure, there being no reason to use this power, or any other, of the viscosity, except to force the calculated results into agreement with the observed values, we think it better to continue the older practice of simply dividing by the relative viscosity and to attribute deviations to shortcomings in the equation. Obviously, there must be many phenomena in concentrated solutions which are not covered by the Falkenhagen treatment, which must be oversimplified for very concentrated solutions.

The new equation of Falkenhagen yields better results than that of Wishaw and Stokes (15). In all such equations, the choice of å is quite arbitrary. For example, in calculating for lithium chloride, Falkenhagen and Leist use a value of å of 4.8 Å; the calculations of Wishaw and Stokes are based on å = 5.2 Å, and Fuoss and Onsager (14) use 4.31 Å in their calculations for the dilute region.

In order to calculate Λ, Λ_0 must be known and a reasonable value for å, the distance of closest approach of the ions, must be assumed. At 25.0° C., the only uncertain parameter is the latter quantity. Two series of calculations have been made (Wishaw–Stokes equation), using slightly different values of this parameter. To obtain a good fit with the Falkenhagen equation, significantly different values of å had to be used. At the higher temperature, the difficulty of not knowing Λ_0 is an additional handicap. For each value of å, we have used a slightly different value of Λ_0. Although Stokes maintains that å is temperature independent we have used a smaller value of å for the higher temperature.

Again, all equations assume constancy of å with increasing concentration. In fact, however, and assuming again that å is a real quantity, the distance of closest approach must decrease with increasing concentration, because a concentration is eventually reached where there is no longer sufficient water in the solution to maintain extensive hydration.

ACKNOWLEDGMENTS

We are indebted to Dr. E. M. Kartzmark for her assistance in the preparation of this paper and with the calculations. As in all work proceeding from this laboratory, most of the expense of the research was borne by a research fund supplied by the National Research Council.

REFERENCES

1. CAMPBELL, A. N. and KARTZMARK, E. M. Can. J. Research, B, **28**, 43 (1950).
2. CAMPBELL, A. N., GRAY, A. P., and KARTZMARK, E. M. Can. J. Chem. **31**, 617 (1953).
3. CAMPBELL, A. N. and KARTZMARK, E. M. Can. J. Chem. **30**, 128 (1952).
4. CAMPBELL, A. N., KARTZMARK, E. M., BEDNAS, M. E., and HERRON, J. T. Can. J. Chem. **32**, 1051 (1954).
5. CAMPBELL, A. N., DEBUS, G. H., and KARTZMARK, E. M. Can. J. Chem. **33**, 1508 (1955).
6. CAMPBELL, A. N. and DEBUS, G. H. Can. J. Chem. **34**, 1232 (1956).
7. KRAUS, C. A. and BURGESS, W. M. J. Am. Chem. Soc. **49**, 1226 (1927).
8. SCATCHARD, G., PRENTISS, S. S., and JONES, P. T. J. Am. Chem. Soc. **56**, 805 (1934).

9. KLOTSCHKO, M. A. and GRIGORJEW, I. G. Akad. Wiss. (U.S.S.R.) Nachr. Abt. physik-chem. Analyse, **21**, 288 (1950). German translation.
10. CAMPBELL, A. N. and GRIFFITHS, J. E. Can. J. Chem. **34**, 1647 (1956).
11. JONES, G. and BRADSHAW, B. C. J. Am. Chem. Soc. **55**, 1780 (1933).
12. WASHBURN, E. W. J. Am. Chem. Soc. **38**, 2431 (1916).
13. FUOSS, R. M. and KRAUS, C. A. J. Am. Chem. Soc. **55**, 2387 (1933).
14. FUOSS, R. M. and ONSAGER, L. Proc. Natl. Acad. Sci. U.S. **41**, 274 (1955).
15. WISHAW, B. F. and STOKES, R. H. J. Am. Chem. Soc. **76**, 2065 (1954).
16. FALKENHAGEN, H., LEIST, M., and KELBG, G. Ann. Physik, (6), **11**, 51 (1952). FALKENHAGEN, H. and LEIST, M. Naturwiss. **24**, 570 (1954). Z. physik. Chem. **205**, 16 (1955).

SPECTRE INFRAROUGE DE HF À L'ÉTAT CRISTALLIN[1]

PAUL A. GIGUÈRE ET NUMAN ZENGIN[2]

RÉSUMÉ

On a mesuré le spectre d'absorption infrarouge entre 300 et 5000 cm.$^{-1}$ de minces films de HF cristallisé à −180° C. La vibration fondamentale produit un doublet intense à 3420 et 3060 cm.$^{-1}$ et un second, plus faible, à 3590 et 3270 cm.$^{-1}$. Toutes les caractéristiques du spectre concordent avec les données actuelles sur la structure cristalline de HF: chaînes parallèles, en zigzag, de molécules reliées par des liaisons hydrogène asymétriques. On a également déduit les dimensions approximatives suivantes:

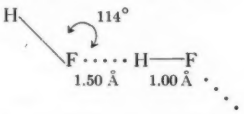

La haute polarité de la molécule et les fortes liaisons hydrogène se manifestent de plusieurs façons: largeur exceptionnelle des bandes (de 150 à 200 cm.$^{-1}$); grand espacement des diverses composantes de la fondamentale dans le cristal; abaissement considérable (quelque 700 cm.$^{-1}$) de la fréquence fondamentale en passant de la molécule libre au solide, résultant d'une diminution de la force de rappel de 8.8 à 6.3×10^5 dynes/cm.; fréquences de libration élevées (1000–1200 cm.$^{-1}$) et forces de rappel intermoléculaires allant jusqu'à 0.6×10^5 dynes/cm.

Les spectres infrarouges et Raman des cristaux moléculaires peuvent fournir des indications précieuses sur l'arrangement des molécules à l'état solide ainsi que sur les forces intermoléculaires. Cette information est particulièrement utile dans le cas des composés de l'hydrogène puisque la diffraction aux rayons X ne permet pas de localiser ces atomes avec précision. Jusqu'à présent on a étudié par ces méthodes les halogénures HCl, HBr et HI (1, 2, 3, 4) mais aucun travail n'est encore paru sur HF à l'état solide. La raison principale en est sans doute la difficulté que présente la manipulation de ce composé extrêmement corrosif. De plus sa tendance marquée à la fluorescence rend presque impossible l'étude de l'effet Raman dans les états condensés. Ainsi une étude récente du spectre Raman de l'acide liquéfié (5) n'a révélé aucune indication de la vibration fondamentale.

MÉTHODE EXPÉRIMENTALE

À cause de la grande réactivité de l'acide fluorhydrique, et en particulier de son action sur le verre, il a fallu des précautions spéciales pour préparer les échantillons. Le gaz, contenu dans un cylindre de fer, était censé pur à 99.9%.* Les seules traces d'impuretés susceptibles d'affecter les résultats (H_2O, 0.04%; H_2S, 0.02%; SO_2, 0.01%) étaient à peine visibles dans les spectres des films les plus épais. Le gaz était transféré sous pression réduite dans un réservoir de cuivre d'environ un demi-litre d'où il était admis par petites bouffées dans la cellule d'absorption. Celle-ci était en verre, du type courant (6); les parois internes étaient recouvertes d'un enduit résistant à l'acide fluorhydrique. À cette fin nous avons d'abord employé une couche suffisamment épaisse de vernis Glyptal qui offre une protection efficace mais finit par se détacher du verre après un certain temps. Par la suite nous y avons substitué la cire Halocarbon 15-00,† également inerte, qui adhère

[1]*Manuscrit reçu le 30 janvier 1958.*
Contribution du Département de Chimie, Université Laval, Québec, Qué.
[2]*Boursier postdoctoral du Conseil National de Recherches, Ottawa, Canada.*
**Produit de "The Matheson Co. Inc.", East Rutherford, New Jersey.*
†Fabriquée par "The Halocarbon Products Corp.", North Bergen, New Jersey.

indéfiniment au verre. Les fenêtres de la cellule étaient faites de disques de chlorure d'argent sauf pour les mesures au-delà de 25 μ où il fallut recourir à l'iodure de césium. Le disque central, sur lequel se condensait le film de HF, était fait des mêmes matériaux; dans le cas de l'iodure de césium un mince film de polyéthylène, suffisamment transparent jusqu'à 40 μ, empêchait l'attaque par l'acide fluorhydrique.

Les canalisations, réduites au minimum, étaient de cuivre rouge. Un robinet à pointeau en laiton permettait de contrôler le débit du gaz; un manomètre de Bourdon à capsule de cuivre indiquait la pression dans le réservoir. Le seul robinet en verre sur la cellule à absorption était lubréfié avec de la graisse Fluorolube MG.* La moindre attaque des parois par l'acide se traduisait par l'apparition dans les spectres de bandes d'absorption des fluosilicates. L'épaisseur des films, telle qu'évaluée d'après la quantité de gaz utilisé et l'étendue de la surface froide, dans l'hypothèse d'une condensation uniforme, variait entre 3 et 5 μ. Leur température n'a pas été mesurée avec précision mais elle devait être d'environ $-180°$ C. avec l'air liquide comme réfrigérant. Les spectres furent enregistrés au moyen d'un spectrographe de Perkin-Elmer, Modèle 12C à double passage. Suivant la région nous avons utilisé des prismes de LiF, NaCl et CsBr calibrés de la façon usuelle (7).

RÉSULTATS

Les bandes d'absorption infrarouges de HF cristallisé se divisent en deux groupes distincts: les fondamentales, de 2.8 à 3.5 μ (Fig. 1) et les vibrations du réseau, au-delà de 6 μ (Fig. 2). Le premier groupe comprend le doublet principal à 3420 et 3060 cm.$^{-1}$. Vu la largeur considérable de ces bandes et leur proximité relative il était difficile de déterminer avec plus de précision la position des maxima. Un second doublet beaucoup moins intense que le premier, à 3590 et 3270 cm.$^{-1}$ présente quelque difficulté d'interprétation. À première vue on pourrait l'attribuer à des combinaisons (somme–différence) des fréquences fondamentales avec une vibration du réseau de l'ordre de 200 cm.$^{-1}$. Cependant les intervalles de fréquence, soient 170, 150 et 210 cm.$^{-1}$ respectivement, ne concordent pas assez bien à cette fin. De plus on devrait s'attendre à trouver une bande semblable vers 2860 cm.$^{-1}$ alors qu'en fait on n'observe qu'un renflement à peine perceptible. Étant donnée la ressemblance générale, à des échelles différentes, des deux doublets il semble plus probable que nous avons affaire ici aux quatre composantes de la vibration fondamentale, puisqu'il y a quatre molécules de HF dans la maille cristalline (8). Normalement deux des composantes devraient être actives en infrarouge et deux en Raman. Cependant il n'est pas inconcevable que toutes quatre apparaissent en infrarouge, surtout si on considère la possibilité de désordre dans la structure du cristal (distribution statistique des liaisons hydrogène) qui détruit la symétrie des sites.

Quant à la bande très floue déjà mentionnée aux environs de 2860 cm.$^{-1}$, et visible seulement dans les échantillons les plus épais, elle peut provenir d'une combinaison d'une fondamentale avec une vibration de réseau ou encore de quelque impureté. Hornig (2) a trouvé une bande analogue à 2616 cm.$^{-1}$ dans le spectre de HCl cristallisé. L'ion H_3O^+ possède une faible bande à cet endroit dans les solutions aqueuses d'acides (9) mais comme nous n'avons pu déceler aucune trace d'absorption vers 1700 cm.$^{-1}$, cette explication se trouve éliminée. Il convient d'ajouter ici qu'aucune indication d'harmoniques ni de bandes de combinaison n'est apparue entre 4000 et 5000 cm.$^{-1}$ probablement parce que les films utilisés étaient trop minces.

Du côté des grandes longueurs d'onde outre une demi-douzaine de bandes extrêmement faibles provenant, semble-t-il, d'impuretés (SO_2, H_2S, etc.), on trouve quatre ou cinq

*Fabriquée par "Hooker Electrochemical Co.", Niagara Falls, New York.

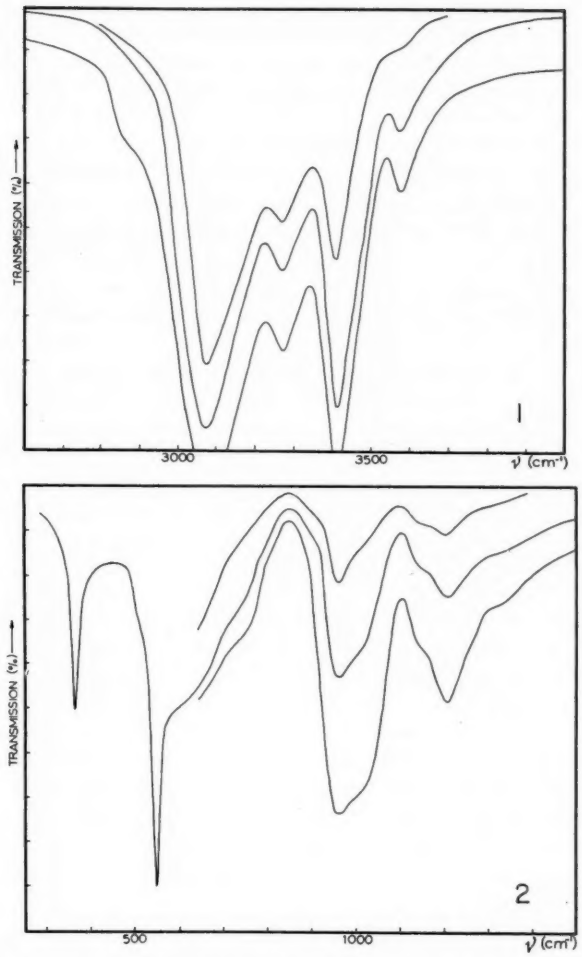

FIG. 1. Bandes d'absorption de HF à l'état cristallin dans la région de la vibration fondamentale.
FIG. 2. Bandes de vibration du réseau cristallin de HF.

bandes assez fortes à 366, 547, 955–1010 et 1204 cm.$^{-1}$. La courbe médiane dans les figures 1 et 2 a été obtenue avec le même échantillon en sorte que les intensités relatives des deux groupes de bandes sont reproduites assez fidèlement. Pour attribuer sans équivoque ces bandes aux divers modes de vibration du réseau cristallin il faudrait connaître le spectre Raman de HF cristallin. À titre d'essai on peut assigner le doublet non résolu à 955–1010 cm.$^{-1}$ ainsi que la bande assez large à 1204 cm.$^{-1}$ à des rotations gênées ou librations. A priori ces fréquences semblent passablement élevées pour de tels modes mais cette situation s'explique par la petitesse du moment d'inertie de la molécule HF ainsi que par l'énergie relativement grande des liaisons hydrogène dans cette substance. Par ailleurs le pic aigu à 366 cm.$^{-1}$ est de fréquence appropriée pour une translation comme on le verra plus loin d'après les forces de rappel intermoléculaires. Enfin l'origine de la

forte bande asymétrique surmontée d'un pic aigu à 547 cm.$^{-1}$ demeure incertaine. Sa fréquence paraît trop élevée pour une translation et un peu basse pour une libration; son intensité est également trop grande pour une harmonique de ν_T. Il se peut qu'elle provienne de mouvements de torsion des chaînes.

DISCUSSION

L'analyse de ces résultats se trouve facilitée par l'étude très poussée de Hornig et son groupe (1, 2, 3, 4) sur les spectres infrarouges de HCl, HBr et HI ainsi que par la détermination par les rayons X de la structure cristalline de HF (8). Ainsi l'on sait que ce cristal orthorhombique contient quatre molécules par maille, avec la symétrie du groupe infini $D_{24}{}^{17}$, quoique la symétrie $D_{24}{}^{16}$ ne soit pas définitivement exclue. Les molécules, reliées par des liaisons hydrogène, forment des chaînes en zigzag quasi-infinies, coplanaires et parallèles au plan 100 (Fig. 3); l'angle entre les molécules adjacentes est de 120°. Une telle structure implique des liaisons hydrogène orientées selon une direction privilégiée, ce qui semble en contradiction avec la nature essentiellement électrostatique de ce genre de liaisons. Cependant Schneider (10) a démontré récemment, en se servant du concept d'orbitale équivalente (11), le rôle important que jouent dans la formation de la liaison hydrogène les "doublets libres" sur l'atome accepteur de proton. À cause de l'hybridation des orbitales du fluor (sp^3) les molécules de HF tendent donc à s'orienter mutuellement suivant un angle à peu près tétragonal.

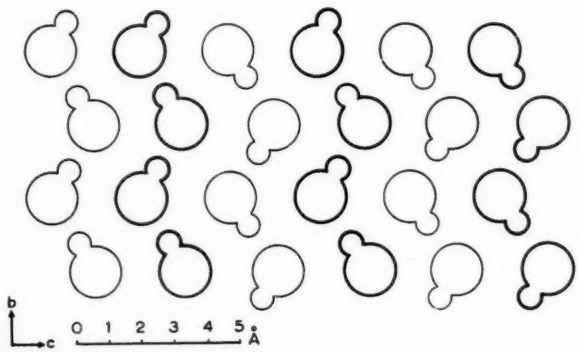

FIG. 3. Arrangement désordonné des chaînes de HF dans deux plans 100 successifs.

Les bandes fondamentales de HF cristallin sont d'abord remarquables par leur grande largeur: de 150 à 200 cm.$^{-1}$ à comparer avec 10 ou 20 cm.$^{-1}$ pour les autres halogénures HX. Cette caractéristique bien connue des composés contenant des liaisons hydrogène a suscité de nombreuses explications. Dans le cas de HF il n'est pas impossible que l'élargissement des bandes soit dû pour une part à un certain désordre dans le cristal. En effet l'analyse aux rayons X a montré la possibilité d'une distribution statistique des liaisons hydrogène, telle que représentée sur la figure 3. Les données présentes favorisent cette explication sans toutefois trancher la question; pour ce faire il faudra recourir à des méthodes plus puissantes telle la diffraction des neutrons. De toute façon ce désordre, s'il existe, ne conduit à aucune entropie résiduelle au zéro absolu puisqu'il ne fait intervenir que deux configurations différentes pour chaque chaîne (8). Contrairement aux autres halogénures d'hydrogène qui présentent à l'état solide des transitions du premier

ou du second ordre, HF garde la même structure cristalline à toute température. Il est évident qu'à cause de la grande polarité de la molécule et des fortes liaisons hydrogène les molécules n'ont pas la liberté de se réorienter dans le cristal.

La fréquence élevée des vibrations fondamentales confirme sans équivoque que la liaison F—H ··· F est asymétrique dans HF à l'état solide contrairement au cas exceptionnel de l'ion HF_2^- (10). Un calcul approximatif basé sur la règle de Badger conduit, à partir d'une fréquence moyenne de 3300 cm.$^{-1}$, à une distance H—F d'environ 1.00 Å. Comme la diffraction aux rayons X a donné 2.49 Å pour la distance minimum entre deux atomes de fluor voisins, il s'ensuit que les liaisons hydrogène sont d'à peu près 1.50 Å dans ce cristal. Dans la vapeur la distance F—H ··· F dans les polymères est de 2.55 Å (12) tandis que dans la molécule libre la distance interatomique est de 0.917 Å (13). On voit donc que les liaisons hydrogène dans HF sont notablement plus courtes, et partant plus fortes, que dans H_2O (1.75 Å); dans cette dernière substance le passage de la vapeur au solide allonge la liaison O—H de 0.96 à 1.01 Å (14).

À la suite de l'analyse de Hornig on sait que dans les cristaux des composés polaires du type HX le rapport des intensités des deux composantes fondamentales I_x et I_y dans le spectre infrarouge varie suivant l'angle α entre molécules voisines d'après la relation

$$I_x/I_y = \tan^2\alpha/2.$$

Des mesures faites sur cinq spectres différents de HF nous ont donné pour le rapport d'intensité des deux bandes à 3420 et 3060 cm.$^{-1}$ les valeurs: 2.31, 2.32, 2.38, 2.42 et 2.48 qui correspondent à des angles allant de 113° à 115°. L'accord avec le valeur trouvée par diffraction des rayons X, 120.1° (8), est satisfaisant surtout si l'on songe à l'incertitude des mesures d'intensité dans le cas présent. Par ailleurs l'écart entre ces diverses valeurs de α est beaucoup moindre que pour HCl et HBr (2). La possibilité, mentionnée par Hornig, d'une orientation partielle des films est évidemment minime pour une substance aussi polaire que HF. De toute façon on n'a jamais observé de différence notable entre les spectres de films déposés sur AgCl et sur NaCl, du moins dans la région de 300 à 1000 cm.$^{-1}$. Notons que des mesures d'intensité faites sur le doublet secondaire à 3590 et 3270 cm.$^{-1}$ conduisent à un angle voisin de 100°, bien que la précision des mesures soit évidemment assez faible ici. Ce résultat renforce l'hypothèse des deux composantes fondamentales déjà invoquée pour ces bandes.

Forces de rappel

Les présents résultats permettent d'évaluer les forces de rappel tant pour la molécule que pour le cristal. Qualitativement l'existence de forces intermoléculaires considérables

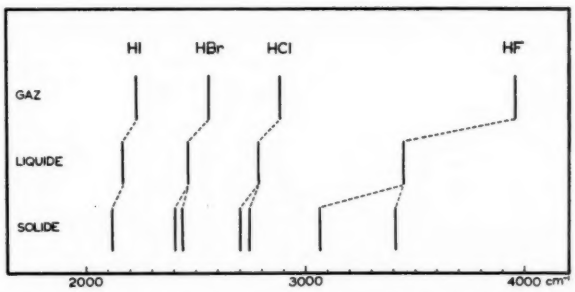

FIG. 4. Comparaison des fréquences de vibration des halogénures d'hydrogène dans les trois états physiques.

dans le cristal de HF se manifeste de trois façons: (*a*) un abaissement inusité de la vibration fondamentale en passant de la molécule libre, 3962 cm.$^{-1}$ (13) au cristal (Fig. 4); (*b*) la séparation extrêmement grande entre les composantes de la vibration fondamentale à l'état solide et enfin; (*c*) les valeurs très élevées des fréquences de libration. Ces observations sont en accord avec le caractère ionique marqué de la liaison H—F et les fortes liaisons hydrogène, 6.7 kcal./mole, selon Pauling (15), qui persistent même à l'état de vapeur.

Nous avons d'abord calculé les forces de rappel, tant principale que secondaires, à partir des quatre présumées composantes de la vibration fondamentale en supposant que le couplage entre les vibrations internes et externes des molécules dans le cristal est faible. Cette hypothèse est naturellement moins justifiable pour HF que pour les autres halogénures d'hydrogène mais elle tient encore en première approximation. En assignant arbitrairement les quatre fréquences comme suit:

$$\nu_1 = 3270 \text{ cm.}^{-1},$$
$$\nu_2 = 3060 \text{ cm.}^{-1},$$
$$\nu_3 = 3420 \text{ cm.}^{-1},$$
$$\nu_4 = 3590 \text{ cm.}^{-1},$$

on arrive aux valeurs suivantes (la notation est celle de Hornig):

$$f_{11} = 6.31 \times 10^5 \text{ dynes/cm.},$$
$$f_{12} = f_{34} = 0.65 \times 10^5 \text{ dynes/cm.},$$
$$f_{13} = f_{24} = 0.015 \times 10^5 \text{ dynes/cm.},$$
$$f_{14} = f_{23} = 0.36 \times 10^5 \text{ dynes/cm.}$$

Par contre, si on n'utilise que les deux composantes majeures on obtient des constantes assez voisines pour les deux forces principales, soient $f_{11} = 5.9$ et $f_{12} = 0.62 \times 10^5$ dynes/cm. Ces quantités demeurent sujettes à revision jusqu'à ce que les fréquences fondamentales dans le spectre Raman du cristal soient connues. Pour le moment il est intéressant de constater que la diminution de la force de rappel interne en passant de la molécule libre au cristal est énormément plus grande pour HF que pour les autres halogénures d'hydrogène (Tableau I). L'amortissement de la vibration de HF dans le cristal accroît son anharmonicité, laquelle se manifeste par un élargissement des bandes d'absorption.

Quant aux modes de libration des molécules dans le réseau cristallin, les fréquences trouvées ici soient 955, 1010 et 1204 cm.$^{-1}$ sont sans doute les plus hautes jamais rencontrées. Il est intéressant de les comparer à celles de la glace à 850 cm.$^{-1}$ (16). Hornig et

TABLEAU I

CONSTANTES MOLÉCULAIRES DES HALOGÉNURES D'HYDROGÈNE

	f_0	f_{11}	f_{12}	r_{H-X}	D	μ
HF	8.83	6.3	0.65	0.917	134	1.9
HCl	4.81	4.31	0.072	1.27	102	1.03
HBr	3.84	3.45	0.048	1.41	86	0.88
HI	2.93	2.66	—	1.60	70	0.38

NOTE: f_0, *constante de force de rappel (en* 10^{-5} *dynes/cm.) pour la molécule libre (17).*
f_{11}, *constante de force de rappel principale dans le cristal (2).*
f_{12}, *constante de force de rappel entre molécules voisines dans le cristal (2).*
r_{H-X}, *distance interatomique (en Å) dans la molécule libre (13).*
D, *énergie de dissociation de la liaison (en kcal./mole) (17).*
μ, *moment polaire (en debyes).*

Osberg (2) ont évalué à 266 cm.$^{-1}$ la fréquence de ce mode dans HCl cristallin, ce qui est en harmonie avec une valeur moyenne de 1100 cm.$^{-1}$ pour HF. Nous avons utilisé cette dernière quantité pour calculer la constante secondaire f_{12} d'après la formule usuelle

$$f = 4\pi^2\nu^2 I/r^2$$

pour une oscillation perpendiculaire à la force de rappel; nous obtenons ainsi presque exactement le même résultat (6.4×10^5 dynes/cm.) que ci-haut. Enfin un calcul très grossier de la fréquence de translation gênée ν_T d'une molécule HF par rapport à ses voisines dans l'hypothèse d'un oscillateur harmonique conduit à une valeur d'environ 330 cm.$^{-1}$.

Des deux facteurs principaux qui affectent les vibrations d'une molécule dans le cristal soient (*a*) le champ de forces créé par l'ensemble des molécules dans leur position d'équilibre et (*b*) le couplage avec les molécules adjacentes, il est clair que le second est énormément plus important dans le cas de HF. La technique dite de dilution isotopique (3) a permis à Hornig de différencier ces deux facteurs dans des "cristaux mixtes" de HCl et DCl. Vu la largeur anormale des bandes d'absorption de HF il est peu probable que cette méthode puisse révéler suffisamment de détails sur les vibrations des molécules isolées ou des paires de molécules dans les mélanges.

ABSTRACT

The infrared absorption of thin crystallized films of HF at −180° C. was measured from 300 to 5000 cm.$^{-1}$. The fundamental vibrations give rise to a strong doublet at 3420 and 3060 cm.$^{-1}$ and a weaker one at 3590 and 3270 cm.$^{-1}$. These bands are remarkably broad owing to the presence of very strong hydrogen bonds. From the intensity ratio of the fundamental components the angle between neighboring HF molecules in the zigzag chains is calculated to be about 114°. Both the splitting of the fundamental components and the vapor–solid shift are unusually large in keeping with the high polarity of the molecule and the strong hydrogen bonds. The "internal" force constant $f_{11} = 6.31 \times 10^5$ dynes/cm. is much lower than for the free molecule, and the "external" force constants are higher, by an order of magnitude, than in the other hydrogen halide crystals. Some five lattice vibrations were found between 350 and 1200 cm.$^{-1}$.

BIBLIOGRAPHIE

1. Hiebert, G. L. et Hornig, D. F. J. Chem. Phys. **20**, 918 (1952).
2. Hornig, D. F. et Osberg, W. E. J. Chem. Phys. **23**, 662 (1955).
3. Hornig, D. F. et Hiebert, G. L. J. Chem. Phys. **27**, 752 (1957).
4. Hiebert, G. L. et Hornig, D. F. J. Chem. Phys. **27**, 1216 (1957).
5. Safari, E. Ann. phys. **9**, 203 (1954).
6. Wagner, E. L. et Hornig, D. F. J. Chem. Phys. **18**, 296 (1950).
7. Downie, A. R., Magoon, M. G., Purcell, T. et Crawford, B., Jr. J. Opt. Soc. Am. **43**, 941 (1953).
8. Atoji, M. et Lipscomb, W. N. Acta Cryst. **7**, 173 (1954).
9. Falk, M. et Giguère, P. A. Can. J. Chem. **35**, 1195 (1957).
10. Schneider, W. G. J. Chem. Phys. **23**, 26 (1955).
11. Lennard-Jones, J. et Pople, J. A. Proc. Roy. Soc. (London), A, **205**, 155 (1951).
12. Bauer, S. H., Beach, Y. J. et Simons, J. H. J. Am. Chem. Soc. **61**, 19 (1939).
13. Herzberg, G. Spectra of diatomic molecules. D. Van Nostrand Company, Inc., New York. 1950.
14. Peterson, S. W. et Lévy, H. A. Acta Cryst. **10**, 70 (1957).
15. Pauling, L. Nature of the chemical bond. Cornell Univ. Press, Ithaca, N.Y. 1941.
16. Giguère, P. A. et Harvey, K. B. Can. J. Chem. **34**, 798 (1956).
17. Cottrell, T. L. The strengths of chemical bonds. Butterworth Scientific Publications, London. 1954.

THE INFRARED CARBONYL STRETCHING BANDS OF ACETOPHENONES SUBSTITUTED IN THE METHYL GROUP[1]

R. NORMAN JONES AND ERNEST SPINNER[2]

ABSTRACT

Measurements have been made of the positions and intensities of the C=O stretching bands in the infrared spectra of compounds of the types C_6H_5—CO—CH_2X, C_6H_5—CO—CHX_2, and C_6H_5—CO—CX_3 where X = —Cl, —Br, —I, —CN, —C_6H_5, and —OH. In most cases two bands are observed, and these are attributed to *gauche* and *cis* conformations associated with hindered rotation about the CO—CH_2X and CO—CHX_2 bonds. The relative positions and intensities of these bands are discussed in terms of the steric, electrical, and mass effects of the substituents.

INTRODUCTION

Rotational isomerism has been observed repeatedly in substances containing the groups —CO—CH_2X and CO—CHX_2 (1, 2, 3, 4, 5). Rotation of the CH_2X or CHX_2 group is restricted and the preferred conformations are those in which an H or X atom eclipses the oxygen atom when the molecule is viewed along the axis of the CO—CH_2X or CO—CHX_2 bond (I, II).

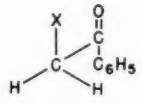

I (cis)

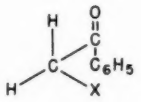

II (gauche)

Bellamy, Thomas, and Williams (4) have studied the C=O stretching bands in the infrared spectra of ω-chloroacetophenone, ω,ω-dichloroacetophenone, and ring-substituted derivatives of the former. In spectra measured in the liquid phase they observed two prominent maxima in the C=O stretching region, whereas a single band only was noted if the spectra were determined on material in the solid state. The relative intensities of the doublet peaks were temperature dependent, the lower frequency band becoming relatively more intense with rising temperature. In a later publication (5), Bellamy and Williams further established that the relative intensities of the two peaks varied with the solvent, the band at higher frequency increasing in relative intensity with change from a solvent of lower polarity (CCl_4) to one of higher polarity ($CH_3.CN$). By analogy with the influence of the C—X conformation on the C=O stretching bands of α-halogenated cyclohexanone derivatives (6, 7, 8, 9), Bellamy and collaborators assigned the doublet band of higher frequency to the *cis* form (I), and, from the temperature effect, they inferred that this is thermodynamically the more stable conformation.

This investigation extends these studies to acetophenone derivatives containing —Br, —I, —C≡N, —C_6H_5, and —OH substituents in the methyl group. The substitution effects on the integrated absorption intensities are also considered.

[1]*Manuscript received February 3, 1958.*
Contribution from the Division of Pure Chemistry, National Research Council, Ottawa, Canada. Presented in part at a meeting of the Chemical Institute of Canada, May 27, 1958.
Issued as N.R.C. No. 4739.
[2]*National Research Council Postdoctorate Fellow.*

EXPERIMENTAL

The spectra were determined in carbon tetrachloride and chloroform solutions on a Perkin-Elmer model 112 double-pass single-beam spectrometer using a calcium fluoride prism at a computed spectral slit width (S') of 1.6 cm.$^{-1}$ (10). The absolute values reported for the positions of the band maxima are correct within ± 1 cm.$^{-1}$ and the reproducibility is accurate to ± 0.5 cm.$^{-1}$. The integrated absorption intensities were determined by method II of Ramsay (11, 12); integration was performed by the use of Simpson's Rule and extended out into the wings of the band to the point where the measured optical density was 0.01. Corrections for finite spectral slit width were not applied since the ratio of S' to the half band width ($\Delta\nu_{\frac{1}{2}}^{(a)}$) was less than 0.2 in all cases except phenacyl alcohol (10). For this compound $\Delta\nu_{\frac{1}{2}}^{(a)} = 8$ cm.$^{-1}$ and the finite slit error on the basis of Ramsay's calculations would amount to about 2%.

The compounds were obtained commercially, or prepared by standard methods, and purified by fractional crystallization, vacuum distillation, vacuum sublimation, or combinations of these techniques. The melting points, boiling points, and refractive indices were consistent with values reported in the literature.

RESULTS AND DISCUSSIONS

The positions and intensities of the C=O stretching bands in both solvents are listed in Table I.

TABLE I

POSITIONS AND INTENSITIES OF THE C=O STRETCHING BANDS IN THE INFRARED SPECTRA OF SUBSTANCES C_6H_5—CO—R

	CCl_4 solution			$CHCl_3$ solution		
Group R	ν_1 (cm.$^{-1}$)	ν_2 (cm.$^{-1}$)	Integrated absorption intensity[a]	ν_1 (cm.$^{-1}$)	ν_2 (cm.$^{-1}$)	Integrated absorption intensity[a]
—CH_3	1691		*2.18, 2.26, 2.18*; 2.20	1683		2.7[b]
—CH_2Cl	1714	1694	*2.02, 1.89, 1.83*; 1.91	1707	1689	*2.16, 2.13, 2.28*; 2.19
—$CHCl_2$	1716	1693	*1.88, 1.85*; 1.87	1710	1687	*2.05, 1.97*; 2.01
—CCl_3	1717.5	—	*1.56, 1.41*; 1.49	1713	—	*1.85, 1.92*; 1.88
—CH_2Br	1709	1688	*2.07, 1.91, 1.94*; 1.97	1702	1684	*2.21, 2.18*; 2.20
—$CHBr_2$	1707	1682	*1.78, 1.84, 1.82*; 1.81	1702	1678	*1.88, 2.04*; 1.96
—CBr_3	1704	—	*1.32, 1.41, 1.44*; 1.39	1700	—	*1.61, 1.54, 1.60*; 1.58
—CH_2I	1701[c]	1683	*2.13, 2.06*; 2.10	1696	1678	*2.27, 2.19*; 2.23
—$CH_2.CN$	1709	—	*2.07, 2.18, 2.08*; 2.11	1703	—	*2.27, 2.33*; 2.30
—$CH_2.C_6H_5$	1698	1685	*2.02, 1.90, 1.98*; 1.97	—	1680	*2.08, 2.26, 2.21*; 2.18
—$CH_2.OH$	1692	—	*1.76, 1.73*; 1.75	1687	—	*2.09, 2.04*; 2.07

[a] *The intensities are expressed in units of 10^4 mole^{-1} liter cm.$^{-2}$. The individual measurements are reported in italics followed by the arithmetical mean in roman type.*
[b] *This figure is taken from the data of G. N. Barrow, J. Chem. Phys.* **21**, *2008 (1953).*
[c] *Inflection.*

Band Positions

The compounds containing the groups —CH_2Cl, —$CHCl_2$,—CH_2Br, —$CHBr_2$, —CH_2I, and —$CH_2.C_6H_5$ give two bands, designated ν_1 and ν_2. The compounds containing —$CH_2.CN$ and —$CH_2.OH$ show one band only, as do those containing —CCl_3 and —CBr_3 groups.

The doublet maxima noted for —CH_2Cl and —$CHCl_2$ agree with the observations of Bellamy and collaborators (4) on these compounds and the band positions in carbon

tetrachloride solution check with the amended values reported by these investigators in their later publication (5). In all cases where doublets are observed the band at higher frequency (ν_1) is relatively more intense in chloroform than in carbon tetrachloride solution, indicating that the ν_1 band is associated with the more polar structure. This is consistent with the assignment of the ν_1 band to the *cis* conformation I.

In any carbonyl compound, the C=O stretching frequency is determined by a combination of steric, electrical, and mass effects of the groups surrounding the C=O bond. These effects have been reviewed in a preceding publication (13). At present the relative importance of the different effects for a given structure cannot be evaluated quantitatively, though certain structures are encountered in which one or other of these effects can be recognized to exercise a dominating influence.

Substitution Effects in the gauche Conformation (Band ν_2)

The band at lower frequency falls in the range 1694–1682 cm.$^{-1}$ in carbon tetrachloride solution and 1689–1678 cm.$^{-1}$ in chloroform. Except for the chlorinated compounds, the band lies below that of acetophenone, and the frequency diminishes in the sequence:

$$\underset{(49.5)}{-CH_2Cl} > \underset{(84)}{-CHCl_2} > \underset{(15)}{-CH_3} > \underset{(94)}{-CH_2Br} > \underset{(91)}{-CH_2.C_6H_5} > \underset{(141)}{-CH_2I} > \underset{(173)}{-CHBr_2}$$

Since electron withdrawal raises the C=O frequency, this sequence shows that the polar effect of the substituent is opposed by mass and/or steric effects that act to lower the frequency. If acetophenone itself is excluded, the above sequence approximates to one of increasing mass, as is indicated by the molecular weights of the groups given above in parenthesis.

Although the mass effect may be predominant, the influence of the electrostatic and steric effects of the substituent is also apparent. The inductive effect should be strongest for chlorine; the increase in the ν_2 frequencies of the chloro compounds can be explained in this way, and it is consistent with the substitution effects of chlorine on the ν_1 band discussed below.

Steric effects should be most in evidence in the bromide and iodide. In these compounds (III) the *ortho* hydrogen atom of the benzene ring and *gauche* halogen atom appear to be in the same steric relationship as in the *ortho*-halogenated acetophenones in the *s-trans* configuration (IV), for which steric interaction effects have been demonstrated (13).

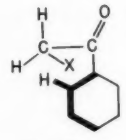

X = Br, I

III

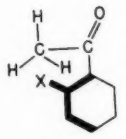

X = Br, I

IV

This steric strain can be released in a number of ways: (*a*) by a slight rotation of the methyl group about the CO—CH_2X axis; (*b*) by a slight rotation of the plane of the benzene ring about the 1,4-axis; (*c*) by increase in the angle α in

.

Of these effects (*a*) should have little effect on the ν_2 frequency and should be inoperative for the disubstituted derivatives, (*b*) should raise the C=O frequency by diminishing the resonance with the aromatic ring, and (*c*) should lower the frequency. In fact *ortho* bromination of acetophenone raises the C=O frequency by 11 cm.$^{-1}$ whereas bromination in the methyl group lowers it by 3 cm.$^{-1}$; the analogy between the steric conditions in these structures is therefore more apparent than real. The steric strain in IV would appear to be relieved largely by rotation of the whole acetyl group with respect to the ring, and the strain in III by opening of the R—CO—R angle.

Substitution Effects on the ν_1 Band

For the ν_1 band the C—O stretching frequency is in all cases greater than that of acetophenone, and diminishes in the series:

$$-CCl_3 > -CHCl_2 > -CH_2Cl > -CH_2CN > -CH_2Br > -CHBr_2 > -CBr_3 > -CH_2I > -CH_2.C_6H_5 > -CH_3.$$

Here the electronegativity of the substituent exercises the dominant influence. The trisubstituted groups $-CCl_3$ and $-CBr_3$ exhibit one band only, and since this lies well above that of acetophenone it is to be classified with the ν_1 series. For the chloro derivatives ν_1 increases with increasing substitution ($-CCl_3 > -CHCl_2 > -CH_2Cl$), whereas for bromination the sequence is reversed ($-CH_2Br > -CHBr_2 > -CBr_3$). The introduction of the first chlorine atom (in the *cis* position) changes the C=O frequency by +23 cm.$^{-1}$, while the further displacements on introduction of the second and third chlorine atoms in the *gauche* positions are +2 and +1.5 cm.$^{-1}$ respectively.* Although small, these additional positive shifts are significant, and they agree with the shifts produced by chlorination on the ν_2 band. The major shift induced by the *cis* C—Cl bond results largely from the direct dipole–dipole interaction across space, while the smaller shifts for the *gauche* C—Cl bonds are associated with the inductive effect acting through the bond system.

The "true" inductive effect of the *gauche* C—Cl bond on ν_1 must be somewhat greater than the 1 to 3 cm.$^{-1}$ actually observed. The *gauche* C—Cl bond will have a small dipole–dipole interaction with the C=O bond of opposite sign to that of the *cis* C—Cl bond. Furthermore the *gauche* C—Cl bond will have small steric and mass effects which will also act to lower the frequency. In the case of the bromo derivatives, these negative mass and steric effects are more important than the positive inductive effect of the *gauche* C—Br bond, and the reversed series is observed with the positive shift for $-CH_2Br$ (18 cm.$^{-1}$) exceeding that for $-CHBr_2$ (16 cm.$^{-1}$) and $-CBr_3$ (13 cm.$^{-1}$).

The low frequency of the single band in phenacyl alcohol suggests a *gauche* conformation, but more probably this molecule is stabilized in the *cis* conformation (V), with the hydrogen bonding being responsible for the excessive lowering of the ν_1 band. This band is symmetrical and very narrow ($\Delta\nu_{\frac{1}{2}}^{(a)} = 8$ cm.$^{-1}$), further evidence that only one molecular species is present.

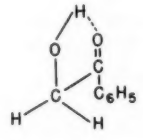

V

**All numerical data quoted in this discussion are for solutions in carbon tetrachloride unless otherwise indicated.*

Band Intensities

The integrated absorption intensity of the C=O stretching band in all types of carbonyl compounds varies over a comparatively small range between 1 and 5 intensity units.* Because the total range of intensity is so limited, it is difficult to evaluate the significance of small intensity changes associated with substitution effects. The situation is different with such bands as N—H stretch and C≡N stretch for which intensities have been observed to vary over a hundredfold range in various types of amines and nitriles (15, 16, 17).

Most of the ω-substituted acetophenones considered in this paper possess two carbonyl bands that overlap extensively. This overlap makes it impossible to evaluate the integrated absorption intensities of the ν_1 and ν_2 bands separately and only the total space integral under the complex band system can be obtained. The figures given in Table I are for this quantity.

In all cases, the integrated absorption intensity of this band system is greater in chloroform solution in carbon tetrachloride; this could indicate that the absorption of ν_1 is greater than that of ν_2, since the *gauche/cis* ratio is less in chloroform. However, the same solvent intensity effect is observed for the trichloro- and tribromo-derivatives and for acetophenone, itself, where the *gauche/cis* ratio is not involved. Most of the enhanced intensity in chloroform must therefore be attributed to a general solvent effect not dependent on the conformation.

In all cases, substitution diminishes the intensity of the carbonyl band system. The main features of these substitution effects are summarized in the series i–v listed below, where the groups are arranged in an order of diminishing band intensity. The sequence is the same in both solvents, though the quantitative differences are not.

(i) $-CH_3 > -CH_2I > -CH_2Br > -CH_2Cl$

(ii) $-CH_3 > -CH_2Cl > -CHCl_2 > -CCl_3$

(iii) $-CH_3 > -CH_2Br > -CHBr_2 > -CBr_3$

(iv) $-CH_3 > -CCl_3 > -CBr_3$

(v) $-CHCl_2 > -CHBr_2$

In series i–iii the intensity falls as the electronegativity of the functional group increases. Series iv and v, however, suggest that in the di- and tri-substituted compounds bromine is more effective than chlorine in lowering the band intensity. This effect is probably predominantly steric as it is only observed in the polysubstituted derivatives.

Substitution Effects on the gauche/cis Ratio

Because of the extensive overlap the integrated absorption intensities cannot be used to determine the equilibrium concentrations of the *gauche* and *cis* species. Some information about this equilibrium can be obtained from the ratio of the extinction coefficients at the peaks of the ν_1 and ν_2 bands. These are summarized in Table II.

The single peak of phenacyl cyanide shows little change in intensity or band width in the two solvents; from the position of the maximum (1709 cm.$^{-1}$ in CCl_4) it can be assumed that this compound exists exclusively in the *cis* conformation. The iodide shows a strong maximum at 1683 cm.$^{-1}$ in the same solvent, with a weak inflection at 1701 cm.$^{-1}$, and therefore exists predominantly, but not exclusively, in the *gauche* form. The iodide and nitrile represent the extremes of *gauche* and *cis* stabilized systems; the other compounds are listed in Table II in a sequence of increasing ratio of $\epsilon^{(a)}_{\nu_2,max}$ to $\epsilon^{(a)}_{\nu_1,max}$, and with some

**The unit of integrated absorption intensity employed here is 10^4 mole^{-1} liter cm.$^{-2}$. (See Ref. 18.)*

TABLE II

MOLECULAR EXTINCTION COEFFICIENTS OF ABSORPTION MAXIMA FOR C=O STRETCHING BANDS IN INFRARED SPECTRA OF SUBSTANCES C_6H_5—CO—R

	—CH_2OH	—CH_2CN	—$CHBr_2$	—$CHCl_2$	—CH_2Cl	—$CH_2.C_6H_5$	—CH_2Br	—CH_2I
A. CCl_4 solution								
$\epsilon^{(a)}_{\nu_1.max}$	700	400	335	245	240	220	116	60[a]
$\epsilon^{(a)}_{\nu_2.max}$	—	—	260	330	375	375	610	700
$\epsilon^{(a)}_{\nu_2.max}/\epsilon^{(a)}_{\nu_1.max}$	0	0	0.78	1.35	1.56	1.70	5.26	11.7
B. $CHCl_3$ solution								
$\epsilon^{(a)}_{\nu_1.max}$	492	444	318	290	262	*b*	145	80
$\epsilon^{(a)}_{\nu_2.max}$	—	—	148	172	214	295	384	470
$\epsilon^{(a)}_{\nu_2.max}/\epsilon^{(a)}_{\nu_1.max}$	0	0	0.47	0.59	1.22	*b*	2.65	5.9

[a] *Inflection.*
[b] *For the* —$CH_2.C_6H_5$ *group the carbonyl band envelope is particularly broad in chloroform solution and could not be resolved.*

reservations this can be identified with the sequence of increasing *gauche/cis* equilibrium ratio.

This series approximates to one of increasing stability of the *cis* form with increased electron-withdrawing effect of the X group. From III we might expect that with increase in the size of the X substituent, the increasing steric hindrance would raise the energy of the *gauche* forms, and so shift the equilibrium in favor of the *cis* conformation. In fact, the reverse appears to be true; in the iodide the equilibrium is greatly in favor of the *gauche* form, in spite of the steric hindrance associated with the large iodine atom. It is evident that we are dealing here with a complex interplay of factors which cannot be evaluated *a priori.*

VALIDITY OF THE ASSIGNMENTS

In assigning the ν_1 and ν_2 bands respectively to the *cis* and *gauche* conformations we have accepted the arguments advanced by Bellamy, Thomas, and Williams (4, 5). These in turn are based partly on an earlier generalization from this laboratory (6) that "*large positive shifts of the* C=O *stretching frequency on α-bromination in the cyclohexanone ring system in the chair configuration occur only when the bromine atom occupies an equatorial position*". This generalization was later extended to other halogens (Ref. 14, p. 478), while Corey and collaborators (7, 8, 9) have shown that conformational assignments based on this rule are consistent with those derived from thermodynamic considerations. Kumler and Huitric (19) have questioned some of Corey's conclusions because they conflicted with dipole moment data. The criticisms however were directed against Corey's assumption of a rigid chair configuration for the cyclohexanone ring in certain compounds, and not against the spectroscopic argument per se.

The existence of spectroscopic effects associated with conformational equilibria in compounds of this type was first recognized by Mizushima and co-workers (2) in chloroacetone. Initially these investigators assigned the C=O band of lower frequency to VI, which they considered thermodynamically more stable than the *gauche* structure VII. This was not consistent with the conclusions of Bellamy, Corey, and ourselves, since it required that the parallel alignment of C=O and C—Cl dipoles should produce

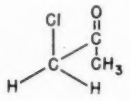

VI

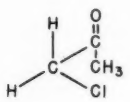

VII

a lesser spectral shift than the *gauche* arrangement. It was however in agreement with our observations in indicating greater thermodynamic stability for the *cis* conformation.

Recently Josien, Castinel, Chiurdoglu, and Vanlanduyt (20) in a reappraisal of Mizushima's data changed the assignment of the vapor-state carbonyl band of chloroacetone; this left the structural assignments for VI and VII unchanged, but indicated greater thermodynamic stability for VII over VI. This presented a complete reversal from the spectroscopic and thermodynamic behavior pattern developed by Bellamy, Corey, and ourselves for α-bromo ketones, and led Josien and collaborators to criticize our original interpretation of the α-halogenated cyclohexanone-type spectra.

The discussion of substitution effects earlier in this paper by no means fully explains the band shifts on the basis of the conformations associated with ν_1 and ν_2, but the situation is a good deal less satisfactory if the assignments are reversed. Without elaborating on this unnecessary detail, it can be noted, for example, that introduction of the first chlorine atom produces a positive displacement of $+23$ cm.$^{-1}$ for ν_1 while the additional displacements produced by the second and third chlorine atoms are $+2$ and $+1.5$ cm.$^{-1}$ respectively. If the ν_1 and ν_2 assignments are reversed this requires that the first (*gauche*) chlorine substituent produces the large displacement while the second (*gauche*) and the third (*cis*) substituents have only small effects. Difficulties of the same kind would be encountered in explaining the relatively small differences observed between mono- and di-halogenated substituents on the ν_2 band and such an assignment is quite untenable.

Finally, the recent re-examination of the spectrum of chloroacetone has led Bellamy and Williams (5) to reverse the assignments for the carbonyl bands of that compound, so that there is now complete consistency with the ω-substituted acetophenone spectra. With this change the conclusions from dipole moment measurements as well as the thermodynamic behavior of these compounds substantiate fully the hypothesis that large positive carbonyl shifts are associated with *cis*-bromination in the α-position.

ACKNOWLEDGMENTS

The acetophenone derivatives were prepared by one of us (E. S.) in the chemistry laboratories of the Manchester College of Science and Technology in connection with an investigation of their ultraviolet spectra. We wish to thank Dr. A. Burawoy for making them available to us for these studies.

REFERENCES

1. Nakagawa, I., Ichishima, I., Kuratani, K., Miyazawa, T., Shimanouchi, T., and Mizushima, S. J. Chem. Phys. **20**, 1720 (1952).
2. Mizushima, S., Shimanouchi, T., Miyazawa, T., Ichishima, I., Kuratani, K., Nakagawa, I., and Shido, N. J. Chem. Phys. **21**, 815 (1953).
3. Josien, M. L. and Calas, R. Compt. rend. **240**, 1641 (1955).
4. Bellamy, L. J., Thomas, L. C., and Williams, R. L. J. Chem. Soc. 3704 (1956).
5. Bellamy, L. J. and Williams, R. L. J. Chem. Soc. 4294 (1957).
6. Jones, R. N., Ramsay, D. A., Herling, F., and Dobriner, K. J. Am. Chem. Soc. **74**, 2828 (1952).
7. Corey, E. J. J. Am. Chem. Soc. **75**, 2301, 3297 (1953).
8. Corey, E. J., Topie, T. H., and Wozniak, W. A. J. Am. Chem. Soc. **77**, 5415 (1955).
9. Corey, E. J. and Burke, H. J. J. Am. Chem. Soc. **77**, 5418 (1955).

10. JONES, R. N. Spectrochim. Acta, **9**, 235 (1957).
11. RAMSAY, D. A. J. Am. Chem. Soc. **74**, 72 (1952).
12. JONES, R. N., RAMSAY, D. A., KEIR, D. S., and DOBRINER, K. J. Am. Chem. Soc. **74**, 80 (1952).
13. JONES, R. N., FORBES, W. F., and MUELLER, W. A. Can. J. Chem. **35**, 504 (1957).
14. JONES, R. N. and SANDORFY, C. The applications of infrared and Raman spectrometry to the eluicidation of molecular structure. *In* Technique of organic chemistry. Vol. IX. *Edited by* A. Weissberger. Interscience Publishers, Inc., New York and London. 1956.
15. RUSSELL, R. A. and THOMPSON, H. W. J. Chem. Soc. 483 (1955).
16. SKINNER, M. W. and THOMPSON, H. W. J. Chem. Soc. 487 (1955).
17. THOMPSON, H. W. and STEEL, G. Trans. Faraday Soc. **52**, 1451 (1956).
18. JONES, R. N., AUGDAHL, E., NICKON, A., ROBERTS, G., and WHITTINGHAM, D. J. Ann. N.Y. Acad. Sci. **69**, 38 (1957).
19. KUMLER, W. D. and HUITRIC, A. C. J. Am. Chem. Soc. **78**, 3369 (1956).
20. JOSIEN, M. L., CASTINEL, C., CHIURDOGLU, G., and VANLANDUYT, E. Compt. rend. **244**, 2383 (1957).

CLASSICAL APPROACH TO THE STRUCTURE OF CONDENSED-RING AROMATIC COMPOUNDS—A REJOINDER TO THE PROBLEM OF DIBENZO(*cd*,*mn*)PYRENE

LAKHBIR SINGH

According to the molecular-orbital treatment of the dibenzo(*cd*,*mn*)pyrene structure given by Lister (2), this molecule should be paramagnetic corresponding to two free electrons. It is a remarkable conclusion, as all other known hydrocarbons of this family including graphite are diamagnetic. The author of the present note, however, believes that the simple classical theory can still provide better guidance in such complicated problems. This approach can be considered reliable even today, as it is known that the earlier electronic theory was essentially correct in all its conclusions, "although expressed in a terminology which now seems old-fashioned" (1).

According to a new classical concept of the aromatic bond developed by the author (3), the π-electrons tend to form a continuous circular coupling round the benzene ring. However, the π-electron coupling in the condensed-ring aromatic compounds cannot be unique and stable, because the π-electrons on the carbon atoms which are common between two or three rings can complete the circular coupling (or the 'sextet') of only one of these rings at a time (4). Thus, the π-electron coupling in these complex molecules remains in a state of turmoil, which is responsible for their peculiar physical and chemical properties.

In naphthalene, each ring alternately becomes fully aromatic. Part of the time, the continuous aromatic coupling gets truncated in both the rings. The π-electrons at the α-positions, which do not form the continuous ring, return round these atoms to complete the π-electron coupling in the side ring. This side ring behaves more or less as a conjugated side chain (for half the time) and is the cause of greater reactivity of the napthalene

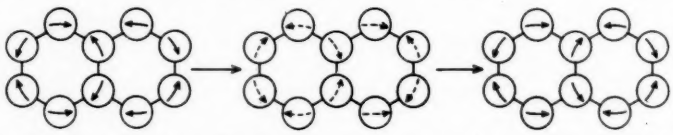

π-Electron coupling in naphthalene. The broken arrows represent the π-electrons on the lower side of the molecular plane.

molecule. In phenanthrene, most of the time a simple double bond remains in the middle ring, because of the greater tendency of the π-electrons to complete the sextets in the two outer rings. This explains the olefinic character of this C_9—C_{10} bond. In pyrene, however, a naphthalene type of coupling in the two middle rings also becomes equally

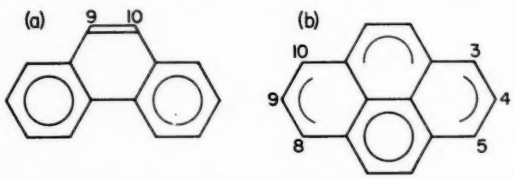

π-Electron coupling in phenanthrene (*a*) and pyrene (*b*).

effective. The transient π-electron coupling among three atoms in this molecule is supported by the reduction product 3,4,5,8,9,10-hexahydropyrene. The two π-electrons on the C_9 and C_{10} positions in the middle ring of anthracene remain uncoupled for part of the time. However, this molecule is not paramagnetic in spite of the abundant chemical evidence in favor of this partial free valence character at these two positions. This is owing to the fact that these π-electrons are not free in the usual sense of this term. They can be called free or uncoupled in a relative sense only. The π-electrons forming the

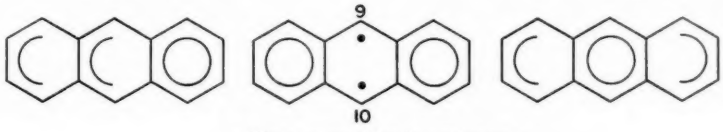

π-Electron coupling in anthracene.

aromatic bond couple on both sides of the molecular plane after each half revolution of these electrons round the carbon atoms (3). The π-electrons at the truncated ends of the aromatic bond couple after one full revolution around the carbon atoms (4) as in a simple covalent bond, while these partially free π-electrons in anthracene couple after one and a half revolutions. This situation arises only momentarily for each π-electron when it is on a C_9 or C_{10} atom. Under these circumstances the spin of the electron cannot be treated as free. These gradations in coupling are, however, reflected in the variations in chemical properties as shown by the benzene carbon atoms, the α-positions in naphthalene, and the C_9 and C_{10} positions in anthracene.

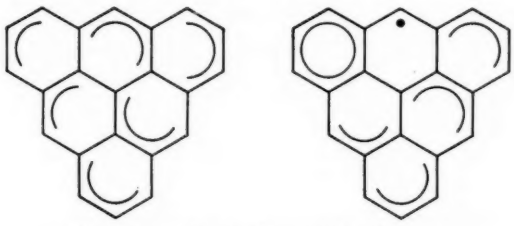

π-Electron coupling in dibenzo(*cd*,*mn*)pyrene.

On the basis of the above considerations, it can be predicted that the dibenzo(*cd*,*mn*)-pyrene hydrocarbon will not be paramagnetic. It may, however, have some free valence character of the anthracene type. The π-electron coupling in it can get truncated in many ways. The actual weight to these possibilities can be decided only after the chemical properties are known.

1. DEWAR, M. J. S. *In* Progress in organic chemistry. Vol. 2. *Edited by* J. W. Cook. Butterworths Scientific Publications, London. 1953. p. 1.
2. LISTER, M. W. Can. J. Chem. **35**, 934 (1957).
3. SINGH, L. Naturwissenschaften, **43**, 466 (1956) (in English).
4. SINGH, L. Naturwissenschaften, **44**, 111 (1957) (in English).

RECEIVED DECEMBER 23, 1957.
PHYSICAL CHEMISTRY DIVISION,
NATIONAL CHEMICAL LABORATORY,
POONA, INDIA.

HELVETICA
CHIMICA
ACTA

SCHWEIZERISCHE
CHEMISCHE GESELLSCHAFT
Verlag Helvetica Chimica Acta
Basel 7 (Schweiz)

Seit 1918 **40** Jahre

CANADIAN JOURNAL OF CHEMISTRY

Notes to Contributors

Manuscripts

(i) ***General.*** Manuscripts, in English or French, should be typewritten, double spaced, on paper 8½×11 in. **The original and one copy are to be submitted.** Tables and captions for the figures should be placed at the end of the manuscript. Every sheet of the manuscript should be numbered.

Style, arrangement, spelling, and abbreviations should conform to the usage of recent numbers of this journal. Names of all simple compounds, rather than their formulas, should be used in the text. Greek letters or unusual signs should be written plainly or explained by marginal notes. Superscripts and subscripts must be legible and carefully placed.

Manuscripts and illustrations should be carefully checked before they are submitted. Authors will be charged for unnecessary deviations from the usual format and for changes made in the proof that are considered excessive or unnecessary.

(ii) ***Abstract.*** An abstract of not more than about 200 words, indicating the scope of the work and the principal findings, is required, except in Notes.

(iii) ***References.*** These should be designated in the text by a key number and listed at the end of the paper, with the number, in the order in which they are cited. The form of the citations should be that used in this journal; in references to papers in periodicals, titles should not be given and only initial page numbers are required. The names of periodicals should be abbreviated in the form given in the most recent *List of Periodicals Abstracted by Chemical Abstracts*. All citations should be checked with the original articles and each one referred to in the text by the key number.

(iv) ***Tables.*** Tables should be numbered in roman numerals and each table referred to in the text. Titles should always be given but should be brief; column headings should be brief and descriptive matter in the tables confined to a minimum. Vertical rules should not be used. Numerous small tables should be avoided.

Illustrations

(i) ***General.*** All figures (including each figure of the plates) should be numbered consecutively from 1 up, in arabic numerals, and each figure referred to in the text. The author's name, title of the paper, and figure number should be written in the lower left corner of the sheets on which the illustrations appear. Captions should not be written on the illustrations (see Manuscripts (i)).

(ii) ***Line Drawings.*** Drawings should be carefully made with India ink on white drawing paper, blue tracing linen, or co-ordinate paper ruled in blue only; any co-ordinate lines that are to appear in the reproduction should be ruled in black ink. Paper ruled in green, yellow, or red should not be used. All lines should be of sufficient thickness to reproduce well. Decimal points, periods, and stippled dots should be solid black circles large enough to be reduced if necessary. Letters and numerals should be neatly made, preferably with a stencil (**do NOT use typewriting**), and be of such size that the smallest lettering will not be less than 1 mm. high when reproduced in a cut of suitable size.

Many drawings are made too large; originals should not be more than 2 or 3 times the size of the desired reproduction. Wherever possible two or more drawings should be grouped to reduce the number of cuts required. In such groups of drawings, or in large drawings, full use of the space available should be made; the ratio of height to width should conform to that of a journal page (5½×7¾ in.) but allowance must be made for the captions..

The original drawings and one set of clear copies (e.g. small photographs) are to be submitted.

(iii) ***Photographs.*** Prints should be made on glossy paper, with strong contrasts. They should be trimmed so that essential features only are shown and mounted carefully, with rubber cement, on white cardboard, with no space between them. In mounting, full use of the space available should be made to reduce the number of cuts required (see Illustrations (ii)). Photographs or groups of photographs should not be more than 2 or 3 times the size of the desired reproduction.

Photographs are to be submitted in duplicate; if they are to be reproduced in groups one set should be mounted, the duplicate set unmounted.

Reprints

A total of 50 reprints of each paper, without covers, are supplied free. Additional reprints, with or without covers, may be purchased at the time of publication.

Charges for reprints are based on the number of printed pages, which may be calculated approximately by multiplying by 0.5 the number of manuscript pages (double-space typewritten sheets, 8½×11 in.) and including the space occupied by illustrations. An additional charge is made for illustrations that appear as coated inserts. Prices and instructions for ordinary reprints are sent out with the galley proof.

Any reprints required in addition to those requested on the author's reprint requisition form must be ordered officially as soon as the paper has been accepted for publication.

Contents

Notes:

Printed in Canada *by* University of Toronto Press